INTERACCIÓN PLANTA-PLANTA PARÁSITA: ESTUDIOS CITOQUÍMICOS DE LA RESISTENCIA A JOPO (OROBANCHE CRENATA) EN LEGUMINOSAS

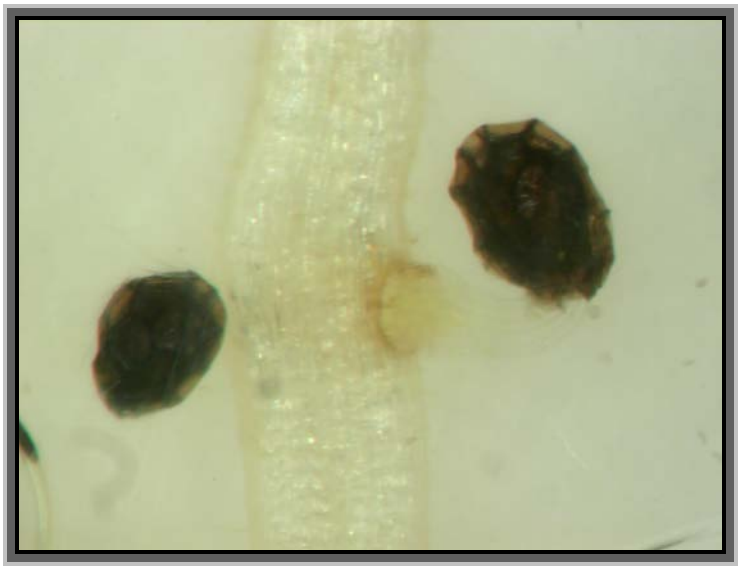

María de los Dolores Lozano Baena

Tesis Doctoral

2011

TITULO: *Interacción planta-planta parásita: estudios citoquímicos de la resistencia a jopo (Orobanche crenata) en leguminosas*

AUTOR: *María Dolores Lozano Baena*

Campus de Rabanales
Ctra. Nacional IV, Km. 396 A
14071 Córdoba

www.uco.es/publicaciones
publicaciones@uco.es

ISBN-13: 978-84-694-9099-0

TÍTULO DE LA TESIS: **Interacción planta-planta parásita: estudios citoquímicos de la resistencia a jopo (*Orobanche crenata*) en leguminosas.**

DOCTORANDO/A: MARÍA DOLORES LOZANO BAENA

ESCRITO RAZONADO DEL RESPONSABLE DE LA LÍNEA DE INVESTIGACIÓN

(Ratificando el informe favorable del director. Sólo cuando el director no pertenezca al programa de doctorado).

D. Juan Gil Ligero, Profesor Titular del departamento de Genética de la Universidad de Córdoba y responsable de la línea de investigación en la que se encuadra la tesis "Interacción planta-planta parásita: estudios citoquímicos de la resistencia a jopo (*Orobanche crenata*) en leguminosas" realizada por María Dolores Lozano Baena, ratifica los informes emitidos por sus dos directores, D. Alejandro Pérez de Luque y D. Diego Rubiales Olmedo. La tesis cumple con los requisitos establecidos para su defensa, englobando tres artículos publicados en revistas SCI de alto índice de impacto de los que la doctoranda es la autora principal o coautora, además de un cuarto manuscrito enviado para su publicación. Además, cumple también con la normativa necesaria para poder obtener la mención de doctorado europeo

Por todo ello, se autoriza la presentación de la tesis doctoral.

Córdoba, 28 de enero de 2011

Firma del responsable de línea de investigación

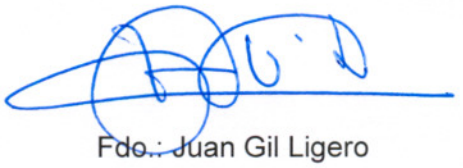

Fdo.: Juan Gil Ligero

TÍTULO DE LA TESIS: **Interacción planta-planta parásita: estudios citoquímicos de la resistencia a jopo (*Orobanche crenata*) en leguminosas.**

DOCTORANDO/A: Mª DOLORES LOZANO BAENA

INFORME RAZONADO DEL/DE LOS DIRECTOR/ES DE LA TESIS

(se hará mención a la evolución y desarrollo de la tesis, así como a trabajos y publicaciones derivados de la misma).

D. Alejandro Pérez de Luque, Dr. Ingeniero Agrónomo e Investigador Titular del Instituto de Investigación y Formación Agraria y Pesquera de Andalucía (IFAPA),

D. Diego Rubiales Olmedo, Dr. Ingeniero Agrónomo y Profesor de Investigación del CSIC,

INFORMAN

Que el trabajo "Interacción planta-planta parásita: estudios citoquímicos de la resistencia a jopo (*Orobanche crenata*) en leguminosas" realizado por María Dolores Lozano Baena bajo su dirección se considera ya finalizado y puede ser presentado para su exposición y defensa como Tesis Doctoral en la Universidad de Córdoba. Fruto de dicho trabajo han sido la publicación de tres artículos en revistas internacionales con alto índice de impacto (Plant Physiology, Jornal of Experimental Botany, Annals of Botany) de los que la doctoranda es autora principal o coautora, y un cuarto artículo cuyo manuscrito se ha enviado para su publicación a Annals of Botany. Asimismo, la doctoranda y la tesis cumplen los requisitos y permisos necesarios para optar a la mención de doctorado europeo.

Por todo ello, se autoriza la presentación de la tesis doctoral.

Córdoba, 31 de enero de 2011

Firma de los directores

Fdo.:Alejandro Pérez de Luque Fdo.: Diego Rubiales Olmedo

Siendo sincera, han sido numerosas las ocasiones en las que he pensado en este momento y en qué escribir o de quién me puedo estar olvidando y casi todas las veces me he vuelto loca al hacerlo. Por eso, espero que me disculpéis si me olvido de alguien, no es esa mi intención y como me conocéis bastante bien, prefiero recordar todos los momentos vividos estos años en lugar de redactar un informe detallado de ellos.

Me gustaría empezar dándoles las gracias a mis directores de tesis que me han tenido que aguantar todos estos años. Sé que no ha sido fácil para vosotros luchar contra mi cabezonería, pero necesitaba de vuestra paciencia para comprender el por qué de vuestras opiniones. Gracias por haberme dado el espacio que necesitaba para entenderos y para entender el trabajo que realizaba. Gracias Diego por darme una oportunidad, por seguir tu intuición y permitirme trabajar en lo que me gusta, en lo que siempre he querido. Y gracias a Alex, por cambiar mi forma de ver las cosas, por permitirme aprender de tus conocimientos y enseñarme el camino cuando ni siquiera era capaz de ver las posibilidades que tenía.

Gracias a Mª Teresa y Jose Ignacio, por haberme permitido trabajar en vuestro grupo de investigación. Con ello he entendido mejor el funcionamiento de las cosas y he podido ver cómo habéis formado más que un grupo, una gran familia.

A mis compañeros del CIFA (ahora IFAPA). Con vosotros empecé mi trabajo en las "camaritas" y en el "laboratorio de molecular". Jamás olvidaré tantas horas ni tantas personas trabajando juntas a la vez en una mesa de 2x1 m^2.

A mis compañeros del IAS (CSIC), ya seáis del "labo", mantenimiento, informática, biblioteca, o conserjería. Todos me habéis ayudado cuando os he necesitado. Gracias a todos por ello.

A toda la gente que me encontré y con la que tuve el placer de trabajar durante mis estancias en el extranjero, porque me hicisteis sentir aceptada estando lejos de casa pese a no conocerme ni conoceros.

Al personal del CIB de Madrid por la colaboración que mantuvimos y que posibilitó, no sólo una publicación, sino también la posibilidad de seguir trabajando juntos.

A mis compañeros de Rabanales que aun en la distancia siempre me ayudabais cuando os hacía una visita sorpresa.

A mis amigos. Jamás olvidaré las caras que poníais cuando os hablaba de trabajo ni vuestros comentarios de "Mª Dolores como siempre tan científica". Gracias por aceptarme tal y como soy.

A mi familia. Ya sé que mi trabajo es difícil de entender y que muchas veces os habéis extrañado cuando os contaba lo que hacía pero pese a todo se que siempre habéis estado orgullosos de mi.

Gracias a todos

ÍNDICE

INTRODUCCIÓN GENERAL QUE JUSTIFIQUE LA TEMÁTICA DE LA TESIS

Orobanche crenata (jopo) es uno de los principales problemas para el cultivo de leguminosas (Fam. Fabaceae) en la zona mediterránea, llegando a producir pérdidas cercanas al 100% de la producción de algunas de las principales especies de interés agronómico como el haba (*Vivia faba* L.), la lenteja (*Lens culinaris* Medick) y el guisante (*Pisum sativum* L.) en zonas muy infectadas. Esta planta holoparásita obligada ataca a la raíz del huésped desarrollando una estructura de fijación denominada haustorio a través de la cual consigue todos los elementos y nutrientes necesarios para su desarrollo. Esto hace que sea muy difícil y costoso su manejo dado que la mayor parte de las pérdidas de producción del cultivo se dan antes siquiera de que el parásito emerja del suelo.

Debido al gran interés que tiene el cultivo de leguminosas, se necesitan estrategias económica y medioambientalmente sostenibles que aumenten la producción combatiendo dichas infecciones. En este sentido, la búsqueda de mecanismos de resistencia para incorporarlos en los programas de mejora es una de las mejores opciones en el manejo y control de jopo.

A pesar de ser un patógeno bien caracterizado en especies susceptibles a su ataque, no es tanto el conocimiento que se tiene sobre los mecanismos de resistencia en las que lo combaten. En este sentido, las especies de leguminosas cultivadas no son de fácil manejo debido a su complejo genoma y a que la mayoría presentan niveles de resistencia muy bajos y poco estables en el tiempo. Además, la complejidad de la interacción y el hecho de que ambos (parásito y huésped) son plantas, limita en gran medida su estudio.

Por todo ello, con esta tesis hemos querido caracterizar la interacción que se da entre la planta parásita *O. crenata* y varias de las principales especies de leguminosas de interés en nuestro país y en toda el área mediterránea.

Trabajos anteriores habían demostrado que existen distintos momentos durante el proceso de infección del jopo en los que el huésped puede presentar mecanismos de defensa frente al mismo. En un primer momento, las semillas de jopo necesitan para germinar de la presencia en el suelo de ciertas sustancias exudadas por las raíces del huésped. Gracias a ello, las semillas una vez germinadas orientan su crecimiento en dirección al huésped. Una vez han contactado con él, comienzan a penetrar en la raíz y intentar desarrollar conexiones con sus haces vasculares para empezar a nutrirse y a crecer, continuando su ciclo de vida. Dichas conexiones las establecen a través del desarrollo de un órgano específico denominado haustorio que actúa de unión entre huésped y parásito.

Si el huésped presenta mecanismos de defensa que impiden al jopo alcanzar sus vasos conductores, entonces estamos ante un mecanismo de defensa *pre-haustorial* y la radícula de jopo muere antes formar el haustorio.

Si la radícula de jopo consigue formar un haustorio y empezar a nutrirse del huésped, éste puede presentar mecanismos de defensa *post-haustoriales* que le impidan seguir creciendo.

De esta forma, para este trabajo se seleccionó en primer lugar la especie *Vicia sativa* que presenta mecanismos de defensa *post-haustoriales*. De esta especie se utilizaron dos genotipos: uno resistente (A01) y otro susceptible (S27) al ataque del jopo, con el fin de determinar el tipo de mecanismo de defensa que presentaba.

Para estudiar los mecanismos de defensa *pre-haustoriales*, se seleccionaron dos cultivares de la especie *Vicia faba* como en el caso anterior, una resistente (Baraca) y la otra susceptible (Prothabon).

Pero el manejo de estas especies así como el de las principales leguminosas de interés comercial presenta grandes dificultades debido a sus características genéticas y condiciones de cultivo. Por ello y con el fin de encontrar un mecanismo de defensa general presente en leguminosas, se seleccionó la especie modelo *M. truncatula* y así, poder determinar en qué forma se defiende esta especie del ataque del jopo. *M. truncatula* permitía un mejor manejo y posibilitaba no sólo encontrar con mayor facilidad nuevas fuentes de resistencia, sino también la posibilidad de traspasar dichas fuentes a especies de interés comercial.

Debido al escaso conocimiento que se poseía sobre los mecanismos de defensa de las leguminosas frente al jopo, optamos por utilizar diferentes técnicas citoquímicas y de microscopía como una primera aproximación a los mecanismos que desencadena la invasión del parásito en el tejido huésped. Estas técnicas permiten la observación directa a nivel celular del proceso infectivo del jopo en la raíz del huésped. Por ello, varios tipos de tinciones fueron seleccionadas con el objetivo de determinar qué mecanismos celulares se desencadenaban

cuando el huésped era invadido por el patógeno, así como la combinación de las mismas con diversas técnicas de microscopia entre ellas la de fluorescencia y la microscopia confocal.

Del mismo modo, la metodología del HPLC de masas (LC-MS/MS) permite la identificación de sustancias simples en mezclas complejas (como es el medio celular de los tejidos de nuestras especies). Así, para determinar los compuestos que producen las células de nuestra interacción jopo-planta huésped, decidimos utilizar esta técnica y así poder identificar y cuantificar las sustancias responsables de la resistencia de nuestro huésped frente al parásito.

Todas estas técnicas combinadas permiten no sólo caracterizar el proceso de infección del jopo en la raíz del huésped, sino también determinar los mecanismos mediante los cuales dicho huésped se defiende ante su invasión.

OBJETIVOS A ALCANZAR

1) Puesta a punto de diferentes técnicas histoquímicas y de microscopia, para esclarecer los mecanismos de defensa/ resistencia de estas leguminosas frente al patógeno *O. crenata*.

2) Estudiar la interacción entre *O. crenata* y líneas resistentes y susceptibles de las leguminosas *Vicia sativa, V. faba* y *Medicago truncatula,* con el fin de identificar los componentes macroscópicos de la resistencia.

3) Identificación y caracterización de los mecanismos defensivos a nivel histoquímico, frente a *O. crenata,* de las leguminosas anteriores.

4) Determinar si la leguminosa *M. truncatula* es una buena candidata como especie modelo para la caracterización de la interacción entre el género *O.* y las principales leguminosas cultivadas.

CAPÍTULO I: "Piensa en tres dimensiones"

Mucilage production during the incompatible interaction between *Orobanche crenata* and *Vicia sativa*

Journal of Experimental Botany (2006) 57: 931-942

Alejandro Pérez-de-Luque[1], María-Dolores Lozano[1], José-Ignacio Cubero[2], Pablo González-Melendi[3], Mari-Carmen Risueño[3] and Diego Rubiales[1]

[1] *CSIC, Instituto de Agricultura Sostenible, Apdo. 4084, 14080 Córdoba, Spain*

[2] *ETSIAM-UCO, Dep. Genética, Apdo. 3048, 14080 Córdoba, Spain*

[3] *CSIC, Centro de Investigaciones Biológicas, Dep. Plant Development and Nuclear Organization, Ramiro de Maeztu 9, 28040 Madrid, Spain*

Abstract

Orobanche spp. (broomrapes) are holoparasites lacking in chlorophyll and totally dependent on their host for their supply of nutrients. *O. crenata* is a severe constraint to legumes cultivation and breeding for resistance remains as one of the best available methods of control. However, little is known about the basis of host resistance to broomrapes. It is a multicomponent event, and resistance based on hampering development and necrosis of broomrape tubercles has been reported. In the present work we studied histologically the formation of mucilage and occlusion of host xylem vessels associated with death of *O. crenata* tubercles. Samples of necrotic *O. crenata* tubercles established on resistant and susceptible vetch genotypes were collected. The samples were fixed, sectioned and stained using different procedures. The sections were observed at the light microscopy level, either under bright field, epi-fluorescence or confocal laser scanning microscopy. A higher proportion of necrotic tubercles was found on the resistant genotype and this was associated with a higher percentage of occluded vessels. Mucilage is composed mainly by carbohydrates (non-esterified pectins) and presence of polyphenols was also detected. The mucilage and other substances composed by parasite secretions and host degraded products was found to block host vessels and obstruct the parasite supply channel, being a quantitative defensive response against *O. crenata* in vetch, and probably also in other legumes and plants. The presence of foreign substances (i.e. parasite secretions) and host degraded products (i.e. carbohydrates from cell walls) inside host vessels seems to activate this response and leads to xylem occlusion and further death of established *Orobanche* tubercles.

Introduction

Broomrapes (*Orobanche* spp.) are obligate root holoparasites which connect to the vascular system of their host plants through a specialised structure known as a haustorium. These parasites are devoid of chlorophyll and totally depend on their hosts for their supply of carbon, nitrogen and inorganic solutes. Some of these species have become a severe constraint to major crops including legumes. This is the case of *O. crenata* (crenate broomrape) which has been known to threaten legume crops since ancient times (Cubero, 1994). It is an important pest in faba bean (*Vicia faba*), pea (*Pisum sativum*), lentil (*Lens culinaris*), vetches (*Vicia* spp.), grass and chickling pea (*Lathyrus sativus* and *L. cicera*) and other grain and forage legumes in the Mediterranean basin and the Middle East (Rubiales *et al*., 2005).

Breeding for resistance is the most economic, feasible and environmental friendly method of control against this parasite. However, despite resistance to *Orobanche* spp. has been reported (Labrousse *et al*., 2001; Rubiales *et al*., 2003a, b; Rubiales *et al*., 2004; Pérez-de-Luque *et al*., 2005a), little is known about the basis of host resistance to these parasites (Joel *et al*., 1996; Pérez-de-Luque *et al*., 2005b). One of the most common incompatible interactions described in the literature is the darkening and/or necrosis of developing tubercles (Dörr *et al*., 1994; Labrousse *et al*., 2001; Pérez-de-Luque *et al*., 2005a, b). Histological studies have revealed that initial vascular connections are established and tubercles develop but they then become dark and the parasite dies at an early developmental stage (Dörr *et al*., 1994; Labrousse *et al*., 2001; Pérez-de-Luque *et al*., 2005b). The presence of substances inside host vessels has been associated with the darkening of broomrape tubercles (Labrousse *et al*., 2001; Zehhar *et al*., 2003; Pérez-de-Luque *et al*., 2005b) and it is possible that these substances block the vessels and interfere with the nutrient flux between host and parasite (Pérez-de-Luque *et al*., 2005b).

Xylem occlusion is a common response to vascular invading pathogens such as bacteria, fungi and viruses, and formation of mucilages and tylosis is tipically associated with resistance against wilt diseases (Beckman *and* Zaroogian, 1967; VanderMolen *et al*., 1983; Rioux *et al*., 1998; Beckman, 2000). Furthermore it has also been reported as a response to wounded tissue (Crews *et al*., 2003). However, it has not been demonstrated as a common response against parasitic plants. In the present work we study the composition and the role of

these substances appearing inside host vessels of *Vicia sativa* resistant to *O. crenata* by the use of different cytochemical and immunofluorescence assays.

Materials and methods

Plant material and growth conditions

Orobanche crenata seeds were collected on *Pisum sativum* infected plants in Cordoba (Spain) during year 2003. *O. crenata* was grown on resistant and susceptible genotypes of common vetch (*Vicia sativa* L., A01 and V27 respectively). The polyethylene bag system described by Linke *et al*. (2001) was used. A strip (11×28 cm) of glass fiber paper (Whatmann GF/A) with disinfected *O. crenata* seeds (40 mg) spread on it was inserted in a polyethylene bag (25×35 cm). In order to ensure homogeneous seed germination, the synthetic germination stimulant GR-24 (10 mg l^{-1}, 5 ml per bag) was added. Fifteen days later germinated vetch seedlings having a radicle length of about 4-5 cm were transferred to the bag, placing them on the upper side of the system. Twenty ml of Hoagland nutrient solution (Hoagland *and* Arnon, 1950) was added to each bag, and refilled later when necessary. The bags were suspended vertically in boxes and the plants were grown in a controlled environment chamber with a day/night temperature of 20ºC ± 0.5ºC, 14 h photoperiod and an irradiance of 200 µmol m^{-2} s^{-1}.

At days 35, 40 and 45, the number of *O. crenata* tubercles was counted, referring those that became necrotic and died as a percentage of the total.

Collection and fixation of samples

Observations were taken using a binocular microscope (Nikon SMZ1000; Nikon Europe B.V., Badhoevedorp, The Netherlands). At 35, 40 and 45 days after inoculation, tubercles of *O. crenata* were sampled at random with the corresponding attached parts of host roots.

For bright field and epi-fluoresence observations at the light microscope, the sampled material was fixed in FAA (ethanol 50% + formaldehyde 5% + glacial acetic acid 10%, in water) for 48 h. Fixed samples were then dehydrated in ethanol series (50, 80, 95, 100, 100%: 12 h each) and transferred to an embedding solvent (Xylene; Panreac Quimica S.A., Montcada i Reixac, Spain) through a xylene-ethanol series (30, 50, 80, 100, 100%: 12 h each)

and finally saturated with paraffin (Paraplast Xtra; Sigma, St. Louis, USA). 7 µm-thick sections were cut with a rotary microtome (Nahita 534; Auxilab S.A., Beriain, Spain) and attached to adhesive-treated microscope slides (polysine slides; Menzel GmbH & Co KG, Braunschweig, Germany).

For inmunofluorescence experiments analysed through confocal laser scanning microscopy, the samples were fixed in 4% formaldehyde in phosphate buffered saline (PBS), pH 7.3 at 4ºC overnight. After washing in PBS (3x15 min), they were stored in 0.1% formaldehyde in PBS at 4ºC. 40µm vibratome sections (Vibratome series 1000, Intracel Electrophysiology and Biochemistry Equipment, Herts, UK) were cut under water and dried down on 3-aminopropyl triethoxy silane (APTES, Sigma)-coated multi-well slides. The sections were dehydrated in a series of 30, 50, 70 and 100% methanol/water, then rehydrated in a series of 70, 50, 30% methanol/water, and finally in PBS, for 5 min at each step. To facilitate penetration of the labelling reagents, the sections were treated with 0.1% Tween 20 in PBS for 15 min at room temperature, then washed in PBS for 5 min and allowed to dry.

Cytochemical methods for light microscopy

After removal of paraffin, the sections were stained with different dyes:

1. Alcian green - safranin (AGS) (Joel, 1983). The slides were dried and mounted with DePeX (BDH). With this staining method, carbohydrates (including cell walls and mucilage) appeared green, yellow or blue, while lignified, cutinized and suberized walls, as well as tannin and lipid material inside cells appeared red (Joel, 1983). Non-stained sections were kept as control, and for examination under the fluorescence microscope.

2. Staining with 0.05% toluidine blue O (TBO) in PO_4 buffer (pH 5.5) during 5-10 min was used. In this case the dye was applied before removal of paraffin (Ruzin, 1999). This method allows the detection of phenolics as well as tannins, lignin and suberin (Baayen *et al*., 1996; Bordallo *et al*., 2002; Mellersh *et al*., 2002; Crews *et al*., 2003).

3. Phloroglucinol (2% in ethanol)-HCl (35%) (Ruzin, 1999) stains the aldehyde groups of lignin and suberin, but quenches lignin autofluorescence and retains suberin fluorescence (Baayen *et al*., 1996; Rioux *et al*., 1998).

4. Aniline blue fluorochrome was used for callose detection under UV fluorescence. The samples were stained during 15-30 min in a solution 0.1% aniline blue fluorochrome in water (Bordallo *et al*., 2002).

5. Pectins were detected using ruthenium red. The samples were immersed during 5 min in a solution 0.05% ruthenium red in water. Non-methyl esterified pectins take a red/pink coloration with this dye (Vallet *et al*., 1996).

The sections were observed using a light microscope (Leica DM-LB, magnification ×100 to ×400; Leica Microsystems Wetzlar GmbH, Wetzlar, Germany) and photographed using a digital camera (Nikon DXM1200F; Nikon Europe B.V., Badhoevedorp, The Netherlands). The samples were also observed by epi-fluorescence under excitation at 450-490 nm (blue-violet).

Immunofluorescence for confocal laser scaning microscopy

After blocking with 5% bovine serum albumine (BSA) in PBS for 5 min, the slides carrying the vibratome sections were incubated with the first antibody undiluted for 1 h: JIM 5 for non-methyl esterified pectins and JIM 7 for methyl esterified pectins (Professor Keith Roberts, John Innes Centre, Norwich, UK). After washing in PBS, they were incubated with a fluorescent anti-rat ALEXA 546 (Molecular Probes Inc., Eugene, OR, USA) antibody applied 1/25 in 3% BSA in PBS for 45 min at room temperature in the dark. Confocal optical section stacks were collected using a Leica TCS-SP2-AOBS-UV confocal laser scanning microscope (Leica Microsystems Wetzlar GmbH, Wetzlar, Germany).

Dye tracer

Naphthol blue black was used as a dye tracer to test the continuity of water and nutrient fluxes between the host root and the parasite tubercles (Jacobsen *et al*., 1992). The distal parts of infected vetch roots were immersed into a dye solution 0.1% naphthol blue black and the root tips cut under the solution. Transpiration was then allowed to proceed for 4-5 hours. Attached tubercles with the corresponding host root part as well as root sections cut at various points (before and after attached tubercles) were sampled. Transverse fresh hand-cut sections of the samples were observed under a light microscope.

Determination of sealed vessels

Samples stained with AGS were used to determine the proportion of vessels filled with different substances. Transverse sections of the haustoria were observed under light microscope, with the host central cylinder centred within the field of view. The central cylinder was divided in four equitable quadrants and the relative position of the haustorium respect these quadrants was recorded. Vessels within quadrants containing the haustorium were considered close to the haustorium, and vessels within quadrants not containing the haustorium were considered away from the haustorium. The number of vessels filled with safranin and alcian green stained substances were recorded, and expressed as a percentage respect to the total number of vessel in each quadrant.

Statistical analysis

Assays were performed with ten replicates per treatment with a completely randomized design. Statistical analysis (ANOVA) was performed with SPSS 10.0 and Statistix 8.0 for Windows. Percentages were transformed according to the formula $Y = \arcsin(\sqrt{X\%/100})$.

A minimum of ten samples from a pull collected from ten replicates were used for each cytochemical assay

Results

The highest proportion of necrotic tubercles was found on the resistant genotype (Table 1). The percentage of necrotic tubercles increased with time in both resistant and susceptible genotypes, but at a much higher rate in the resistant one.

Table 1. *Proportion of O. crenata necrotic tubercles (incompatible interactions) after their establishment on susceptible and resistant vetches.*

Genotype	**Necrotic tubercles (%)**		
	35 d.a.i.	**40 d.a.i.**	**45 d.a.i.**
V. sativa V27 (Susceptible)	8.0 (0.21±0.06)	15.9 (0.33±0.08)	27.6 (0.48±0.09)
V. sativa A01 (Resistant)	13,8 (0.31±0.09)	51,4 (0.80±0.14)	61,5 (0.95±0.17)

Data are expressed as a percentage of the total number of established tubercles. d.a.i., days after inoculation. Log-transformed data with SE shown in parentheses alongside back-transformed means.

Vessels of susceptible roots in a compatible interaction contained no mucilage, but in some cases the presence of safranin-staining substance could be detected at a low proportion (Fig. 1). During an incompatible interaction there was a higher percentage of vessels filled with substances in resistant vetch than in susceptible vetch. Within an incompatible interaction more than half of the vessels near the haustorium were filled with the safranin-staining substance in the resistant genotype. There was a higher proportion of vessels filled with mucilage opposite than next to the haustorium in resistant vetch.

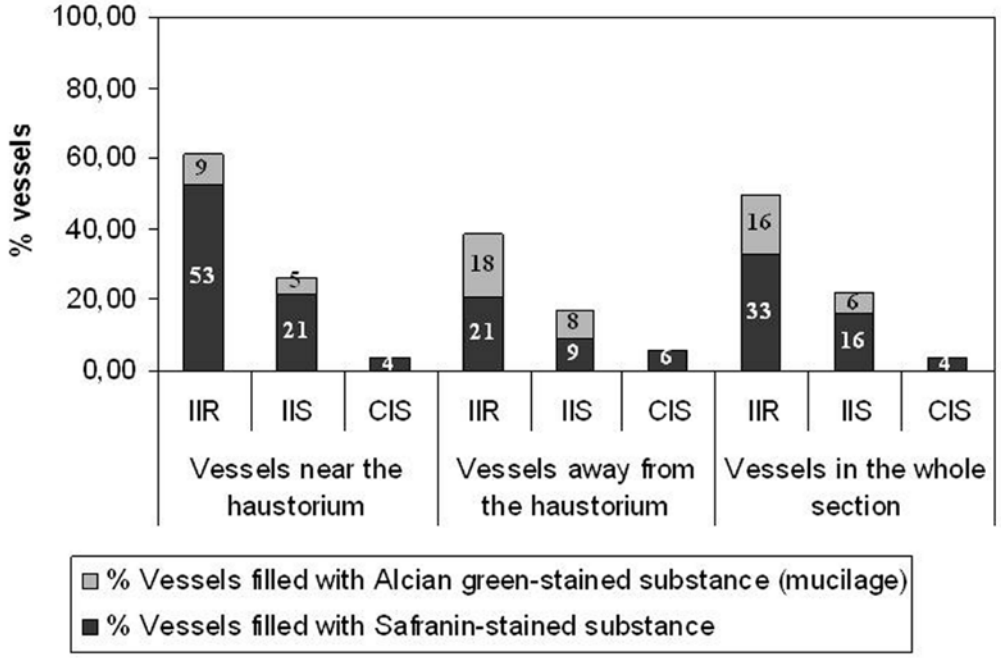

Fig. 1. *Proportion of vessels filled with mucilage and other substances depending on the interaction between host and parasite: IIR, incompatible interaction on resistant host; IIS, incompatible interaction on susceptible host; CIS, compatible interaction on susceptible host. Samples collected 45 days after inoculation were used.*

Table 2 shows the reactions of different tissues to the histochemical tests in incompatible interactions in resistant vetch. Carbohydrates, including carboxylated polysaccharides and pectins, were detected using alcian green, TBO and ruthenium red dyes mainly in the apoplast (Fig. 2A-C).

Table 2. *Reaction of tissues to different cytochemical assays in an incompatible interaction in resistant vetch.*

Cytochemical assays	Specificity	Colour[a]	Vessels			Parenchyma			Fibers			Endodermis			Mucilages	Interface host-parasite
			ml[b]	w	l	ml	w	p	ml	w	p	ml	w	p		
AGS stain	Carbohydrates	Blue – green (B)	+	-	+	+	-	-	+	-	-	-	-	-	+	-
	Lignin, suberin, cutin, tannins, lipids	Red (B)	+	+	+	+	-	-	+	+	+	+	-	-	-	+
TBO stain	Polyphenols	Green – blue, turquoise (B)	+	+	+	+	+	-	+	+	+	-	+	-	+	+
	Carboxylated polysaccharides	Pink (B)	+	-	+	+	-	-	-	+	-	-	-	-	+	-
Phloroglucinol – HCl stain	Lignin, suberin, polyphenols	Red (B)	+	+	+	+	-	-	+	+	+	+	+	-	+	+
	Suberin	Blue – white (F)	-	-	-	-	-	-	-	-	-	-	+	-	-	-
Aniline blue fluorochrome	Callose	Blue – white (F)	+	+	-	+	+	+	-	-	-	-	-	-	-	+
Ruthenium red stain	Non – esterified pectins	Pink (B)	+	-	+	+	+	-	+	-	+	+	-	-	+	+

The presence of staining in the tissue is indicated by (+) and the absence by (-). Samples collected 45 days after inoculation were used

[a] Observed under brightfield (B) or epi-fuorescence (F)

[b] ml: middle lamellae; w: cell wall; l: lumen; p: protoplasma

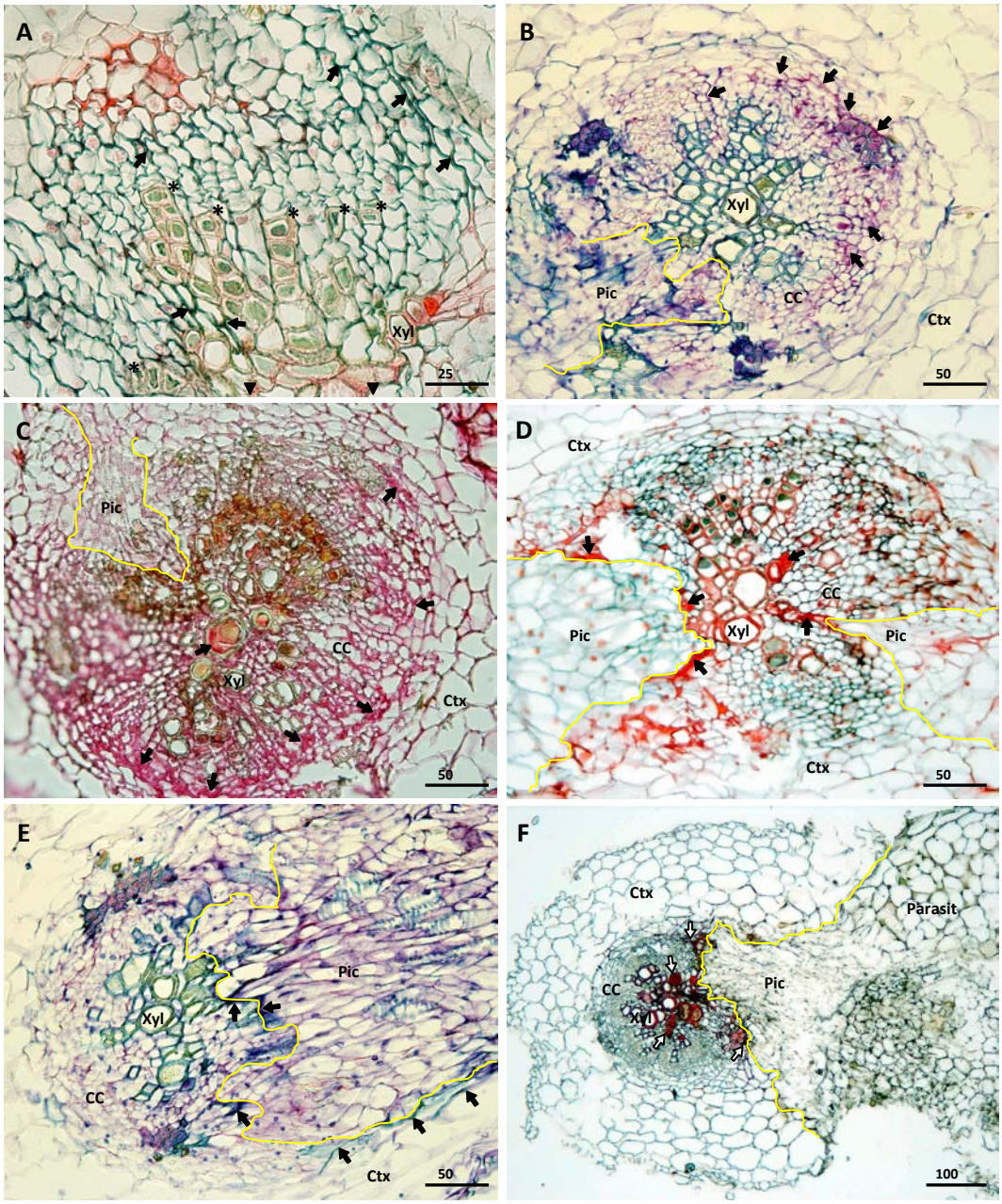

Fig. 2. *Cross sections of incompatible interactions of Orobanche crenata on resistant vetch (Vicia sativa line A01) stained following different procedures. (A) AGS staining showing accumulation of carbohydrates (arrows, green colour) in the apoplast of areas opposite the haustorium. Neighbouring xylem vessels filled with mucilage can also be observed (asterisks). Arrowheads indicate the direction where the haustorium was located. (B) Idem as (A) with TBO staining showing accumulation of carboxylated polysaccharides (arrows, pink colour) in parenchymatic cells. (C) Idem as (A) with ruthenium red staining indicating presence of non-esterified pectins (arrows, pink colour). (D) AGS staining showing areas and vessels dyed with safranin next to the haustorium (arrows, red colour). (E) TBO staining indicating presence of polyphenols and lignins (arrows, blue-turquoise colour). (F) Idem as (E) with phloroglucinol-HCl staining showing lignins and polyphenols (arrows, red colour). Yellow lines delimit parasite from host tissues. CC, central cylinder; Ctx, cortex; Pic, parasite intrusive cells (haustorium); Xyl, xylem vessel.*

A more intense staining for carbohydrates was detected in zones opposite the haustorium of necrotic tubercles than that of healthy tubercles. An intense staining for polyphenols and lignins with AGS, TBO and phloroglucinol was seen in zones next to the haustorium of necrotic tubercles (Fig. 2D-F). The staining appeared also in the apoplast and in the interface between host and parasite. Lignification of host cell walls in contact with parasite tissues was observed at different points and on consecutive sections. These lignified walls formed a ring surrounding the parasite intruding tissues and corresponded to cells from the host endodermis and/or pericycle. Figure 3 shows a 3D diagram of this phenomenon.

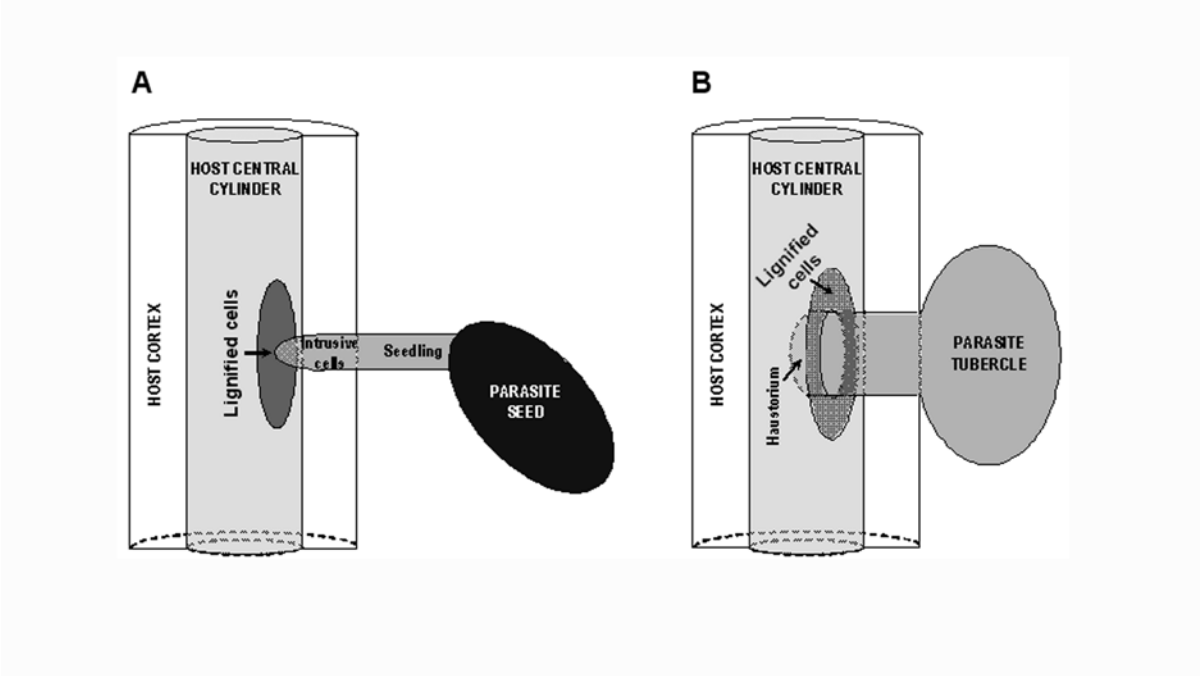

Fig. 3. *Scheme of O. crenata penetration process into a resistant host. (A) The parasite meets a physical barrier (lignified cells) before reaching the host central cylinder. (B) The parasite successfully overcomes the host barrier and penetrates into the central cylinder, but lignified cells still remain surrounding the intruding tissues like a ring.*

The presence of suberin was restricted only to the endodermal cells (Fig. 4A, B), and callose accumulated in some parenchyma cells, in the interface host-parasite and in the middle lamellae and cell wall of some xylem vessels (Fig. 4C-F).

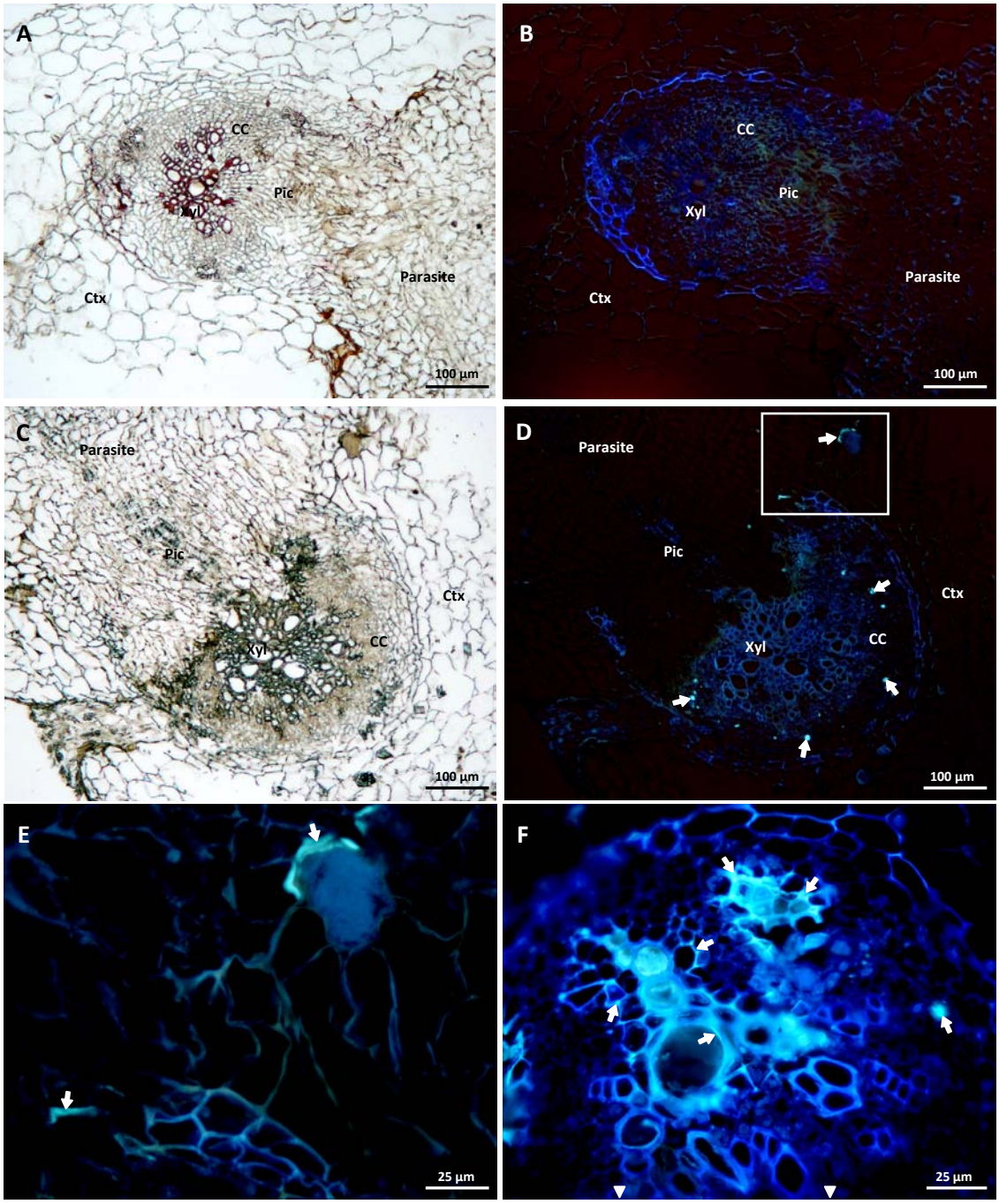

Fig. 4. *Cross sections of incompatible interactions of Orobanche crenata on resistant vetch (Vicia sativa line A01) stained for suberin and callose detection. (A) Section stained with Phloroglucinol-HCl in order to quench lignin autofluorescence. (B) Idem as (A) observed by epi-fluorescence under blue-violet excitation. Suberized cell walls can be observed (blue fluorescence), mainly corresponding to the endodermis. Absence of lignin fluorescence can be observed (for example, xylem vessels). The fluorescence of endodermal cells is disrupted at the point of penetration of the parasite (haustorium). (C) Light micrograph of a section stained for callose detection. (D) Idem as (C) observed by epi-fluorescence under blue-violet excitation. Callose depositions show a blue-white fluorescence (arrows). (E) Detail of (D) showing callose deposition in cortical cell walls in contact with parasite tissues (arrows). (F) Detail of a central cylinder showing callose depositions in xylem walls and parenchyma cells (arrows). Arrowheads indicate the direction where the haustorium was located. CC, central cylinder; Ctx, cortex; Pic, parasite intrusive cells (haustorium); Xyl, xylem vessel.*

Staining consecutive sections with different dyes allowed us to characterise the composition of mucilage and other substances inside the xylem vessels (Fig. 5). Mucilage stained with alcian green from AGS staining, indicates a carbohydrate composition (Fig. 5A, E). This was confirmed by the pink colour after TBO staining, that corresponds to carboxylated polysaccarides (Fig. 5B). The pink/red colour obtained with ruthenium red indicated the presence of non-methyl esterified pectins (Fig. 5C). Presence of polyphenols was also confirmed by blue/turquoise staining with TBO (Fig. 5B) and red staining with phloroglucinol (Fig. 5F) and the absence of lipids, tannins, suberin and lignin because of the negative staining with safranin from AGS (Fig. 5A, E). The mucilage was colourless in non – stained sections, whereas the other substances found inside host vessels showed a natural brownish yellow colouration. This substance stained strongly red with safranin from AGS (Fig. 5A, E), was positive also for ruthenium red (Fig. 5C), phloroglucinol (Fig. 5F), and TBO originated a green staining (Fig. 5B, D). All this indicated the presence of polyphenols, pectins, lignins and probably lipids and/or tannins, but not suberin due to the lack of fluorescence using phloroglucinol staining (Fig. 4B).

Positive staining with ruthenium red showed non – esterfied pectins being also part of these components (Fig. 5C). Contrary to the homogeneous aspect showed by the mucilage, this substance presented a heterogeneous aspect and a granular structure (Fig. 5D).

In order to confirm that the mucilage was mainly composed of non-methyl esterified pectins, immunostaining was performed with antibodies JIM 5 and JIM 7. An intense staining was observed in the core of the haustorium and adjacent areas for non-esterified pectins (Fig 6A), whereas little presence of esterified pectins was detected (Fig. 6B) and mainly restricted to host cortical cell walls opposite the haustorium. In no case esterified pectins were located inside host vessels (Fig. 6D). Non-esterified pectins were located in the apoplast, between intercellular spaces and inside host xylem vessels (Fig. 6C, E, F), and in vascular parenchyma cells opposite the haustorium (Fig. 6E, F), being this last a confirmation of the important role of these cells in the synthesis and secretion of the mucilage.

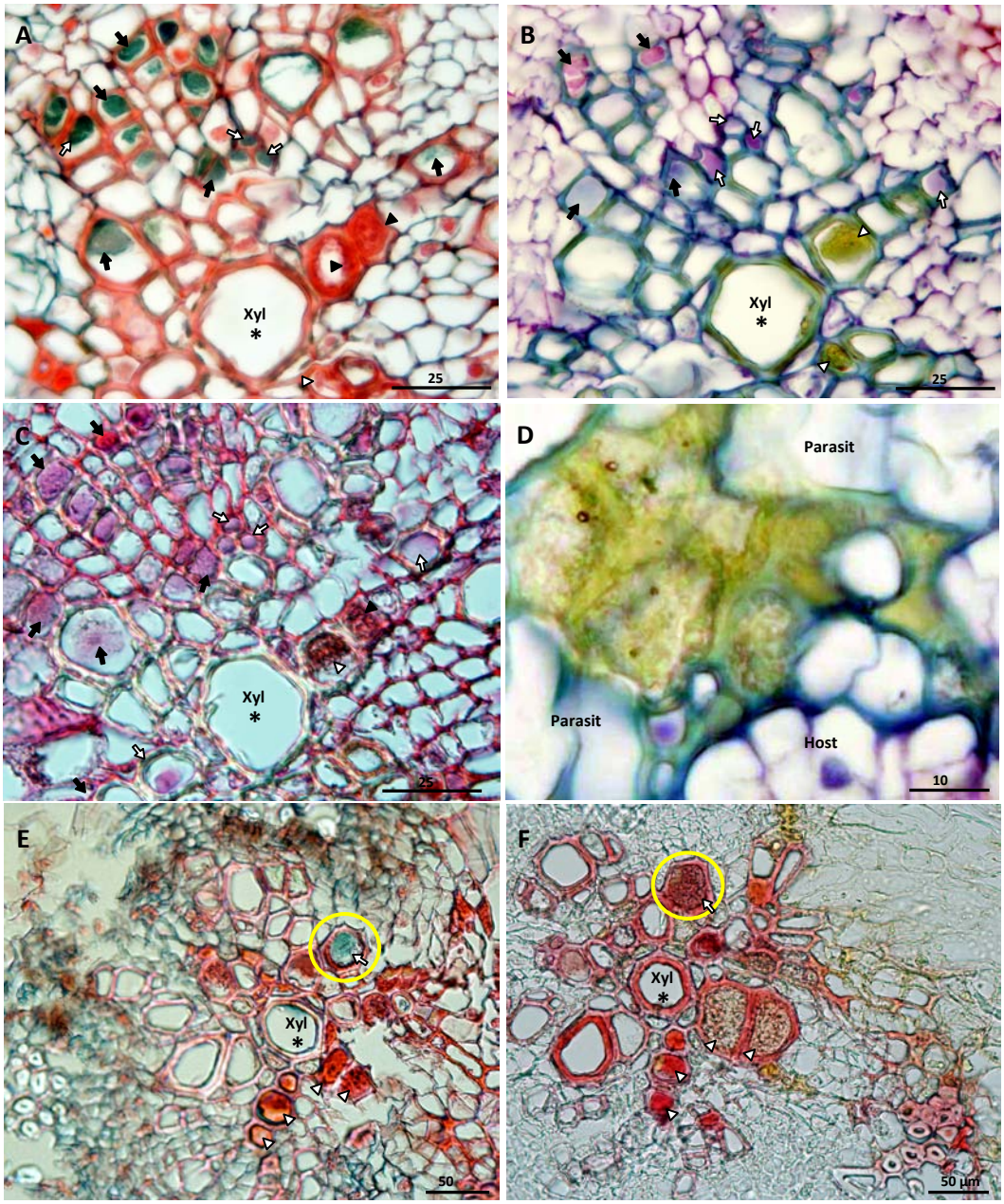

Fig. 5. *Cross sections of incompatible interactions of Orobanche crenata on resistant vetch (Vicia sativa line A01) stained for characterisation of mucilage composition. (A), (B) and (C), sections from the same series stained with AGS, TBO and ruthenium red respectively. Arrows indicate mucilage inside xylem vessels and arrowheads other filling substances. Asterisk indicates sections of the same xylem vessel as a reference. Green colour in (A) corresponds to carbohydrates and red colour with lignin, and/or lipids. Pink colour in (B) corresponds to carboxylated polysaccharides and blue/turquoise with polyphenols. Pink colour in (C) corresponds to non-methyl esterified pectins. (D) Detail of the other substance(s) found inside xylem vessels, in this case located within the interface host-parasite, and stained with TBO. A granular structure and heterogeneous aspect can be observed. (E) and (F), sections from the same series stained with AGS and phloroglucinol-HCl respectively. Arrows indicate mucilage inside xylem vessels and arrowheads other filling substances. A yellow circle indicates the same xylem vessel in both sections. Asterisk indicates sections of the same xylem vessel as a reference. Green colour in (E) corresponds to carbohydrates and red colour with lignin and/or lipids. Red colour in (F) corresponds to lignin and polyphenols. Xyl, xylem vessel.*

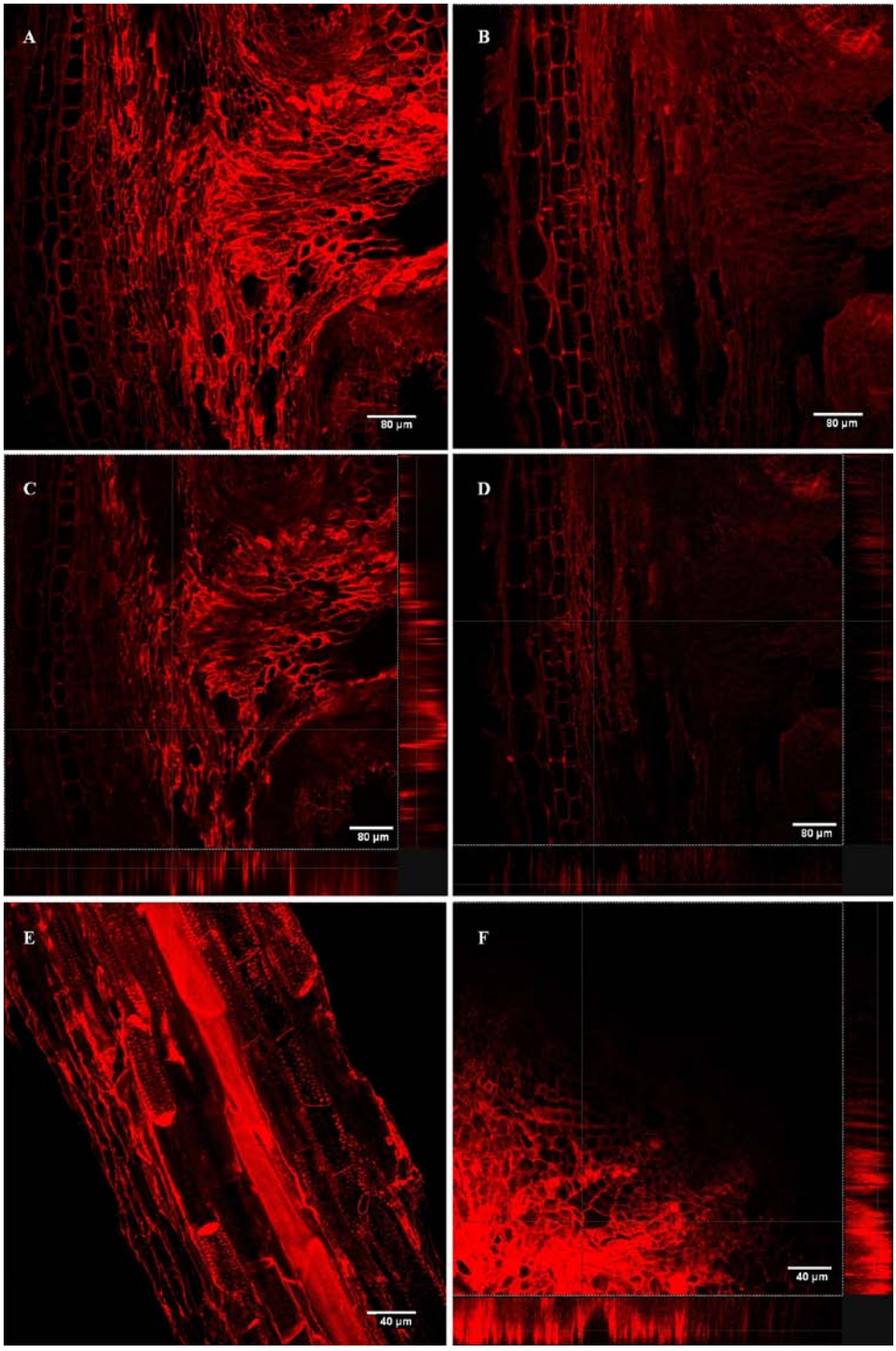

Fig. 6. *Localization of methyl esterified and non-methyl esterified pectins with antibodies JIM 7 and JIM 5 respectively. The images were obtained using confocal microscopy and are full Z-series projections in (A), (B) and (E), and single optical sections with projections on X and Y in (C), (D) and (F). (A) Longitudinal section of the haustorium in an incompatible interaction showing localization of non-methyl esterified pectins. (B) Idem as (A) showing localization of methyl esterified pectins. (C) Single section from (A) with the corresponding projections on X and Y of virtual sections indicated by white lines. (D) Single section from (B) with the corresponding projections on X and Y of virtual sections indicated by white lines. (E) Longitudinal section of an infected resistant vetch root showing localization of non- methyl esterified pectins inside xylem vessels filled with*

mucilage. Accumulation of non-methyl esterified pectins can be observed also within intercellular spaces and cell walls of vascular parenchyma cells (arrows). Red points in the xylem vessels correspond to non-lignified areas from which the mucilage can penetrate into the vessels. Arrowheads indicate the direction where the haustorium was located. (F) Single cross section of an infected resistant vetch root showing localization of non-methyl esterified pectins inside xylem vessels and intercellular spaces and cell walls of vascular parenchyma cells. Projections on X and Y of virtual sections (white lines) of the whole series are shown. Arrowheads indicate the position where the haustorium was located.

When naphthol blue black was applied into the transpiration stream of roots, it was confined to the vascular bundles and stained the areas it was moving through. In compatible interactions, the vessels of the healthy tubercles and the haustorium were stained (Fig. 7A, B). On the contrary, the dye did not reach the necrotic tubercles of incompatible interactions either the haustorium or nearby host vascular tissues, but reached host vessels opposite and away the haustorium (Fig. 7C, D).

Fig. 7. *Presence of naphthol blue black dye tracer within host and parasite tissues in compatible and incompatible interactions. (A) Compatible interaction on susceptible vetch showing the dye blue colouration of vascular tissues along the root. (B) Hand section of a well developed O. crenata tubercle on susceptible vetch showing the dye blue colouration of the vascular tissues. (C) Incompatible interaction on resistant vetch showing the localization of dye blue colouration only before the point of attachment by the tubercle. (D) Hand section of a necrotic O. crenata tubercle on resistant vetch showing sealed vessels and absence of the dye inside parasite vessels.*

Discussion

Xylem occlusion as a putative defensive response against parasitic plants has been reported previously (Labrousse *et al*., 2001; Zehhar *et al*., 2003; Pérez-de-Luque *et al*., 2005b). However no detailed studies about this phenomenon had been undertaken. The results presented here suggest that it is a quantitative trait, expressed against *O. crenata* at higher intensity within resistant than within susceptible vetch genotypes. The response is quantitative not only in the amount of incompatible infection units (Table 1), but also in the amount of mucilage accumulating inside vessels within incompatible interactions (Fig. 1).

The mucilage is presumably produced by vascular parechyma cells near xylem vessels, as indicated by the more intense staining for carbohydrates observed in resistant plants (Fig. 2A), the immunostaining for non-esterified pectins with JIM 5 (Fig. 6E, F) and by the presence of a higher proportion of vessels away from the haustorium filled with mucilage (Fig 1). This is in agreement with previous reports about mucilage production and secretion (Shi *et al*., 1992; Baayen *et al*., 1996; Dong *et al*., 1997; Rioux *et al*., 1998; Crews *et al*., 2003). Despite Vander Molen *et al*. (1983) suggested that occlusion gels congeal in host vessels after dissolution of carbohydrates from host cell walls by pathogen enzymes, we have not found evidences of this. However, the safranin-staining substance accumulated in vessels near the haustorium is probably composed, partially at least, by host cells components released by *O. crenata* enzymatic activity.

The main components of the mucilage seem to be carbohydrates, specifically non-methyl esterified pectins, and polyphenols to a lesser extent. This composition confers good properties to the gel in order to act as a permanent seal: the mixture can be polymerised by peroxidases to form a stable adhesive (Crews *et al*., 2003). This idea is supported by the accumulation of peroxidase in vessels of rice challenged by a vascular pathogen reported by Young *et al*. (1995) and the increased levels of peroxidase activity found by Pérez-de-Luque *et al*. (2005a) in resistant peas to *O. crenata* showing this kind of incompatible reaction (i.e. necrotic tubercles and mucilage production). Being the composition similar to that described for mucilage produced against other vascular pathogens (Shi *et al*., 1992; Baayen *et al*., 1996; Kpémoua *et al*., 1996; Dong *et al*., 1997; Rioux *et al*., 1998; Tagne *et al*., 2002) we assume that this is the same response found in those other pathogenic systems.

The question arising is why this defensive mechanism is activated if the parasite does not invade host vessels in the same way as a vascular pathogen (i.e. fungi or bacteria spread along xylem lumen). A first hypothesis could be that the host recognises a wound in the tissues when the parasite penetrates, and the mucilage production is activated as reported by

Crews *et al*. (2003). However, the mucilage production would be observed also in susceptible plants during compatible interactions, and that is not the case (Fig. 1). Thus, to find out a more satisfactory answer, we paid attention to the safranin staining substance accumulating in vessels near the haustorium. As previously stated (Pérez-de-Luque *et al*., 2005b) and confirmed by the present results (Table 1), this substance always accumulates in areas near the core of the haustorium and a similar substance was found at the attachment area of *O. crenata* seedlings and surrounding parasite intrusive tissues (Pérez-de-Luque *et al*., 2005b). This substance seems to be, at least partially, parasite originated, because it also appears only on the external parasite interface near the attachment and penetration point (Pérez-de-Luque *et al*., 2005b). The role of this substance seems to be an anchoring device for the parasite in order to penetrate host tissues by mechanical pressure (Joel *et al*., 1996). Lipids probably take part in the composition of this secretion just as non-methyl esterified pectins (Fig. 5A, C and 6A, C), conferring the adhesive properties. But the parasite also releases enzymes to allow penetration between host cells (Singh *and* Singh, 1993; Antonova *and* Ter Borg, 1996; Losner-Goshen *et al*., 1998). These enzymes dissolve components from the host cell walls and middle lamellae, such as pectins, polyphenols and lignins, which will became part of the secretion, as suggested by the staining with AGS, ruthenium red, phloroglucinol and TBO (Fig 5). In fact, the secretion can be considered as a pull of different substances and components, including enzymes, originated mainly from the parasite, but also from the host. This could explain the heterogeneous aspect and granular structure it presents (Fig 5D). When the parasite is hampered during the penetration attempts, it releases a higher amount of secretions (i.e. enzymes and adhesives) to overcome the host resistance (Joel *et al*., 1996; Pérez-de-Luque *et al*., 2005b). The presence of a ring of lignified host cells surrounding the parasite intruding tissues probably corresponds to a previous barrier to penetration broken by the parasite (Fig. 3). If the parasite is successful and establishes vascular connections with the host, the excess of secretions and dissolved cell wall components leak through the apoplast and reaches the neighbouring host vessels (Pérez-de-Luque *et al*., 2005b). At this time, the presence of foreign substances inside host vessels may activate the production and accumulation of mucilage. Also the degraded products from host cell walls, as carbohydrates, can act as endogenous elicitors of defence responses (Aldington *and* Fry, 1993; Moerschbacher *et al*., 1999). Finally, accumulation of mucilage, secretions and degraded products block host vessels and does not allow nutrient flux between host and parasite (Fig. 7), causing further parasite death.

In conclusion, mucilage production can be considered as a quantitative defensive reaction taking place against *O. crenata* in vetch, and probably also in other legumes (Pérez-de-Luque *et al*., 2005b) and plants (Labrousse *et al*., 2001; Zehhar *et al*., 2003). It seems to be activated by the presence of foreign substances (i.e. parasite secretions) and host degraded products (i.e. carbohydrates from cell walls) inside host vessels, and leads to obstruction of parasite supply channel and further death of established *Orobanche* tubercles.

Acknowledgements

We thank to Ana Moral for her help in the realisation of this work and the Confocal Microscopy Service of the CIB-CSIC (Madrid) where observations were made.

A P-d-L was a visiting researcher at the Plant Development group at the CSIC-Madrid funded by the Consejería de Innovación, Ciencia y Empresa de la Junta de Andalucía. P G-M is a researcher at the CSIC funded by the programme "Ramón y Cajal" of the Spanish Ministry of Education and Science.

JIM 5 and JIM 7 antibodies were kindly supplied by Professor Keith Roberts from John Innes Centre in Norwich (UK).

This research was supported by the projects AGL2002-03248 and BOS2002-03550.

References

Aldington S and Fry SC. 1993. Oligosaccharins. *Advances in Botanical Research* **19:** 1-101.

Antonova TS and Ter Borg SJ. 1996. The role of peroxidase in the resistance of sunflower against *Orobanche cumana* in Russia. *Weed Research* **36:** 113-121.

Baayen RP, Ouellette GB, Rioux D. 1996. Compartmentalization of decay in carnations resistant to *Fusarium oxysporum* f. sp. dianthi. *Phytopathology* **86:** 1018-1031.

Beckman CH. 2000. Phenolic-storing cells: keys to programmed cell death and periderm formation in wilt disease resistance and in general defence responses in plants? *Physiological and Molecular Plant Pathology* **57:** 101-110.

Beckman CH and Zaroogian GE. 1967. Origin and composition of vascular gel in infected banana roots. *Phytopathology* **57:** 11-13.

Bordallo JJ, Lopez-Llorca LV, Jansson HB, Salinas J, Persmark L, Asensio L. 2002. Colonization of plant roots by egg-parasitic and nematode-trapping fungi. *New Phytologist* **154:** 491-499.

Cubero JI. 1994. Breeding work in Spain for *Orobanche* resistance in faba bean and sunflower. In: Pieterse AH, Verkleij JAC, ter Borg SJ, eds. *Biology and management of Orobanche, Proceedings of the Third International Workshop on Orobanche and related Striga research*. Amsterdam: Royal Tropical Institute, 465-473.

Crews LJ, McCully ME, Canny MJ. 2003. Mucilage production by wounded xylem tissue of maize roots - time course and stimulus. *Functional Plant Biology* **30:** 755-766.

Dong Z, McCully ME, Canny MJ. 1997. Does *Acetobacter diazotrophicus* live and move in the xylem of sugarcane stems? Anatomical and physiological data. *Annals of Botany* **80:** 147-158.

Dörr I, Staack A, Kollmann R. 1994. Resistance of *Hellianthus* to *Orobanche* - histological and cytological studies. In: Pieterse AH, Verkleij JAC, eds. *Biology and management of Orobanche, Proceedings of the Third International Workshop on Orobanche and related Striga Research*. Amsterdam: Royal Tropical Institute, 276-289.

Hoagland DR and Arnon DI. 1950. The water-culture method for growing plants without soil. *California Agricultural Experiment Station Circular* 347. University of California, Berkeley, USA.

Jacobsen KR, Fisher DG, Maretzki A, Moore PH. 1992. Developmental changes in the anatomy of the sugarcane stem in relation to phloem unloading and sucrose storage. *Botanical Acta* **105:** 70-80.

Joel DM. 1983. AGS (Alcian Green Safranin) - A simple differential staining of plant material for the light microscope. *Proceedings RMS* **18:** 149-151.

Joel DM, Losner-Goshen D, Hershenhorn J, Goldwasser Y, Assayag M. 1996. The haustorium and its development in compatible and resistant host. In: Moreno MT, Cubero JI, Berner D, Joel DM, Musselman LJ, Parker C, eds. *Advances in parasitic plant research*. Córdoba: Junta de Andalucía, Consejería de Agricultura y Pesca, 531-541.

Kpemoua K, Boher B, Nicole M, Calatayud P, Geiger JP. 1996. Cytochemistry of defense responses in cassava infected by *Xanthomonas campestris* pv. manihotis. *Canadian Journal of Microbiology* **42:** 1131-1143.

Labrousse P, Arnaud MC, Serieys H, Bervillé A, Thalouarn P. 2001. Several Mechanisms are involved in resistance of *Helianthus* to *Orobanche cumana* Wallr. *Annals of Botany* **88:** 859-868.

Linke K-H, Joel DM, Kroschel J. 2001. Observations of the underground development. Polybag system. In: Kroschel J, ed. *A technical manual for parasitic weed research and extension*. Dordrecht: Kluwer Academic Publishers, 56-58.

Losner-Goshen D, Portnoy VH, Mayer AM, Joel DM. 1998. Pectolytic activity by the haustorium of the parasitic plant *Orobanche* L. (Orobanchaceae) in host roots. *Annals of Botany* **81:** 319-326.

Mellersh DG, Foulds IV, Higgins VJ, Heath MC. 2002. H_2O_2 plays different roles in determining penetration failure in three diverse plant-fungal interactions. *The Plant Journal* **29:** 257-268.

Moerschbacher BM, Mierau M, Graeβner B, Noll U, Mort AJ. 1999. Small oligomers of galacturonic acid are endogenous suppressors of disease resistance reactions in wheat leaves. *Journal of Experimental Botany* **50:** 605-612.

Pérez-de-Luque A, Jorrín J, Cubero JI, Rubiales D. 2005a. Resistance and avoidance against *Orobanche crenata* in pea (*Pisum* spp.) operate at different developmental stages of the parasite. *Weed Research* **45:** 379-387.

Pérez-de-Luque A, Rubiales D, Cubero JI, Press MC, Scholes J, Yoneyama K, Takeuchi Y, Plakhine D, Joel DM. 2005b. Interaction between *Orobanche crenata* and its host legumes: Unsuccessful haustorial penetration and necrosis of the developing parasite. *Annals of Botany* **95:** 935-942.

Rioux D, Nicole M, Simard M, Ouellette GB. 1998. Immunocytochemical evidence that secretion of pectin occurs during gel (gum) and tylosis formation in trees. *Phytopathology* **88:** 494-505.

Rubiales D, Alcántara C, Sillero JC. 2004. Variation in resistance to crenate broomrape (*Orobanche crenata*) in species of *Cicer*. *Weed Research* **44:** 27-32.

Rubiales D, Pérez-de-Luque A, Cubero JI, Sillero JC. 2003a. Crenate broomrape (*Orobanche crenata*) infection in field pea cultivars. *Crop Protection* **22:** 865-872.

Rubiales D, Pérez-de-Luque A, Joel DM, Alcántara C, Sillero JC. 2003b. Characterization of resistance in chickpea to crenate broomrape (*Orobanche crenata*). *Weed Science* **51:** 702-707.

Rubiales D, Pérez-de-Luque A, Sillero JC, Román B, Kharrat M, Khalil S, Joel DM, Riches C. 2005b. Screening techniques and sources of resistance against parasitic weeds in grain legumes. *Euphytica* **144:** in press.

Ruzin SE. 1999. Plant microtechnique and microscopy. 1st ed. New York: Oxford University Press.

Shi J, Mueller WC, Beckman CH. 1992. Vessel occlusion and secretory activities of vessel contact cells in resistant or susceptible cotton plants infected with *Fusarium oxysporum* f. sp. vasinfectum. *Physiological and Molecular Plant Pathology* **40:** 133-147.

Singh A and Singh M. 1993. Cell wall degrading enzymes in *Orobanche aegyptiaca* and its host *Brassica campestris*. *Physiologia Plantarum* **89:** 177-181.

Tagne A, Neergaard E, Hansen HJ, The C. 2002. Studies of host-pathogen interaction between maize and *Acremonium strictum* from Cameroon. *European Journal of Plant Pathology* **108:** 93-102.

Vallet C, Chabbert B, Czaninski Y, Monties B. 1996. Histochemistry of lignin deposition during sclerenchyma differentiation in alfalfa stems. *Annals of Botany* **78:** 625-632.

VanderMolen GE, Labavitch JM, Strand LL, DeVay JE. 1983. Pathogen-induced vascular gels: Ethylene as a host intermediate. *Physiologia Plantarum* **59:** 573-580.

Young SA, Guo A, Guikema JA, White FF, Leach JE. 1995. Rice cationic peroxidase accumulates in xylem vessels during incompatible interactions with *Xanthomonas oryzae* pv oryzae. *Plant Physiology* **107:** 1333-1341.

Zehhar N, Labrousse P, Arnaud MC, Boulet C, Bouya D, Fer A. 2003. Study of resistance to *Orobanche ramosa* in host (oilseed rape and carrot) and non-host (maize) plants. *European Journal of Plant Pathology* **109:** 75-82.

CAPÍTULO II: "Que los árboles no te impidan ver el bosque"

Resistance to broomrape (*Orobanche crenata*) in faba bean (*Vicia faba*): cell wall changes associated with pre-haustorial defensive mechanisms

Annals of Applied Biology (2007) 151: 89-98

Alejandro Pérez-de-Luque[1], María-Dolores Lozano[2], María-Teresa Moreno[1], Pilar S. Testillano[3] and Diego Rubiales[2]

[1] *IFAPA-CICE (Junta de Andalucía), CIFA "Alameda del Obispo", Área de Mejora y Biotecnología, Apdo. 3092, E-14080 Córdoba, Spain.*

[2] *CSIC, Instituto de Agricultura Sostenible, E-14080 Córdoba, Apdo. 4084, Spain*

[3] *CSIC, Centro de Investigaciones Biológicas, Dep. Plant Development and Nuclear Organization, Ramiro de Maeztu 9, E-28040 Madrid, Spain*

Abstract

Broomrapes (*Orobanche* spp.) are parasitic angiosperms which attach to the roots of the hosts in order to take water and nutrients from them. No complete control measures are available to date, but breeding for resistance remains as one of the most feasible and environmental friendly methods. However, the mechanisms governing the interaction between these parasites and the host are yet not well understood. We studied the cellular changes associated with the resistance to *O. crenata* in faba bean as mechanisms involved or responsible for resistance. Two cultivars of faba bean, resistant and susceptible to *O. crenata* infection, were used. The evolution of the infection and the changes in the cell and tissue organization and wall components of the host cells were followed and evaluated in both genotypes. Samples of compatible and incompatible interactions were fixed and sectioned, and specific cytochemical methods for different cell components were applied, results being analyzed under light and epifluorecence microscopy. A higher proportion of *O. crenata* seedlings unable to penetrate the root was found on the resistant genotype. Reinforcement of cell walls by callose deposition hampers parasite penetration through the cortex. Lignification of endodermal cells prevents further penetration of the parasite into the central cylinder.

Introduction

The existence of parasitic plants attacking crops is known from ancient times (Cubero *and* Moreno, 1996). This is particularly true for the broomrapes (*Orobanche* spp.), which are obligate root holoparasites. Devoid of chlorophyll, they totally depend on the hosts for the supply of carbon, nitrogen and inorganic solutes, which they obtain through a specialised structure (haustorium) connected to the vascular system of their host plants. This haustorium is formed after the parasite has germinated in the presence of stimulants from the host root, developed a seedling, attached to the host root and penetrated into the central cylinder (Parker *and* Riches, 1993; Press *and* Graves, 1995). Following vascular connection with the host, the parasite develops a tubercle that later on will originate an apex which will evolve into a flowering stem.

O. crenata (crenate broomrape) is an important pest in legumes, affecting mainly faba bean (*Vicia faba*), pea (*Pisum sativum*), lentil (*Lens culinaris*), vetches (*Vicia* spp.), grass and chickling pea (*Lathyrus sativus* and *L. cicera*) and other grain and forage legumes in the Mediterranean basin and Middle East (Rubiales *et al*., 2006). Despite several methods having been developed in order to control these parasites, including mechanical, biological and chemical practices (Parker *and* Riches, 1993; Jurado-Expósito *et al*., 1996, 1997; Joel 2000; Rubiales *et al*., 2003*a*; Eizenberg *et al*., 2004; Pérez-de-Luque *et al*., 2004*a*, *b*), breeding for resistance remains as the most economic, feasible and environmental friendly method of control. However, resistance to *Orobanche* in legumes is a complex multicomponent event, difficult to access, scarce and of low heritability (Cubero *and* Hernández, 1991; Cubero, 1994; Cubero *and* Moreno, 1999), which makes breeding for resistance a difficult task. Hence, a detailed knowledge of the mechanisms underlying such resistance is necessary to improve breeding programs and help breeders to identify new sources of resistance when turning to wild relatives.

Resistance to *Orobanche* spp. has been reported in different crops including sunflower (*Helianthus annuus*) (Labrousse *et al*., 2001) and legumes (Rubiales *et al*., 2003*a*, *b*; Rubiales *et al*., 2004; Pérez-de-Luque *et al*., 2005*a*), but little is known about the basis of host resistance to these parasites (Joel *et al*., 1996; Pérez-de-Luque *et al*., 2005*b*). It is tempting to compare infection by parasitic plants with infection by fungi, but despite analogies being present, there are also many differences (Mayer, 2006). Studying resistance against parasitic plants presents some handicaps compared with other pathosystems, as parasite and host are

relatively close organisms that share many morphological, physiological and biochemical traits. And the question becomes more complicated because the interaction implies two plants which merge their tissues. At this point, cytological and cytochemical studies are powerful tools to unveil the mechanisms underlying the plant-parasitic plant interaction. These methodologies have been applied recently with success to studying the interactions *O. crenata*-pea (Pérez-de-Luque *et al*., 2005*b*, 2006*a*), *O. crenata*-vetch (Pérez-de-Luque *et al*., 2005*b*, 2006*b*) and *O. cumana*-sunflower (Echevarría-Zomeño *et al*., 2006).

The aim of the present work was to analyse, for the first time, the changes in cell and tissue organization and components accompanying the resistant response, as defence mechanisms implicated in the resistance of faba bean against *O. crenata,* specifically those which hamper parasite penetration into the host root and do not allow formation of the endophyte (haustorium) and connection with the vascular tissues.

Material and Methods

Plant material and growth conditions

Orobanche crenata was grown on resistant and susceptible cultivars of faba bean (*Vicia faba*, Baraca and Prothabon respectively). The glass rhizotron system described by Rubiales *et al*. (2006) was used. It involves growing host and parasite in sand and vermiculite (3:1) held in the gap between two glass sheets (Fig. 1). Two cork strips of 0.5 cm thickness are placed between both glasses in left and right sides, and the lower side is sealed with a porous material (foam rubber) that allows nutrient solution to penetrate. A strip (11×12 cm) of glass fiber paper (Whatmann GF/A) with disinfected *O. crenata* seeds (40 mg) spread on it was inserted in the upper part of the plate, on the sand. Faba bean seedlings, with a root length of about 5-6 cm, were placed on the paper in the upper side of the plates. Plates were placed vertically and irrigated with Hoagland nutrient solution (Hoagland *and* Arnon, 1950). The plants were grown in a controlled environment chamber with a day/night temperature of 20^0C ± 0.5^0C, a 14h photoperiod and an irradiance of 200 µmol m^{-2} s^{-1}.

O. crenata seed germination was evaluated 20 days after transplantation, by using a binocular microscope (Nikon SMZ1000; Nikon Europe B.V., Badhoevedorp, The Netherlands). Five hundred seeds located close (<3 mm) to the faba bean root were observed, and the number of those germinated counted and expressed as percentage of the total. Seeds

were considered to be germinated when the germ tube was at least 0.1 mm long. At 25 days after transplanting, the number of *O. crenata* seedlings touching faba bean roots was counted. Those that became necrotic or caused a darkening of the host at the point of contact, were expressed as a percentage of the total number of successfully attached seedlings.

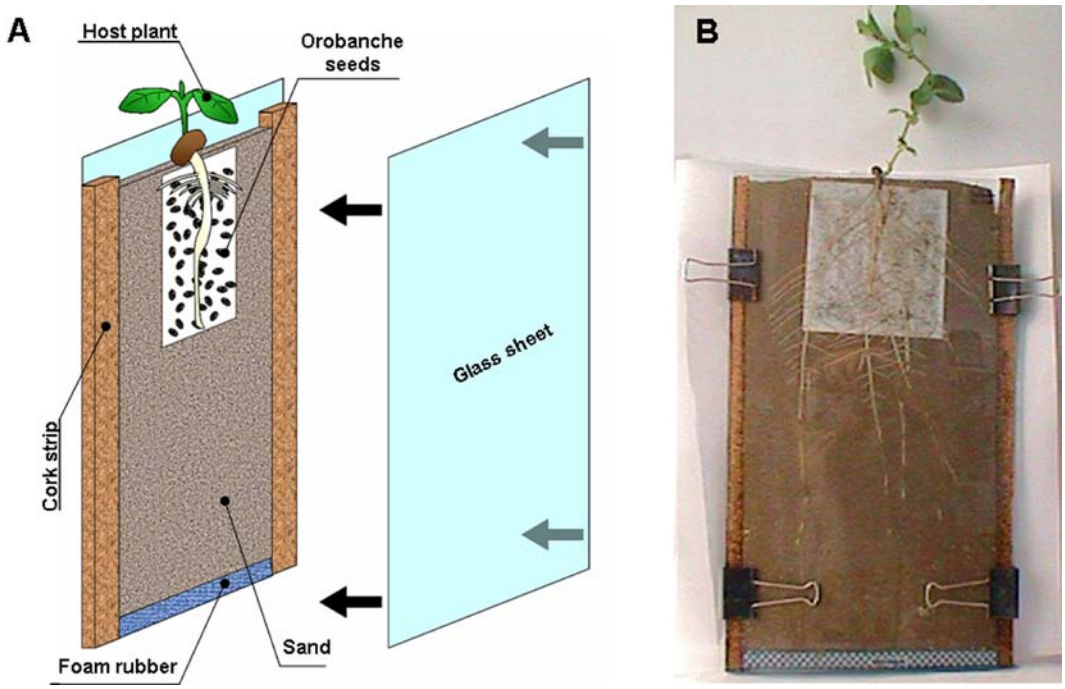

Fig. 1 *Glass rhizotron system for inoculation of faba bean with Orobanche crenata. (a) Schematic representation of the system. (b) General view of the system.*

Faba bean root length and *O. crenata* tubercle formation were evaluated 40 days after transplanting. Root length was estimated according to Tennant (1975). Tubercles were counted and classified according to their developmental stage (Ter Borg *et al*., 1994): S1, tubercles <2 mm; S2, tubercles >2mm but without root formation; S3, tubercles with crown root; S4, sprout already visible remaining underground; S5, shoot emergence; S6, flowering; S7, setting of seeds. Values were expressed as total number of tubercles per plant, number of tubercles per centimetre of host root length, and number and percentage of tubercles at S1-S4 developmental stage. The percentage of germinated seeds that established a tubercle was also estimated.

Collection and processing of samples for cytochemistry

At 25 days after transplanting, seedlings of *O. crenata* were sampled at random with the corresponding attached parts of host roots. The sampled material was fixed either in FAA (ethanol 50%+formaldehyde 5%+glacial acetic acid 10%, in water) for 48 h or Karnovsky (paraformaldehyde 4%+glutaraldehyde 5%, in 0.025M cacodilate buffer) for 4 h.

FAA-fixed samples were then dehydrated in an ethanol series (50, 80, 95, 100, 100%: 12 h each) and transferred to an embedding solvent (xylene; Panreac Quimica S.A., Montcada i Reixac, Spain) through a xylene-ethanol series (30, 50, 80, 100, 100%: 12 h each) and finally saturated with paraffin (Paraplast Xtra; Sigma, St. Louis, USA). Sections (7 μm) were cut with a rotary microtome (Nahita 534; Auxilab S.A., Beriain, Spain) and attached to adhesive-treated microscope slides (polysine slides; Menzel GmbH & Co KG, Braunschweig, Germany).

Karnovsky-fixed samples were dehydrated in an acetone series and embedded in an acrylic resin, Historesin 8100 (Leica Microsystems Wetzlar GmbH, Wetzlar, Germany). Resin polymerization was performed at 4ºC overnight. Semi-thin sections (2 μm) were cut with a glass knife in an ultratome Pyramitome (LKB, Sweden) and attached to microscope slides.

Cytochemical methods for light and epifluorescence microscopy

After removal of paraffin, FAA-fixed sections were stained with the following dyes: (i) Alcian green - safranin (AGS) (Joel, 1983). The slides were dried and mounted with DePeX (BDH) mounting medium. With this staining method, carbohydrates (including cell walls and mucilage) appeared green, yellow or blue, while lignified, cutinized and suberized walls, as well as tannin and lipid material inside cells appeared red (Joel, 1983). (ii) Phloroglucinol (2% in ethanol)-HCl (35%) (Ruzin, 1999) stains the aldehyde groups of lignin and suberin, but quenches lignin autofluorescence and retains suberin fluorescence (Baayen *et al*., 1996; Rioux *et al*., 1998). (iii) Aniline blue fluorochrome was used for callose detection under UV fluorescence. Samples were stained during 15-30 min in a solution 0.1% aniline blue fluorochrome in water (Bordallo *et al*., 2002).

Semi-thin (2 μm) historesin sections of Karnovsky-fixed samples were stained with 0.05% toluidine blue O (TBO) in phosphate buffer (pH 5.5) during 1 min (Ruzin, 1999). This

method allows detection of phenolics as well as tannins, lignin and suberin (Baayen *et al*., 1996; Bordallo *et al*., 2002; Mellersh *et al*., 2002; Crews *et al*., 2003).

Sections were observed using a light microscope (Leica DM-LB, magnification ×100 to ×400; Leica Microsystems Wetzlar GmbH, Wetzlar, Germany) and photographed using a digital camera (Nikon DXM1200F; Nikon Europe B.V., Badhoevedorp, The Netherlands). Samples were also observed by epi-fluorescence under excitation at 450-490 nm (blue-violet) with the same microscope.

Statistical analysis

Assays were performed with ten replicates per treatment with a completely randomized design. Statistical analysis (ANOVA) was performed with SPSS 10.0 and Statistix 8.0 for Windows. Percentages were transformed according to the formula $Y = \arcsin(\sqrt{(X\%/100)})$.

Results

Resistance against *Orobanche* has been divided into several steps, including induction of parasite germination, penetration/establishment and tubercle development. Resistant plants stop parasite infection and/or development in at least one of these steps. Both cultivars showed no significant differences inducing germination of *O. crenata* seeds (about 45% of germination) (Table 1). The percentage of germinated *O. crenata* seeds developing a tubercle was higher in the susceptible cultivar Prothabon (1.34%) than in the resistant one Baraca (0.04%) (more than 30 times fold). This resulted in 127.0 established tubercles per Prothabon plant whereas only in 3.4 per Baraca plant. No differences were found in the root length of both genotypes, but in order to avoid escape due to low root biomass, the number of established tubercles were referred to the root length. The relation remained between both cultivars, with Prothabon presenting the highest number of established tubercles per cm of root (0.38) compared with Baraca (0.01).

Most of the established tubercles in both cultivars remained in stages 1 and 2 of development at the end of the experiment (Table 2). Only in Prothabon did a significant number (22.1%) develop on the crown root (stage 3) and some (0.3%) also developed at the apex (stage 4).

Table 1 *Orobanche crenata* seed germination and tubercle formation in faba bean[a]

Faba Bean Cultivar	Germination at 0–3 mm from Host Root (%)[b]	Germinated Seeds that Establish a Tubercle (%)[b]	Number of Tubercles per Plant	Host Root Length (cm)	Tubercles per centimetre of Host Root Length
Baraca (resistant)	43.8 ± 2.4 (0.72 ± 0.03)	0.04 ± 0.01 (0.018 ± 0.004)	3.4 ± 0.9	336.7 ± 26.5	0.01 ± 0.00
Prothabon (susceptible)	46.4 ± 3.5 (0.75 ± 0.04)	1.34 ± 0.41 (0.107 ± 0.016)	127.0 ± 26.4	342.9 ± 24.3	0.38 ± 0.08

[a]Values are given as mean ± standard error; d.f. = 9.
[b]Log transformed data with standard error are shown in parentheses alongside back-transformed mean values.

Table 2 Attached *Orobanche crenata* seedlings unable to develop tubercles and developmental stage of already established tubercles[a]

Faba Bean Cultivar	Attached Seedlings Unable to Develop Tubercles (%)[b]	Developmental Stage							
		S1		S2		S3		S4	
		Number of Tubercles	Percentage[b]	Number of Tubercles	Percentage[b]	Number of Tubercles	Percentage[b]	Number of Tubercles	Percentage[b]
Baraca (resistant)	68.5 ± 1.8 (0.98 ± 0.02)	1.29 ± 0.7	37.5 ± 12.6 (0.38 ± 0.18)	1.9 ± 0.5	54.1 ± 15.3 (0.88 ± 0.22)	0.3 ± 0.2	8.4 ± 3.2 (0.12 ± 0.08)	0.0 ± 0.0	0.0 ± 0.0 (0.00 ± 0.00)
Prothabon (susceptible)	39.4 ± 2.3 (0.68 ± 0.02)	28.4 ± 7.7	22.4 ± 1.8 (0.48 ± 0.02)	70.1 ± 17.1	55.2 ± 2.5 (0.81 ± 0.03)	28.0 ± 3.4	22.1 ± 2.5 (0.52 ± 0.03)	0.4 ± 0.2	0.3 ± 0.2 (0.03 ± 0.02)

[a]Values are given as mean ± standard error; d.f. = 9.
[b]Log transformed data with standard error are shown in parentheses alongside back-transformed mean values.

A darkening of the tissues around the attachment and penetration point was observed in some cases (Fig. 2b). The seedlings could not develop further, became dark and did not result in a tubercle. The percentage of these attached *O. crenata* seedlings unable to develop a tubercle was also determined for both genotypes (Table 2), resulting in a higher percentage of aborted penetration attempts in Baraca (68.5%) compared with Prothabon (39.4%).

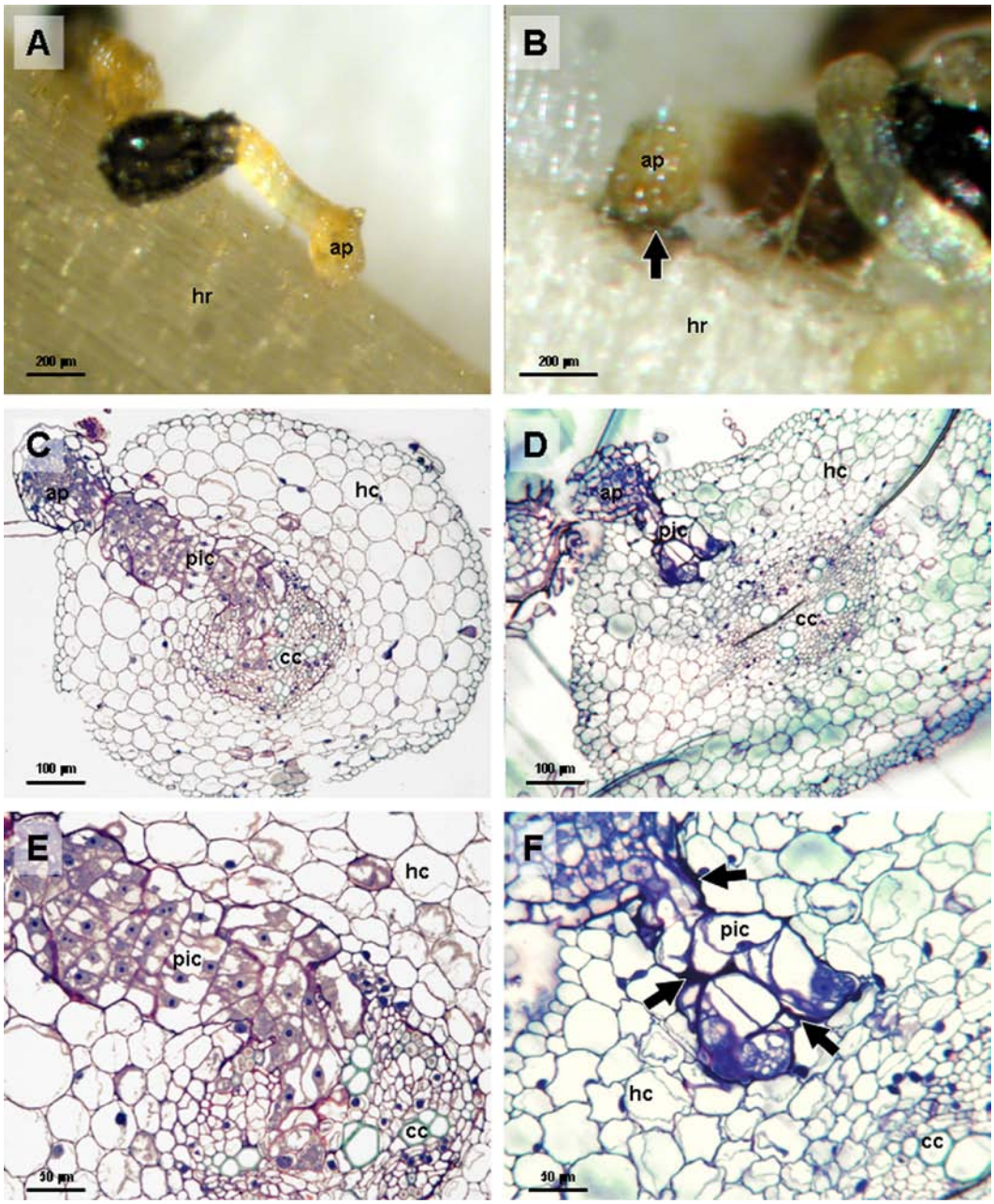

Fig. 2 *Compatible and incompatible reactions of Orobanche crenata in faba bean. (a) Successful attachment and penetration on susceptible faba bean. (b) Incompatible reaction on resistant faba bean. Arrow indicates darkening of host tissues at the attachment point. (c) Cross section of a compatible interaction stained with TBO*

showing penetration of parasite cells through the host tissues. (d) Cross section of an incompatible interaction stained with TBO showing parasite cells halted in the host cortex. (e) Detail of (c) showing how the parasite cells have reached the central cylinder of the host. (f) Detail of (d) showing accumulation of a dark stained deposit around the penetration pathway of the parasite (arrows). hr, host root; ap, parasite appressorium; pic, parasite intrusive cells; hc, host cortex; cc, host central cylinder.

In order to analyze the changes in cell structure and components associated with the mechanisms of resistance behind this reaction, cytochemical analyses were performed. Staining of historesin embeded samples with TBO revealed a different level of penetration of the parasite intrusive cells in susceptible (Fig. 2c, e) and resistant (Fig. 2d, f) cultivars. In root cross sections of Prothabon (susceptible) samples, the parasite cells were observed penetrating throughout the whole root and reaching the central cylinder (Fig. 2c, e). However, in resistant plants of Baraca cultivar, the parasite cells appeared stopped at the cortex (Fig. 2d, f). It seems that the parasite is unable to penetrate into the host central cylinder and appeared to be stopped in both the cortex and/or the endodermis (Fig. 2d, f). Moreover, an accumulation of dark-blue stained substances around the penetration pathway during incompatible interactions was observed (Fig. 2f).

Staining with alcian-green-safranin (AGS) of paraffin embeded samples also revealed that the penetration of the parasite is stopped at the root cortex in resistant plants (Fig. 3a, b). AGS staining makes carbohydrates (including cell walls and mucilage) to appear green, yellow or blue, while lignified, cutinized and suberized walls appear red. In the resistant plant roots, AGS-stained sections showed that the substances around the penetration pathway are of heterogeneous nature. The observation of these sections under epifluorescence microscopy with blue excitation showed no fluorescence emission from the substances or neighbouring host cells and walls (Fig. 3c). Neither observation under polarized light showed any special feature (Fig. 3d).

Accumulation of callose around the penetration pathway of the parasite has been detected using aniline blue fluorochrome (Fig. 4a-d), as a key feature associated with the major mechanism responsible for stopping parasite penetration in the host cortex. As revealed by the aniline blue specific staining, the accumulation of callose occurred in the walls of the host cells surrounding the parasite and this accumulation was localized mostly in certain wall regions, specifically in those directly in contact with the parasite cells (Fig. 4b, c, d). The reinforcement of host cells walls by callose accumulation originates a characteristic

bottleneck aspect of the parasite intrusive tissues (Figures 2f, 3b, 4a). No callose depositions were detected in compatible interactions collected on susceptible plants (data not shown).

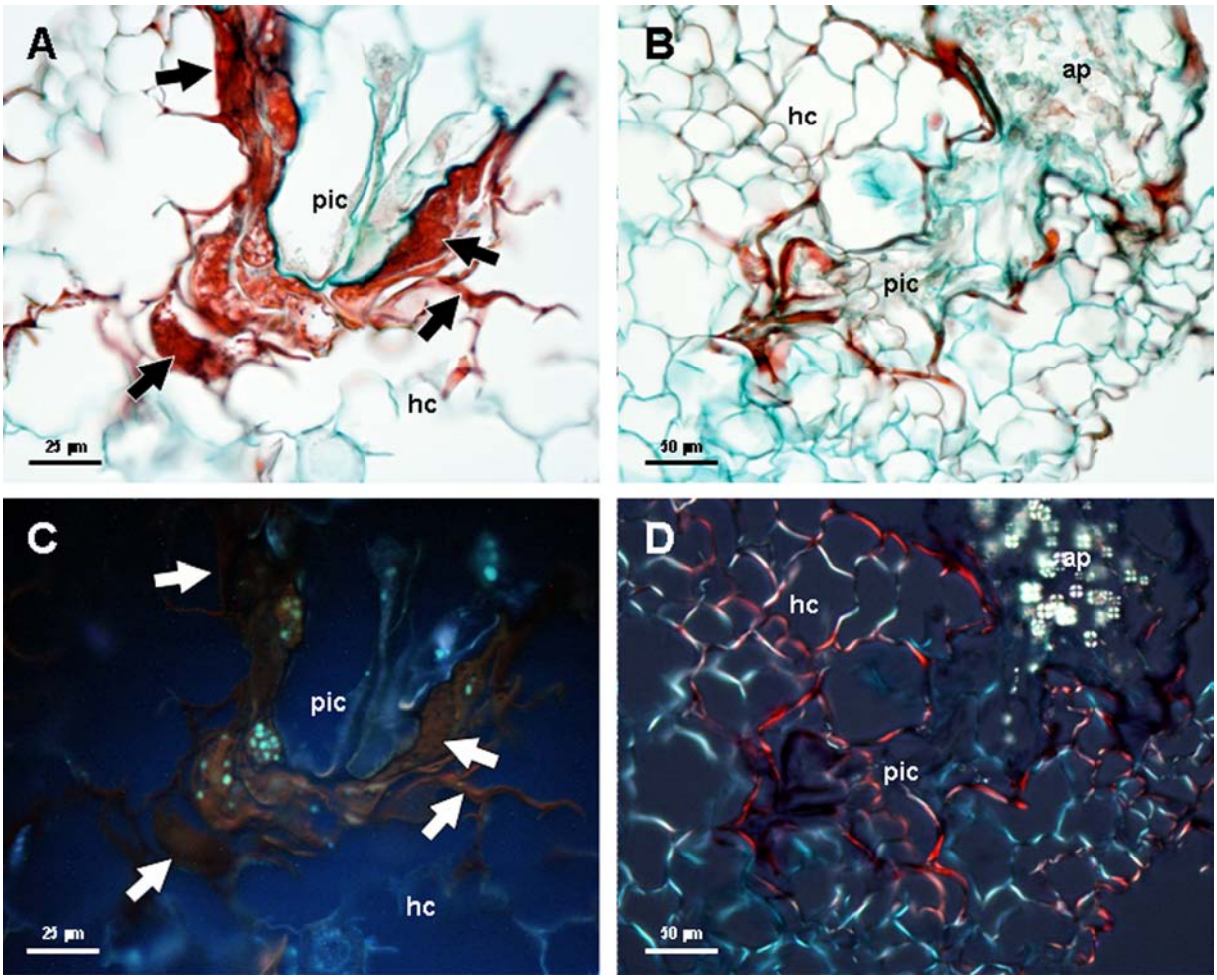

Fig. 3 *Incompatible interactions stained with AGS. (a) Detail of parasite cells halted in the host cortex showing an intense red coloration of the material accumulated in the apoplastic interfase. (b) Parasite intrusive cells showing a 'bottleneck' aspect due to difficulties found during the penetration attempt. (c) The same as (a) under epifluorescence showing absence of emission from the accumulated substances. (d) The same as (b) under polarized light showing the absence of suberised or lignified cell walls. ap, parasite appresorium; pic, parasite intrusive cells; hc, host cortex.*

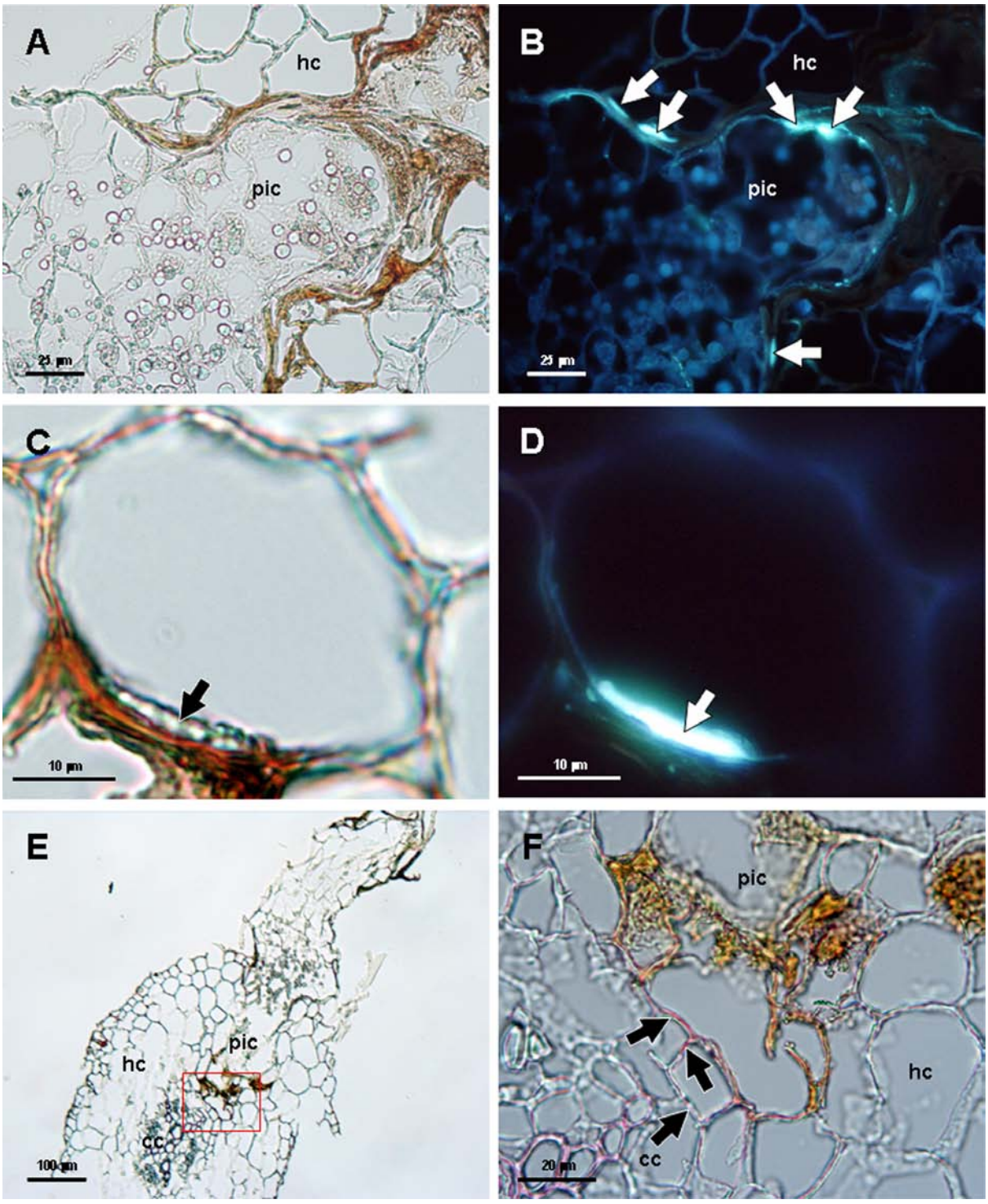

Fig. 4 *(a) Incompatible interaction stained with aniline blue fluorochrome and observed under light microscope. (b) The same as (a) observed under epifluorescence and showing accumulation of callose around the penetration pathway of the parasite (arrows). (c) Detail of a faba bean cell stained with aniline blue fluorochrome showing accumulation of material on the cell wall in contact with the parasite tissues (arrow). (d) The same as (c) but observed under epifluorescence and showing callose deposition on the cell wall (arrow). (e) Incompatible interaction stained with phloroglucinol-HCl and showing the parasite intrusive cells reaching the endodermis. (f) Detail of (e) showing lignification of endodermal cell walls in contact with parasite tissues (arrows). pic, parasite intrusive cells; hc, host cortex; cc, host central cylinder.*

In some cases, in the resistant plants, the parasite is not being stopped in the cortex and reaches the endodermis (Fig. 4e, f). The phloroglucinol-HCl procedure for lignin provided specific staining of the endodermal cell walls at the point of the cessation of the parasite (Fig. 4e, f). This result indicates that a lignification of endodermal cell walls in contact with parasitic tissues takes place (Fig. 4e, f). Again, no presence of lignification was detected in samples collected on susceptible plants (data not shown).

Discussion

As clearly demonstrated in other studies (Labrousse *et al*., 2001; Pérez-de-Luque *et al*., 2005*a*), resistance to *Orobanche* can be divided into different steps. In our work, contrary to previous results obtained with other legumes (Rubiales *et al*., 2003*a,b*; Sillero *et al*., 2005; 2006; Pérez-de-Luque *et al*., 2005*a*), low induction of germination of parasite seeds does not seem to be a determinant factor in the resistant faba bean cultivar studied. However, stoppage of parasite penetration through host tissues and hampering of tubercle development appear as the main available defence responses found in the resistant faba bean. The darkening around the attachment and penetration point of the parasite has been widely described as an incompatible interaction in resistant plants against root parasitic angiosperms (Lane *and* Bailey, 1992; Dörr *et al*., 1994; Goldwasser *et al*., 1997; Pérez-de-Luque *et al*., 2005*b*). Our study shows that it is a quantitative trait, because it is present also in the susceptible cultivar Prothabon but to a lesser extent compared with the resistant Baraca. It is important to notice that the resistance found in Baraca is also incomplete; a few individuals are able to overcome the barriers and develop a tubercle. This confirms previous works assuring that resistance to *Orobanche* is complex (Cubero *and* Hernández, 1991; Cubero, 1994; Cubero *and* Moreno, 1999). This darkening around the attachment point has been usually assumed as a hypersensitive response (HR) because of the dark coloration of host tisúes, but there is no conclusive evidence supporting that a HR really occurs in a manner similar to that described for fungal infection (Heath, 1999; Richael *and* Gilchrist, 1999). In fact, other studies about the incompatible interaction between *Orobanche* spp. and resistant hosts have shown that no HR is present (Rubiales *et al*., 2003*b*; Pérez-de-Luque *et al*., 2005*b*, 2006*a*; Echevarría-Zomeño *et al*., 2006). For that reason, cytochemical studies were developed in order to unveil the nature of such defence response.

No HR was detected when samples of the incompatible interaction were dissected. The accumulation of substances around the penetration pathway of the parasite intrusive cells seems to be responsible for the dark coloration observed at the attachment point as previously reported (Pérez-de-Luque *et al*., 2005*b*). This accumulation can only be observed in the case of incompatible interactions and a possible explanation for it was given previously (Joel *et al*., 1996; Pérez-de-Luque *et al*., 2005*b*, 2006*b*): when the parasite is hampered during the penetration attempts, it releases a higher amount of secretions (i.e. enzymes and adhesives) to overcome the host resistance. An analogous phenomenon was described for the interaction between parasites of the Santalaceae and incompatible hosts (Kuijt, 1969). The nature of these substances remains undetermined to date, but studies with *O. crenata* and other legumes suggests that such accumulation of substances would correspond with an excess of enzymes and adhesive substances excreted by the parasite and degraded products from the host cell walls (Pérez-de-Luque *et al*., 2005*b*, 2006*a*). In other cases (*O. cumana* - *Helianthus annuus*) these secretions contain phenolic compounds excreted by the host leading to the creation of a toxic environment for the parasite (Echevarría-Zomeño *et al*., 2006), but we have not found evidence for this in our study (i.e. fluorescence).

Reinforcement of host cell walls by callose deposition, a ß-1,3-glucan polymer, appears as the main factor responsible for resistance in this case. This is a type of cell wall fortification rapidly developed under pathogen invasion (Hammond-Kosack & Jones, 1996; Brown *et al*., 1998). Despite it has been previously reported in resistant pea to *O. crenata* (Pérez-de-Luque *et al*., 2006*a*), this is the first time it is observed in sufficient amounts and locations to stop the parasite penetration. Because the reinforcement of cell walls by callose requires cross-linking of hydroxyproline-rich glycoproteins (HRGPs) (Brown *et al*., 1998), it is possible that protein cross-linking will be also taking place in this case, but we did not observe it (data not shown). Although the main role of callose here seems to be cell wall reinforcement, we cannot discard another role as a reservoir of ß-glucans elicitors as suggested by Esquerré-Turgayé *et al*. (2000). In this case, ß-glucans degraded from the cell walls would release oligosaccharides, which could play an important role as elicitors of defence responses (Aldington *and* Fry, 1993).

Complementary to callose depositions, if the parasite is able to pierce the cortex and reaches the endodermis, lignification of the cells takes place. This lignification of host pericycle and endodermis was reported as the main resistance factor in *Vicia sativa* against *O. crenata* penetration (Pérez-de-Luque *et al*., 2005*b*), and prevents the parasite reaching the

central cylinder and establishing a haustorium with vascular connections. Other reports described lignification of host cortex and xylem elements (Dörr *et al*., 1994; Antonova *and* Ter Borg, 1996) and unspecific tissues (De Ruck *et al*., 1995; Goldwasser *et al*., 1999). In this work, however, we have observed that lignification of cell walls is set in play after stoppage of parasite intrusive cells in the host cortex has been overcome.

In addition to these, a retarded development of the few established individuals was observed in resistant faba bean. This can be explained by delayed penetration and establishment due to the barriers activated by the resistant host; it would take more time for the parasite to establish a functional haustorium because it must overcome the mechanisms of resistance. But at this point we cannot discard another possible mechanism of resistance, like partial occlusion of host xylem vessels by mucilage (Pérez-de-Luque *et al*., 2005*b*, 2006*b*) but not being as drastic as leading to parasite death. We cannot discard neither an incompatibility between host and parasite tissues at the hormonal level, preventing a normal development of the haustorium and vascular connections. More studies are needed to investigate this hypothesis.

In conclusion, stoppage of *O. crenata* seedling penetration in the host root is a quantitative response in faba bean and is associated with reinforcement of host cell walls in contact with the parasite intrusive cells. At the first stage, the reinforcement takes place in the cortex by callose deposition. However, if the parasite later overcomes this barrier, a lignification of endodermal cells prevents further penetration into the central cylinder and formation of an haustorium.

Acknowledgements

We thank A. Moral for her help in the realisation of this work. A P-d-L was a visiting researcher at the Plant Development group at the CIB-CSIC (Madrid) funded by the Consejería de Innovación, Ciencia y Empresa de la Junta de Andalucía. A P-d-L acknowledges a postdoctoral contract at the IFAPA-CICE funded by the programme "Juan de la Cierva" of the Spanish Ministry of Education and Science. This research was supported by the project EUFABA (QLK5-CT-2002-02307-07).

References

Aldington S and Fry SC. 1993. Oligosaccharins. *Advances in Botanical Research* **19:** 1-101.

Antonova TS and Ter Borg SJ. 1996. The role of peroxidase in the resistance of sunflower against *Orobanche cumana* in Russia. *Weed Research* **36:** 113-121.

Baayen RP, Ouellette GB, Rioux D. 1996. Compartmentalization of decay in carnations resistant to *Fusarium oxysporum* f. sp. dianthi. *Phytopathology* **86:** 1018-1031.

Bordallo JJ, Lopez-Llorca LV, Jansson HB, Salinas J, Persmark L, Asensio L. 2002. Colonization of plant roots by egg-parasitic and nematode-trapping fungi. *New Phytologist* **154:** 491-499.

Brown I, Trethowan J, Kerry M, Mansfield J, Bolwell GP. 1998. Localization of components of the oxidative cross-linking of glycoproteins and of callose synthesis in papillae formed during the interaction between non-pathogenic strains of *Xanthomonas campestris* and French bean mesophyll cells. *The Plant Journal* **15**: 333-343.

Cubero JI. 1994. Breeding work in Spain for *Orobanche* resistance in faba bean and sunflower. In: Pieterse AH, Verkleij JAC, ter Borg SJ, eds. *Biology and management of Orobanche, Proceedings of the Third International Workshop on Orobanche and related Striga research*. Amsterdam: Royal Tropical Institute, 465-473.

Cubero JI and Hernández L. 1991. Breeding faba bean (*Vicia faba* L.) for resistance to *Orobanche crenata* Forsk. *Options Méditerranéennes* **10**: 51-57.

Cubero JI and Moreno MT. 1996. Parasitic plant science: a quarter century. In: Moreno MT, Cubero JI, Berner D, Joel D, Musselman LJ, Parker C, eds. *Advances in parasitic plant research*. Sevilla, Spain: Junta de Andalucía, Consejería de Agricultura y Pesca, 15-23.

Cubero JI and Moreno MT. 1999. Studies on resistance to *Orobanche crenata* in *Vicia faba*. In: Cubero JI, Moreno MT, Rubiales D, Sillero JC, eds. *Resistance to Bromrape, the State of the Art*. Sevilla, Spain: Junta de Andalucía, Consejería de Agricultura y Pesca, 9-15.

Crews LJ, McCully ME, Canny MJ. 2003. Mucilage production by wounded xylem tissue of maize roots - time course and stimulus. *Functional Plant Biology* **30:** 755-766.

De Ruck E, Tena M, Jorrín J. 1995. La lignificación como respuesta defensiva de girasol (*Helianthus* spp.) frente a la infección por plantas parásitas (*Orobanche cernua*). In: *XIX Congreso de la Sociedad Española de Bioquímica*. Córdoba, 225.

Dörr I, Staack A, Kollmann R. 1994. Resistance of *Helianthus* to *Orobanche* - histological and cytological studies. In: Pieterse AH, Verkleij JAC, ter Borg SJ, eds. *Proc. 3rd International Workshop on Orobanche and Related Striga Research*. Amsterdam, The Netherlands: Royal Tropical Institute, 276-289.

Echevarría-Zomeño S, Pérez-de-Luque A, Jorrín J, Maldonado AM. 2006. Pre-haustorial resistance to broomrape (*Orobanche cumana*) in sunflower (*Helianthus annuus*): cytochemical studies. *Journal of Experimental Botany* **57**: 4189-4200.

Eizenberg H, Goldwasser Y, Golan S, Plakhine D, Hershenhorn J. 2004. Egyptian broomrape (*Orobanche aegyptiaca*) control in tomato with sulfonylurea herbicides - Greenhouse studies. *Weed Technology* **18**: 490-496.

Esquerré-Tugayé MT, Boudart G, Dumas B. 2000. Cell wall degrading enzymes, inhibitory proteins, and oligosaccharides participate in the molecular dialogue between plants and pathogens. *Plant Physiology and Biochemistry* **38**: 157-163.

Goldwasser Y, Kleifeld Y, Plakhine D, Rubin B. 1997. Variation in vetch (*Vicia* spp.) response to *Orobanche aegyptiaca*. *Weed Science* **45**: 756-762.

Goldwasser Y, Hershenhorn J, Plakhine D, Kleifeld Y, Rubin B. 1999. Biochemical factors involved in vetch resistance to *Orobanche aegyptiaca*. *Physiological and Molecular Plant Pathology* **54:** 87-96.

Hammond-Kosack KE, Jones JDG. 1996. Resistance gene-dependent plant defense responses. *The Plant Cell* **8**: 1773-1791.

Heath MC. 1999. The enigmatic hypersensitive response: induction, execution, and role. *Physiological and Molecular Plant Pathology* **55**: 1-3.

Hoagland DR and Arnon DI. 1950. The water-culture method for growing plants without soil. *California Agricultural Experiment Station Circular* 347. University of California, Berkeley, USA.

Joel DM. 1983. AGS (Alcian Green Safranin) - A simple differential staining of plant material for the light microscope. *Proceedings RMS* **18:** 149-151.

Joel DM. 2000. The long-term approach to parasitic weeds control: manipulation of specific developmental mechanisms of the parasite. *Crop Protection* **19**: 753-758.

Joel DM, Losner-Goshen D, Hershenhorn J, Goldwasser Y, Assayag M. 1996. The haustorium and its development in compatible and resistant host. In: Moreno MT, Cubero JI, Berner D, Joel D, Musselman LJ, Parker C, eds. *Advances in parasitic plant research*. Sevilla, Spain: Junta de Andalucía, Consejería de Agricultura y Pesca, 531-541.

Jurado-Expósito M, Castejón-Muñoz M, García-Torres L. 1996. Broomrape (*Orobanche crenata*) control with Imazethapyr applied to pea (*Pisum sativum*) seed. *Weed Technology* **10**: 774-780.

Jurado-Expósito M, Castejón-Muñoz M, García-Torres L. 1997. Broad bean and lentil seed treatments with imidazolines for the control of broomrape (*Orobanche crenata*). *Journal of Agricultural Science* **129**: 307-314.

Kuijt J. 1969. *The biology of parasitic flowering plants*. Berkeley, USA: University of California Press.

Labrousse P, Arnaud MC, Serieys H, Bervillé A, Thalouarn P. 2001. Several mechanisms are involved in resistance of *Helianthus* to *Orobanche cumana* Wallr. *Annals of Botany* **88:** 859-868.

Lane JA and Bailey JA. 1992. Resistance of cowpea and cereals to the parasitic angiosperm *Striga*. *Euphytica* **63**: 85-93.

Mayer AM. 2006. Pathogenesis by fungi and parasitic plants: similarities and differences. *Phytoparasitica* **34**: 3-16.

Mellersh DG, Foulds IV, Higgins VJ, Heath MC. 2002. H_2O_2 plays different roles in determining penetration failure in three diverse plant-fungal interactions. *The Plant Journal* **29:** 257-268.

Parker C and Riches CR. 1993. *Parasitic weeds of the world: biology and control*. Wallingford, UK: CAB International.

Pérez-de-Luque A, Jorrín J, Rubiales D. 2004a. Crenate broomrape control in pea by foliar application of benzothiadiazole (BTH). *Phytoparasitica* **32**: 21-29.

Pérez-de-Luque A, Sillero JC, Moral A, Cubero JI, Rubiales D. 2004b. Effect of sowing date and host resistance on the establishment and development of *Orobanche crenata* in faba bean and common vetch. *Weed Research* **44**: 282-288.

Pérez-de-Luque A, Jorrín J, Cubero JI, Rubiales D. 2005a. Resistance and avoidance against *Orobanche crenata* in pea (*Pisum* spp.) operate at different developmental stages of the parasite. *Weed Research* **45**: 379-387.

Pérez-de-Luque A, Rubiales D, Cubero JI, Press MC, Scholes J, Yoneyama K, Takeuchi Y, Plakhine D, Joel DM. 2005b. Interaction between *Orobanche crenata* and its host legumes: Unsuccessful haustorial penetration and necrosis of the developing parasite. *Annals of Botany* **95**: 935-942.

Pérez-de-Luque A, González-Verdejo CI, Lozano MD, Dita MA, Cubero JI, González-Melendi P, Risueño MC, Rubiales D. 2006a. Protein cross-linking, peroxidase and β-1,3-endoglucanase involved in resistance of pea against *Orobanche crenata*. *Journal of Experimental Botany* **57**: 1461-1469.

Pérez-de-Luque A, Lozano MD, Cubero JI, González-Melendi P, Risueño MC, Rubiales D. 2006b. Mucilage production during the incompatible interaction between *Orobanche crenata* and *Vicia sativa*. *Journal of Experimental Botany* **57**: 931-942.

Press MC and Graves JD. 1995. *Parasitic plants*. London, UK: Chapman & Hall.

Richael C and Gilchrist D. 1999. The hypersensitive response: A case of hold or fold? *Physiological and Molecular Plant Pathology* **55**: 5-12.

Rioux D, Nicole M, Simard M, Ouellette GB. 1998. Immunocytochemical evidence that secretion of pectin occurs during gel (gum) and tylosis formation in trees. *Phytopathology* **88:** 494-505.

Rubiales D, Pérez-de-Luque A, Cubero JI, Sillero JC. 2003a. Crenate broomrape (*Orobanche crenata*) infection in field pea cultivars. *Crop Protection* **22:** 865-872.

Rubiales D, Pérez-de-Luque A, Joel DM, Alcántara C, Sillero JC. 2003b. Characterization of resistance in chickpea to crenate broomrape (*Orobanche crenata*). *Weed Science* **51:** 702-707.

Rubiales D, Alcántara C, Sillero JC. 2004. Variation in resistance to crenate broomrape (*Orobanche crenata*) in species of *Cicer*. *Weed Research* **44:** 27-32.

Rubiales D, Pérez-de-Luque A, Fernández-Aparicio M, Sillero JC, Román B, Kharrat M, Khalil S, Joel DM, Riches C. 2006. Screening techniques and sources of resistance against parasitic weeds in grain legumes. *Euphytica* **147**: 187-199.

Ruzin SE. 1999. *Plant microtechnique and microscopy*. New York, USA: Oxford University Press.

Sillero JC, Moreno MT, Rubiales D. 2005. Sources of resistance to crenate broomrape in *Vicia* species. *Plant Disease* **89**: 22-27.

Sillero JC, Cubero JI, Fernández-Aparicio M, Rubiales D. 2006. Search for resistance to crenate broomrape (*Orobanche crenata*) in *Lathyrus. Lathyrus Lathyrism Newsletters* **4**: 7-9.

Tennant D. 1975. A test of a modified line intersect method of estimating root length. *Journal of Ecology* **63**: 995-1001.

Ter Borg SJ, Willemsen A, Khalil SA, Saber HA, Verkleij JAC, Pieterse AH. 1994. Field study of the interaction between *Orobanche crenata* Forsk. and some lines of *Vicia faba*. *Crop Protection* **13**: 611-616.

CAPÍTULO III: "Accepted with minus comments"

Medicago truncatula as a model for non-host resistance in legumes – parasitic plants interactions

Plant Physiology (2007) 145: 437-449

María-Dolores Lozano-Baena[1], Elena Prats[1], María-Teresa Moreno[2], Diego Rubiales[1] and Alejandro Pérez-de-Luque[2]

[1] *CSIC, Institute for Sustainable Agriculture, Apdo. 4084, 14080 Córdoba, Spain*

[2] *IFAPA (Junta de Andalucía), Centro "Alameda del Obispo", Área de Mejora y Biotecnología, Apdo. 3092, 14080 Córdoba, Spain*

Abstract

Orobanche crenata (crenate broomrape) is a root parasitic weed that represents a major constraint for grain legume production in Mediterranean and West Asian countries. *Medicago truncatula* has emerged as an important model plant species for structural and functional genomics. The close phylogenic relationship of *M. truncatula* with crop legumes increases its value as a resource for understanding resistance against *Orobanche* spp. Different cytological methods were used to study the mechanisms of resistance against *O. crenata* of two accessions of *M. truncatula,* showing early and late acting resistance. In the early resistance accession (SA27774) we found that the parasite died before a tubercle had formed. In the late resistance accession (SA4327) the parasite became attached without apparent problems to the host roots but most of the established tubercles turned dark and died before emergence. The results suggest that there are defensive mechanisms acting in both accessions but with a time gap, that is crucial for a higher success avoiding parasite infection.

Introduction

Orobanche crenata is one of the most important parasitic plants attacking legume crops in Mediterranean area, devastating crops and making unusable infested land (Rubiales, 2001-2003). Being a broomrape (*Orobanche* ssp.), *O. crenata* is an obligate root holoparasite lacking in chlorophyll and depending entirely on the host for its supply of nutrients (Joel *et al*., 2007). The knowledge of the mechanisms of resistance against the parasite is crucial in order to develop strategies of control, like breeding for resistance. With this purpose, we have chosen *Medicago truncatula* as an *O. crenata* host model plant due to its characteristics.

M. truncatula is an annual forage legume in Mediterranean area. Contrary to other legume crops, *M. truncatula* is an autogamous self-fertile plant with a small and diploid genome, a short life cycle and a prolific seed production (Blondon *et al*., 1994). Its simple genetics, the development of new tools and methods for molecular and genetic analysis, and the complete genome sequence (http://www.medicago.org), provide researchers with a valuable data set and making it interesting as a legume model species for laboratory studies (Cook *et al*., 1997; Cook, 1999) and also, in pathogenic interactions (Ellwood *et al*., 2007; Pérez-de-Luque *et al*., 2007a).

Nowadays, the most numerous and important works about parasitic plants were focused on the development in susceptible host, as *Orobanche* spp. (Joel *and* Losner-Goshen, 1994; Neumann *et al*., 1999), *Striga* spp. (Dörr, 1997; Reiss *and* Bailey, 1998), *Cuscuta* spp. (Vaughn, 2002; 2003), *Viscum* spp. (Heide-Jørgensen, 1987) and others (Heide-Jørgensen *and* Kuijt, 1993; 1995). But little is known about the basis of host resistance to these parasites, just finding the work of Joel *et al*. (1996) introducing this subject. In the last years only some histological studies of the resistant interactions have been undertaken (Dörr *et al*., 1994; Antonova *and* Ter Borg, 1996; Gowda *et al*., 1999; Goldwasser *et al*., 2000a; Labrousse *et al*., 2001; Rubiales *et al*., 2003b; Zehhar *et al*., 2003; Pérez-de-Luque *et al*., 2005b; 2006a, b).

This lack of knowledge is due to the complexity of this interaction. The study of this host–parasite interaction presents important limitations because they both are plants, what implies sharing similar morphological, physiological and biochemical traits. In order to solve it, we have chosen cytological and cytochemical techniques as powerful tools to reveal the mechanisms underlying the host-parasitic plants interaction. These studies, complemented with –omic studies, using *M. truncatula* as a host model, will be a valuable addition to our knowledge about the plant–parasitic plant interactions.

In this work we have used two *M. truncatula* accessions previously evaluated against *O. crenata* infection (Rodriguez-Conde *et al*., 2004). We have identified one of them as early resistant to broomrape infection (SA27774), because no establishment or development of parasites can be observed. The other one was characterized as late resistant (SA4327), because despite parasites established and developed, most of them were unable to evolve into mature plants. Cytochemical studies revealed that the defensive mechanisms are activated at different time points in each accession, which implies a different observation of the phenotype of the resistance and a higher success avoiding parasite infection for the early resistant accession.

Materials and Methods

Plant material and growth conditions

Orobanche crenata was grown on accessions of *Medicago truncatula* showing early or late resistance to this pathogen (accessions SA27774 and SA4327 respectively).

The Petri dish system described by Pérez-de-Luque *et al*. (2005a) and Rubiales *et al*. (2006) was used for *in vitro* cultivation of the *M. truncatula* plants and inoculation with *O. crenata* seeds.

M. truncatula seeds were supplied from the SARDI Genetic Resource Centre (GRC) in Australia (Origin: YUG). Seeds were scarified with a metal sheet and sterilized in commercial bleach (20% in sterile water) for 10 minutes. For synchronize germination, seeds were place at 4ºC for 36 hours in sterile water. During this period, we replaced sterile water 2 or 3 times to help germination. After that, seeds were rinsed with sterile water at room temperature for 3 or 4 h, changing it 6 or 8 times. Finally, seed were placed in Petri dishes on wet glass fibre filter papers (Whatmann GF/A) and kept in darkness at 20ºC for 1-2 days. When the radicle reached 2 cm length, seedlings were transferred to new dishes (15 cm diameter) with perlite and new glass fibre papers (Pérez-de-Luque *et al*., 2005a).

O. crenata seeds were collected from infected faba bean plants at Córdoba during 2000. They were disinfected with formaldehyde according to González-Verdejo *et al*. (2005) and spread on the glass fibre paper (~8 mg) where the *M. truncatula* roots were growing. In order to prevent exposure of the parasite seeds - host roots to direct light, the dishes containing test

plants inoculated with parasite seeds were sealed with parafilm and covered with aluminium foil. Then, the upward growing host plants were placed vertically in trays with Hoagland nutrient solution (Hoagland *and* Arnon, 1950) and grown in a controlled environment chamber at 20ºC ± 0.5ºC with a day/night 14 h photoperiod and an irradiance of 200 µmol m^{-2} s^{-1}.

At the same time plants were growing, *O. crenata* seeds were conditioned. For conditioning, parasite seeds need to be in darkness at 20ºC for ten days (Pérez-de-Luque *et al*., 2005a).

After conditioning period, we applied 5 ml of the synthetic stimulant GR24 (1 mg/ml) (Magnus *et al*., 1992) on the paper with the seeds (for *O. crenata* homogeneous germination induction) (Rubiales *et al*., 2003b).

Minirizhotron studies

The infection process was followed using a binocular microscope (Nikon SMZ1000; Nikon Europe B.V., Badhoevedorp, The Netherlands). 15 days after GR24 application, the percentage of *O. crenata* attach seedlings on *M. truncatula* roots was calculated. The total of 200 *O. crenata* seedlings close (< 3 mm) to the *M. truncatula* roots were visualised in each Petri dish and the number of attached seedlings was referred to the total number of seedlings. At 22 days after GR24 application, the percentage of compatible and incompatible attachments against total attachments was scored. An attachment was considered compatible when it resulted in tubercle formation. Finally, 30 days after GR24 application established broomrapes were quantified and expressed as absolute value per plant. In addition, the number of darkened tubercles was recorded and expressed as a percentage respect to the total number of established tubercles per plant.

Collection and fixation of samples

Observations were taken using a binocular microscope. At 15 days after GR24 application, seedlings of *O. crenata* were sampled at random with the corresponding attached parts of host roots.

For staining methods and confocal laser scanning microscopy, the samples were fixed in 4% formaldehyde in phosphate buffered saline (PBS), pH 7.3 at 4ºC overnight. After washing in PBS (3x15 min), they were stored in 0.1% formaldehyde in PBS at 4ºC.

Fixed samples were then dehydrated in ethanol series (50, 80, 95, 100, 100%: 12 h each) and transferred to an embedding solvent (Xylene; Panreac Quimica S.A., Montcada i Reixac, Spain) through a xylene-ethanol series (30, 50, 80, 100, 100%: 12 h each) and finally saturated with paraffin (Paraplast Xtra; Sigma, St. Louis, USA). 7 µm-thick sections were cut with a rotary microtome (Nahita 534; Auxilab S.A., Beriain, Spain) and attached to adhesive-treated microscope slides (polysine slides; Menzel GmbH & Co KG, Braunschweig, Germany).

Staining methods

After removal of paraffin, sections were stained with different dyes:

1. Staining with 0.05% toluidine blue O (TBO) in PO_4 buffer (pH 5.5) during 5-10 min was used. In this case the dye was applied before removal of paraffin (Ruzin, 1999). This method allows the detection of phenolics as well as tannins, lignin and suberin (Baayen *et al*., 1996; Bordallo *et al*., 2002; Mellersh *et al*., 2002; Crews *et al*., 2003).

2. Alcian green - safranin (AGS) (Joel, 1983). The slides were dried and mounted with DePeX (BDH). With this staining method, carbohydrates (including cell walls and mucilage) appeared green, yellow or blue, while lignified, cutinized and suberized walls, as well as tannin and lipid material inside cells appeared red (Joel, 1983). Non-stained sections were kept as control, and for examination under the fluorescence microscope.

3. Phloroglucinol (2% in ethanol)-HCl (35%) (Ruzin, 1999) were applied covering tissue sections for 30 minutes and observed by using light and fluorescence microscopy. This compound stains the aldehyde groups of lignin and suberin, but quenches lignin autofluorescence and retains suberin fluorescence (Baayen *et al*., 1996; Rioux *et al*., 1998).

4. Aniline blue fluorochrome was used for callose detection under UV fluorescence (340-380 nm). The samples were stained during 15-30 min in a solution 0.1% aniline blue fluorochrome in water (Bordallo *et al*., 2002).

Transverse sections were observed using a light microscope (Leica DM-LB, magnification ×100 to ×400; Leica Microsystems Wetzlar GmbH, Wetzlar, Germany) and photographed using a digital camera (Nikon DXM1200F; Nikon Europe B.V., Badhoevedorp, The Netherlands). The samples were also observed by epi-fluorescence under excitation at 340-380 nm (UV).

Fluorescence microscopy

Hand cut sections (with a razor blade) were obtained from fresh root samples to observe accumulation of phenolic compounds by epi-fluorescence under excitation at 340-380 nm (UV).

Confocal laser scanning microscopy

Ten fresh samples of *O. crenata* seedlings with the corresponding attached parts of host roots were immersed in a solution of 0.1% (w/v) diphenyl boric acid 2-aminoethylester (Naturstoffreagenz A: NA) in buffer (100 mM KPi pH 6.8, 1% NaCl (w/v)) according to Hutzler *et al*. (1998). This treatment induces secondary fluorescence of flavonoids. Confocal optical section stacks were collected using a Leica TCS-SP2-AOBS-UV confocal laser scanning microscope (Leica Microsystems Wetzlar GmbH, Wetzlar, Germany) with an excitation wavelength of 488 nm and emission spectra monitored from 515-670 nm. The emission spectra corresponding to 515-590 nm was monitored through one channel (green channel), and the emisión spectra corresponding to 590-670 nm was monitored through another channel (red channel). Analysis of confocal images was performed with the LEICA software LCS, version 2.5 Build 1227.

Cell viability assay

Trypan blue dye exclusion was used to assess cell viability. Samples were immersed in a commercial Trypan Blue solution of 50% (Sigma, St. Louis, USA) and observed using a light microscope. Viable (alive) and non-viable (dead) cells were identified microscopically, under bright field optics, as those that had excluded and taken up the trypan blue stain respectively.

Extraction of total phenolics and identification of phytoalexins

The Petri dish system was used for plant material collection from *Medicago truncatula* accessions showing early or late resistance (SA27774 and SA4327 respectively) to *Orobanche crenata* as described before. *Medicago truncatula* roots from non-infected and infected plants were sampled 30 days after GR24 application, date corresponding to establishment of the parasite. For non-infected plants, small root pieces (~ 1 cm) were sampled at random. For infected plants, parts of the root with an *Orobanche crenata* attachment were sampled, removing the parasite tissues. Then, samples were washed with tap and then distilled water, blotted dry with filter paper, frozen in liquid nitrogen and stored at -80ºC until biochemical analysis (Pérez-de-Luque *et al*., 2005a). Frozen root tissue (0.04 g fresh weight) was homogenized in 1 ml methanol by using a pestle and mortar. After filtering off the solvent extract, the residue was further sequentially extracted twice with a similar volume of methanol and centrifuged twice at 15 000 g for 15 min. The combined solvent extracts were dried and phenolic compounds were re-suspended in 0.24 ml of methanol. The pellet residue was re-suspended in 0.08 mL of 2 M NaOH and incubated at 70ºC for 16 h. The suspension was cooled down, neutralized with 0.08 mL of 2 M HCl and centrifuged (15 000 g for 15 min). Then, the suspension were dried and re-suspended in the same volume of methanol. TLC analysis of the methanolic extract was performed according to Prats *et al*. (2003), by using Silicagel 60 F254 plates (Merk) and diethyl eter:hexane (70:30 v/v) as the mobile phase. Plate was visualised under UV light (254 nm) lamp. Scopoletin (from Sigma, Spain), medicarpin, pisatin and maackiain (from Plantech, UK) were used as standards.

Statistical analysis

Minirizhotron assays were performed with two plants per Petri dish and ten Petri dishes per *M. truncatula* accession (SA27774 and SA4327). Data were recorded from three randomised areas in each plant. In order to study possible interactions due to cultivation of plants in different dishes, each Petri dish was treated as a block and an ANOVA was performed (Statistix v1.1 for Windows). No significant differences were found between blocks, so each Petri dish was considered as a replicate. For cytochemical and confocal studies, at least ten samples were selected at random from several Petri dishes for each study. Percentages were transformed according to the formula $Y = \arcsin(\sqrt{X\%/100})$ prior to statistical treatment.

Results

Minirhizotron studies

This system allowed the study of the infection process in both accessions of *M. truncatula* and the collection of samples at the right time for cytochemical analysis. It also permitted a quantitative study of the expression of the resistance, allowing characterization of both accessions as early and late resistant plants. Addition of GR24 to the minirhizotrons assured a high and homogeneous germination of *O. crenata* seeds (40%). A similar number of attachments was formed on both accessions during first 3 weeks (Table 1).

Table 1. *Phenotypic components of the resistance to Orobanche crenata observed in Medicago truncatula* per plant.

Data shown as mean ± SE. Data with the same letter within the same column are not significantly different (HSD, P<0.05)

Accession	15 d after GR24		22 d after GR24		30 d after GR24	
	Total number of *Oc* seedlings attached to *Mt* roots*	**% *Oc* seedlings attached to *Mt* roots***	**Total number of *Oc* seedlings attached to *Mt* roots***	**% *Oc* seedlings developed into tubercle**	**Total number of *Oc* Tubercles established on *Mt* roots**	**% of unviable *Oc* tubercles (darkened)**
SA4327	23.0a ± 1.58	11.5a ± 0.79	27.4a ± 2.87	80.5a ± 4.85	23.6a ± 2.36	67.9a ± 2.55
SA27774	23.4a ± 1.82	11.7a ± 0.91	31.6a ± 1.51	7.7b ± 1.45	4.3b ± 0.63	49.7a ± 9.30

* From a total of 200 seedlings per plant

However, both accessions differed already by this time on percentage of *O. crenata* germinated seeds in contact with *M. truncatula* roots that successfully formed a tubercle, being the success on tubercle formation much lower in SA27774 (7.7%). This reaction was characterized by stoppage of parasite seedlings penetration into the host root, usually accompanied by darkening of host and/or parasite tissues around the point of attachment. On the contrary, at the same observation date, most of the attachments in SA4327 had evolved to small tubercles. As a consequence, 30 days after GR24 application there were almost no tubercles (4.3) in accession SA27774 contrasting with the number of them established on SA4327 (23.6). But a new incompatible reaction was found at this point: more than half of the tubercles (67.9%) on SA4327 had become dark and stopped their development.

Samples of both kind of incompatible interactions, and compatible interactions, were collected and used for cytochemical studies.

Light and fluorescence microscopy

In order to characterise the mechanisms of resistance setting in play by the host, different histochemical procedures were employed. For comparison, tissues of the *M. truncatula* accession SA4087 were included as controls. This accession is the most susceptible one to *O. crenata* attack described to date (Rodriguez-Conde *et al*., 2004).

Sections of both, successful and unsuccessful penetration attempts, are presented in Figure 1, corresponding to accessions SA4087 (Fig. 1, A and B), SA4327 (Fig. 1, C and D) and SA27774 (Fig. 1, E and F) respectively. The toluidine blue O (TBO) staining was used as a general dye in order to get preliminary information about the incompatible interaction. In accessions SA4087 and SA4327, the parasite was able to pierce through the cortex and penetrated into the host central cylinder, beginning the development of the haustorium. Parasite intrusive cells in SA27774 also reached the host central cylinder but some abnormalities were observed. A dark stained deposit accumulated at the interface between host and parasite and a wall thickening inside host xylem vessels next to parasite tissues was developed (Fig. 1F).

Staining of sections from the early resistance accession with alcian green – safranin (AGS) confirmed that parasite intrusive cells reached the host central cylinder, but an intense red coloration of the parasite tissues (corresponding to non-carbohydrate substances) was observed (Fig. 2, A and D), contrary to the common green staining (carbohydrates) expected for normal and healthy tissues in SA4087 (Fig. 2G). The parasite tissues also presented a disrupted and disorganised aspect. Accumulation of a red-stained material in the apoplast within and around the penetration pathway of the parasite was observed (Figure 2, A and D) corresponding with the dark stained material (unspecific substances) found using the TBO procedure. Host cells in contact and near the parasite tissues were impregnated with this red substance, and it was also present inside some host xylem vessels (Fig 2D). Observation of samples under UV excitation (340-380 nm) revealed a strong blue-white fluorescence from the walls and middle lamellae of cells surrounding the parasite intrusive tissues, including some xylem vessels (Figure 2, B, C and E). This fluorescence was shown only in host vessels near or in contact with the parasite cells (Fig. 2, C and E), but not in those located away from the infection point. The thickening of the cell walls found inside the xylem vessels also presented this fluorescence (Fig. 2E).

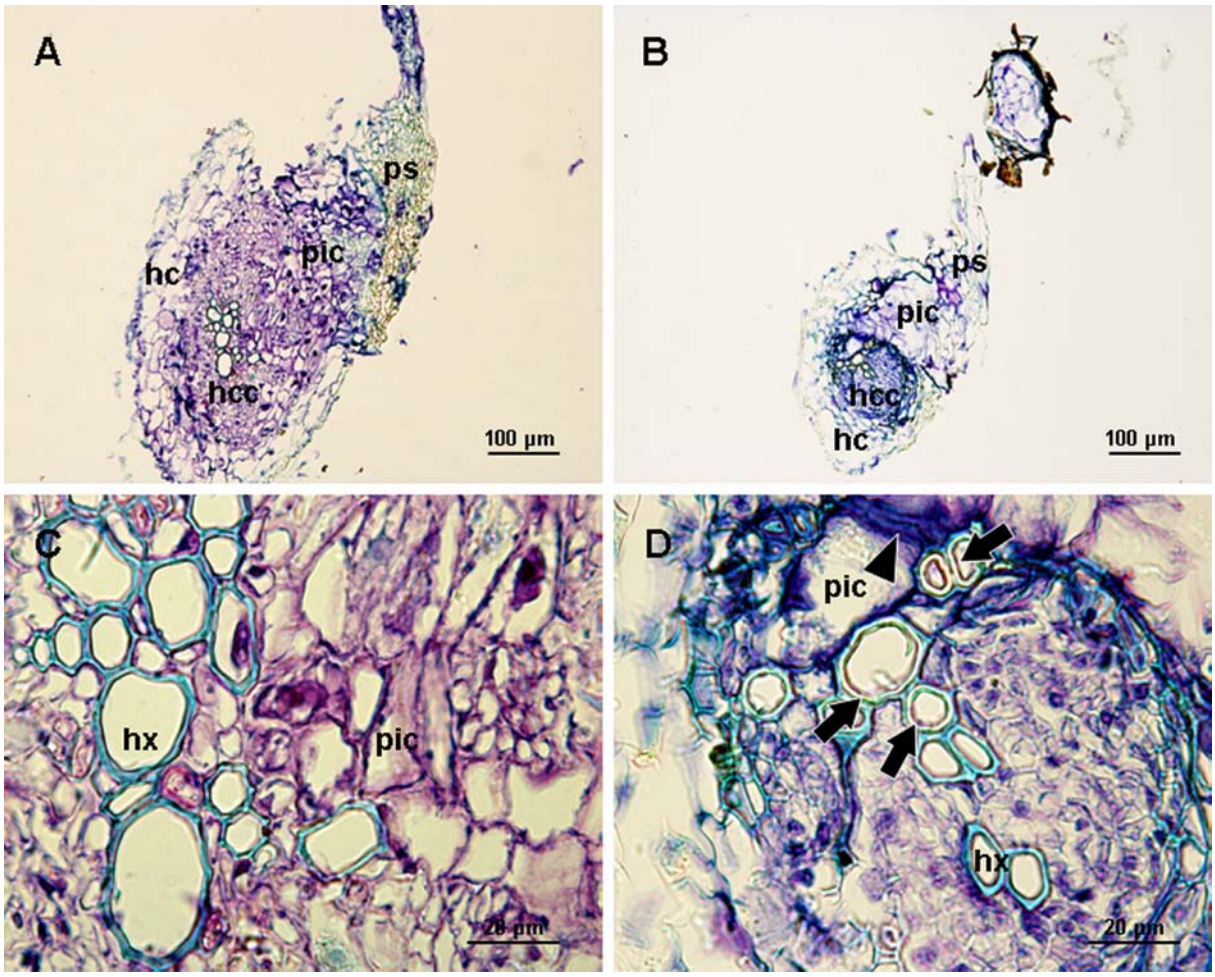

Fig. 1. *Sections stained with Toluidine Blue O (TBO). (A) Cross section of a successful O. crenata seedling penetration on SA4087 accession of M. truncatula. (B) Detail of (A) showing the central cylinder and host xylem vessels in contact with parasite cells. Some parasite vessels begin to develop connecting with the host xylem vessels. (C) Cross section of a successful O. crenata seedling penetration on SA4327 accession of M. truncatula. (D) Detail of (C) showing the central cylinder and host xylem vessels in contact with parasite cells. (E) Cross section of an unsuccessful O. crenata seedling penetration on SA27774 accession of M. truncatula. (F) Detail of (E) showing the thickening of host xylem walls (arrows) in contact with parasite cells and accumulation of a dark stained substance (arrowhead). ps: parasite seedling; pic: parasite intrusive cells; hc: host cortex; hcc: host central cylinder; hx: host xylem vessels; px: parasite xylem vessels.*

Observation of samples under polarized light proved that the secondary thickening of xylem walls was not due to birefringence (O'Brien *and* McCully, 1981), as it is common in the case of lignified and suberized walls (Fig. 2F).

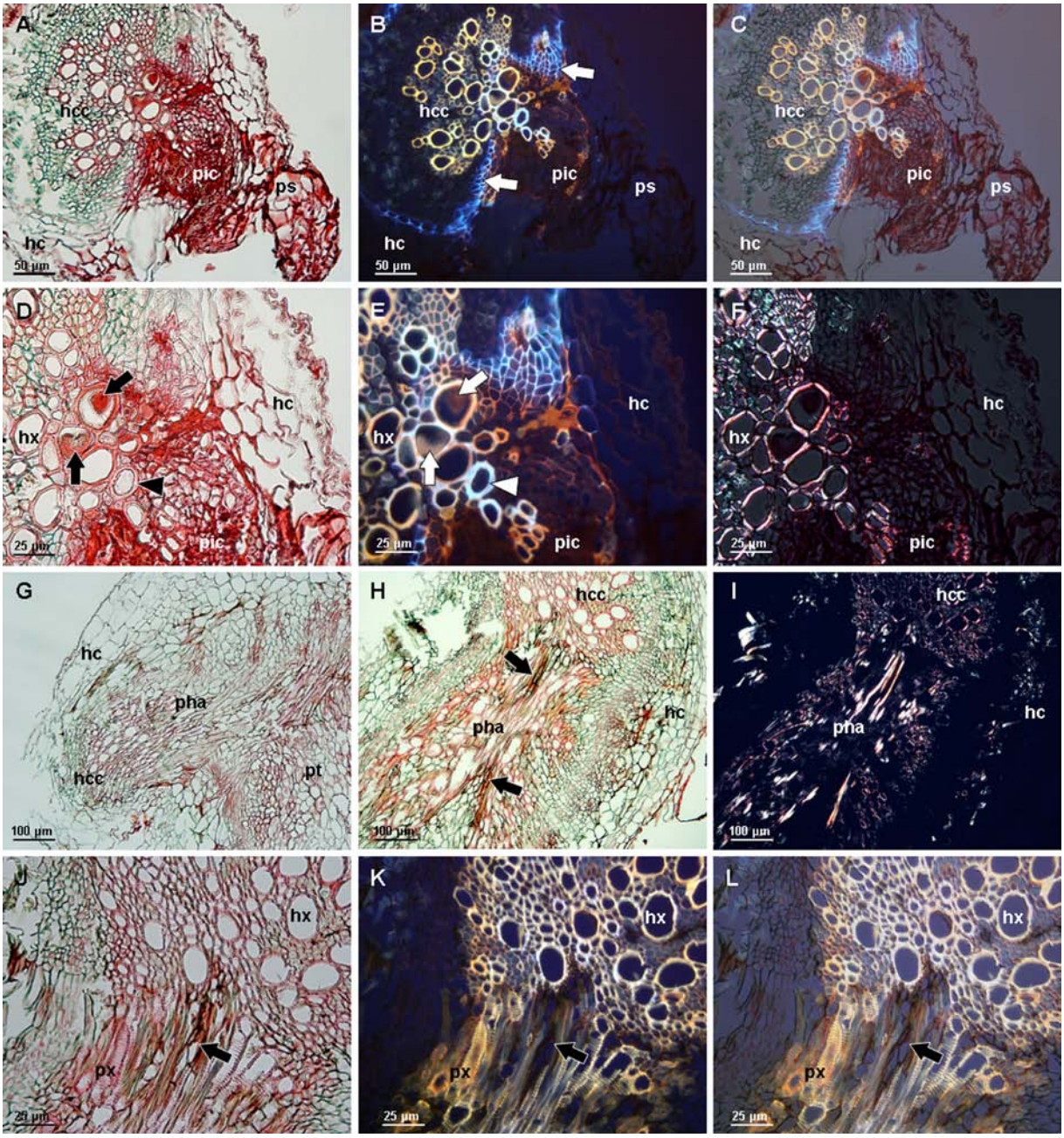

Fig. 2. *Sections stained with Alcian Green – Safranin (AGS). (A) Cross section of an unsuccessful O. crenata seedling penetration on SA27774 accession of M. truncatula. (B) The same section observed under UV excitation (340-380 nm) showing an intense fluorescence in host cells in contact with parasite tissues (arrows). (C) Overlay of (A) and (B) showing the localization of the fluorescent cells. (D) Detail of (A) showing accumulation of substances (non-carbohydrates) inside host xylem vessels (arrows) and thickening of xylem vessels in contact with parasite cells (arrowhead). (E) Idem as (D) observed under UV excitation (340-380 nm) and showing blue fluorescence from the thickened xylem cell walls (arrowhead). (F) Idem as (D) observed under polarized light showing no changes in the cell walls birefringence of thickened xylem vessels. (G) Cross section of a successful established O. crenata tubercle on SA4087 accession. (H) Cross section of a darkened established O. crenata tubercle on SA4327 accession. (I). Idem as (H) observed under polarized light. (J) Detail of a cross section of a darkened established O. crenata tubercle on SA4327 accession showing accumulation of a*

dark brown substance inside parasite xylem vessels and the apoplast of the haustorium (arrow). (K) Idem as (J) observed under UV excitation (340-380 nm) and showing quenched autofluorescence from the vessels covered by the dark brown substance (arrow). ps: parasite seedling; pic: parasite intrusive cells; hc: host cortex; hcc: host central cylinder; hx: host xylem vessels; pha: parasite haustorium; pt: parasite tubercle; px: parasite xylem vessels.

Sections of tubercles becoming dark on the late resistant accession and stained with the same technique (AGS) showed a normal aspect at the first sight (Fig. 2H) compared with those corresponding to healthy tubercles (Fig. 2G). However, a few details were observed: firstly, the presence of a dark brown deposit in the apoplast and some vessels from the haustorium (Fig. 2J) which did not stained; and secondly, the presence of a slight blue-white fluorescence in host xylem walls in contact with the haustorium (Fig. 2K). The dark deposit did not present fluorescence and quenched that of the impregnated vessels (Fig. 2K). It also eliminated the birefringence of the affected vessels (Fig. 2I) under polarized light. The blue-white fluorescence was very similar to that found in the case of the early resistant accession (Fig. 2, B, C and E).

In order to check the possible role of lignins and suberins in this resistance, phloroglucinol-HCl staining was used (Fig. 3). In compatible interactions on SA4087, xylem walls appeared with a light pink stain (Fig. 3, E and F), indicating their normal lignification. However, an intense red colouration was observed in walls of xylem vessels near the parasite intrusive cells in sections of incompatible interactions on SA27774 (Fig. 3, A and C). These vessels presented also the thickened walls observed with TBO and AGS staining. Some xylem vessels were also filled with a material which was strongly stained with this method. When observed under UV excitation (340-380 nm) (Fig. 3, B and D), lignin autofluorescence was quenched by the staining, and only suberin fluorescence remained. As can be seen in Fig. 3B and 3D, only the suberized walls corresponding to the endodermal cells showed fluorescence: lignified cell walls did not fluoresce.

To identify other mechanisms implicated in reinforcement of host cell walls against *Orobanche* penetration, aniline blue fluorochrome was used for identification of callose under UV excitation (340-380 nm) (Fig. 4). Our results showed that host cell walls from the cortex (Fig. 4C) in contact with parasite intrusive tissues and some cells in the central cylinder (Fig. 4D) presented a slight accumulation of callose. No presence of callose was detected in compatible interactions (Fig. 4F).

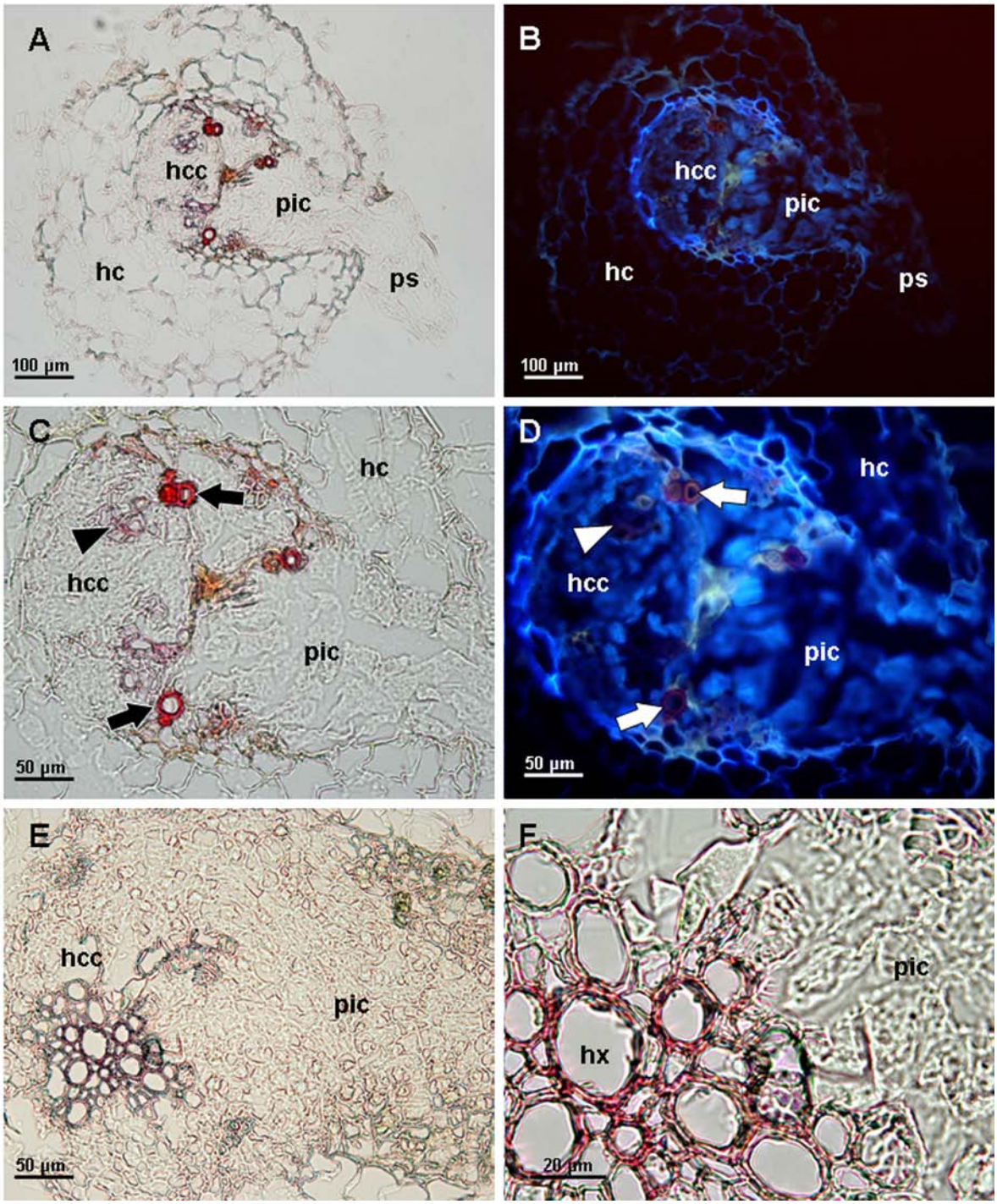

Fig. 3. *Sections stained with Phloroglucinol–HCl. (A) Cross section of an unsuccessful O. crenata seedling penetration on SA27774 accession of M. truncatula. (B) The same section observed under UV excitation (340-380 nm). (C) Detail of (A) showing accumulation of substances (polyphenols) inside host xylem vessels and thickening of their cell walls (arrows) compared with normal xylem vessels stained with the dye (arrowhead). (D) Idem as (C) observed under UV excitation (340-380 nm) and showing blue fluorescence corresponding to suberin from endodermal cells, and the quenched fluorescence from normal lignified xylem walls (arrowhead) and thickened xylem walls (arrows). (E) Cross section of a successful O. crenata seedling penetration on SA4087 accession of M. truncatula. (F) Detail of (E) showing the normal staining of host xylem walls. ps: parasite seedling; pic: parasite intrusive cells; hc: host cortex; hcc: host central cylinder; hx: host xylem vessels.*

Observations of fresh hand cut sections were taken under UV excitation (340-380 nm) (Fig. 5) to detect the presence of phenolic compounds. No fluorescence in tissues was detected neither in uninfected roots (Fig. 5, A and B) or compatible interactions (Fig. 5, C and D). On the contrary, a strong fluorescence was found in host tissues adjacent to parasite intrusive cells (Fig. 5, E and F) and haustoria (Fig. 5, G and H) in sections of incompatible interactions.

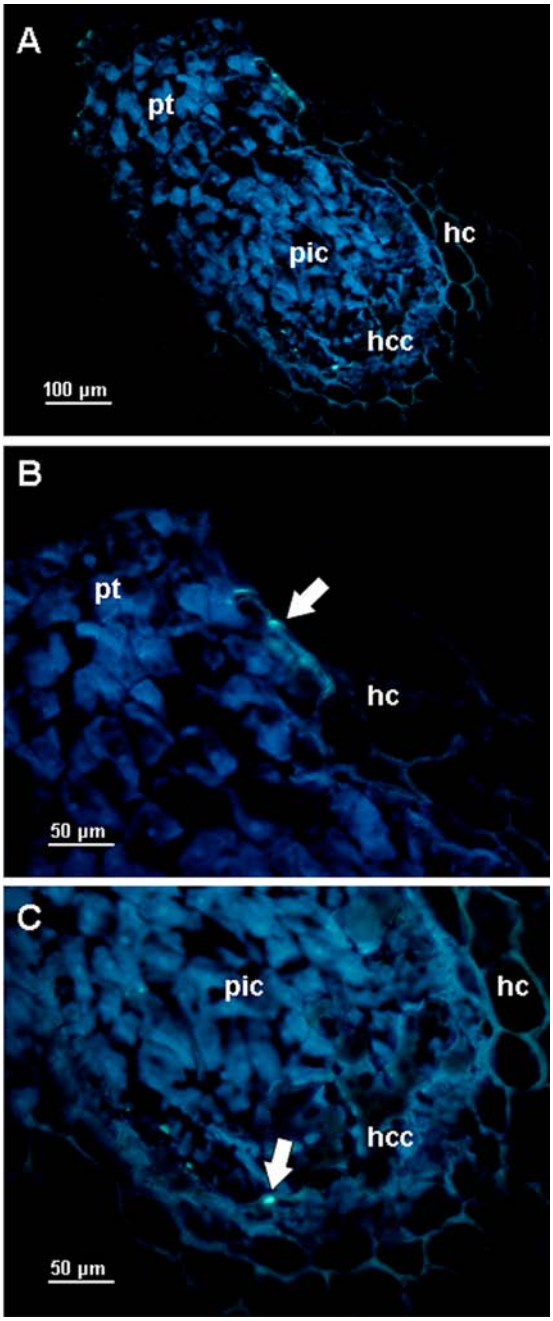

Fig. 4. *Sections stained with Aniline Blue Fluorochrome . (A) General view of a cross section of an incompatible interaction on SA27774 accession of M. truncatula observed under bright field. (B) Idem as (A) observed under UV excitation (340-380 nm). (C) Detail of (B) showing callose depositions (arrow) in cell walls from the host*

cortex in contact with parasite cells. (D) Idem as (C) showing callose depositions (arrow) in cell walls from the host central cylinder. (E) Cross section of a compatible interaction on SA4087 accession of M. truncatula observed under bright field. (F) Idem as (E) observed under UV excitation (340-380 nm). No presence of callose is detected. pt: parasite tubercle; pic: parasite intrusive cells; hc: host cortex; hcc: host central cylinder.

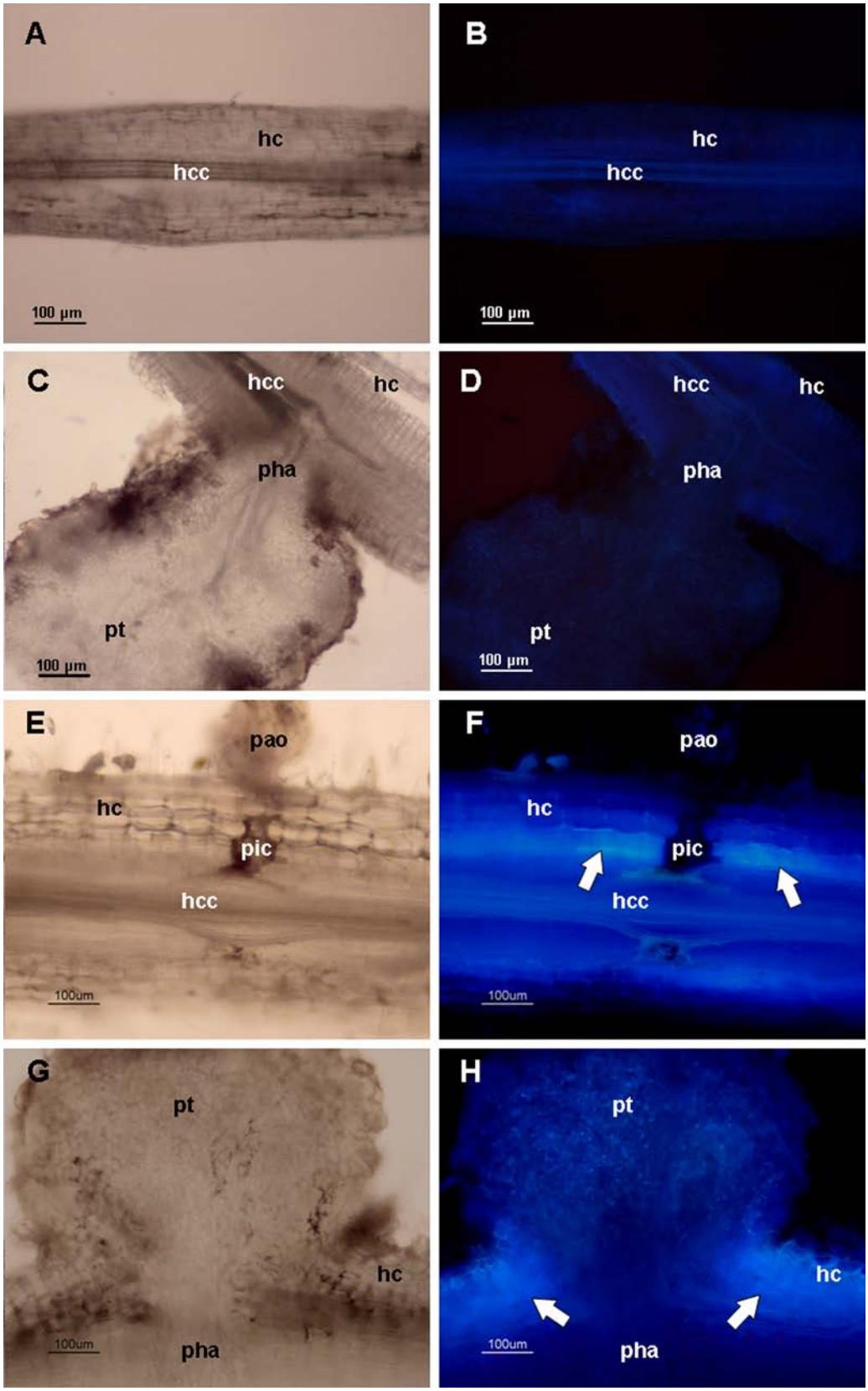

Fig. 5. *Hand cut fresh sections for fluorescence observation (A) Longitudinal section of an uninfected M. truncatula root observed under bright field. (B) Idem as (A) observed under UV excitation (340-380 nm). (C) Longitudinal section of a successful established O. crenata tubercle on SA4327 accession of M. truncatula observed under bright field. (D) Idem as (C) observed under UV excitation (340-380 nm). (E) Longitudinal section of an unsuccessful O. crenata seedling penetration on SA27774 accession of M. truncatula observed under bright field. (F) Idem as (E) observed under UV excitation (340-380 nm) and showing a strong fluorescence from host cells in contact with parasite tissues (arrows). (G) Cross section of a darkened O. crenata tubercle on SA4327 accession observed under bright field. (H) Idem as (G) observed under UV excitation (340-380 nm) and showing a strong fluorescence from host cells in contact with parasite tissues (arrows). hc: host cortex; hcc: host central cylinder; pha: parasite haustorium; pt: parasite tubercle; pao: parasite attachment organ; pic: parasite intrusive cells.*

Confocal laser scanning microscopy

Confocal microscopy studies were developed in order to get a more secure localization of phenolic compounds in tissues (Fig. 6). The emission spectra were collected using two channels (green and red) for the same excitation, in order to check differences in the fluorescence of the accumulated compounds. The fluorescence was detected within the host central cylinder (Fig. 6, A-D) and cortical cells (Fig. 6, E-H) in incompatible interactions on the early resistant accession (SA27774). Also accumulation of phenolics was observed in the attachment organ of some parasites in contact with the host root (Fig. 6, A-D).

Regarding incompatible interactions on the late resistant accession (SA4327), accumulation of phenolics was observed in the haustoria and tubercles of the parasite (Fig. 6, I-L) and within host xylem vessels connected with the parasite haustorium (Fig. 6, M-O). No presence of phenolics compounds was detected in compatible interactions on both accessions, SA4327 (Fig. 6P) and SA4087 (data not shown).

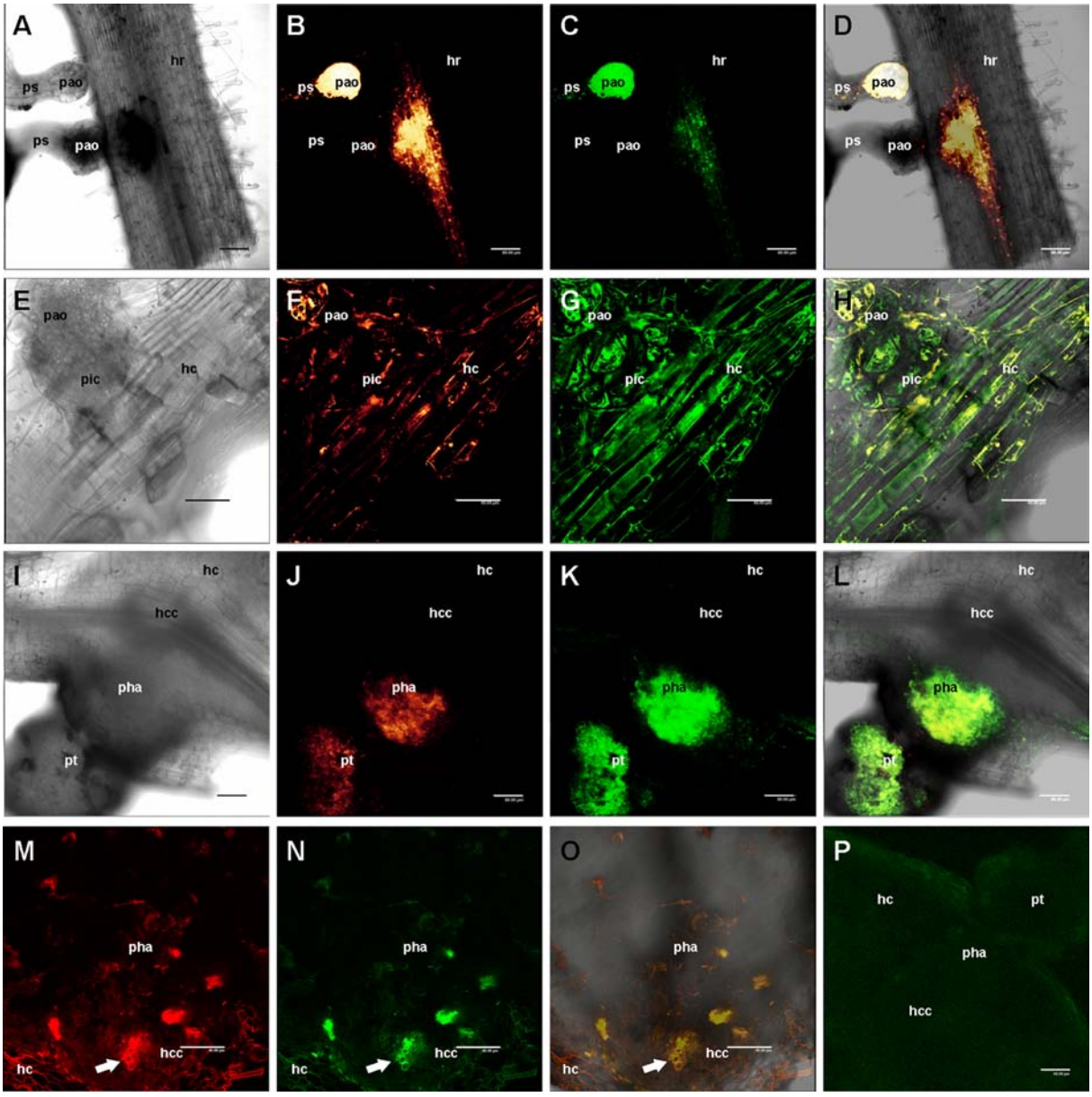

Fig. 6. *Localization of phenolic compounds using confocal laser microscopy. The images are single optical sections in (B), (C), (F), (G), (J), (K), (M), (N) and (P). Figures (B), (F), (J) and (M) correspond to emission spectra collected within the red channel (590-670 nm). Figures (C), (G), (K), (N) and (P) correspond to emission spectra collected within the green channel (515-590 nm). (A) Incompatible interaction of O. crenata on SA27774 accession of M. truncatula (transmission). A darkening of the attachment organ and root tissues can be observed. (B) Optical section of (A) showing intense fluorescence (red channel) in the host central cylinder and in the youngest attachment organ. (C) Idem as (B) through the green channel. (D) Overlay of (A), (B) and (C) showing the localization of the fluorescence in tissues. (E) Detail of an unsuccessful O. crenata seedling penetration on SA27774 accession (transmission). (F) Optical section of (E) showing intense fluorescence (red channel) in the host cells and in the parasite intrusive cells. (G) Idem as (F) through the green channel. (H) Overlay of (E), (F) and (G) showing the localization of the fluorescence in tissues. (I) Darkened O. crenata tubercle on SA4327 accession of M. truncatula (transmission). (J) Optical section of (I) showing intense fluorescence (red channel) in the haustorium and distal parts of the tubercle. (K) Idem as (J) through the green*

channel. (L) Overlay of (I), (J) and (K) showing the localization of the fluorescence in tissues. (M) Optical section of a darkened O. crenata tubercle on SA4327 accession showing intense fluorescence (red channel) in the host xylem vessels (arrow). (N) Idem as (M) through the green channel. (O) Overlay of (M) and (N) with a transmission image showing the localization of the fluorescence in tissues. (P) Optical section of a normal O. crenata tubercle on SA4327 accession. No fluorescence (green channel) can be detected. ps: parasite seedling; pao: parasite attachment organ; hr: host root; pic: parasite intrusive cells; hc: host cortex; hcc: host central cylinder; pha: parasite haustorium; pt: parasite tubercle. Scale bar: 80 µm in (A)-(D), (I)-(L), (P); 40 µm in (E-H), (M)-(O).

Cell viability assay

Trypan blue staining was used in fresh hand cut sections to check the viability of the cells in compatible and incompatible interactions (Fig. 7). In compatible interactions (Fig. 7, A and B) and uninfected roots (Fig. 7E) all the cells exclude the dye, confirming they were alive. However, the parasite intrusive cells and those corresponding to the attachment organ (Fig. 7, C and D) in incompatible interactions were clearly stained by the dye, indicating no viable cells. Moreover, parasite cells located in the distal part of the tubercle in incompatible interactions on the late resistant accession were also stained (Fig. 7F) and consequently were not viable.

Identification of phytoalexins

TLC plates showed the presence of known phytoalexins in the methanolic extracts of inoculated plants from both, soluble and cell wall bound phenolics fractions (Fig. 8). Medicarpin and maackiain were found in the soluble phenolic fraction of inoculated plants of both *M. truncatula* accessions. Scopoletin was identified in the cell wall bound phenolic fraction of inoculated plants of *M. truncatula* accession SA4327. Pisatin was not detected in any of the extracts. Several other compounds appeared on the TLC plate corresponding to soluble phenolics from inoculated plants, but they did not correlated with any of the phytoalexins used as standards. The retention factor (Rf) of the known phytoalexins were 0.158 for scopoletin, 0.526 for pisatin, 0.595 for maackiain and 0.632 for medicarpin.

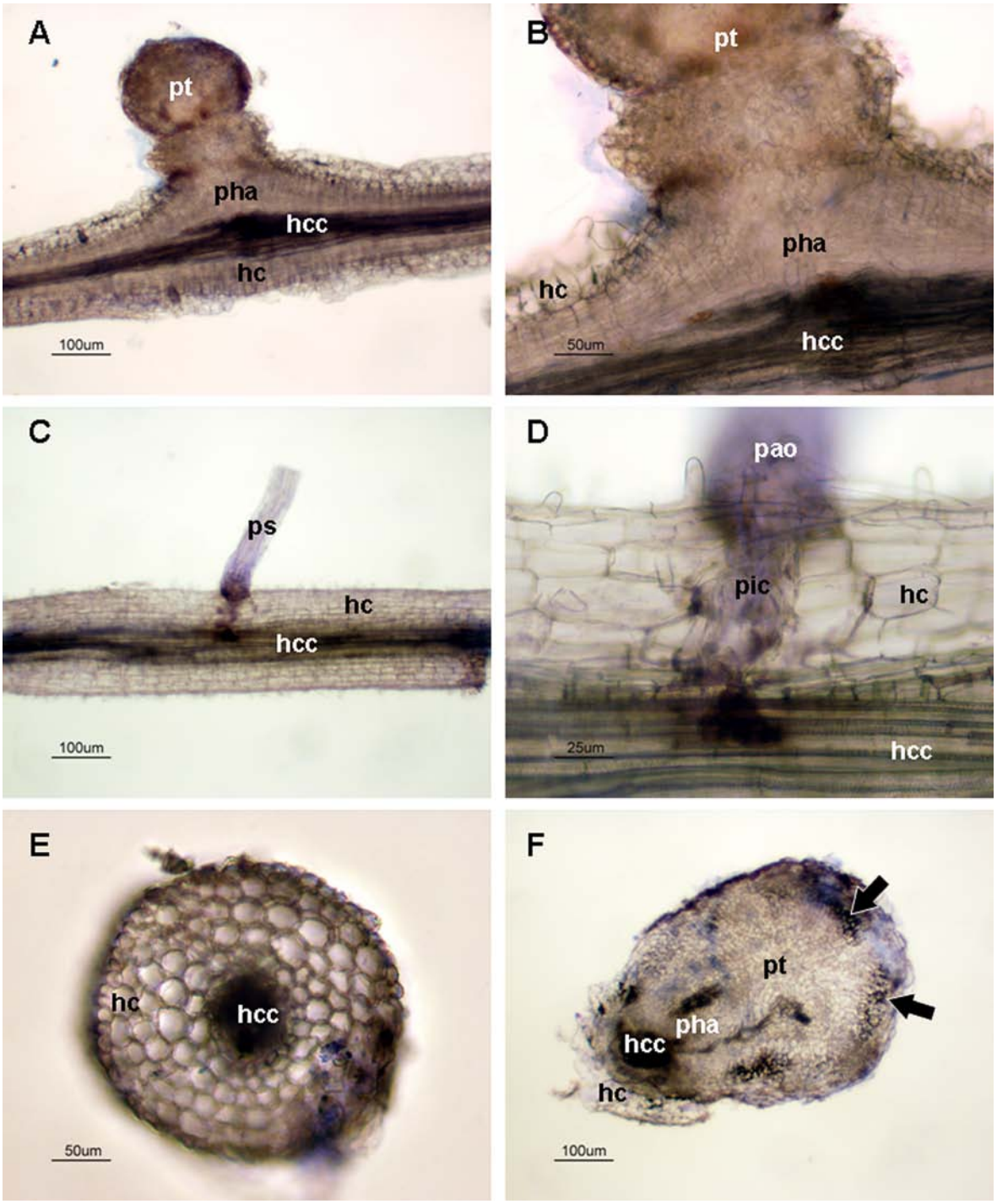

Fig. 7. *Hand cut fresh sections stained for cell viability. (A) Longitudinal section of a normal O. crenata tubercle on SA4327 accession of M. truncatula. (B) Detail of (A) showing the absence of stained cells in host and parasite tissues. (C) Longitudinal section of an unsuccessful O. crenata seedling penetration on SA27774 accession of M. truncatula. (D) Detail of (C) showing stained cells corresponding to the parasite intrusive cells and the attachment organ, indicating their loss of viability. (E) Cross section of an uninfected M. truncatula root showing the absence of stained cells. (F) Cross section of a darkened O. crenata tubercle on SA4327 accession showing stained cells (arrows) in the distal part of the tubercle. pt: parasite tubercle; pha: haustorium; hc: host cortex; hcc: host central cylinder; ps: parasite seedling; pao: parasite attachment organ; pic: parasite intrusive cells.*

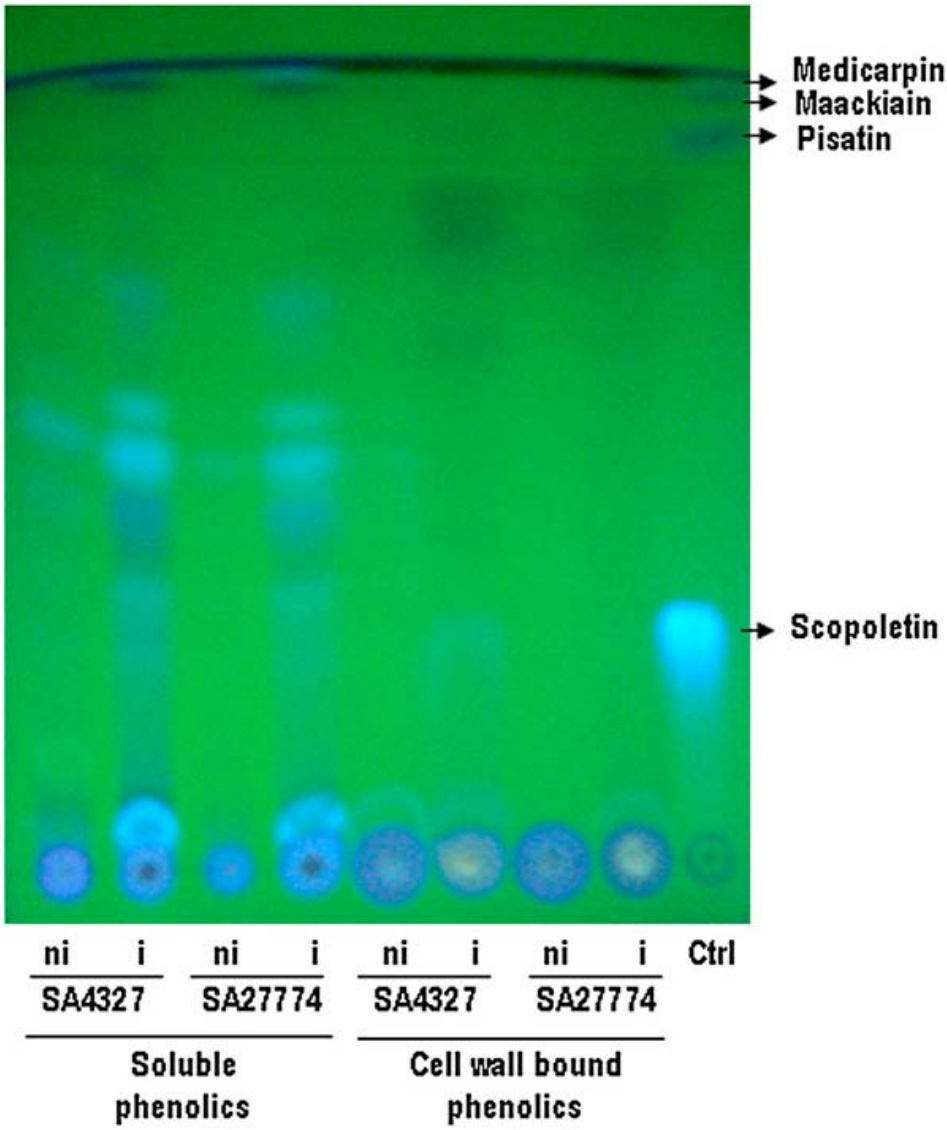

Figure 8*. TLC plate of the methanolic extract from root samples of O. crenata inoculated (i) and non inoculated (ni) M. truncatula plants. Ctrl: control with standard phytoalexins (scopoletin, medicarpin, pisatin and maackiain).*

Discussion

Mechanisms of resistance against *O. crenata* were characterized in two genotypes of *M. truncatula*. One of them, SA27774, shows an early expression of the resistance to this parasitic plant, and does not allow the establishment of the parasite. On the contrary, SA4327 is infected with *O. crenata* and allows the establishment and development of parasite tubercles. However, it is not completely susceptible to the pathogen attack, and a late resistance is expressed after tubercles establishment. This does not prevent completely the development of the parasitic plant, but limits the amount of individuals of the pathogen

growing on it. Both kind of incompatible interactions, appearing before or after the development of the parasite haustorium, have been previously reported in resistant host to parasitic plants (Labrousse *et al*., 2001; Serghini *et al*., 2001; Rubiales *et al*., 2003b; Zehhar *et al*., 2003; Pérez-de-Luque *et al*., 2005a,b; 2006a,b; Echevarría-Zomeño *et al*., 2006). They are indicative of resistance, but the exact nature of the mechanisms underlying such resistance is not well understood. For example, stoppage of seedling penetration has been usually associated to a hypersensitive response (HR) (Dörr *et al*., 1994; Goldwasser *et al*., 1997), but there is no conclusive evidence that a HR really occurs in these interactions (Rubiales *et al*., 2003b; Pérez-de-Luque *et al*., 2005b) in a manner similar to that described for fungal attack (Heath, 1999; Richael *and* Gilchrist, 1999). For that reason, histological and histochemical studies are of great value in order to know what is really happening inside host tissues.

The cytological data show that the penetration of *O. crenata* in the early resistant *M. truncatula* accession (SA27774) is stopped once the parasite intrusive cells have reached the host central cylinder. This is the first time that a pre-haustorial mechanism of resistance against parasitic root plants is located inside the central cylinder of the host. Usually, the pre-haustorial defensive mechanisms against parasitic plants have been located in the host cortex (Echevarría-Zomeño *et al*., 2006; Pérez-de-Luque *et al*., 2006a; 2007b) or the endodermis (Pérez-de-Luque *et al*., 2005b; 2006a; 2007b). This kind of resistance is also different to that found in rice and maize against the parasite *Striga* spp. (Gurney *et al*., 2003; 2006) where the parasite is stopped before penetrating the central cylinder, probably due to physical barriers as described in the case of *Orobanche* spp. But once the parasite reached the central cylinder, a haustorium was developed connecting with the hosts vascular tissues, and resistance relied on post-haustorial mechanisms such as sealing of vessels by mucilage (Pérez-de-Luque *et al*., 2005a; 2006b). Moreover, for the first time is also described a post-haustorial defensive mechanism different from the sealing of vessels (Pérez-de-Luque *et al*., 2005a; 2006b) in the late resistant *M. truncatula* accession (SA4327).

The only physical barrier detected against the parasite intrusion is the thickening of host xylem walls. This was reported some time ago (Dörr *et al*., 1994), and our results indicate that the secondary thickening of the xylem walls is composed by some kind of lignin, or at least (because no birefringence was detected) by some kind of polyphenol. Although some callose depositions were located, their presence was not enough or well located enough to stop broomrape penetration as has been recently found in faba bean (Pérez-de-Luque *et al*., 2007b). In this last case, big callose depositions were located in host cell walls in contact with

parasite tissues (i.e. at the point of the resistance) stopping the parasite penetration. However we cannot discard a possible role of callose as a reservoir of β-glucans elicitors (Esquerré-Tugayé *et al*., 2000) as suggested in the case of pea-*O. crenata* (Pérez-de-Luque *et al*., 2006a).

So the lack of strong physical barriers preventing the parasite penetration into the host must be complemented and reinforced by another type of defensive mechanism: The fluorescence points towards the presence of phenolic compounds (phytoalexins) as the mechanism responsible to stop parasite intrusion, as has been recently reported in the sunflower – *O. cumana* interaction (Echevarría-Zomeño *et al*., 2006). However, contrary to what has been shown in that work, in which suberization plays a crucial role stopping *O. cumana* penetration in the cortex, no physical barriers appears in *M. truncatula* roots, and the parasite intrusive cells are able to pierce easily through the cortex and the endodermis, reaching the vascular cylinder. At this moment, an intense release of phenolic compounds at the infection point takes place, through the host cells in contact with the parasite tissues and the xylem vessels. Medicarpin and maackiain have been found as part of the soluble phenolics fraction in inoculated plants, and both phytoalexins have been previously reported as implicated in defence against pathogens (Cachinero *et al*., 2002). This maybe creates an unpleasant environment for the parasite intrusive cells, contributing to their further death and avoiding the development of an haustorium. Moreover, these phenolic compounds seem to be secreted to the external part of the root, affecting broomrape seedlings attached near a previous unsuccessful penetration attempt. This is not strange, because accumulation and secretion of phytoalexins against parasitic plants has been previously reported (Goldwasser *et al*., 1999; Serghini *et al*., 2001; Echevarría-Zomeño *et al*., 2006). The absence of dead host cells in this case, confirmed by the viability test, supports that this defensive mechanism is not a HR. However, other mechanisms of resistance acting at the same time cannot be discarded. For example, hormonal compatibility between host and parasite is needed in order to develop a functional haustorium (Joel and Pérez-de-Luque, unpublished results), and a lack of this compatibility could affect the normal parasite growth.

In the case of the late resistance found in SA4327, the accumulation and secretion of phenolic compounds seems to be operating but at a later stage. Once the parasite has formed a haustorium and established vascular connections with the host, the last one produces phenolic compounds which are translocated through the vascular system and reach the parasite. The first evidence for this is the presence of a dark deposit in parasite vessels of the haustorium.

This deposit probably corresponds with the oxidation of phenolic compounds, what usually originates dark brown components (Takahama, 2004). The fluorescence found in host vessels, haustoria and tubercles implies that the host is poisoning the parasite established tubercles releasing phytoalexins through the vascular connections. These phytoalexins accumulates in the tubercles by the sink effect that *O. crenata* has once it has been connected with the host root. The presence of parasite dead cells in the same areas were phenolic compounds accumulate within the tubercles could indicate that the accumulation of toxic metabolites (phenolics) from the host plant is killing the parasite. The presence of soluble phenolics like medicarpin and maackiain also supports the idea of excretion of phytoalexins. As in the previous case, other(s) defensive mechanism(s) cannot be discarded, including the lack of hormonal compatibility. The presence of scopoletin in the cell wall bound phenolics fraction could be an indicative of further development of physical barriers not detected at this point by cytochemical methods. All these results are in accordance with those obtained by Dita *et al*. (2007), who found an activation of genes related with the synthesis of phenolic compounds also in early and late resistant accessions to *O. crenata*. The main difference was, like in this case, a matter of time: similar genes were activated but with a time gap between them.

Conclusion

Recent studies have revealed that multiple factors are involved in resistance to parasitic plants. Behind the observation of incompatible interactions (unsuccessful attachment-penetration and darkening of established tubercles) underlies a complex system of multiple mechanisms of resistance. To date, most of those described were based mainly in physical barriers preventing parasite penetration into the host central cylinder (pre-haustorial mechanisms) and blocking of host vessels disrupting the nutrient fluxes between host and parasite (post-haustorial mechanisms). In this work we presented for the first time one mechanisms of resistance, accumulation of phytoalexins (phenolic compounds), that does not rely on physically stopping parasite penetration into the host: the parasite penetrates reaching the central cylinder, but it seems to be poisoned and killed before developing a haustorium. Despite other mechanisms of resistance could be involved, a crucial difference between both accessions is the moment at which the host detects and reacts against the parasite. It determines a more effective resistance against the pathogen: the earliest the parasite is detected, the most effective are the defensive mechanisms activated, and the infection is lower.

Acknowledgements

We thank the microscopy service of the University of Córdoba-SCAI where CLM observations were made. A P-d-L is a researcher at the IFAPA funded by the programme "Juan de la Cierva" of the Spanish Ministry of Education and Science.

References

Antonova TS and Ter Borg SJ. 1996. The role of peroxidase in the resistance of sunflower against *Orobanche cumana* in Russia. *Weed Res* **36**: 113-121.

Baayen RP, Ouellette GB, Rioux D. 1996. Compartmentalization of decay in carnations resistant to *Fusarium oxysporum* f. sp. dianthi. *Phytopathology* **86**: 1018-1031.

Blondon F, Marie D, Brown S, Kondorosi A. 1994. Genome size and base composition in *Medicago sativa* and *M. truncatula* species. *Genome* **37**: 264-275.

Bordallo JJ, Lopez-Llorca LV, Jansson HB, Salinas J, Persmark L, Asensio L. 2002. Colonization of plant roots by egg-parasitic and nematode-trapping fungi. *New Phytol* **154**: 491-499.

Cachinero JM, Hervás A, Jiménez-Díaz RM, Tena M. 2002. Plant defence reactions against fusarium wilt in chickpea induced by incompatible race 0 of *Fusarium oxysporum* f.sp. ciceris and nonhost isolates of *F. oxysporum*. *Plant Pathol* **51**: 765–776.

Cook DR. 1999. *Medicago truncatula*: a model in the making. *Curr Opin Plant Biol* **2**: 301-304.

Cook DR, VandenBosh K, De Bruijn FJ, Huguet T. 1997. Model legumes get the nod. *Plant Cell* **9**: 275-281.

Crews LJ, McCully ME, Canny MJ. 2003. Mucilage production by wounded xylem tissue of maize roots - time course and stimulus. *Funct Plant Biol* **30**: 755-766.

Dita MA, Die JV, Román B, Krajinski F, Küster H, Moreno MT, Cubero JI, Rubiales D. 2007. Gene expression profiling of *Medicago truncatula* roots in response to the parasitic plant *Orobanche crenata*. *Planta*, submitted.

Dörr I, Staack A, Kollmann R. 1994. Resistance of Helianthus to *Orobanche* – histological and cytological studies. In AH Pieterse, JAC Verkleij, SJ ter Borg, eds, Biology and management of *Orobanche*, Proceedings of the Third International Workshop on *Orobanche* and related *Striga* research. Royal Tropical Institute, Amsterdam, pp 276-289.

Dörr I. 1997. How *Striga* parasitizes its host: a TEM and SEM study. *Ann Bot* **79**: 463-472.

Echevarría-Zomeño S, Pérez-de-Luque A, Jorrín J, Maldonado AM. 2006. Pre–haustorial resistance to broomrape (*Orobanche cumana*) in sunflower (*Helianthus annuus*): cytochemical studies. *J Exp Bot* **57**: 4189-4200.

Ellwood S, Lichtenzveig J, Pfaff T, Kamphuis L, Oliver R. 2007. Fungi. In: *The Medicago truncatula handbook*, http://www.noble.org/MedicagoHandbook.

Esquerré-Tugayé MT, Boudard G, Dumas B. 2000. Cell wall degrading enzymes, inhibitory proteins, and oligosaccharides participate in the molecular dialogue between plants and pathogens. *Plant Physiol Biochem* **38**:157–163.

Goldwasser Y, Kleifeld Y, Plakhine D, Rubin B. 1997. Variation in vetch (*Vicia* spp.) response to *Orobanche aegyptiaca*. *Weed Sci* **45**: 756-762.

Goldwasser Y, Hershenhorn J, Plakhine D, Kleifeld Y, Rubin B. 1999. Biochemical factors involved in vetch resistance to *Orobanche aegyptiaca*. *Physiol Mol Plant P* **54**: 87–96.

Goldwasser Y, Plakhine D, Kleifeld Y, Zamski E, Rubin B. 2000. The differential susceptibility of vetch (*Vicia* spp.) to *Orobanche aegyptiaca*: anatomical studies. *Ann Bot* **85**: 257-262.

González-Verdejo CI, Barandiaran X, Moreno MT, Cubero JI, Di-Pietro A. 2005. An improved axenic system for studying pre-infection development of the parasitic plant *Orobanche ramosa*. *Ann Bot* **96**: 1121-1127.

Gowda BS, Riopel JL, Timko MP. 1999. NRSA-1: a resistance gene homolog expressed in roots of non-host plants following parasitism by *Striga asiatica* (witchweed). *Plant J* **20**: 217-230.

Gurney AL, Grimanelli D, Kanampiu F, Hoisington D, Scholes JD, Press MC. 2003. Novel sources of resistance to *Striga hermonthica* in *Trypsacum dactyloides* a wild relativesof maize. *New Phytol* **160**: 557-568.

Gurney AL, Press MC, Scholes JD. 2006. A novel form of resistance in rice to the angiosperm parasite *Striga hermonthica*. *New Phytol* **169**: 199-208.

Heath MC. 1999. The enigmatic hypersensitive response: induction, execution, and role. *Physiol Mol Plant Pathol* **55**: 1-3.

Heide-Jørgensen HS. 1987. Development and ultrastructure of the haustorium of *Viscum minimum*. I: The adhesive disk. *Can J Bot* **67**: 1161-1173.

Heide-Jørgensen HS and Kuijt J. 1993. Epidermal derivatives as xylem elements and transfer cells: a study of the host-parasite interface in two species of *Triphysaria* (Scrophulariaceae). *Protoplasma* **174**: 173-183.

Heide-Jørgensen HS and Kuijt J. 1995. The haustorium of the root parasite *Triphysaria* (Scrophulariaceae), with special reference to xylem bridge ultrastructure. *Amer J Bot* **82**: 782-797.

Hoagland DR and Arnon DI. 1950. The water-culture method for growing plants without soil. California Agricultural Experiment Station Circular 347. University of California, Berkeley.

Hutzler P, Fischbach R, Heller W, Jungblut TP, Reuber S, Schmitz R, Veit M, Weissenbock G, Schnitzler J. 1998. Tissue localization of phenolic compounds in plants by confocal laser scanning microscopy. *J Exp Bot* **49**: 953-965.

Joel DM. 1983. AGS (Alcian Green Safranin) - A simple differential staining of plant material for the light microscope. Proc RMS **18**: 149-151.

Joel DM and Losner-Goshen D. 1994. The attachment organ of the parasitic angiosperms *Orobanche cumana* and *O. aegyptiaca* and its development. *Can J Bot* **72**: 564-574.

Joel DM, Losner-Goshen D, Hershenhorn J, Goldwasser Y, Assayag M. 1996. The haustorium and its development in compatible and resistant host. In MT Moreno, JI Cubero, D Berner, D Joel, LJ Musselman, C Parker, eds. Advances in parasitic plant research. Junta de Andalucía, Consejería de Agricultura y Pesca, Sevilla, pp 531-541.

Joel DM, Hershenhorn Y, Eizenberg H, Aly R, Ejeta G, Rich PJ, Ransom JK, Sauerborn J, Rubiales D. 2007. Biology and Management of Weedy Root Parasites. In J Janick, ed, *Horticultural Reviews*, Vol 33. John Wiley & Sons, Hoboken, pp 267-349.

Labrousse P, Arnaud MC, Serieys H, Bervillé A, Thalouarn P. 2001. Several mechanisms are involved in resistance of *Helianthus* to *Orobanche cumana* Wallr. *Ann Bot* **88**: 859-868.

Mangnus EM, Stommen PLA, Zwanenburg B. 1992. A standardized bioassay for evaluation of potential germination stimulants for seeds of parasitic weeds. *J Plant Growth Regul* **11**: 91-98.

Mellersh DG, Foulds IV, Higgins VJ, Heath MC. 2002. H_2O_2 plays different roles in determining penetration failure in three diverse plant-fungal interactions. Plant J **29**: 257-268.

Neumann U, Vian B, Weber, HC, Sallé G. 1999. Interface between haustoria of parasitic members of the Scrophulariaceae and their host: a histochemical and inmunocytochemical approach. *Protoplasma* **207**: 84-97.

O'Brien TP and McCully ME. 1981. The study of plant structure. Principles and selected methods. Termarcarphi Pty. Ltd., Melbourne.

Pérez-de-Luque A, Jorrín J, Cubero JI, Rubiales D. 2005a. Resistance and avoidance against *Orobanche crenata* in pea (*Pisum* spp.) operate at different developmental stages of the parasite. *Weed Res* **45**: 379-387.

Pérez-de-Luque A, Rubiales D, Cubero JI, Press MC, Scholes J, Yoneyama K, Takeuchi Y, Plakhine D, Joel DM. 2005b. Interaction between *Orobanche crenata* and its host legumes: Unsuccessful haustorial penetration and necrosis of the developing parasite. *Ann Bot* **95**: 935-942.

Pérez-de-Luque A, González-Verdejo CI, Lozano MD, Dita MA, Cubero JI, González-Melendi P, Risueño MC, Rubiales D. 2006a. Protein cross-linking, peroxidase and β-1,3-endoglucanase involved in resistance of pea against *Orobanche crenata*. *J Exp Bot* **57**: 1461-1469.

Pérez-de-Luque A, Lozano MD, Cubero JI, González-Melendi P, Risueño MC, Rubiales D. 2006b. Mucilage production during the incompatible interaction between *Orobanche crenata* and *Vicia sativa*. *J Exp Bot* **57**: 931-942.

Pérez-de-Luque A, Lozano MD, Maldonado AM, Jorrín JV, Dita MA, Die J, Román B, Rubiales D. 2007a. *Medicago truncatula* as a model for studying interactions between root parasitic plants and legumes. In: *The Medicago truncatula handbook,* http://www.noble.org/MedicagoHandbook

Pérez-de-Luque A, Lozano MD, Testillano PS, Moreno MT, Rubiales D. 2007b. Resistance to broomrape (*Orobanche crenata*) in faba bean (*Vicia faba*): cell wall changes associated with pre-haustorial defensive mechanisms. *Ann Appl Biol* **151**: 89-98.

Prats E, Bazzalo ME, Leon A, Jorrin J. 2003. Accumulation of soluble phenolic compounds in sunflower capitula correlates with resistance to *Sclerotinia sclerotiorum*. *Euphitica* **132**: 321-329.

Reiss GC and Bailey JA. 1998. *Striga* gesnerioides parasitising cowpea: development of infection structures and mechanisms of penetration. *Ann Bot* **81**: 431-440.

Richael C and Gilchrist D. 1999. The hypersensitive response: A case of hold or fold? *Physiol Mol Plant Pathol* **55**: 5-12.

Rioux D, Nicole M, Simard M, Ouellette GB. 1998. Immunocytochemical evidence that secretion of pectin occurs during gel (gum) and tylosis formation in trees. *Phytopathology* **88**: 494-505.

Rodríguez-Conde MF, Moreno MT, Cubero JI, Rubiales D. 2004. Characterization of the *Orobanche* - *Medicago truncatula* association for studying early stages of the parasite-host interaction. *Weed Res* **44**: 218-223.

Rubiales D. 2001. Parasitic plants: an increasing threat. *Grain Legumes* **33**: 10-11.

Rubiales D, Sillero JC, Román MB, Moreno MT, Fondevilla S, Pérez-de-Luque A, Cubero JI, Zermane N, Kharrat M and Khalil S. 2002. Management of broomrape in Mediterranean agriculture. In: AEP, ed, Legumed: Grain Legumes in the Mediterranean Agriculture. European Association for Grain Legume Research, Rabat, pp 67-73.

Rubiales D. 2003. Parasitic plants, wild relatives and the nature of resistance. *New Phytol* **160**: 459-461.

Rubiales D, Pérez-de-Luque A, Joel DM, Alcántara C, Sillero JC. 2003b. Characterization of resistance in chickpea to crenate broomrape (*Orobanche crenata*). *Weed Sci* **51**: 702-707.

Rubiales D, Pérez-de-Luque A, Fernández-Aparicio M, Sillero JC, Román B, Kharrat M, Khalil S, Joel DM, Riches C. 2006. Screening techniques and sources of resistance against parasitic weeds in grain legumes. *Euphyt* **147**: 187-199.

Ruzin SE. 1999. Plant microtechnique and microscopy. Oxford University Press, Oxford.

Serghini K, Pérez-De-Luque A, Castejón-Muñoz M, García-Torres L, Jorrín JV. 2001. Sunflower (*Helianthus annuus L.*) response to broomrape (*Orobanche cernua* Loefl.) parasitism: induced synthesis and excretion of 7-hydroxylated simple coumarins. *J Exp Bot* **52**: 2227-2234.

Takahama U. 2004. Oxidation of vacuolar and apoplastic phenolic substrates by peroxidase: Physiological significance of the oxidation reactions. *Phytochem Rev* **3**: 207-219.

Vaughn KC. 2002. Attachment of the parasitic weed dodder to the host. *Protoplasma* **219**: 227-237.

Vaughn KC. 2003. Dodder hyphae invade the host: a structural and immunocytochemical characterization. *Protoplasma* **220**: 189-200.

Zehhar N, Labrousse P, Arnaud MC, Boulet C, Bouya D, Fer A. 2003. Study of resistance to *Orobanche ramosa* in host (oilseed rape and carrot) and non-host (maize) plants. *European J Plant Pathol* **109**: 75-82.

CAPÍTULO IV: "¡Acábalo YA!"

Resistance to *Orobanche crenata* in the model legume *Medicago truncatula*: the flavonoid response

Annals of Botany (2011): Submitted

María-Dolores Lozano-Baena[1], Elena Prats[1], Diego Rubiales[1] and Alejandro Pérez-de-Luque[2]

[1] *CSIC (Institute for Sustainable Agriculture), Apdo. 4084, 14080 Córdoba, Spain* and

[2] *IFAPA, Avda. Menendez Pidal s/n, PO Box 3092, 14004 Córdoba, Spain*

Background and Aims

Orobanche crenata Forsk. (crenate broomrape) is a weedy root parasite that represent the major constraint for legume crops in Mediterranean Basin and West Asia. This obligate root holoparasite depends completely on its host for all nutritional requirements. Little is known on resistance mechanisms in legume crops such as faba bean, vetches and pea what is hampered by their complex genome and physiology and the little genomic resources available. To facilitate identification of genes and metabolic pathways activated in resistance reactions we have studied the response against *O. crenata* attack using the model legume *Medicago truncatula* Gaertn. (barrel medic). *M. truncatula* seems to defend from *O. crenata* infection mainly using chemical compounds i.e. flavonoids (phytoalexins). These phenolic compounds are well known in plant kingdom due to their antifungal and antimicrobial activity. In this work we identified and quantified by the first time some of the flavonoids acting against *O. crenata* invasion using two *M. truncatula* accessions with different resistances.

Methods

To identify and quantify some of the flavonoids produced by *M. truncatula* as response to the *O. crenata* attack, we have used high performance liquid chromatography with UV and mass spectrometric detection (LC-MS/MS) systems as well recognized methods to profile flavonoids in plant tissue extracts.

Key Results

Three of the standards (naringenin, daidzein and formononetin) were identified and quantified in the analysed root tissues for soluble phenolic samples but only formononetin appeared in both inoculated and non inoculated roots (naringenin and daidzein were only detected in inoculated roots of the SA4327 accession). No standard was detected in cell wall-bound phenolic extracts. Medicarpin, genistein, chlorogenic acid and scopoletin were not detected in any case and maackiain could not be analysed due to its instability.

Conclusions

This is the first report of flavonoids presents in the plant-plant parasite interaction *M. truncatula-O. crenata* such as defence response against this parasite. Our results probed that the model legume *M. truncatula* produces certain flavonoids (phytoalexins), defending itself and avoiding *O. crenata* attack.

Introduction

Crenate broomrapes (*Orobanche crenata* Forsk.) are root holoparasitic plants specialized in attacking cool season legume crops. This parasitic weed represents the major constraint for grain and forage legume production in Mediterranean and West Asian countries, resulting in complete yield loss with severe infestations and removing otherwise productive land from effective use for very long periods of time (Rubiales *et al*., 2006; Joel *et al*., 2007). Legumes are an important crop family to humans as a source of food, feed for livestock and raw materials for industry (Graham *and* Vance, 2003).

Phytoalexins are polycyclic compounds (phenolics) commonly-know by plant pathologists due to their antifungal, antiinsect and antimicrobial activity (Dakota *and* Phillips, 1996). These compounds are synthesized "de novo" in response to pathogen elicitors or damages via phenylpropanoid pathway (Dixon *et al*., 2002; Yu *and* McGonigle, 2005). Legumes are known to produce and accumulate specific phytoalexins named isoflavonoids as defence against different attacks including UVB light, anaerobic mediums, heavy metals, herbivorous and pathogens (Aoki *et al*., 2000; Dixon *and* Sumner, 2003). Phenolics have recently been shown to as plant defence compounds against broomrapes (Pérez-de-Luque *et al*., 2005a; Echevarría-Zomeño *et al*., 2006; Lozano-Baena *et al*., 2007) as in other plant-plant parasite interactions (Ueda *and* Sugimoto, 2010). For this reason, qualitative and quantitative determination of isoflavonoids expressed in legume crops against pathogens is important to understand plant defences and to design control strategies.

Unfortunately, little genomic resources are available for most cool season grain and forage legumes such as faba beans (*Vicia faba* L.), lentils (*Lens culinaris* Medik), peas (*Pisum sativum* L.) or vetches (*Vicia sativa* L.). Nevertheless, *Medicago truncatula* Gaertn. (barrel medic) has been selected as a model legume (Benedito *et al*., 2008; Rispail *et al*., 2010) because of its small diploid genome, self-fertility, short life cycle, high seed production, ease of cultivation and possibility of genetic transformation. Development of techniques and methods for molecular and genetic analysis and the genome sequence (http://www.medicago.org) provide new tools which make *M. truncatula* a suitable model for legume genomic research.

Different mechanisms of resistance against *O. crenata* have been reported in *M. truncatula* germplasm (Rodríguez-Conde *et al*., 2004; Fernández-Aparicio *et al*., 2008). Accessions SA4327 and SA27774 have been the subject of recent cytological and molecular

studies revealing that both accessions present similar defence mechanisms but acting at different timing, being the resistance of SA27774 early acting and that of SA4327 late acting (Lozano-Baena *et al*., 2007; Pérez-de-Luque *et al*., 2007; Castillejo *et al*., 2009). Thus, resistance act in SA27774 during host tissues invasion, whereas in SA4327 acts after establishment of vascular connections.

Cytological studies showed that resistance is due to accumulation of compounds (i.e. phenolics) (Lozano-Baena *et al*., 2007) in host tissues around infection points that accumulate into parasite. The same reaction has been described in the interaction of *O. cumana* with its host sunflower (*Helianthus annus* L.) where fluorescence and confocal laser microscopy (CLM) observations revealed accumulation of phenolic compounds during the incompatible reaction (Echevarría-Zomeño *et al*., 2006). Sealing of vessels or callose found before in sunflower (Echevarría-Zomeño *et al*., 2006) was not evident if *M. truncatula*.

In the present study, we identified and quantified some of the flavonoids produced by *M. truncatula* as response to the *O. crenata* attack using high performance liquid chromatography with UV and mass spectrometric detection (LC-MS/MS) systems as well recognized methods to profile flavonoids in plant tissue extracts (Prasain *et al*., 2004; Deavours *and* Dixon, 2005). As standards, we have selected some of the main *M. truncatula* flavonoids of the phenylpropanoid pathway probed as defence compounds in pathogen invasions (Naoumkina *et al*., 2007; Farag *et al*., 2008; Lozano-Baena *et al*., 2007), in its close relative alfalfa (*M. sativa* L.) (He *and* Dixon, 2000), as well as in other species (Shimada *et al*., 2000) (Fig. 1). Specifically, chlorogenic acid is a product of cinnamic acid metabolism (Steck, 1968), an important intermediate of lignin biosynthesis with anti-pathogenic properties (Jöet *et al*., 2010) and has been reported to be produced by alfalfa under stress conditions (Jorrín *and* Dixon, 1990). Scopoletin is a coumarin, a class of secondary metabolites with antimicrobial properties and derived from phenylpropanoid pathway in plants, that is involved too in lignin biosynthesis (Kai *et al*., 2008). Naringenin were selected due to be the start point to other phenolic synthesis (i.e. flavones, flavonols, anthocyanins and condensed tannins) with defensive roles against parasites, and the precursor of the mainly isoflavonoids analysed (Deavours *and* Dixon, 2005; Farag *et al*., 2008; Limem *et al*., 2008) (Fig. 2) i.e. daidzein and genistein (next steps in this metabolic pathway). Moreover, these simple isoflavonoids are not only phytoalexin precursors but they inhibit the growth of microorganisms themselves (Dakota *and* Phillips, 1996). Daidzein plays another important role in this pathway due to be the precursor of phytoalexins in legume plants (Dixon *et al*.,

1996; He *and* Dixon, 2000; Shimada *et al*., 2000; Dixon *et al*., 2002; Deavours *and* Dixon, 2005; Yu *and* McGonigle, 2005), specifically, two pterocarpans directly related with *M. truncatula* defence response: medicarpin (the major phytoalexin produced in alfalfa) and its precursor formononetin (Dixon *et al*., 1996; Naoumkina *et al*., 2007; Farag *et al*., 2008). And finally, maackiain is an important phytoalexin pterocarpan with antifungal activity and precursor of pisatin (another phytoalexin), present in pea (Aoki *et al*., 2000).

Therefore, to identify the presence and concentration of these standards in samples could help in understanding *M. truncatula* / *O. crenata* interaction.

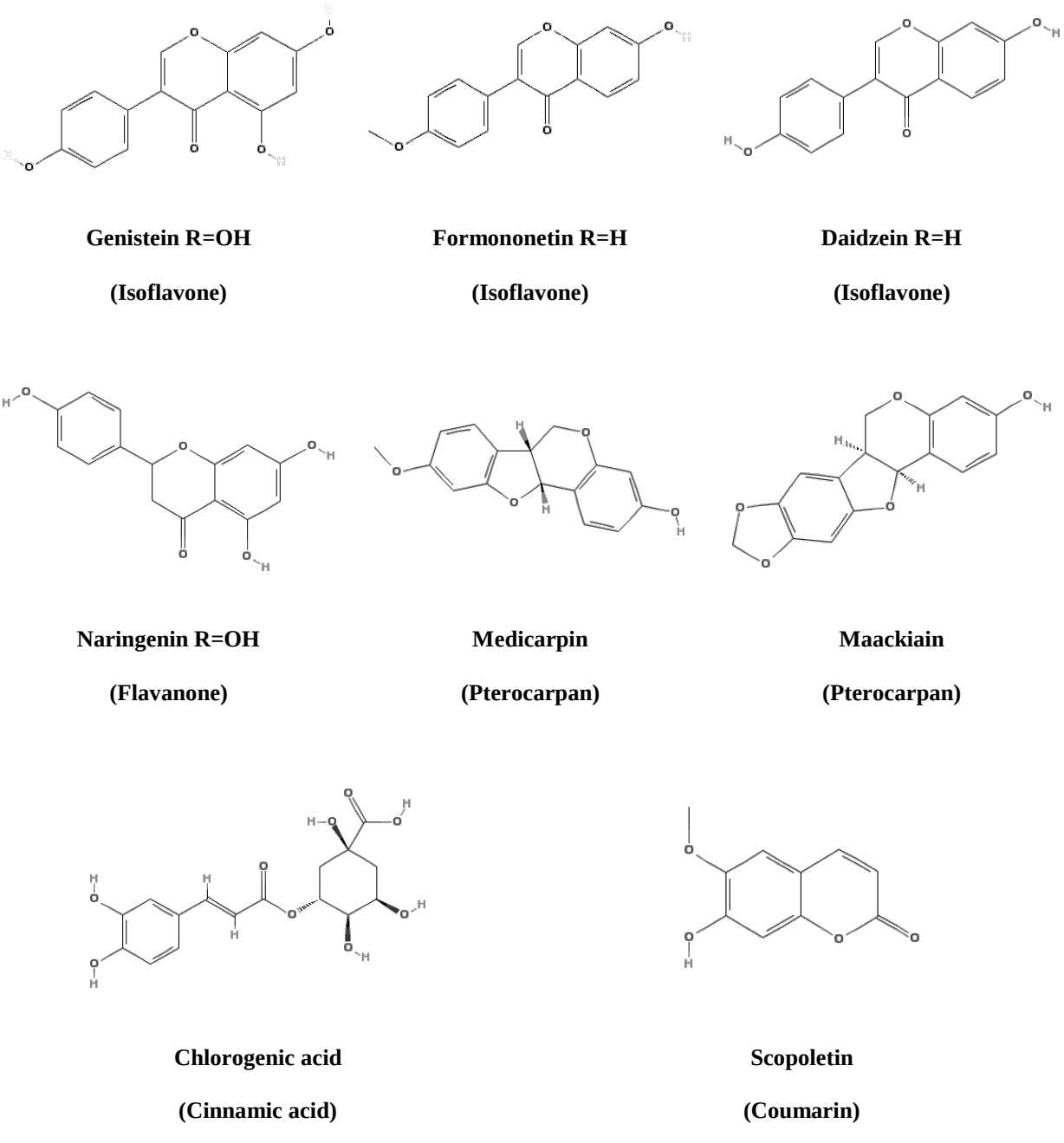

Genistein R=OH

(Isoflavone)

Formononetin R=H

(Isoflavone)

Daidzein R=H

(Isoflavone)

Naringenin R=OH

(Flavanone)

Medicarpin

(Pterocarpan)

Maackiain

(Pterocarpan)

Chlorogenic acid

(Cinnamic acid)

Scopoletin

(Coumarin)

Fig. 1. *Structure of analysed phytoalexins.*

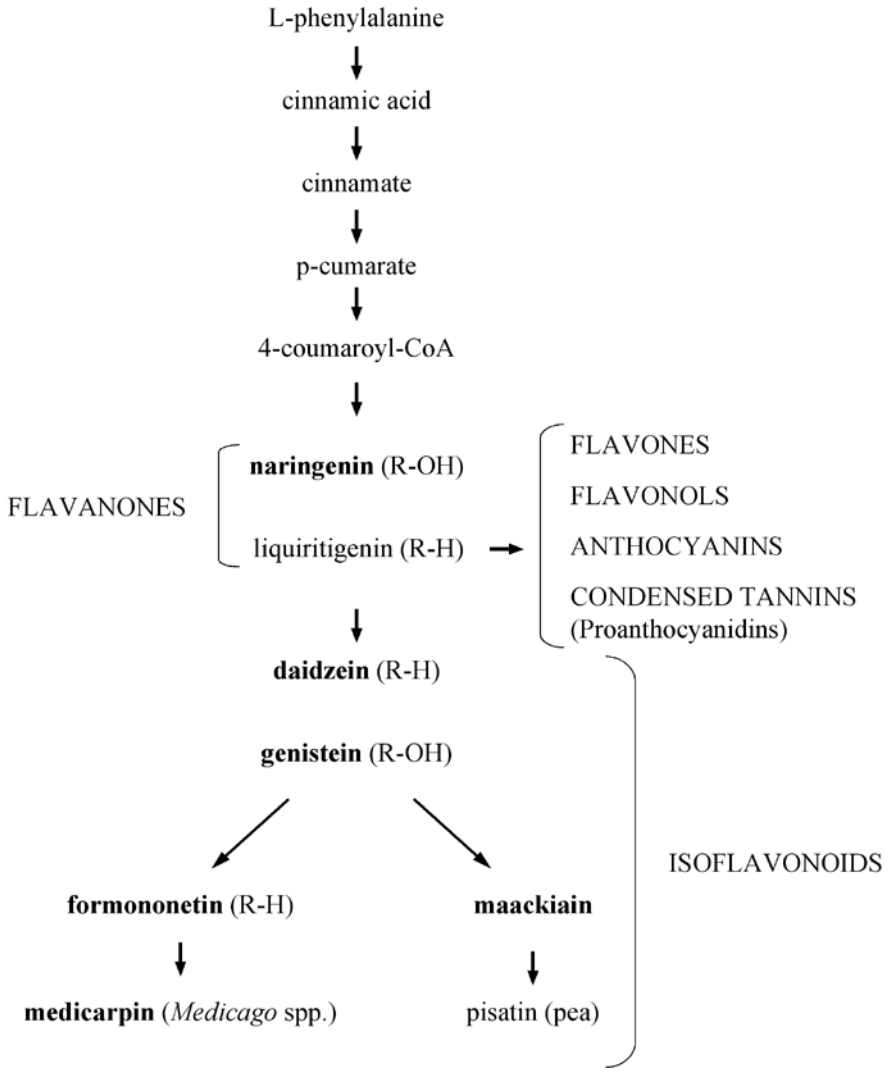

Fig. 2. *Phenylpropanoid pathway.*

Materials and Methods

Plant material and growth conditions

Crenate broomrape was grown on two *Medicago truncatula* accessions showing early and late resistance to this pathogen (accessions SA27774 and SA4327, respectively). The petri dish system described by Pérez-de-Luque *et al*. (2005a) was used for in vitro cultivation of the *M. truncatula* plants and inoculation with *O. crenata* seeds. *M. truncatula* seeds were supplied from the South Australian Research and Development Institute Genetic Resource Centre in Australia (origin: Morocco for SA27774 and Yugoslavia for SA4327). Seeds were scarified slightly scratching the cuticle with a razor blade and sterilized in commercial bleach (20% in sterile water) for 10 min. For synchronized germination, seeds were placed at 4ºC for

36 h in sterile water. During this period, sterile water was replaced two or three times to help germination. After that, seeds were rinsed with sterile water at room temperature for 3 h, changing it six times. Finally, seeds were placed in petri dishes on wet glass fibre filter papers (Whatmann GF/A) and kept in darkness at 20ºC for 1 to 2 days. When the radicle reached 2 cm length, seedlings were transferred to new dishes (15 cm diameter) with perlite and new glass fibre papers (Pérez-de-Luque *et al*., 2005a). *O. crenata* seeds were collected from infected faba bean (*Vicia faba*) plants at Córdoba (Spain) during 2000. They were disinfected with formaldehyde according to González-Verdejo *et al*. (2005) and spread on the glass fibre paper (approximately 8 mg) where *M. truncatula* roots were growing. At the same time, some seedlings were kept without inoculation as controls. To prevent exposure of the parasite seeds and host roots to direct light, the dishes containing test plants were covered with aluminium foil. Then, the upward growing host plants were placed vertically in trays with Hoagland nutrient solution (Hoagland *and* Arnon, 1950) and grown in a controlled environment chamber at 20ºC ± 0.5ºC with a day/night 14 h photoperiod and an irradiance of 200 µmol m^{-2} s^{-1}. At the same time plants were growing, crenate broomrape seeds were conditioned. For conditioning, parasite seeds need to be in a humid environment in darkness at 20ºC for 10 days (Pérez-de-Luque *et al*., 2005a).

After conditioning period, we applied 5 ml of the synthetic stimulant GR24 (0.01 mg/ml; Magnus *et al*., 1992) on the paper with the seeds for *O. crenata* homogenous germination induction.

Collection of samples

Root samples were harvested 15 days after GR24 application, time at which many of the haustorium are formed (Fig. 3) and plant defence mechanisms are expected to be acting. Another indication of the best moment to collect samples was the aspect that *O. crenata* radicles showed during collection. When samples were harvested, we could observe morphological differences between *M. truncatula* accessions and *O. crenata* parasites corresponding with the aspect described before (Fig. 3). Tissue samples collected from SA4327 showed a healthy appearance and growing as expected but *O. crenata* radicles infecting SA27774 had stopped their development and both, host and parasite close tissues seemed dark.

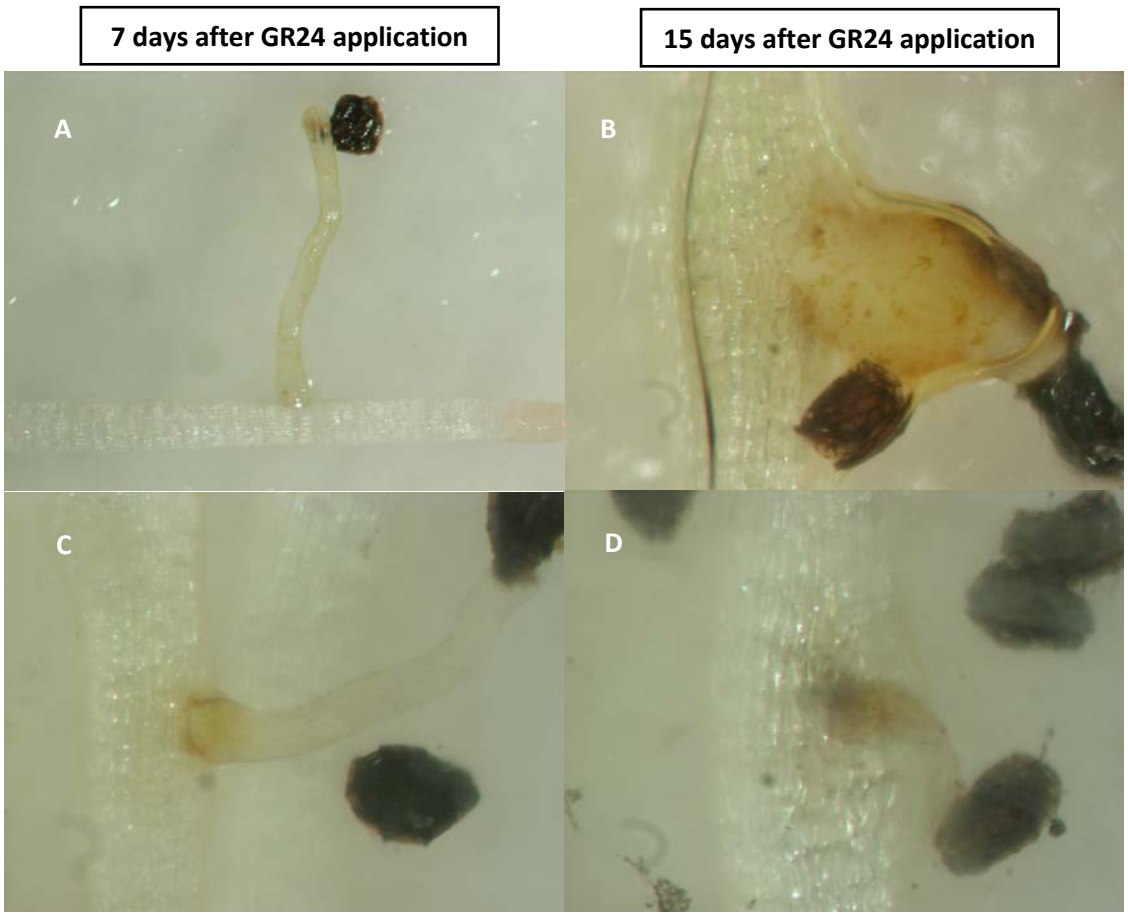

Fig. 3. *Images illustrate O. crenata parasite attacking M. truncatula roots in "initial" infection stage (7 days after GR24 application) and "well develop" stage (15 days after GR24) observed under bright field. Images A and B show roots from M. truncatula SA4327 accession with O. crenata attached seedlings and tubercle (respectively). Images C and D show roots from SA27774 accession with attached seedlings. No SA27774 tubercles were observed in this time gap. Arrows shows the darkening around the infection point observed in SA27774 and parasite tissues.*

For non inoculated plants, small root pieces (approximately 1 cm) were sampled at random. For inoculated plants, parts of the root with a crenate broomrape attachment were sampled, removing the parasite tissues. Then, samples were washed with tap and distilled water, blotted dry with filter paper, frozen in liquid nitrogen, and stored at -80ºC until biochemical analysis (Pérez-de-Luque *et al*., 2005a).

Observations were taken using a binocular microscope (Nikon SMZ1000; Nikon Europe B.V.). Triplicate biological replicates were collected for both control and inoculated samples.

Extraction of phenolics

Frozen root tissues (0.04 g fresh weight) were homogenized in 1 ml methanol (MeOH) by using a pestle and mortar. After filtering off the solvent extract, the residue was further sequentially extracted twice with a similar volume of MeOH and centrifuged twice at 15,000g for 15 min. The combined solvent extracts were dried and phenolic compounds were resuspended in 0.24 ml of MeOH for further analysis of soluble phenolics. The pellet residue was resuspended in 0.08 ml of 2 M NaOH and incubated at 70ºC for 16 h. The suspension was cooled down, neutralized with 0.08 ml of 2 M HCl, and centrifuged (15,000g for 15 min). Then, the suspension was collected and analysed as extract of cell wall-bound phenolics.

Chemicals

The flavonoids (used as standards) formononetin, daidzein, genistein, naringenin, maackiain and medicarpin were purchased from Plantech (www.plantechuk.co.uk, Reading, UK); scopoletin and chlorogenic acid were purchased from Sigma-Aldrich (www.sigmaaldrich.com) (Fig. 1). Standards were chosen based on their previous reported role in the plant defence process and represent the principal steps of the phenylpropanoid pathway.

Quantification of total phenolics

The determination of total phenolic content was performed by the Folin-Ciocalteu method (Prats, 2002). Absorbance of both, soluble and cell wall-bound phenolic extracts was measured colorimetrically in a Synergy HT multi-detection microplate reader (Biotek Instruments, Winooski, VT, USA). Data analysis was carried out using BioTek's Gen5 Data Analysis Software.

LC-ESI-MS/MS Analyses: Identification and quantification of phytoalexins

A Varian 1200 L Triple-Quadrupole tandem mass spectrometer (S.C.A.I., UCO) was used equipped with an electrospray ionization (ESI) source under negative ionization (NI). Chromatographic separation was performed on a C18 column 150 x 2 mm inner diameter (id). The mobile phase consisted of (A) double distilled water containing 0.1% formic acid and (B) a solution of acetonitrile 75% and methanol 25% (v/v). The mobile phase was pumped at a flow rate of 0.2 ml/ min and the injection volume was 10 μl. The gradient started with 10% B and increased linearly to 100% B over 10 min. Compounds were subjected to collision-induced dissociation in the multiple reaction monitoring (MRM) mode.

Statistical Analysis

Total phenolic determination assays were performed with 4 replicates per treatment and LC-ESI-MS/MS analyses with three replicates per treatment, with a completely randomized design. Statistical analysis (ANOVA) was performed with Statistix 9.0 for Windows.

Results

O. crenata seeds germinated 7 days after GR24 application and broomrape attachments on *M. truncatula* roots were developed 15 days after GR24 application as usual. At this point, we could observe differences in the aspect of the attached seedlings between accessions: SA4327 attached seedlings presented a healthy appearance (Fig. 3A and B). On the contrary, SA27774 attached seedlings and the host tissues surrounding parasite attachment showed a dark appearance and no further healthy tubercles developed (Fig. 3C and D).

Quantification of total phenolics

Total soluble and cell wall-bound phenolic content was determinated in *M. truncatula* root tissue extracts of non inoculated and inoculated plants with *O. crenata* parasite corresponding to plants sampled 15 days after GR24 application (a synthetic germination stimulant). Data are presented in Fig. 4.

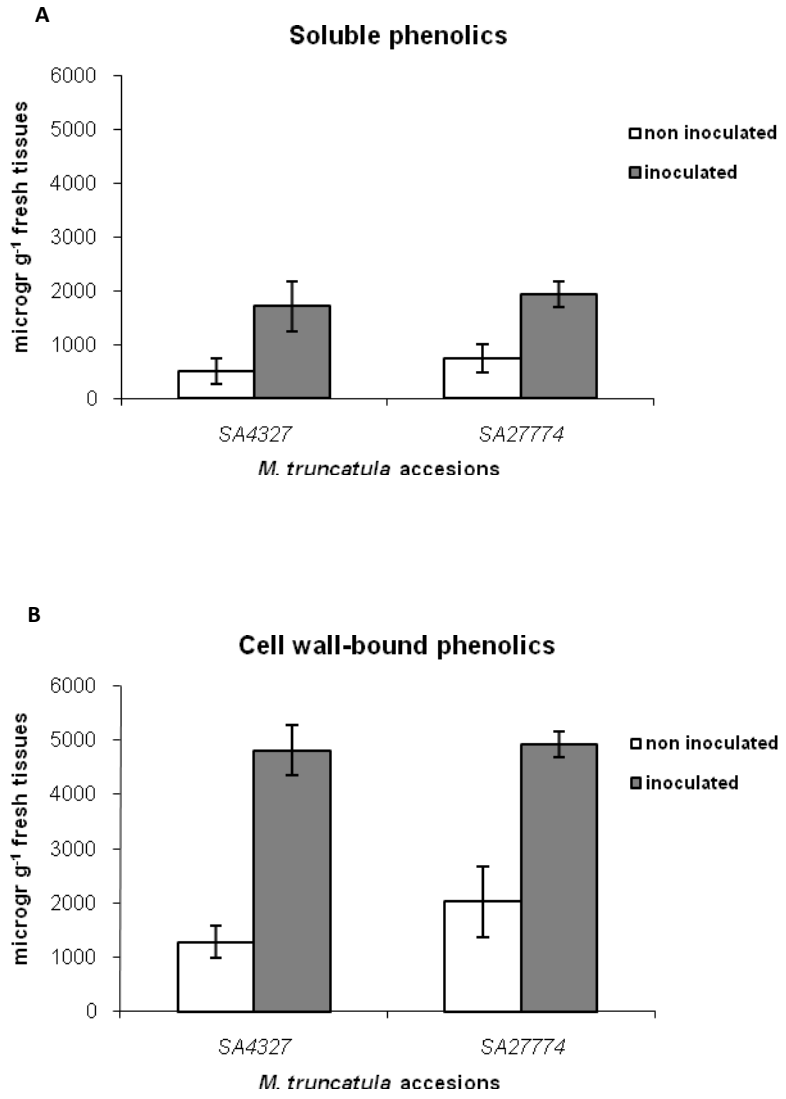

Fig. 4. *Total soluble (A) and cell wall-bound (B) phenolics in non inoculated and O. crenata inoculated M. truncatula roots. Plant root samples were collected 15 days after GR24 application. Concentration of phenolics is indicated as micrograms of chlorogenic acid per gram of fresh tissues.*

Root extracts from inoculated plants presented a twofold higher phenolic level, both soluble and cell wall-bound respect to non inoculated plants. However, significant differences between accessions were not detected (Fig. 4A, B).

For soluble phenolics (Fig. 4A), values ranged between 1935 μg of phenolics per g of fresh in inoculated tissues of accession SA27774 and 505.5 $\mu g \cdot g^{-1}$ of fresh tissues corresponding to non inoculated tissues of SA4327. Roots from SA4327 inoculated tissues

and SA27774 non inoculated tissues had 1710.6 and 750 μg of phenolics per gr of fresh tissues respectively. Cell wall-bound phenolics data showed similar results with the highest phenolic concentration in SA27774 inoculated tissues (4920 $\mu g \cdot g^{-1}$ of fresh tissues) and the lowest value of SA4327 non inoculated tissues (1281 $\mu g \cdot g^{-1}$ of fresh tissues) (Fig. 4B).

LC-ESI-MS/MS Analyses

LC-MS technique was used to identify and quantify phytoalexins produced by *M. truncatula* cell roots in response to *O. crenata* attack (Fig. 5). Our samples were analysed using both: positive-ion ESI mass spectra, which provided a greater number of fragment ions for each component that aided in structural identification, and negative-ion ESI, which yielded better sensitivity and higher signal to noise ratios (Huhman *and* Sumner, 2002). However no differences were observed between these methods in analysed samples.

Three of the standards (naringenin, daidzein and formononetin) were identified and quantified in the analysed root tissues for soluble phenolic samples but only formononetin appeared in both inoculated and non inoculated roots (naringenin and daidzein were only detected in inoculated roots of the SA4327 accession). No standard was detected in cell wall-bound phenolic extracts. Medicarpin, genistein, chlorogenic acid and scopoletin were not detected in any case and maackiain could not be analysed due to its instability.

Significant differences between samples were detected in formononetin accumulation. Firstly, although formononetin was identified in control samples its presence is more than twice in inoculated tissue extracts. Secondly, we found differences between accessions so that the highest and lowest formononetin concentration (i.e. 4108.4 and 1096.2 ngr gr^{-1} fresh tissues respectively) appears in SA27774 accession. However, formononetin concentration in SA4327 non inoculated samples is higher than SA27774 non inoculated. In this sense, SA4327 inoculated samples have lower formononetin levels than the inoculated SA27774 roots.

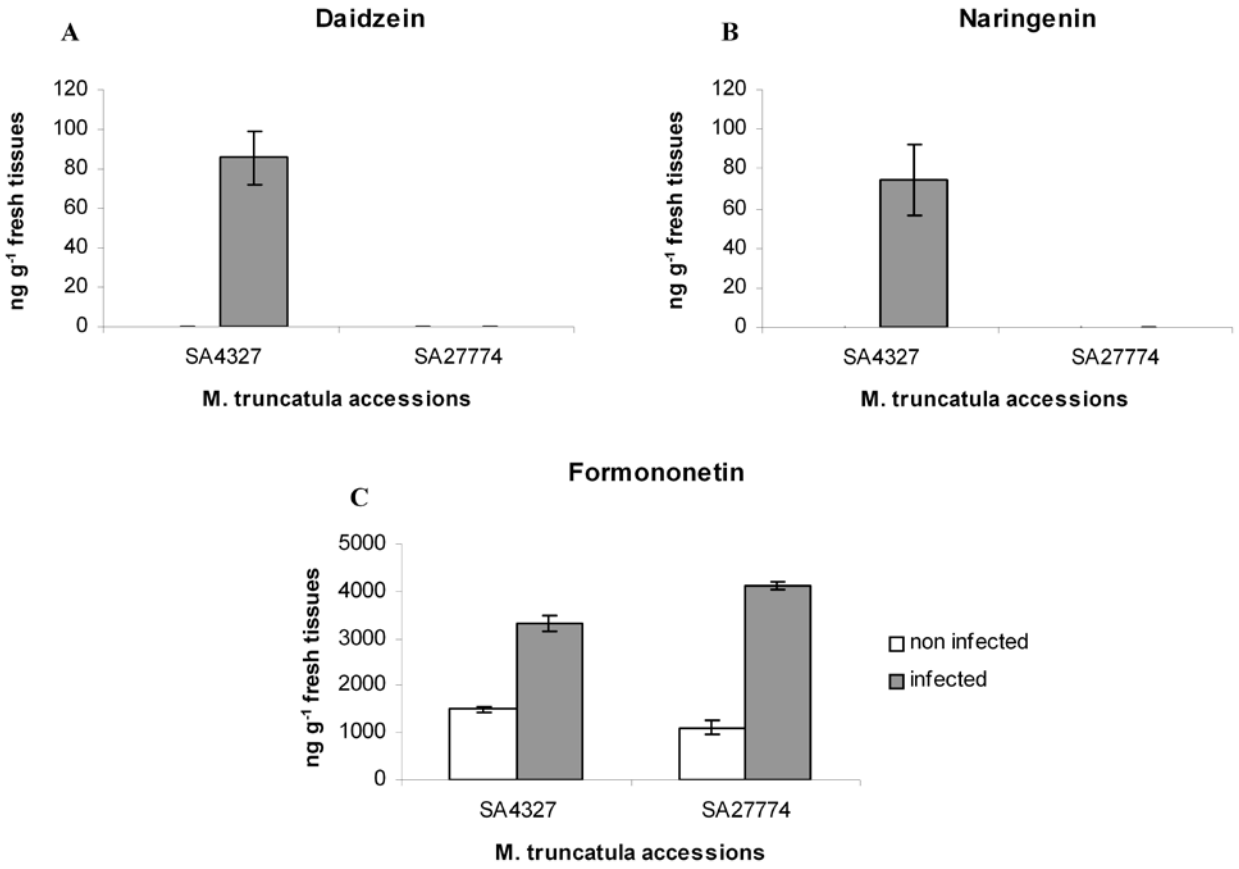

Fig. 5*. LC-MS Analysis: naringenin (A), daidzein (B) and formononetin (C) concentration in non inoculated and O. crenata inoculated M. truncatula roots corresponding to soluble phenolic samples. Plant root samples were collected 15 days after GR24 application.*

Regarding standards found in SA4327 accession, formononetin concentration in inoculated samples (3308.9 ngr gr^{-1} fresh tissues) is so much higher in comparison with naringenin and daidzein (74.187 and 85.57 ngr gr^{-1} fresh tissues respectively). No significant differences between naringenin and daidzein concentration were detected.

When chromatograms of inoculated and non inoculated samples were compared, we could observe that LC-MS detected other peaks, apart from our standards, present in inoculated samples that did not appear in non inoculated. Now, we are working in order to identify these compounds present only in infected samples.

Discussion

O. crenata invasion process can be divided into different phases and plant hosts have developed different resistance mechanisms which act in all of them (Pérez-de-Luque *et al*., 2008). In the first phase of *O. crenata* life cycle, parasite seeds germinate and grow towards host stimulated by the presence in the soil of some specific chemicals exuded by its roots. Because *M. truncatula* is a poor host of *O. crenata* the percentage of *O. crenata* seeds germinated in presence of *M. truncatula* root exudates is very low (Rodriguez-Conde *et al*., 2004). To solve this problem, researchers normally use exogenous application of the synthetic germination stimulant GR24. With its addition, the percentage of *O. crenata* germinated seeds reach the 40-50% increasing the number of contacting radicles and attached seedlings (Fernández-Aparicio *et al*., 2008). For this reason, we have chosen the GR24 application such as start point of *O. crenata* infection process. Afterwards, we can observe the first emerged radicles 5 days after its application and the 40-50% of germinated seeds in a week. After that, infection process continues as normally, appearing attached tubercles to *M. truncatula* roots growing 15 days after GR24 application.

We centred our work in the next phase of *O. crenata* life cycle when radicles start to penetrate *M. truncatula* root tissues. At this level, host plants activate the pre-haustorial resistance mechanisms aiming to hamper the parasite attempt to reach the central cylinder and establish vascular connection with host vessels. However, whether parasite reaches to establish host vascular connections, it starts to develop the haustorium (a specialized structure to suck water and nutrient from host). In order to avoid this, host plant activates the post-haustorial mechanisms of resistance and finally, try to stop parasite tubercle growth (Pérez-de-Luque *et al*., 2008). Whatever the resistance mechanism which is acting in this interaction, it should be taking place at this phase. For this reason, samples were collected at this time gap in order to determine this defence reaction.

Quantification of total phenolics

In general, phytoalexins are not detectable in healthy tissues or they can be found in very low concentrations (i.e. constitutive metabolism) or as sugar conjugates stored in vacuoles (then named phytoanticipins) (Dixon *et al*., 1996; Dakota *and* Phillips, 1996). They are secreted as defence compounds by cells immediately adjacent to infected sites and

accumulate in dead and dying cells within these localized regions. These compounds are synthesized rapidly after infection due to the de novo activation of secondary metabolic pathways (i.e. phenylpropanoid pathway), which divert primary metabolic precursors into the production of phytoalexins (Yu *and* McGonigle, 2005).

In legumes, isoflavonoid phytoalexins are the products of the phenylpropanoid pathway involved in defence against pathogens (Dixon *et al*., 1996). In our previous study (Lozano-Baena *et al*., 2007), we showed that *M. truncatula* produced some toxic compounds against *O. crenata* infection, stopping parasite growth. These observations suggested the possibility of phenolic compound accumulation as a defence strategy by infected legume plants. They inhibited development of *O. crenata* attached seedlings and caused a browning reaction in radicles and tubercles.

Our results show high concentration of phenolics in extracted samples (Fig. 4). Phenolics were detected in all samples with no significant differences between host accessions but with pathogen presence. The presence of phenolics in non inoculated samples could be due to constitutive metabolism (Dakota *and* Phillips, 1996; Farag *et al*., 2007). But, our results probe that inoculation (i.e. infection) process induced a very high increase of these compounds in samples, duplicating their concentration (Fig. 4).

The increase of phenolic compounds was observed in both soluble and cell wall-bound fractions but it was higher in cell wall-bound extracts where inoculated SA4327 accession has more than three times the concentration regarding to non inoculated samples. A similar fact occurs in SA27774 accession (Fig. 4). This suggest that cell wall-bound phenolics have a more important role in *M. truncatula* defence response but the less concentration of phenolics in soluble fractions can be explained in a different way. In this sense, soluble phenolics are synthesised and excreted close to parasite tissues and confocal studies have shown that parasite accumulate these phenolics within itself (Lozano-Baena *et al*., 2007). Indeed, they established a flux between host and parasite in which *O. crenata* radicles and tubercles showed an accumulation of phenolics removing them from host root tissues. Moreover, once phenolics reach parasite intrusive tissues and due to their strong antioxidant properties (Limem *et al*., 2008), they are rapidly oxidated into other chemical forms and getting their toxic function. These two facts, could contribute to detect a lower concentration of soluble phenolics in root samples. On the contrary, cell wall-bound phenolics are fixed into cell walls and extraction method recovers them in all their original form and concentration.

On the other hand, the high level of cell wall-bound phenolics in samples suggests that cells are accumulating these compounds in walls with defensive function acting such as physical barriers reinforcing cell walls and trying to hamper parasite penetration (Pérez-de-Luque *et al*., 2005b). Using specific stainings Lozano-Baena *et al*. (2007) showed the thickening of host vascular cell walls by phenolics accumulation but showed that these thickened walls presented no lignins which could strengthen them. Thus, it is not clear that these phenolics are from metabolic branch of lignins synthesis (normal pathway to imparts mechanical strength to stems and trunks, and hydrophobicity to water-conducting vascular elements) (Dixon *et al*., 1996) and moreover, these phenolics do not stopped parasite intrusion because it reached the endodermis and vascular vessels of the host. This suggests that the accumulation of these phenolics does not act as strong physical barrier and probably could have other function.

LC-ESI-MS/MS Analyse

Total phenolic determination just provides evidences about the presence and concentration of phenolic compounds in harvested samples but no identification and quantification of them are possible. For this reason, LC-MS technique was selected in this work because of its reliability, high sensitivity and selectivity identifying and quantifying specific compounds in a complex mixture (Caboni *et al*., 2008). Other authors have presented plant phenolic compounds as defence against Orobanche ssp. (Serghini *et al*., 2001; Echevarría-Zomeño *et al*., 2006; Lozano-Baena *et al*., 2007) but this is the first time that a work analyze and quantify their role in the interaction between *O. crenata* and the model legume *M. truncatula*.

Using LC-MS technique, neither chlorogenic acid nor scopoletin were detected in any of analysed samples. These phenolics are directly involved in phenylpropanoid pathway, for example as precursors of lignin biosynthesis (Fig. 2). In agreement with this, lignins were not observed before in inoculated roots of *M. truncatula* (Lozano-Baena *et al*., 2007).

On the other hand, phenylpropanoid pathway is responsible for flavonoid synthesis (Fig. 2) such as naringenin and LC-MS analysis confirms the presence of this flavanone such as soluble phenolic but only in SA4327 inoculated samples (Fig. 5B). This fact point naringenin, as principal step of this pathway, as one of the first flavonoids appeared in host tissues after

parasite intrusive cells detection. Once naringenin is metabolized, the first isoflavonoids of the phenylpropanoid pathway are daidzein and genistein. Genistein were not detected by LC-MS analysis and daidzein had a similar concentration as naringenin and appeared in the same samples (i.e. SA4327 inoculated samples) (Fig. 5A).

All this data support the idea that phenylpropanoid pathway is activated in *M. truncatula* defence response. Indeed, no control (i.e. non inoculated) samples have showed traces of any of the standard flavonoids used except formononetin (Fig. 5). This suggests that no defence response is acting in this samples and formononetin detection is due to basal metabolism (Dakota *and* Phillips, 1996). Furthermore, LC-MS analysis confirmed that intrusive cells of *O. crenata* parasite induce the accumulation of formononetin like soluble phenolic in all *M. truncatula* extracted root tissues nearby infected point (Fig. 5C). Formononetin (derived from daidzein metabolization) is the precursor of medicarpin, a constitutive polyphenol of *M. truncatula* (Farag *et al*., 2007) and its close relative alfalfa, and main isoflavonoid responsible of its defence response to pathogens (He *and* Dixon, 2000; Deavours *and* Dixon, 2005; Naoumkina *et al*., 2007; Farag *et al*., 2008).

In this sense, LC-MS analysis of inoculated samples revealed a considerable accumulation of formononetin of non inoculated roots. In addition, we found significant difference between accessions, so inoculated SA27774 samples have more concentration of formononetin than inoculated SA4327 (Fig. 5C). This may be due to the difference between defence reactions occurring in *M. truncatula* accessions and the time-gap selected to collect samples.

The final step of phenylpropanoid pathway in *M. truncatula* is the conversion of formononetin into the phytoalexin medicarpin (Dixon *et al*., 1996). Other authors have demonstrated that cell suspensions of *M. truncatula* accumulated the isoflavonoid phytoalexin medicarpin in response to yeast elicitor or methyl jasmonate (Naoumkina *et al*., 2007) and to fungi (Harrison *and* Dixon, 1993). Results indicate that mechanisms underlying accumulation of medicarpin differ depending on the nature of the stimulus.

Unfortunately, we could not detect medicarpin in root tissue as expected. The absence of medicarpin could be explaining by several reasons: firstly, we chose as time sampling 15 days after GR24 application, period of time necessary to allow pathogen germinate, take contact with host roots and initiate host tissue invasion. Hence, when we collected samples probably we selected them in another pathway step so medicarpin levels could not be

detected. Secondly, the extraction method separate detected compounds depending on their state in plant tissues (i.e. soluble or cell wall-bound). TLC analysis identified medicarpin as part of the soluble phase in extracted samples (Lozano-Baena *et al*., 2007) and if medicarpin is secreted by *M. truncatula* root cells and transported to *O. crenata* parasite to stop its intrusion, this fact could difficult its detection in root extracted samples. This circumstance was showed by Lozano-Baena *et al* (2007) where phenolic flux from host tissues to parasite and further accumulation was detected in *O. crenata* established seedlings and tubercles by fluorescence.

Because no standards were detected in cell wall-bound analysed samples, we conclude that these compounds are not involved in this defence reaction. Therefore, phytoalexins responsibles of host cell walls reinforcement could not be identified. In this sense, phenylpropanoid pathway produce many different polyphenols that could be the cause of this reaction i.e. flavones, flavonols, etc (Fig. 2). These polyphenols act bounded to cell wall perhaps limiting the absorption of water and nutrients by the parasite from host vessels, and reducing tubercles growth.

Altogether, in this work we have demonstrated that the model legume *M. truncatula* produces certain compounds i.e. flavonoids as phytoalexins in order to defend itself from the *O. crenata* parasite attack. These compounds (derived from phenylpropanoid pathway) have been identified and their concentration in host tissues quantified to determine their role in this plant-parasitic plant interaction.

Acknowledgements

This work was supported by project AGL2008-01239.

References

Aoki T, Akashi T, Ayabe S. 2000. Flavonoids of Leguminous plants: Structure, biological activity and biosinthesis. *Journal Plant Research* **113:** 475-488.

Benedito VA, Torres-Jerez I, Murray JD, Andriankaja A, Allen S, Kakar K, Wandrey M, Verdier J, Zuber H, Ott T, Moreau S, Niebel A, Frickey T, Weiller G, He1 J, Dai1 X, Zhao PX, Tang Y, Udvardi MK. 2008. A gene expression atlas of the model legume *Medicago truncatula*. *The Plant Journal* **55**: 504-513.

Caboni P, Sarais G, Angioni A, Vargiu S, Pagnozzi D, Cabras P, Casida JE. 2008. Liquid chromatography-Tandem mass spectrometric ion-switching determination of chlorantraniliprole and flubendiamide in fruits and vegetables. *Journal of Agricultural and Food Chemistry* **56**: 7696-7699.

Castillejo MA, Maldonado AM, Dumas-Gaudot E, Fernández-Aparicio M, Susin R, Rubiales D, Jorrín J. 2009. Differential expression proteomics to investigate responses and resistance to *Orobanche crenata* in *Medicago truncatula*. *BMC Genomic*s 10: 294. doi:10.1186/1471-2164-10-294.

Dakota FD and Phillips DA. 1996. Diverse functions of isoflavonoids in legumes transcend anti-microbial definitions of phytoalexins. *Physiological and Molecular Plant Pathology* **49**: 1-20.

Deavours B.E. and Dixon R.A. 2005. Metabolic Engineering of Isoflavonoid Biosynthesis in alfalfa. *Plant Physiology* **138**: 2245-2259.

Dixon RA and Sumner LW. 2003. Legume natural products: understanding and manipulating complex pathways for human and animal health. *Plant Physiology* **131**: 878-885.

Dixon RA, Lamb CJ, Masoud S, Sewalt VJH, Paiva NL. 1996. Metabolic engineering: prospects for crop improvement through the genetic manipulation of phenylpropanoid biosynthesis and defence responses - a review. *Gene* **179**: 61-71.

Dixon RA, Achnine L, Kota P, Liu C, Reddy MSS, Wang L. 2002. The phenylpropanoid pathway and plant defence-a genomics perspective. *Molecular Plant Pathology* **3**: 371-390.

Echevarría-Zomeño S, Pérez-de-Luque A, Jorrín J, Maldonado AM. 2006. Pre-haustorial resistance to broomrape (*Orobanche cumana*) in sunflower (*Helianthus annuus*): cytochemical studies. *Journal of Experimental Botany* **57**: 4189-4200.

Farag MA, Huhman DV, Lloyd Z, Sumner LW. 2007. Metabolic profiling and systematic identification of flavonoids and isoflavonoids in roots and cell suspension cultures of *Medicago truncatula* using HPLC-UV-ESI-MS and GC-MS. *Phytochemistry* **68**: 342-354.

Farag MA, Huhman DV, Dixon RA, Sumner LW. 2008. Metabolomics reveals novel pathways and differential mechanistic and elicitor-specific responses in phenylpropanoid and isoflavonoid biosynthesis in *Medicago truncatula* cell cultures. *Plant Physiology* **146**: 387-402.

Fernández-Aparicio M, Pérez-de-Luque A, Prats E, Rubiales D. 2008. Variability of interaction between barrel medic (*Medicago truncatula*) genotypes and *Orobanche* species. *Annals of Applied Biology* **153**: 117-126.

González-Verdejo CI, Barandiaran X, Moreno MT, Cubero JI, Di-Pietro A. 2005. An improved axenic system for studying pre-infection development of the parasitic plant *Orobanche ramosa*. *Annals of Botany* **96**: 1121-1127.

Graham PH, Vance CP. 2003. Legumes: importance and constraints to greater use. *Plant Physiology* **131**: 872-877.

Harrison MJ, Dixon RA. 1993. Isoflavonoid accumulation and expression of defence gene transcripts during the establishment of vesicular-arbuscular mycorrhizal associations in roots of *Medicago truncatula*. *Molecular Plant-Microbe Interactions* **6**: 643-654.

He XZ and Dixon RA. 2000. Genetic manipulation of isoflavone 7-O-methyltransferase enhances biosynthesis of 4'-O-methylated isoflavonoid phytoalexins and disease resistance in alfalfa. *The Plant Cell* **12**: 1689-1702.

Hoagland DR and Arnon DI. 1950. The water-culture method for growing plants without soil. California Agricultural Experiment Station Circular 347. University of California, Berkeley.

Huhman D and Sumner L. 2002. Metabolic profiling of saponins in *Medicago sativa* and *Medicago truncatula* using HPLC coupled to an electrospray ion-trap mass spectrometer. *Phytochemistry* **59**: 347-360.

Joel DM, Hershenhorn Y, Eizenberg H, Aly R, Ejeta G, Rich PJ, Ransom JK, Sauerborn J, Rubiales D. 2007. Biology and Management of Weedy Root Parasites. In: J. Janick ed. Horticultural Reviews. Hoboken, **33**: 267-350.

Jöet T, Salmona J, Laffargue A, Descroix F, Dussert S. 2010. Use of the growing environment as a source of variation to identify the quantitative trait transcripts and modules of co-expressed genes that determine chlorogenic acid accumulation. *Plant, Cell and Environment* **33**: 1220-1233.

Jorrín J and Dixon A. 1990. Stress Responses in Alfalfa (*Medicago sativa* L.) II. Purification, Characterization, and Induction of Phenylalanine Ammonia-Lyase Isoforms from Elicitor-Treated Cell Suspension Cultures. *Plant Phisiology* **92**: 447-455.

Kai K, Mizutani M, Kawamura N, Yamamoto R, Tamai M, Yamaguchi H, Sakata K, Shimizu B. 2008. Scopoletin is biosynthesized via ortho-hydroxylation of feruloyl CoA by a 2-oxoglutarate-dependent dioxygenase in *Arabidopsis thaliana*. *The Plant Journal* **55**: 989-999.

Limem I, Guedon E, Hehn A, Bourgaud F, Ghedira LC, Engasser JM, Ghoul M. 2008. Production of phenylpropanoid compounds by recombinant microorganisms expressing plant-specific biosynthesis genes. *Process Biochemistry* **43**: 463-479.

Lozano-Baena MD, Moreno MT, Rubiales D, Pérez-de-Luque A. 2007. *Medicago truncatula* as a model for non-host resistance in legume-parasitic plant interactions. *Plant Physiology* **145**: 437-449.

Magnus EM, Stommen PLA, Zwanenburg B. 1992. A standardized bioassay for evaluation of potential germination stimulants for seeds of parasitic weeds. *Journal of Plant Growth Reguation* **11**: 91-98.

Naoumkina M, Farag MA, Sumner LW, Tang Y, Liu CJ, Dixon RA. 2007. Different mechanisms for phytoalexin induction by pathogen and wound signals in *Medicago truncatula*. *PNAS* **104**: 17909-17915.

Pérez-de-Luque A, Jorrín J, Cubero JI, Rubiales D. 2005a. *Orobanche crenata* resistance and avoidance in pea (*Pisum* spp.) operate at different developmental stages of the parasite. *Weed Research* **45**: 379-387.

Pérez-de-Luque A, Rubiales D, Cubero JI, Press MC, Scholes J, Yoneyama K, Takeuchi Y, Plakhine D, Joel DM. 2005b. Interaction between *Orobanche crenata* and its host legumes: unsuccessful haustorial penetration and necrosis of the developing parasite. *Annals of Botany* **95**: 935-942.

Pérez-de-Luque A, Lozano-Baena MD, Maldonado AM, Jorrín JV, Dita MA, Die J, Román B, Rubiales D. 2007. *Medicago truncatula* as a model for studying interactions between root parasitic plants and legumes. In: U Mathesius, EP Journet, LW Sumner, eds. The *Medicago truncatula* Handbook. The Samuel Roberts Noble Foundation, Ardmore: OK 1-31.

Pérez-de-Luque A, Moreno T, Rubiales D. 2008. Host plant resistance against broomrapes (*Orobanche* spp.): defence reactions and mechanisms of resistance. *Annals of Applied Biology* **152**: 131-141.

Pérez-de-Luque A, Fondevilla S, Pérez-Vich B, Aly R, Thoirons S, Simiers P, Castillejo MA, Fernández-Martínez JM, Jorrín J, Rubiales D, Delavaults P. 2009. Understanding *Orobanche* and *Phelipanche*-host plant interactions and developing resistance. *Weed Research* **49**: 8-22.

Prasain JK, Wang CC, Barnes S. 2004. Mass spectrometric methods for the determination of flavonoids in biological samples. *Free Radical Biology and Medicine* **37**: 1324-1350.

Prats E, Rubiales D, Jorrín J. 2002. Acibenzolar-s-methylinduced resistance to sunflower rust (*Puccinia helianthi*) is associated with an enhancement of coumarins on foliar surface. *Physiological and Molecular Plant Pathology* **60**: 155-162.

Rispail N, Kaló P, Kiss GB, Ellis THN, Gallardo K, Thompson RD, Prats E, Larrainzar E, Ladrera R, González EM, Arrese-Igor C, Ferguson BJ, Gresshoff PM, Rubiales D. 2010. Model legumes contribute to faba bean breeding. *Field Crops Research* **115**: 253-269.

Rodríguez-Conde MF, Moreno MT, Cubero JI, Rubiales D. 2004. Characterization of the *Orobanche-Medicago truncatula* association for studying early stages of the parasite-host interaction. *Weed Research* **44**: 218-223.

Rubiales D, Pérez-de-Luque A, Fernández-Aparicio M, Sillero JC, Román B, Kharrat M, Khalil S, Joel DM, Riches C. 2006. Screening techniques and sources of resistance against parasitic weeds in grain legumes. *Euphytica* **147**: 187-199.

Serghini K, Pérez-De-Luque A, Castejón-Muñoz M, García-Torres L, Jorrín JV. 2001. Sunflower (*Helianthus annuus* L.) response to broomrape (*Orobanche cernua* Loefl.) parasitism: induced synthesis and excretion of 7-hydroxylated simple coumarins. *Journal of Experimental Botany* **52**: 2227-2234.

Shimada N, Akashi T, Aoki T, Ayabe S. 2000. Induction of isoflavonoid pathway in the model legume *Lotus japonicus*: molecular characterization of enzymes involved in phytoalexin biosynthesis. *Plant Science* **160**: 37-47.

Steck W. 1968. Metabolism of cinnamic acid in plants: Chlorogenic acid formation. *Phytochemistry* **7**: 1711-1717.

Ueda H and Sugimoto Y. 2010. Vestitol as a chemical barrier against intrusion of parasitic plant *Striga hermonthica* into *Lotus japonicas* roots. *Bioscience biotechnology and biochemistry* **74**: 1662-1667.

Yu Oliver and McGonigle B. 2005. Metabolic engineering of isoflavone biosynthesis. *Advances in Agronomy* **86**: 147-190.

RESULTADOS Y DISCUSIÓN GENERALES

Los resultados obtenidos en estos trabajos de tesis muestras varios tipos de mecanismos de resistencia en leguminosas en respuesta al ataque de la especie de planta parásita *O. crenata*.

En el primer capítulo, encontramos una gran mayoría de tubérculos del parásito necrosados en el genotipo resistente de *V. sativa*. Los cortes realizados de dichas muestras, presentan un establecimiento de conexiones vasculares de *O. crenata* con los vasos conductores de la planta huésped y un estado de desarrollo del parásito avanzado. Por el contrario, los cortes realizados en el genotipo resistente presentan una obstrucción de dichos vasos por una sustancia coloreada con varios tipos de tinción: AGS (safranina), TBO (toulidina), rojo de rutenio y floroglucinol. Dichas tinciones son específicas de carbohidratos y pectinas así como de polifenoles y ligninas por lo que la sustancia que tapona los vasos conductores de la raíz huésped sería una especie de mucílago compuesta por los mismos. Dichas tinciones también muestran un engrosamiento de las paredes de los vasos xilemáticos de la raíz cercanos al punto de infección y de las células que los rodean. También se utilizaron técnicas de inmunotinción encaminadas a determinar qué tipo de pectinas aparecían en las células cercanas al tejido del parásito. Por último, la aplicación del nactofenol (tinción in vivo) determinó la existencia de conexiones vasculares funcionales entre las interacciones susceptibles huésped-parásito, justo al contrario de las resistentes donde la tinción no alcanzaba a teñir el tejido del parásito.

Estos resultados nos permitieron concluir que la especie de leguminosa *V. sativa* presenta una respuesta defensiva post-haustorial a la invasión de la especie de planta parásita *O. crenata* ya que permitía el establecimiento y la formación de conexiones vasculares del parásito en la línea resistente pero no su desarrollo. Dicha respuesta defensiva consiste en la producción por parte de las células de la raíz del huésped de una serie de sustancias a modo de mucílago que taponaban los vasos vasculares de la zona infectada imposibilitando el paso de agua y nutrientes desde huésped al parásito. Además, dichas células cercanas a la infección también presentaban lignificaciones y engrosamientos de sus paredes celulares así como la presencia de ciertos depósitos de calosa, hecho que contribuía también a imposibilitar el desarrollo del parásito ya que actuaban como barrera física ante su penetración en el tejido radicular huésped. Los cortes-tinciones realizados también probaron que dicha respuesta defensiva es cuantitativa, es decir, a mayor producción de mucílago y de reforzamiento de las

paredes celulares del huésped, mayor es la fuerza de dicha resistencia. De hecho, también se encontró cierta producción de mucílago en cortes de interacciones compatibles del genotipo susceptible pero que debido a su escasez, no conseguían obstruir las conexiones establecidas por los tubérculos de *O. crenata* en la raíz huésped.

En el segundo capítulo, encontramos un mayor porcentaje de tubérculos desarrollándose en el genotipo susceptible de la especie *V. faba* mientras que la mayoría de radículas de *O. crenata* que intentaban penetrar en la raíz del genotipo resistente se oscurecían y morían antes de llegar al estadio de tubérculo. La tinción TBO aplicada en las muestras determinó claras diferencias entre ambos genotipos: en el caso de tubérculos sanos establecidos en la raíz huésped (genotipo susceptible), los cortes realizados mostraban haustorios bien desarrollados y conexiones vasculares directas con los vasos conductores de la raíz huésped. Por el contrario, los cortes de radículas oscurecidas (genotipo resistente) mostraban cómo las células intrusivas del parásito no habían alcanzado dichos vasos, y habían detenido su penetración en el cortex y la endodermis de la raíz. Los mismos resultados se obtuvieron con la tinción AGS que mostraba cómo alrededor de las células de la raíz en contacto con el parásito aparecía una intensa coloración de una sustancia de naturaleza heterogénea que se acumulaba en dichas uniones. También se encontraron considerables acumulaciones de calosa alrededor del parásito a modo de barrera que detenían su avance en el interior de la raíz.

En algunos casos, las células intrusivas del parásito conseguían traspasar estas barreras pero su avance se detenía en la endodermis radicular. A este nivel, las tinciones mostraban lignificaciones de las paredes celulares de la endodermis que parecían ser las responsables de parar el avance del parásito.

Al igual que en el caso de *V. sativa*, concluimos que la respuesta defensiva que presentaba *V. faba* es una respuesta cuantitativa dado que también aparece en el genotipo susceptible pero en escasa medida por lo que no es capaz de detener el ataque de *O. crenata*. Pero al contrario que en el caso de *V. sativa*, en la especie *V. faba* aparecen como respuesta defensiva mecanismos pre-haustoriales dado que el parásito *O. crenata* no era capaz de establecer conexiones vasculares con el xilema de la raíz huésped.

Por último, la especie *M. truncatula* presentó un tipo de respuesta defensiva totalmente distinto al encontrado en las especies de leguminosas antes descritas.

En un principio, *M. truncatula* parecía presentar el mimo tipo de respuesta defensiva que encontramos en *V. faba* dado que en el genotipo resistente seleccionado, las radículas en contacto con la raíz se oscurecían antes de llegar al estadio de tubérculo al contrario que en el susceptible en el que aparecían un mayor número de tubérculos desarrollándose en la raíz huésped. Esto inducía a pensar que *M. truncatula* presentaba una respuesta defensiva pre-haustorial al ataque de *O. crenata*. Pero una observación más detallada de las muestras reveló que estos tubérculos aparentemente sanos, con el tiempo empezaban a presentar signos de oscurecimiento (al igual que ocurría en las radículas del genotipo resistente), para finalmente detener su crecimiento y morir (resistencia post-haustorial). Estas observaciones a nivel macroscópico parecían indicar que ambos genotipos presentaban la misma resistencia al ataque de *O. crenata* pero que por algún motivo, esta resistencia era más lenta en el genotipo que permitía el desarrollo de tubérculos en sus raíces. De esta forma, nuestras muestras presentaban dos tipos de interacciones: en el genotipo supuestamente susceptible encontrábamos interacciones compatibles en las que el parásito se desarrollaba hasta el estadio de tubérculo mientras que, en el genotipo resistente, encontrábamos interacciones incompatibles en las que el parásito moría antes de alcanzar el estadio de tubérculo.

Para averiguar qué mecanismos desencadenaba la intrusión de *O. crenata* en la raíz huésped se volvieron a utilizar las técnicas citoquímicas antes explicadas mediante un análisis microscópico detallado de las muestras cortadas.

Los cortes de las interacciones compatibles teñidos con AGS y TBO mostraban cómo el parásito había conseguido alcanzar el cilindro central de la raíz y desarrollar un haustorio funcional estableciendo conexiones vasculares con los vasos conductores de la misma.

Los mismos cortes pero de las interacciones incompatibles, también mostraban cómo el parásito había conseguido alcanzar el cilindro central de la raíz pero al contrario que en el caso anterior, en las muestras no aparecían conexiones vasculares entre *O. crenata* y el xilema de *M. truncatula* (no se había desarrollado ningún haustorio) y en su lugar, aparecía una coloración oscura intensa rodeando la zona por la que el parásito había penetrado. Las muestras teñidas con AGS mostraban que una intensa coloración de esa zona oscurecida pero que no se correspondía con carbohidratos como ocurría en el caso de *V. sativa*. Esta tinción también reveló un engrosamiento de los haces vasculares de la raíz de *M. truncatula* cercanos al tejido invasor del parásito y de la presencia en el interior de los mismos de una sustancia que por su coloración, tampoco se correspondía con carbohidratos. Las zonas oscurecidas y

engrosadas de la raíz también aparecían teñidas cuando la tinción de TBO era aplicada sobre las muestras cortadas.

La observación de estas muestras usando la microscopía de fluorescencia reveló una intensa fluorescencia en los vasos xilemáticos cercanos al parásito, cosa que no ocurría en las zonas alejadas del punto de infección. Un posterior análisis de estas muestras mediante el uso de luz polarizada demostró que dicha fluorescencia no era debida a la presencia de ligninas en las pareces de las células radiculares del huésped como ocurría en el caso de las especies anteriores analizadas.

Al aplicar estas mismas técnicas en las muestras cortadas de las interacciones compatibles, encontramos que en los haustorios inicialmente en desarrollo, también aparecían (aunque en menor medida) zonas marcadas de la misma forma que en el caso de las interacciones incompatibles. La tinción con floroglucinol no reveló signos de lignificación en las paredes del xilema que pudiera explicar el engrosamiento de las mismas. De igual forma, la fluorescencia determinó la acumulación de ciertas sustancias alrededor de la zona infectada. Dicha fluorescencia parecía corresponderse con la presencia en las mismas de sustancias de tipo fenólico. Al contrario que en el caso de *V. faba*, no se encontraron depósitos de calosa lo suficientemente considerables como para ser responsables de la parada del avance de la radícula de *O. crenata* en el interior de la raíz.

Para determinar más claramente qué tipo de sustancia era la que parecía acumularse alrededor de la zona infectada, se realizaron cortes en fresco de diversas muestras (radículas y tubérculos), así como de secciones de la raíz de *M. truncatula* sin infectar. Estos cortes fueron observados bajo luz fluorescente y mostraron una intensa fluorescencia en las zonas que rodeaban el punto de infección de las interacciones incompatibles, sobre todo, en los vasos xilemáticos cercanos al mismo. Dicha fluorescencia no aparecía ni en los cortes de raíz sin infectar ni en los de tubérculos de las interacciones compatibles. Dicha fluorescencia se correspondía con la presencia de sustancias de tipo fenólico en las muestras. También se utilizó la microscopía confocal como prueba de la presencia de compuestos fenólicos en las muestras. Con esta técnica no se detectó fluorescencia en las muestras analizadas de interacciones compatibles, justo al contrario que en las muestras de interacciones incompatibles donde aparecía fluorescencia tanto en los vasos xilemáticos, como en el cortex de la raíz y en el interior de los tejidos del parásito. Esta fluorescencia se correspondía con la presencia en las muestras de sustancias de tipo fenólico.

La viabilidad de las células presentes en esta interacción se testó utilizando la tinción de azul de tripán. De esta forma, las células vivas incorporan el colorante pero no lo acumulan, expulsándolo al exterior mientras que las células muertas lo absorben pero no son capaces de expulsarlo por lo que lo acumulan y se tiñen de oscuro. En el caso de cortes de raíz no infectados y de cortes de muestras de interacciones compatibles, no aparecían células teñidas con el colorante, justo al revés que en el caso de las muestras de interacciones incompatibles en las que, las células alrededor de la zona infectada aparecían claramente teñidas.

Por último, para la identificación del tipo de compuesto fenólico que presentaban las muestras se utilizaron placas de TLC (cromatografía en capa fina) y una serie de compuestos fenólicos patrón conocidos. De estos, se identificaron la medicarpina y la maackiaina en las fracciones de fenólicos solubles de las muestras infectadas analizadas de ambos genotipos de *M. truncatula*. La escopoletina fue detectada en la fracción de fenólicos unidos a pared del genotipo que permitía la instalación de interacciones compatibles mientras que la pisatina no apareció en ninguna de las muestras analizadas.

En conclusión, podemos decir que *M. truncatula* se defiende del ataque de *O. crenata* produciendo una serie de compuestos fenólicos (algunos de los cuales se pudieron identificar). La producción y secreción de estos compuestos en la zona de raíz infectada es la responsable de parar el avance del patógeno en el interior de la raíz y de su posterior muerte. Concretamente, en el caso de las interacciones incompatibles, la respuesta defensiva aparece en las primeras fases de invasión del parásito, impidiendo que alcance a establecer conexiones vasculares con los vasos xilemáticos de la raíz. Por el contrario, en el caso de las interacciones compatibles, el parásito alcanza a formar dichas conexiones desarrollando un haustorio aunque finalmente, la acumulación progresiva de las mismas sustancias que en el caso anterior, impedirá que el parásito consiga seguir su crecimiento.

La presencia e identificación de sólo algunos de los compuestos fenólicos presentes en la respuesta defensiva de M. truncatula frente a la invasión de O. crenata nos llevó a buscar mecanismos para esclarecer en mayor medida cuáles eran las sustancias responsables de dicha resistencia.

Con esta idea, decidimos ampliar el trabajo comenzado en el tercer capítulo de esta tesis con otro artículo más, en el que nos centramos en la identificación y cuantificación de dichas sustancias.

Para ello, en un primer momento decidimos determinar la concentración de fenólicos totales que aparecían en nuestras muestras separados en dos fases: fenólicos solubles y fenólicos ligados a paredes celulares. El análisis de muestras inoculadas y no inoculadas de *M. truncatula* reveló que los fenólicos estaban presentes en ambos tipos de muestras aunque su concentración era dos veces mayor en las muestras inoculadas que en las no inoculadas. Esto nos indujo a pensar que la raíz presentaba unos niveles basales de estos compuestos y que el proceso infectivo de *O. crenata* elevaba considerablemente su presencia en los tejidos de la raíz del huésped. Este aumento de la concentración de fenólicos en las muestras aparecía en mayor proporción en la fracción de fenólicos ligados a pared. Una posible explicación a este fenómeno es el hecho de que, los fenólicos solubles son más susceptibles de ser metabolizados o acumulados en los tejidos del parásito, retirando así su presencia de las muestras y reduciendo su concentración en el tejido radicular del huésped. Por el contrario, los fenólicos ligados a pared no sólo conservaban su composición sino que no se producía una disminución de su concentración al quedar retenidos por las paredes celulares del huésped.

Pero este análisis general sólo nos permitía conocer la concentración total de fenólicos de las muestras, no permitiendo el análisis individual del tipo de fenólicos presentes. Además, no determinó diferencias en la presencia de fenólicos entre ambos tipos de interacciones. Por ello, se utilizó la técnica de LC-MS/MS como método para la identificación y cuantificación individual de los mismos así como para intentar ver diferencias entre ambos tipos de interacciones.

De los patrones analizados, se consiguieron identificar tres fenólicos en la fracción de fenólicos solubles las muestras de raíz: la daidzeina, la naringenina y la formononetina. Todas estas sustancias se correspondían con distintos pasos metabólicos de la ruta fenilpropanoide (responsable de la producción de los distintos tipos de compuestos fenólicos en las células). De los tres, sólo la formononetina apareció en todos los tipos de muestras analizadas (tanto inoculadas como no inoculadas) de los dos tipos de interacciones (compatibles e incompatibles), viéndose un considerable aumento de la concentración de formononetina debido al proceso de infección de *O. crenata*. Por el contrario, la naringenina y la daidzeina sólo se presentaron en las muestras analizadas de interacciones compatibles.

De esta forma concluimos que *M. truncatula* produce una serie de compuestos fenólicos que actúan como defensa frente a la invasión de *O. crenata*. Estos compuestos proceden de la activación de la ruta fenilpropanoide en los tejidos de la raíz huésped y son acumulados en la

zona infectada impidiendo el desarrollo del parásito dentro de la raíz. Además, se he podido determinar la concentración en las muestras de tres de estos compuestos, destacando la formononetina cuya concentración se ve considerablemente aumentada por el proceso infectivo del parásito.

RESUMEN GENERAL

El presente trabajo para su presentación como tesis doctoral recopila una serie de experimentos encaminados a la determinación y caracterización de la relación que se establece entre la especie de planta parásita *Orobanche crenata* (jopo) y las principales especies de cultivos de leguminosas que se ven afectadas por dicho parásito en el área Mediterránea. *O. crenata* es uno de los principales problemas que afectan al cultivo de leguminosas en nuestra área, llegando devastar cosechas e inutilizar los terrenos de cultivo durante décadas produciendo así, enormes pérdidas económicas al sector agrícola. Por ello, es necesario el encontrar medidas de control que ayuden a combatir la presencia de este parásito en nuestros cultivos.

En este sentido, el primer capítulo describe el proceso infectivo del jopo sobre dos especies de vicias (una resistente a su ataque y otra susceptible) mediante el uso de técnicas citoquímicas y cortes de tejidos sanos/ infectados, además del uso de la microscopía Confocal Laser. Gracias a ello, pudimos determinar que la resistencia que presenta esta especie frente al jopo es debida a la producción por parte del huésped de una serie de sustancias que taponan los vasos conductores del xilema de la zona afectada por el parásito, impidiendo así que éste pueda tomar de la planta el agua y los nutrientes que necesita para su desarrollo.

En el segundo capítulo se utiliza como especie huésped del jopo el haba (*Vicia faba*), caracterizando dicha infección mediante la combinación de técnicas citoquímicas de tinción y diferentes técnicas de microscopía de fluorescencia. En esta ocasión, el huésped impide el desarrollo de nuestro parásito reforzando las paredes de las células en contacto con los tejidos intrusivos del jopo, deteniendo de esta forma el proceso infección.

En el tercer capítulo se seleccionó como huésped la especie *M. truncatula* con el fin de obtener un modelo representativo en leguminosas que ayudara a caracterizar el proceso infectivo del jopo y que fuera fácilmente aplicable al resto de especies cultivadas de leguminosas de más difícil manejo. En este trabajo, cabe destacar la puesta a punto de las técnicas de cultivo, recolección y análisis utilizadas, con el fin de adaptarlas al manejo de *M. truncatula* para su posterior análisis.

Por último, el cuarto capítulo se presenta como una continuación del trabajo realizado en el tercer capítulo ya que éste determinó que la resistencia presente en *M. truncatula* está relacionada con la presencia de ciertas sustancias fenólicas halladas en los tejidos infectados del huésped. Con el fin de identificar dichas sustancias, se determinó la presencia y concentración de los fenólicos totales que había en las muestras así como del uso de la técnica LC-MS/MS para la identificación individual de los mismos.

RESUMEN GENERAL (english version)

In the present work, we have included a serial of reports aimed to determine and characterize the relation established between the root parasitic weed *Orobanche crenata* (crenate broomrapes) and some of the principal legume crops which act such as its host.

This parasitic plant represents the major constraint for grain and forage legume production in Mediterranean and West Asian countries, resulting in complete yield loss with severe infestations and removing otherwise productive land from effective use for very long periods of time. For this reason, the knowledge of the mechanisms of resistance against this pest is crucial to develop strategies of control.

With this purpose, the first report describes the *O. crenata* infection process attacking two vetches species (one susceptible, and the other one resistant) using citoquemical methods in infected and non infected host tissues. Also, laser confocal microscopy was employed in analysed samples. Due to this methodology, we could conclude that this host plant defend itself accumulating some secretions, and degraded products block host vessels and does not allow nutrient flux between host and parasite, causing further parasite death.

In chapter two, we selected as host two cultivars of the legume *Vicia faba* (faba bean). In this report, the interaction *O. crenata*/ *V. faba* was analysed using different citoquemical methods combined with some microscopy techniques. Results showed that the stoppage of *O. crenata* seedling penetration in the host root is associated with reinforcement of host cell walls in contact with the parasite intrusive cells.

Due to the difficult of most cool season grain and forage legume management and the complexity of their genome, we selected in chapter three as *O. crenata* host the legume *Medicago truncatula* in order to obtain a model which helps to characterize the *O. crenata* infection process and which permits establish a model easily applicable to other legume crops. In this report, we concluded that *M. truncatula* seemed to defend itself producing some phenolics compounds which poison parasite and avoid its attack.

Finally, last chapter arose from the need to continue the work of the previous report to identify and quantify the phenolic compounds that produces *M. truncatula* host against parasite. With this objective, LC-MS/MS technique was applied and probed that flavonoid compounds are implicated in this defence reaction.

CONCLUSIONES FINALES

1) Las especies de leguminosas estudiadas: *Vicia sativa*, *V. faba* y *Medicago truncatula*, presentan distintos mecanismos de defensa frente a la especie de planta parásita *Orobanche crenata*.

2) La producción de mucílago puede considerarse como una reacción defensiva cuantitativa, que tiene lugar en *V. sativa* frente al ataque de *O. crenata*.

3) Esta respuesta defensiva parece desencadenarse por la presencia en los tejidos del huésped de ciertas sustancias producidas por el parásito y de los propios tejidos degradados del huésped por el proceso infectivo.

4) Dicho mucílago llega a taponar completamente los vasos conductores del huésped próximos a la zona infectada, produciendo la muerte del parásito en el estadio de tubérculo.

5) En el caso de *V. faba*, el proceso de infección de *O. crenata* se detiene en los primeros estadios del desarrollo del mismo.

6) La primera barrera que forma el huésped aparece en el córtex del tejido radicular como acumulaciones de calosa que detienen la intrusión de las radículas de *O. crenata*.

7) Si *O. crenata* consigue superar dicha barrera, se produce una lignificación de las células de la endodermis del huésped, impidiendo que el parásito alcance el cilindro central y por lo tanto, la formación del haustorio.

8) La especie modelo *M. truncatula* presenta un tipo distinto de mecanismo de defensa, como sería la producción de ciertas sustancias tóxicas para *O. crenata* (fitoalexinas).

9) Dichas sustancias no actúan como una barrera física sino más bien química, ya que parece producirse un envenenamiento y muerte de las células invasivas de *O. crenata* cuando pretenden alcanzar el cilindro central del tejido huésped.

10) Los diferentes cortes histológicos, así como el análisis de dichas fitoalexinas, revela que existe una diferencia en el tiempo de respuesta de las líneas de *M. truncatula* analizadas

frente a la infección. De esta forma, cuanto más rápidamente se produce la aparición de dichos compuestos en el tejido huésped, más efectiva es la respuesta defensiva del mismo y menor la infección.

11) Finalmente, tres de las principales fitoalexinas de la ruta fenilpropanoide (formononetina, daidzeina y naringenina) han sido identificadas y su concentración quantificada en los tejidos infectados del huésped. Estos compuestos están directamente implicados en la resistencia de la especie *M. truncatula* frente a la invasión del parásito *O. crenata*.

12) De estas tres fitoalexinas, destacan los resultados obtenidos para la formononetina, viéndose que existe una relación directa entre la invasión de *O. crenata* y un incremento en su concentración en los tejidos infectados del huésped.

FINAL CONCLUSIONS

1) The analyzed species: *Vicia sativa, V. faba* y *Medicago truncatula*, present different defence mechanism against the parasitic plan *Orobanche crenata*.

2) Mucilage production can be considered as a quantitative defensive reaction taking place against *O. crenata* in *V. sativa*.

3) The production of mucilage seems to be activated by the presence of foreign substances (i.e. parasite secretions) and host-degraded products (i.e. carbohydrates from cell walls) inside host vessels.

4) The accumulation of mucilage leads to the obstruction of the parasite supply channel and to the death of established *Orobanche* tubercles.

5) Stoppage of *O. crenata* seedling penetration in the host root is a quantitative response in faba bean.

6) In a first stage, reinforcement takes place in the cortex by callose deposition in host cell walls.

7) If the parasite later overcomes the previous barrier, lignification of endodermal cell walls prevents further penetration into the central cylinder and formation of a haustorium.

8) The accumulation of phytoalexins (phenolic compounds) is the mechanism of resistance present in the tested *M. truncatul*a accessions against *O. crenata* parasite infection process.

9) This mechanism does not rely on physically stopping parasite penetration into the host: the parasite penetrates reaching the central cylinder, but it seems to be poisoned and killed before developing a haustorium.

10) A crucial difference between both *M. truncatula* accessions is the moment at which the host detects and reacts against the parasite. It determines a more effective resistance

against the pathogen: the earliest the parasite is detected, the most effective are the defensive mechanisms activated, and the infection is lower.

11) Three of the most important phytoalexins derived from phenylpropanoid pathway have been identified (i.e. formononetin, daidzein and naringenin) and their concentration in host tissues quantified as responsibles of the defence reaction in the plant-parasitic plant interaction *M. truncatula*-*O. crenata*.

12) Formononetin seems to be the most significant phytoalexin analyzed due to the direct relation between infection process and its concentration in host infected tissues: parasite intrusion raises formononetin presence in tested samples.

ARTÍCULOS PUBLICADOS

Journal of Experimental Botany Advance Access published February 10, 2006

Journal of Experimental Botany, Page 1 of 12
doi:10.1093/jxb/erj078

Journal of Experimental Botany

RESEARCH PAPER

Mucilage production during the incompatible interaction between *Orobanche crenata* and *Vicia sativa*

Alejandro Pérez-de-Luque[1,*], M. Dolores Lozano[1], José I. Cubero[2], Pablo González-Melendi[3], M. Carmen Risueño[3] and Diego Rubiales[1]

[1] *CSIC, Instituto de Agricultura Sostenible, Apdo. 4084, E-14080 Córdoba, Spain*

[2] *ETSIAM-UCO, Dep. Genética, Apdo. 3048, E-14080 Córdoba, Spain*

[3] *CSIC, Centro de Investigaciones Biológicas, Dep. Plant Development and Nuclear Organization, Ramiro de Maeztu 9, E-28040 Madrid, Spain*

Received 19 September 2005; Accepted 29 November 2005

Abstract

***Orobanche* spp. (broomrapes) are holoparasites lacking in chlorophyll and totally dependent on their host for their supply of nutrients. *O. crenata* is a severe constraint to legumes cultivation and breeding for resistance remains as one of the best available methods of control. However, little is known about the basis of host resistance to broomrapes. It is a multicomponent event, and resistance based on hampering development and necrosis of broomrape tubercles has been reported. In the present work, the formation of mucilage and occlusion of host xylem vessels associated with the death of *O. crenata* tubercles were studied histologically. Samples of necrotic *O. crenata* tubercles established on resistant and susceptible vetch genotypes were collected. The samples were fixed, sectioned and stained using different procedures. The sections were observed at the light microscopy level, either under bright field, epi-fluorescence or confocal laser scanning microscopy. A higher proportion of necrotic tubercles was found on the resistant genotype and this was associated with a higher percentage of occluded vessels. Mucilage is composed mainly by carbohydrates (non-esterified pectins) and the presence of polyphenols was also detected. The mucilage and other substances composed by parasite secretions and host-degraded products was found to block host vessels and obstruct the parasite supply channel, being a quantitative defensive response against *O. crenata* in vetch, and probably also in other legumes and plants. The presence of foreign substances (i.e. parasite secretions) and host-degraded products (i.e. carbohydrates from cell walls) inside host vessels seems to activate this response and leads to xylem occlusion and further death of established *Orobanche* tubercles.**

Key words: Histology, legumes, necrosis, *Orobanche crenata*, parasitic plants, resistance, vascular gel, *Vicia sativa*, wilt diseases, xylem mucilage.

Introduction

Broomrapes (*Orobanche* spp.) are obligate root holoparasites which connect to the vascular system of their host plants through a specialized structure known as a haustorium. These parasites are devoid of chlorophyll and totally depend on their hosts for their supply of carbon, nitrogen, and inorganic solutes. Some of these species have become a severe constraint to major crops including legumes. This is the case of *O. crenata* (crenate broomrape) which has been known to threaten legume crops since ancient times (Cubero, 1994). It is an important pest in faba bean (*Vicia faba*), pea (*Pisum sativum*), lentil (*Lens culinaris*), vetches (*Vicia* spp.), grass and chickling pea (*Lathyrus sativus* and *L. cicera*), and other grain and forage legumes in the Mediterranean basin and the Middle East (Rubiales *et al*., 2006).

Breeding for resistance is the most economic, feasible and environmentally friendly method of control against this parasite. However, despite the fact that resistance to *Orobanche* spp. has been reported (Labrousse *et al*., 2001; Rubiales *et al*., 2003*a*, *b*, 2004; Pérez-de-Luque

* To whom correspondence should be addressed. E-mail: bb2pelua@uco.es

et al., 2005*a*), little is known about the basis of host resistance to these parasites (Joel *et al*., 1996; Pérez-de-Luque *et al*., 2005*b*). One of the most common incompatible interactions described in the literature is the darkening and/or necrosis of developing tubercles (Dörr *et al*., 1994; Labrousse *et al*., 2001; Pérez-de-Luque *et al*., 2005*a*, *b*). Histological studies have revealed that initial vascular connections are established and tubercles develop, but they then become dark and the parasite dies at an early developmental stage (Dörr *et al*., 1994; Labrousse *et al*., 2001; Pérez-de-Luque *et al*., 2005*b*). The presence of substances inside host vessels has been associated with the darkening of broomrape tubercles (Labrousse *et al*., 2001; Zehhar *et al*., 2003; Pérez-de-Luque *et al*., 2005*b*) and it is possible that these substances block the vessels and interfere with the nutrient flux between host and parasite (Pérez-de-Luque *et al*., 2005*b*).

Xylem occlusion is a common response to vascular invading pathogens such as bacteria, fungi, and viruses, and formation of mucilages and tylosis is typically associated with resistance against wilt diseases (Beckman and Zaroogian, 1967; VanderMolen *et al*., 1983; Rioux *et al*., 1998; Beckman, 2000). Furthermore, it has also been reported as a response to wounded tissue (Crews *et al*., 2003). However, it has not been demonstrated as a common response against parasitic plants. In the present work, the composition and the role of these substances appearing inside host vessels of *Vicia sativa* resistant to *O. crenata* were studied by the use of different cytochemical and immunofluorescence assays.

Materials and methods

Plant material and growth conditions

Orobanche crenata seeds were collected on *Pisum sativum* infected plants in Cordoba (Spain) during year 2003. *O. crenata* was grown on resistant and susceptible genotypes of common vetch (*Vicia sativa* L., A01 and V27, respectively). The polyethylene bag system described by Linke *et al*. (2001) was used. A strip (11×28 cm) of glass fibre paper (Whatmann GF/A) with disinfected *O. crenata* seeds (40 mg) spread on it was inserted in a polyethylene bag (25×35 cm). In order to ensure homogeneous seed germination, the synthetic germination stimulant GR-24 (10 mg l^{-1}, 5 ml per bag) was added. Fifteen days later germinated vetch seedlings having a radicle length of about 4–5 cm were transferred to the bag, placing them on the upper side of the system. Twenty ml of Hoagland nutrient solution (Hoagland and Arnon, 1950) was added to each bag, and refilled later when necessary. The bags were suspended vertically in boxes and the plants were grown in a controlled environment chamber with a day/night temperature of 20±0.5 °C, 14 h photoperiod and an irradiance of 200 μmol m^{-2} s^{-1}.

At days 35, 40, and 45, the number of *O. crenata* tubercles was counted, referring those that became necrotic and died as a percentage of the total.

Collection and fixation of samples

Observations were taken using a binocular microscope (Nikon SMZ1000; Nikon Europe BV, Badhoevedorp, The Netherlands). At 35, 40, and 45 d after inoculation, tubercles of *O. crenata* were sampled at random with the corresponding attached parts of host roots.

For bright field and epi-fluoresence observations at the light microscope, the sampled material was fixed in FAA (50% ethanol+5% formaldehyde+10% glacial acetic acid, in water) for 48 h. Fixed samples were then dehydrated in ethanol series (50, 80, 95, 100, 100% for 12 h each) and transferred to an embedding solvent (Xylene; Panreac Quimica SA, Montcada i Reixac, Spain) through a xylene-ethanol series (30, 50, 80, 100, 100% for 12 h each) and finally saturated with paraffin (Paraplast Xtra; Sigma, St Louis, USA). 7 μm-thick sections were cut with a rotary microtome (Nahita 534; Auxilab SA, Beriain, Spain) and attached to adhesive-treated microscope slides (polysine slides; Menzel GmbH & Co KG, Braunschweig, Germany).

For inmunofluorescence experiments analysed through confocal laser scanning microscopy, the samples were fixed in 4% formaldehyde in phosphate buffered saline (PBS), pH 7.3 at 4 °C overnight. After washing in PBS (3×15 min), they were stored in 0.1% formaldehyde in PBS at 4 °C. 40 μm vibratome sections (Vibratome series 1000, Intracel Electrophysiology and Biochemistry Equipment, Herts, UK) were cut under water and dried down on 3-aminopropyl triethoxy silane (APTES, Sigma)-coated multi-well slides. The sections were dehydrated in a series of 30, 50, 70, and 100% methanol/water, then rehydrated in a series of 70, 50, 30% methanol/water, and finally in PBS, for 5 min at each step. To facilitate penetration of the labelling reagents, the sections were treated with 0.1% Tween 20 in PBS for 15 min at room temperature, then washed in PBS for 5 min and allowed to dry.

Cytochemical methods for light microscopy

After removal of paraffin, the sections were stained with different dyes: (i) Alcian green: safranin (AGS) (Joel, 1983). The slides were dried and mounted with DePeX (BDH). With this staining method, carbohydrates (including cell walls and mucilage) appeared green, yellow or blue, while lignified, cutinized and suberized walls, as well as tannin and lipid material inside cells appeared red (Joel, 1983). Non-stained sections were kept as control, and for examination under the fluorescence microscope. (ii) Staining with 0.05% toluidine blue O (TBO) in PO_4 buffer (pH 5.5) during 5–10 min was used. In this case the dye was applied before removal of paraffin (Ruzin, 1999). This method allows the detection of phenolics as well as tannins, lignin, and suberin (Baayen *et al*., 1996; Bordallo *et al*., 2002; Mellersh *et al*., 2002; Crews *et al*., 2003). (iii) Phloroglucinol (2% in ethanol)–HCl (35%) (Ruzin, 1999) stains the aldehyde groups of lignin and suberin, but quenches lignin autofluorescence and retains suberin fluorescence (Baayen *et al*., 1996; Rioux *et al*., 1998). (iv) Aniline blue fluorochrome was used for callose detection under UV fluorescence. The samples were stained during 15–30 min in a solution 0.1% aniline blue fluorochrome in water (Bordallo *et al*., 2002). (v) Pectins were detected using ruthenium red. The samples were immersed during 5 min in a solution 0.05% ruthenium red in water. Non-methyl-esterified pectins take a red/pink coloration with this dye (Vallet *et al*., 1996).

The sections were observed using a light microscope (Leica DM-LB, magnification ×100 to ×400; Leica Microsystems Wetzlar GmbH, Wetzlar, Germany) and photographed using a digital camera (Nikon DXM1200F; Nikon Europe BV, Badhoevedorp, The Netherlands). The samples were also observed by epi-fluorescence under excitation at 450–490 nm (blue-violet).

Immunofluorescence for confocal laser scaning microscopy

After blocking with 5% bovine serum albumin (BSA) in PBS for 5 min, the slides carrying the vibratome sections were incubated with the first antibody undiluted for 1 h: JIM 5 for non-methyl-esterified

pectins and JIM 7 for methyl-esterified pectins (Professor Keith Roberts, John Innes Centre, Norwich, UK). After washing in PBS, they were incubated with a fluorescent anti-rat ALEXA 546 (Molecular Probes Inc., Eugene, OR, USA) antibody applied 1/25 in 3% BSA in PBS for 45 min at room temperature in the dark. Confocal optical section stacks were collected using a Leica TCS-SP2-AOBS-UV confocal laser scanning microscope (Leica Microsystems Wetzlar GmbH, Wetzlar, Germany).

Dye tracer

Naphthol blue black was used as a dye tracer to test the continuity of water and nutrient fluxes between the host root and the parasite tubercles (Jacobsen *et al*., 1992). The distal parts of infected vetch roots were immersed into a dye solution 0.1% naphthol blue black and the root tips cut under the solution. Transpiration was then allowed to proceed for 4–5 h. Attached tubercles with the corresponding host root part as well as root sections cut at various points (before and after attached tubercles) were sampled. Transverse fresh hand-cut sections of the samples were observed under a light microscope.

Determination of sealed vessels

Samples stained with AGS were used to determine the proportion of vessels filled with different substances. Transverse sections of the

Table 1. *Proportion of* O. crenata *necrotic tubercles (incompatible interactions) after their establishment on susceptible and resistant vetches*

Data are expressed as a percentage of the total number of established tubercles. dai, days after inoculation. Log-transformed data with SE shown in parentheses alongside back-transformed means.

Genotype	Necrotic tubercles (%)		
	35 dai	40 dai	45 dai
V. sativa V27 (susceptible)	8.0 (0.21±0.06)	15.9 (0.33±0.08)	27.6 (0.48±0.09)
V. sativa A01 (resistant)	13.8 (0.31±0.09)	51.4 (0.80±0.14)	61.5 (0.95±0.17)

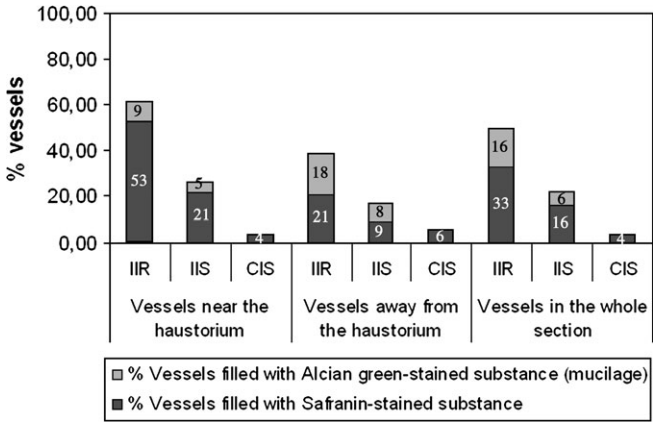

Fig. 1. Proportion of vessels filled with mucilage and other substances depending on the interaction between host and parasite: IIR, incompatible interaction on resistant host; IIS, incompatible interaction on susceptible host; CIS, compatible interaction on susceptible host. Samples collected 45 d after inoculation were used.

Table 2. *Reaction of tissues to different cytochemical assays in an incompatible interaction in resistant vetch*

Cytochemical assays	Specificity	Colour[a]	Vessels			Parenchyma			Fibres			Endodermis			Mucilages	Interface host–parasite
			ml[b]	w	l	ml	w	p	ml	w	p	ml	w	p		
AGS stain	Carbohydrates	Blue-green (B)	+	–	+	+	–	–	+	–	–	–	–	–	+	–
	Lignin, suberin, cutin, tannins, lipids	Red (B)	+	+	+	+	–	–	+	+	+	+	–	–	–	+
TBO stain	Polyphenols	Green-blue, turquoise (B)	+	+	+	+	+	–	+	+	+	–	+	–	+	+
	Carboxylated polysaccharides	Pink (B)	+	–	+	+	–	–	–	+	–	–	–	–	+	–
Phloroglucinol–HCl stain	Lignin, suberin, polyphenols	Red (B)	+	+	+	+	–	–	+	+	+	+	+	–	+	+
	Suberin	Blue-white (F)	–	–	–	–	–	–	–	–	–	–	+	–	–	–
Aniline blue fluorochrome	Callose	Blue-white (F)	+	+	–	+	+	+	–	–	–	–	–	–	–	+
Ruthenium red stain	Non-esterified pectins	Pink (B)	+	–	+	+	+	–	+	–	+	+	–	–	+	+

[a] Observed under brightfield (B) or epi-fuorescence (F).
[b] The presence of staining in the tissue is indicated by (+) and the absence by (–). Samples collected 45 dai were used. ml: middle lamellae; w: cell wall; l: lumen; p: protoplasma.

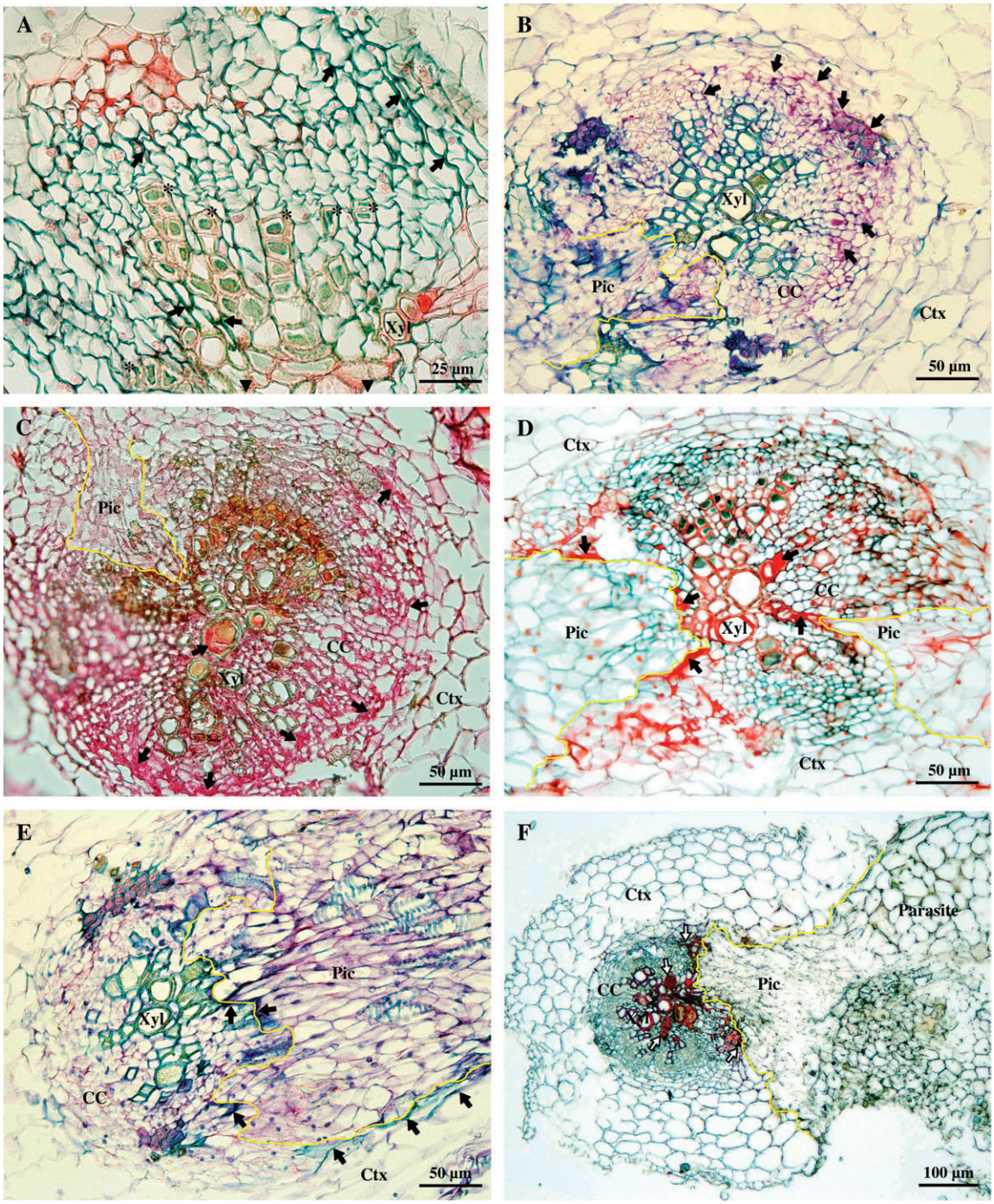

Fig. 2. Cross-sections of incompatible interactions of *Orobanche crenata* on resistant vetch (*Vicia sativa* line A01) stained following different procedures. (A) AGS staining showing accumulation of carbohydrates (arrows, green colour) in the apoplast of areas opposite the haustorium. Neighbouring xylem vessels filled with mucilage can also be observed (asterisks). Arrowheads indicate the direction where the haustorium was located. (B) The same as (A) with TBO staining showing the accumulation of carboxylated polysaccharides (arrows, pink colour) in parenchymatic cells. (C) The same as (A) with ruthenium red staining indicating the presence of non-esterified pectins (arrows, pink colour). (D) AGS staining showing areas and vessels dyed with safranin next to the haustorium (arrows, red colour). (E) TBO staining indicating the presence of polyphenols and lignins (arrows, blue-turquoise colour). (F) The same as (E) with phloroglucinol-HCl staining showing lignins and polyphenols (arrows, red colour). Yellow lines delimit parasite from host tissues. CC, central cylinder; Ctx, cortex; Pic, parasite intrusive cells (haustorium); Xyl, xylem vessel.

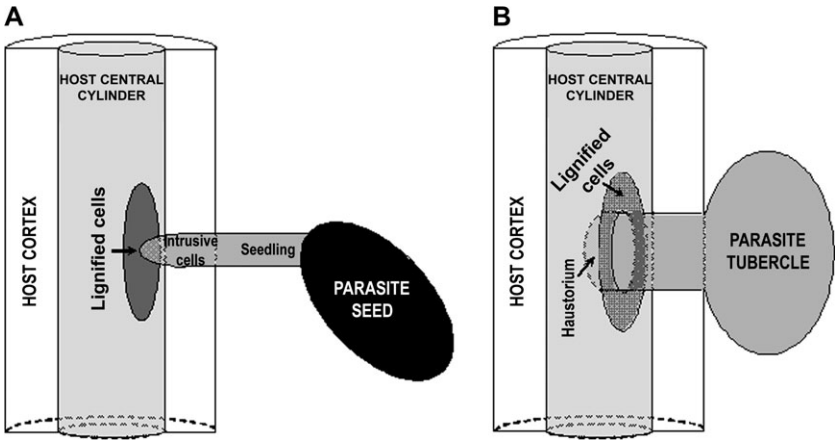

Fig. 3. Scheme of *O. crenata* penetration process into a resistant host. (A) The parasite meets a physical barrier (lignified cells) before reaching the host central cylinder. (B) The parasite successfully overcomes the host barrier and penetrates into the central cylinder, but lignified cells still remain surrounding the intruding tissues like a ring.

haustoria were observed under the light microscope, with the host central cylinder centred within the field of view. The central cylinder was divided in four equitable quadrants and the relative position of the haustorium with respect to these quadrants was recorded. Vessels within quadrants containing the haustorium were considered close to the haustorium, and vessels within quadrants not containing the haustorium were considered away from the haustorium. The number of vessels filled with safranin and alcian green-stained substances were recorded, and expressed as a percentage with respect to the total number of vessels in each quadrant.

Statistical analysis

Assays were performed with ten replicates per treatment with a completely randomized design. Statistical analysis (ANOVA) was performed with SPSS 10.0 and Statistix 8.0 for Windows. Percentages were transformed according to the formula

$$Y = \arcsin\left(\sqrt{(X\%/100)}\right).$$

A minimum of ten samples from a pull collected from ten replicates were used for each cytochemical assay.

Results

The highest proportion of necrotic tubercles was found on the resistant genotype (Table 1). The percentage of necrotic tubercles increased with time in both resistant and susceptible genotypes, but at a much higher rate in the resistant one.

Vessels of susceptible roots in a compatible interaction contained no mucilage, but in some cases the presence of safranin-staining substance could be detected at low proportions (Fig. 1). During an incompatible interaction there was a higher percentage of vessels filled with substances in resistant vetch than in susceptible vetch. Within an incompatible interaction more than half of the vessels near the haustorium were filled with the safranin-staining substance in the resistant genotype. There was a higher proportion of vessels filled with mucilage opposite to rather than next to the haustorium in resistant vetch.

Table 2 shows the reactions of different tissues to the histochemical tests in incompatible interactions in resistant vetch. Carbohydrates, including carboxylated polysaccharides and pectins, were detected using alcian green, TBO, and ruthenium red dyes mainly in the apoplast (Fig. 2A–C). A more intense staining for carbohydrates was detected in zones opposite the haustorium of necrotic tubercles than that of healthy tubercles. An intense staining for polyphenols and lignins with AGS, TBO and phloroglucinol was seen in zones next to the haustorium of necrotic tubercles (Fig. 2D–F). The staining also appeared in the apoplast and in the interface between host and parasite. Lignification of host cell walls in contact with parasite tissues was observed at different points and on consecutive sections. These lignified walls formed a ring surrounding the parasite intruding tissues and corresponded to cells from the host endodermis and/or pericycle. Figure 3 shows a 3D diagram of this phenomenon. The presence of suberin was restricted only to the endodermal cells (Fig. 4A, B), and callose accumulated in some parenchyma cells, in the host–parasite interface and in the middle lamellae and cell wall of some xylem vessels (Fig. 4C–F).

Staining consecutive sections with different dyes allowed the composition of mucilage and other substances inside the xylem vessels to be characterized (Fig. 5). Mucilage stained with alcian green from AGS staining, indicates a carbohydrate composition (Fig. 5A, E). This was confirmed by the pink colour after TBO staining, that corresponds to carboxylated polysaccarides (Fig. 5B). The pink/red colour obtained with ruthenium red indicated the presence of non-methyl-esterified pectins (Fig. 5C). The presence of polyphenols was also confirmed by blue–turquoise staining with TBO (Fig. 5B) and red staining with phloroglucinol (Fig. 5F) and the absence of lipids, tannins, suberin, and lignin because of the negative staining with safranin from AGS (Fig. 5A, E). The mucilage was colourless in non-stained sections, whereas the other

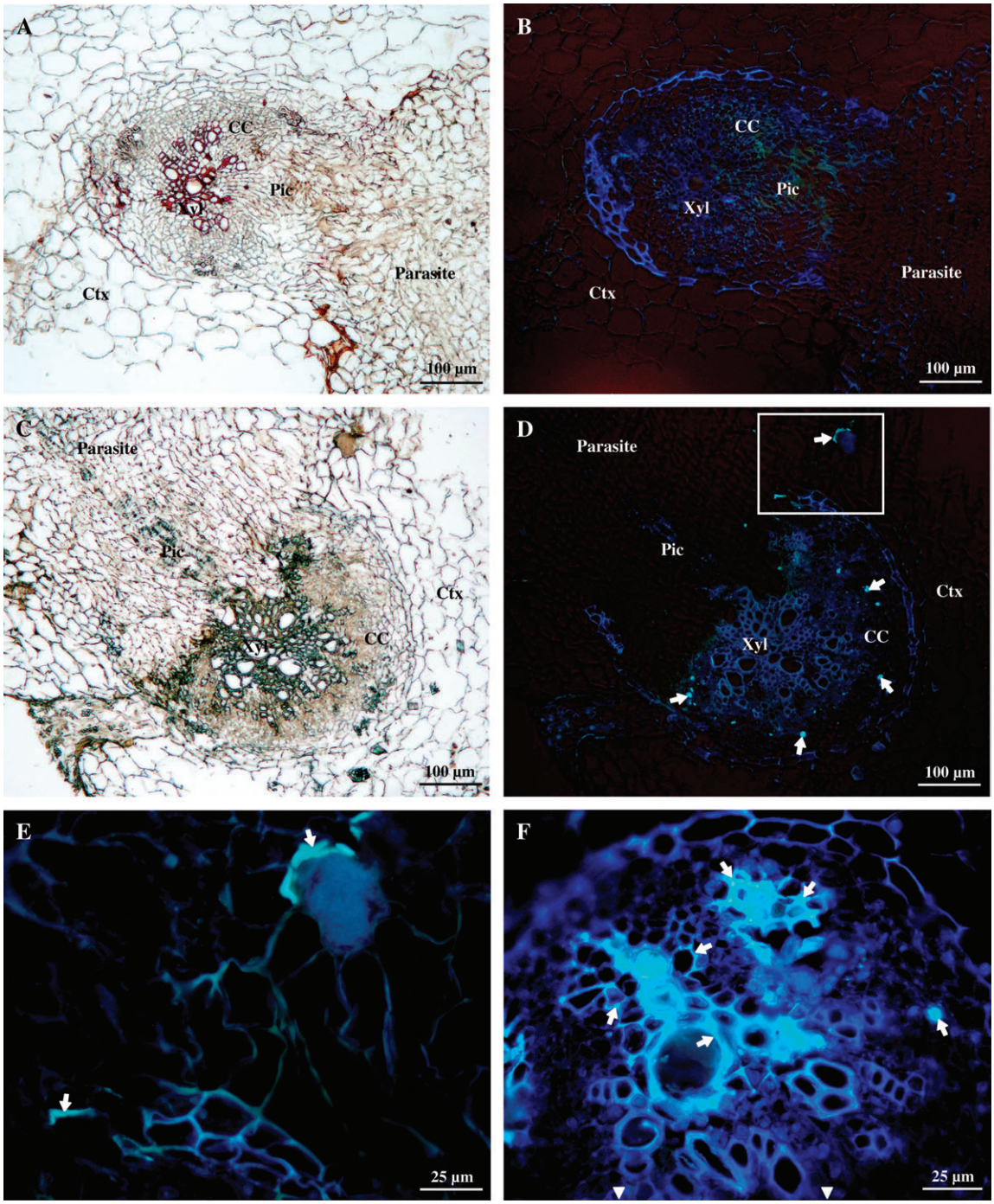

Fig. 4. Cross-sections of incompatible interactions of *Orobanche crenata* on resistant vetch (*Vicia sativa* line A01) stained for suberin and callose detection. (A) Section stained with phloroglucinol-HCl in order to quench lignin autofluorescence. (B) The same as (A) observed by epi-fluorescence under blue-violet excitation. Suberized cell walls can be observed (blue fluorescence), mainly corresponding to the endodermis. The absence of lignin fluorescence can be observed (for example, xylem vessels). The fluorescence of endodermal cells is disrupted at the point of penetration of the parasite (haustorium). (C) Light micrograph of a section stained for callose detection. (D) The same as (C) observed by epi-fluorescence under blue-violet excitation. Callose depositions show a blue-white fluorescence (arrows). (E) Detail of (D) showing callose deposition in cortical cell walls in contact with parasite tissues (arrows). (F) Detail of a central cylinder showing callose depositions in xylem walls and parenchyma cells (arrows). Arrowheads indicate the direction where the haustorium was located. CC, central cylinder; Ctx, cortex; Pic, parasite intrusive cells (haustorium); Xyl, xylem vessel.

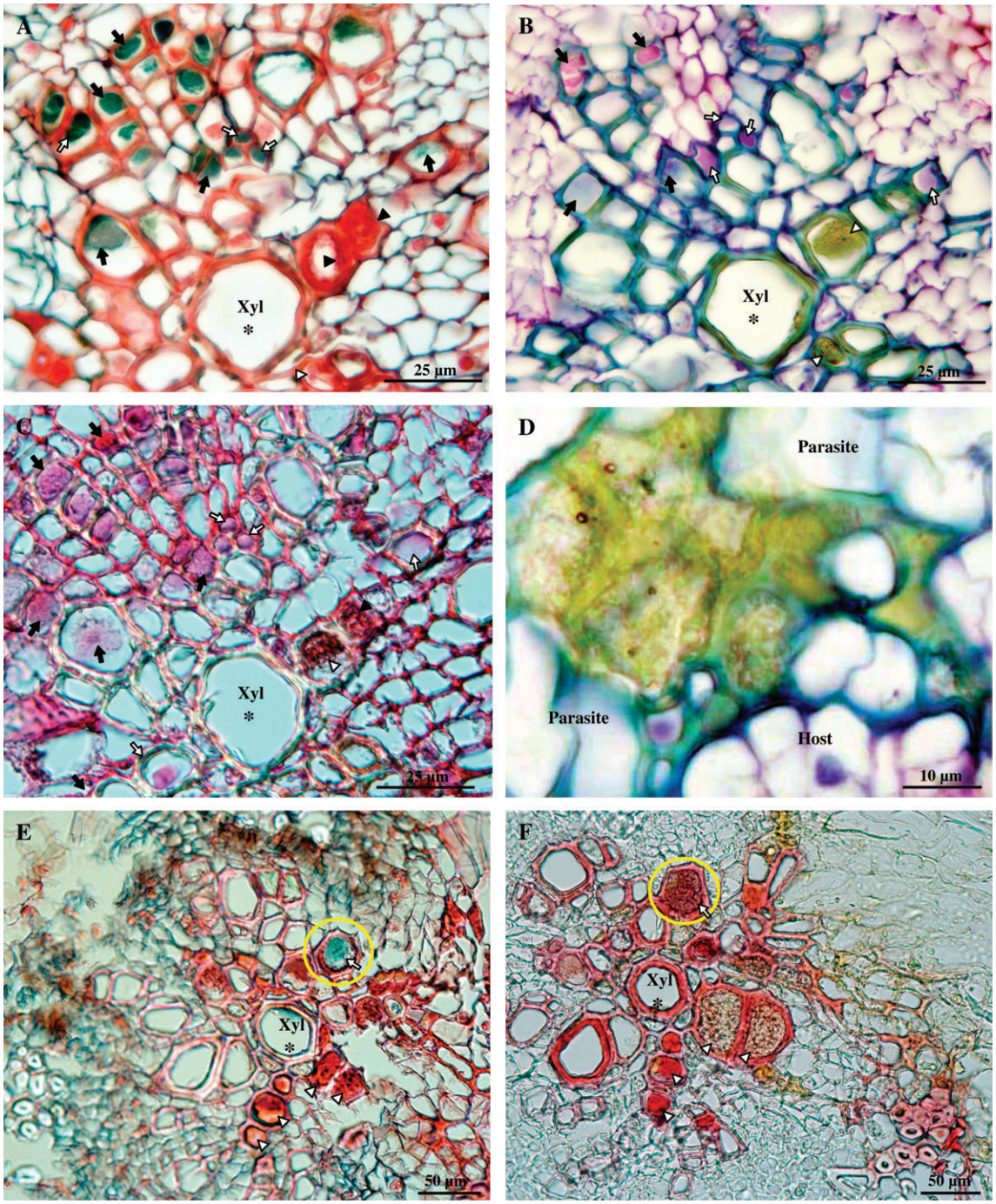

Fig. 5. Cross-sections of incompatible interactions of *Orobanche crenata* on resistant vetch (*Vicia sativa* line A01) stained for characterization of mucilage composition. (A–C) Sections from the same series stained with AGS, TBO, and ruthenium red, respectively. Arrows indicate mucilage inside xylem vessels and arrowheads other filling substances. Asterisk indicates sections of the same xylem vessel as a reference. Green colour in (A) corresponds to carbohydrates and red colour with lignin, and/or lipids. Pink colour in (B) corresponds to carboxylated polysaccharides and blue–turquoise with polyphenols. Pink colour in (C) corresponds to non-methyl-esterified pectins. (D) Detail of the other substance(s) found inside xylem vessels, in this case located within the interface host–parasite, and stained with TBO. A granular structure and heterogeneous aspect can be observed. (E, F) Sections from the same series stained with AGS and phloroglucinol-HCl, respectively. Arrows indicate mucilage inside xylem vessels and arrowheads other filling substances. A yellow circle indicates the same xylem vessel in both sections. Asterisk indicates sections of the same xylem vessel as a reference. Green colour in (E) corresponds to carbohydrates and red colour with lignin and/or lipids. Red colour in (F) corresponds to lignin and polyphenols. Xyl, xylem vessel.

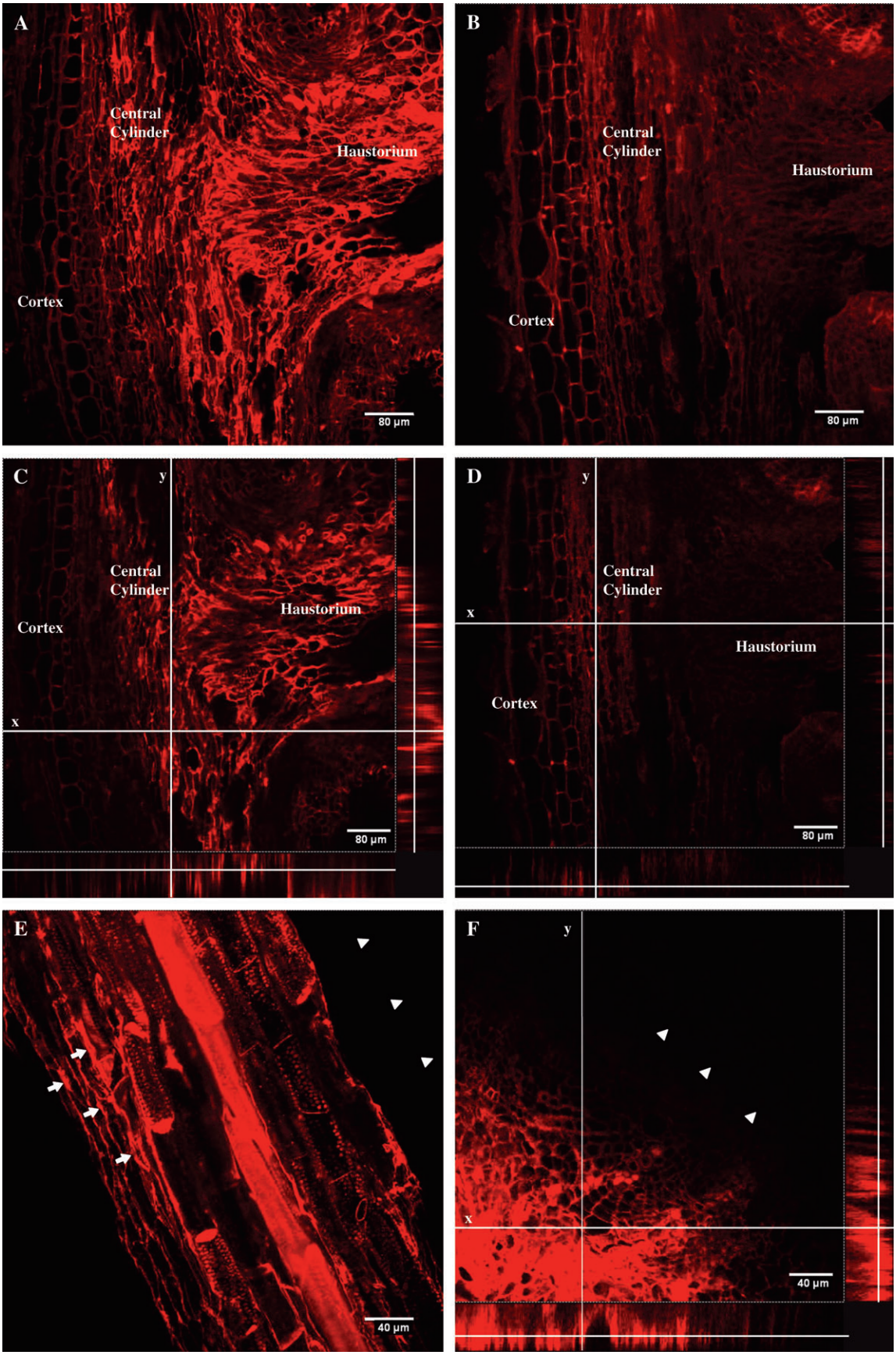
A
Central Cylinder
Haustorium
Cortex
80 µm
B
Central Cylinder
Haustorium
Cortex
80 µm
C
y
Central Cylinder
Haustorium
Cortex
x
80 µm
D
y
Central Cylinder
x
Haustorium
Cortex
80 µm
E
40 µm
F
y
x
40 µm

substances found inside host vessels showed a natural brownish yellow coloration. This substance stained strongly red with safranin from AGS (Fig. 5A, E), was positive also for ruthenium red (Fig. 5C), phloroglucinol (Fig. 5F), and TBO originated a green staining (Fig. 5B, D). All this indicated the presence of polyphenols, pectins, lignins, and probably lipids and/or tannins, but not suberin due to the lack of fluorescence using phloroglucinol staining (Fig. 4B). Positive staining with ruthenium red showed non-esterified pectins also being part of these components (Fig. 5C). Contrary to the homogeneous aspect showed by the mucilage, this substance presented a heterogeneous aspect and a granular structure (Fig. 5D).

In order to confirm that the mucilage was mainly composed of non-methyl-esterified pectins, immunostaining was performed with antibodies JIM 5 and JIM 7. An intense staining was observed in the core of the haustorium and adjacent areas for non-esterified pectins (Fig. 6A), whereas little presence of esterified pectins was detected (Fig. 6B) and was mainly restricted to host cortical cell walls opposite the haustorium. In no case were esterified pectins located inside host vessels (Fig. 6D). Non-esterified pectins were located in the apoplast, between intercellular spaces, and inside host xylem vessels (Fig. 6C, E, F), and in vascular parenchyma cells opposite the haustorium (Fig. 6E, F), this last being a confirmation of the important role of these cells in the synthesis and secretion of the mucilage.

When naphthol blue black was applied into the transpiration stream of roots, it was confined to the vascular bundles and stained the areas it was moving through. In compatible interactions, the vessels of the healthy tubercles and the haustorium were stained (Fig. 7A, B). By contrast, the dye did not reach the necrotic tubercles of incompatible interactions either in the haustorium or nearby host vascular tissues, but reached host vessels opposite to and away from the haustorium (Fig. 7C, D).

Discussion

Xylem occlusion as a putative defensive response against parasitic plants has been reported previously (Labrousse *et al*., 2001; Zehhar *et al*., 2003; Pérez-de-Luque *et al*., 2005*b*). However, no detailed studies about this phenomenon had been undertaken. The results presented here suggest that it is a quantitative trait, expressed against *O. crenata* at a higher intensity within resistant compared with susceptible vetch genotypes. The response is quantitative not only in the amount of incompatible infection units (Table 1), but also in the amount of mucilage accumulating inside vessels within incompatible interactions (Fig. 1).

The mucilage is presumably produced by vascular parechyma cells near xylem vessels, as indicated by the more intense staining for carbohydrates observed in resistant plants (Fig. 2A), the immunostaining for non-esterified pectins with JIM 5 (Fig. 6E, F) and by the presence of a higher proportion of vessels away from the haustorium filled with mucilage (Fig. 1). This is in agreement with previous reports about mucilage production and secretion (Shi *et al*., 1992; Baayen *et al*., 1996; Dong *et al*., 1997; Rioux *et al*., 1998; Crews *et al*., 2003). Despite VanderMolen *et al*. (1983) suggesting that occlusion gels congeal in host vessels after dissolution of carbohydrates from host cell walls by pathogen enzymes, no evidence for this has been found. However, the safranin-staining substance accumulated in vessels near the haustorium is probably composed, partially at least, by host cell components released by *O. crenata* enzymatic activity.

The main components of the mucilage seem to be carbohydrates, specifically non-methyl-esterified pectins, and polyphenols to a lesser extent. This composition confers good properties to the gel in order to act as a permanent seal: the mixture can be polymerized by peroxidases to form a stable adhesive (Crews *et al*., 2003). This idea is supported by the accumulation of peroxidase in vessels of rice challenged by a vascular pathogen reported by Young *et al*. (1995) and the increased levels of peroxidase activity found by Pérez-de-Luque *et al*. (2005*a*) in resistant peas to *O. crenata* showing this kind of incompatible reaction (i.e. necrotic tubercles and mucilage production). Being of a composition similar to that described for mucilage produced against other vascular pathogens (Shi *et al*., 1992; Baayen *et al*., 1996; Kpémoua *et al*., 1996; Dong *et al*., 1997; Rioux *et al*., 1998; Tagne *et al*., 2002) it was assumed that this is the same response as found in those other pathogenic systems.

The question arising is why this defensive mechanism is activated if the parasite does not invade host vessels in the

Fig. 6. Localization of methyl-esterified and non-methyl-esterified pectins with antibodies JIM 7 and JIM 5, respectively. The images were obtained using confocal microscopy and are full Z-series projections in (A), (B) and (E), and single optical sections with projections on X and Y in (C), (D) and (F). (A) Longitudinal section of the haustorium in an incompatible interaction showing localization of non-methyl-esterified pectins. (B) The same as (A) showing localization of methyl esterified pectins. (C) Single section from (A) with the corresponding projections on X and Y of virtual sections indicated by white lines. (D) Single section from (B) with the corresponding projections on X and Y of virtual sections indicated by white lines. (E) Longitudinal section of an infected resistant vetch root showing localization of non-methyl-esterified pectins inside xylem vessels filled with mucilage. Accumulation of non-methyl-esterified pectins can also be observed within intercellular spaces and cell walls of vascular parenchyma cells (arrows). Red points in the xylem vessels correspond to non-lignified areas from which the mucilage can penetrate into the vessels. Arrowheads indicate the direction where the haustorium was located. (F) Single cross-section of an infected resistant vetch root showing localization of non-methyl-esterified pectins inside xylem vessels and intercellular spaces and cell walls of vascular parenchyma cells. Projections on X and Y of virtual sections (white lines) of the whole series are shown. Arrowheads indicate the position where the haustorium was located.

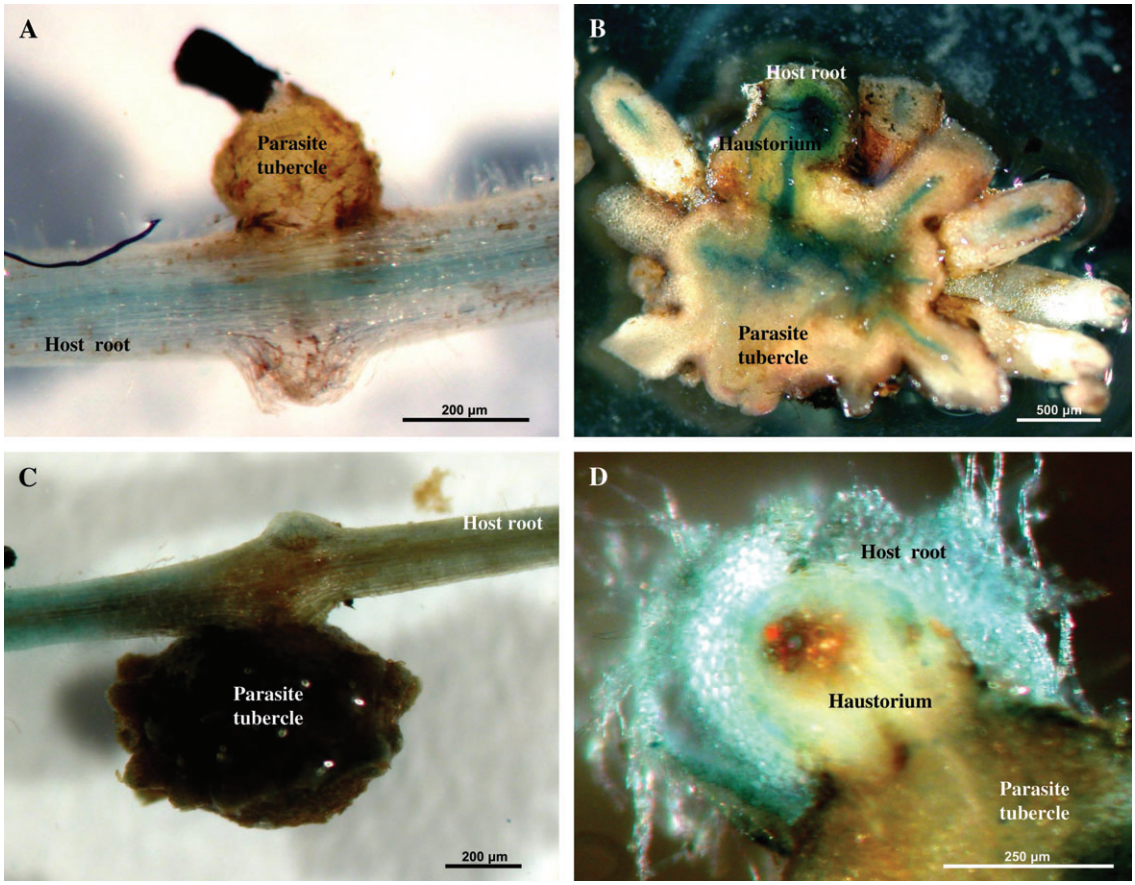

Fig. 7. Presence of naphthol blue black dye tracer within host and parasite tissues in compatible and incompatible interactions. (A) Compatible interaction on susceptible vetch showing the dye blue coloration of vascular tissues along the root. (B) Hand section of a well-developed *O. crenata* tubercle on susceptible vetch showing the dye blue coloration of the vascular tissues. (C) Incompatible interaction on resistant vetch showing the localization of dye blue coloration only before the point of attachment by the tubercle. (D) Hand section of a necrotic *O. crenata* tubercle on resistant vetch showing sealed vessels and the absence of the dye inside parasite vessels.

same way as a vascular pathogen (i.e. fungi or bacteria spread along the xylem lumen). A first hypothesis could be that the host recognizes a wound in the tissues when the parasite penetrates, and mucilage production is activated as reported by Crews *et al*. (2003). However, the mucilage production would also be observed in susceptible plants during compatible interactions, and that is not the case (Fig. 1). Thus, in order to find out a more satisfactory answer, attention was paid to the safranin-staining substance accumulating in vessels near the haustorium. As previously stated (Pérez-de-Luque *et al*., 2005b) and confirmed by the present results (Table 1), this substance always accumulates in areas near the core of the haustorium and a similar substance was found at the attachment area of *O. crenata* seedlings and surrounding parasite intrusive tissues (Pérez-de-Luque *et al*., 2005*b*). This substance seems to be, at least partially, parasite originated, because it only appears on the external parasite interface near the attachment and penetration point (Pérez-de-Luque *et al*., 2005*b*). The role of this substance seems to be an anchoring device for the parasite in order to penetrate host tissues by mechanical pressure (Joel *et al*., 1996). Lipids probably take part in the composition of this secretion as well as non-methyl-esterified pectins (Figs 5A, C, 6A, C), conferring the adhesive properties. But the parasite also releases enzymes to allow penetration between host cells (Singh and Singh, 1993; Antonova and Ter Borg, 1996; Losner-Goshen *et al*., 1998). These enzymes dissolve components from the host cell walls and middle lamellae, such as pectins, polyphenols, and lignins, which will became part of the secretion, as suggested by the staining with AGS, ruthenium red, phloroglucinol, and TBO (Fig. 5). In fact, the secretion can be considered as a pull of different substances and components, including enzymes, originated mainly from the parasite, but also from the host. This could explain the heterogeneous aspect and granular structure it presents (Fig. 5D). When the parasite is hampered during the penetration attempts, it releases a higher amount of secretions (i.e. enzymes and adhesives) to overcome the host resistance (Joel *et al*., 1996; Pérez-de-Luque *et al*., 2005*b*). The presence of a ring of lignified host cells surrounding the parasite intruding tissues probably

corresponds to a previous barrier to penetration broken by the parasite (Fig. 3). If the parasite is successful and establishes vascular connections with the host, the excess of secretions and dissolved cell wall components leak through the apoplast and reach the neighbouring host vessels (Pérez-de-Luque *et al*., 2005*b*). At this time, the presence of foreign substances inside host vessels may activate the production and accumulation of mucilage. The degraded products from host cell walls, as carbohydrates, can act as the endogenous elicitors of defence responses (Aldington and Fry, 1993; Moerschbacher *et al*., 1999). Finally, the accumulation of mucilage, secretions, and degraded products block host vessels and does not allow nutrient flux between host and parasite (Fig. 7), causing further parasite death.

In conclusion, mucilage production can be considered as a quantitative defensive reaction taking place against *O. crenata* in vetch, and probably also in other legumes (Pérez-de-Luque *et al*., 2005*b*) and plants (Labrousse *et al*., 2001; Zehhar *et al*., 2003). It seems to be activated by the presence of foreign substances (i.e. parasite secretions) and host-degraded products (i.e. carbohydrates from cell walls) inside host vessels, and leads to the obstruction of the parasite supply channel and to the death of established *Orobanche* tubercles.

Acknowledgements

We thank Ana Moral for her help in the realization of this work and the Confocal Microscopy Service of the CIB-CSIC (Madrid) where observations were made.

A P-d-L was a visiting researcher at the Plant Development group at the CSIC-Madrid funded by the Consejería de Innovación, Ciencia y Empresa de la Junta de Andalucía. P G-M is a researcher at the CSIC funded by the programme 'Ramón y Cajal' of the Spanish Ministry of Education and Science.

JIM 5 and JIM 7 antibodies were kindly supplied by Professor Keith Roberts from John Innes Centre in Norwich (UK).

This research was supported by the projects AGL2002-03248 and BOS2002-03550.

References

Aldington S, Fry SC. 1993. Oligosaccharins. *Advances in Botanical Research* **19,** 1–101.

Antonova TS, Ter Borg SJ. 1996. The role of peroxidase in the resistance of sunflower against *Orobanche cumana* in Russia. *Weed Research* **36,** 113–121.

Baayen RP, Ouellette GB, Rioux D. 1996. Compartmentalization of decay in carnations resistant to *Fusarium oxysporum* f. sp. *dianthi. Phytopathology* **86,** 1018–1031.

Beckman CH. 2000. Phenolic-storing cells: keys to programmed cell death and periderm formation in wilt disease resistance and in general defence responses in plants? *Physiological and Molecular Plant Pathology* **57,** 101–110.

Beckman CH, Zaroogian GE. 1967. Origin and composition of vascular gel in infected banana roots. *Phytopathology* **57,** 11–13.

Bordallo JJ, Lopez-Llorca LV, Jansson HB, Salinas J, Persmark L, Asensio L. 2002. Colonization of plant roots by egg-parasitic and nematode-trapping fungi. *New Phytologist* **154,** 491–499.

Cubero JI. 1994. Breeding work in Spain for *Orobanche* resistance in faba bean and sunflower. In: Pieterse AH, Verkleij JAC, ter Borg SJ, eds. *Biology and management of* Orobanche. Proceedings of the Third International Workshop on *Orobanche* and related *Striga* Research. Amsterdam: Royal Tropical Institute, 465–473.

Crews LJ, McCully ME, Canny MJ. 2003. Mucilage production by wounded xylem tissue of maize roots:time-course and stimulus. *Functional Plant Biology* **30,** 755–766.

Dong Z, McCully ME, Canny MJ. 1997. Does *Acetobacter diazotrophicus* live and move in the xylem of sugarcane stems? Anatomical and physiological data. *Annals of Botany* **80,** 147–158.

Dörr I, Staack A, Kollmann R. 1994. Resistance of *Helianthus* to *Orobanche*: histological and cytological studies. In: Pieterse AH, Verkleij JAC, eds. *Biology and management of* Orobanche. Proceedings of the Third International Workshop on *Orobanche* and related *Striga Research.* Amsterdam: Royal Tropical Institute, 276–289.

Hoagland DR, Arnon DI. 1950. The water-culture method for growing plants without soil. *California Agricultural Experiment Station Circular* 347. University of California, Berkeley, USA.

Jacobsen KR, Fisher DG, Maretzki A, Moore PH. 1992. Developmental changes in the anatomy of the sugarcane stem in relation to phloem unloading and sucrose storage. *Botanical Acta* **105,** 70–80.

Joel DM. 1983. AGS (Alcian Green Safranin): a simple differential staining of plant material for the light microscope. *Proceedings of the Royal Microscopical Society* **18,** 149–151.

Joel DM, Losner-Goshen D, Hershenhorn J, Goldwasser Y, Assayag M. 1996. The haustorium and its development in compatible and resistant host. In: Moreno MT, Cubero JI, Berner D, Joel DM, Musselman LJ, Parker C, eds. *Advances in parasitic plant research.* Córdoba: Junta de Andalucía, Consejería de Agricultura y Pesca, 531–541.

Kpémoua K, Boher B, Nicole M, Calatayud P, Geiger JP. 1996. Cytochemistry of defense responses in cassava infected by *Xanthomonas campestris* pv. manihotis. *Canadian Journal of Microbiology* **42,** 1131–1143.

Labrousse P, Arnaud MC, Serieys H, Bervillé A, Thalouarn P. 2001. Several mechanisms are involved in resistance of *Helianthus* to *Orobanche cumana* Wallr. *Annals of Botany* **88,** 859–868.

Linke K-H, Joel DM, Kroschel J. 2001. Observations of the underground development. Polybag system. In: Kroschel J, ed. *A technical manual for parasitic weed research and extension.* Dordrecht: Kluwer Academic Publishers, 56–58.

Losner-Goshen D, Portnoy VH, Mayer AM, Joel DM. 1998. Pectolytic activity by the haustorium of the parasitic plant *Orobanche* L. (Orobanchaceae) in host roots. *Annals of Botany* **81,** 319–326.

Mellersh DG, Foulds IV, Higgins VJ, Heath MC. 2002. H_2O_2 plays different roles in determining penetration failure in three diverse plant–fungal interactions. *The Plant Journal* **29,** 257–268.

Moerschbacher BM, Mierau M, Graeβner B, Noll U, Mort AJ. 1999. Small oligomers of galacturonic acid are endogenous suppressors of disease resistance reactions in wheat leaves. *Journal of Experimental Botany* **50,** 605–612.

Pérez-de-Luque A, Jorrín J, Cubero JI, Rubiales D. 2005*a.* Resistance and avoidance against *Orobanche crenata* in pea (*Pisum* spp.) operate at different developmental stages of the parasite. *Weed Research* **45,** 379–387.

Pérez-de-Luque A, Rubiales D, Cubero JI, Press MC, Scholes J, Yoneyama K, Takeuchi Y, Plakhine D, Joel DM. 2005*b.*

Interaction between *Orobanche crenata* and its host legumes: unsuccessful haustorial penetration and necrosis of the developing parasite. *Annals of Botany* **95,** 935–942.

Rioux D, Nicole M, Simard M, Ouellette GB. 1998. Immunocytochemical evidence that secretion of pectin occurs during gel (gum) and tylosis formation in trees. *Phytopathology* **88,** 494–505.

Rubiales D, Alcántara C, Sillero JC. 2004. Variation in resistance to crenate broomrape (*Orobanche crenata*) in species of *Cicer*. *Weed Research* **44,** 27–32.

Rubiales D, Pérez-de-Luque A, Cubero JI, Sillero JC. 2003*a.* Crenate broomrape (*Orobanche crenata*) infection in field pea cultivars. *Crop Protection* **22,** 865–872.

Rubiales D, Pérez-de-Luque A, Joel DM, Alcántara C, Sillero JC. 2003*b.* Characterization of resistance in chickpea to crenate broomrape (*Orobanche crenata*). *Weed Science* **51,** 702–707.

Rubiales D, Pérez-de-Luque A, Sillero JC, Román B, Kharrat M, Khalil S, Joel DM, Riches C. 2006. Screening techniques and sources of resistance against parasitic weeds in grain legumes. *Euphytica* **144,** (in press).

Ruzin SE. 1999. *Plant microtechnique and microscopy*, 1st edn. New York: Oxford University Press.

Shi J, Mueller WC, Beckman CH. 1992. Vessel occlusion and secretory activities of vessel contact cells in resistant or susceptible cotton plants infected with *Fusarium oxysporum* f. sp. *vasinfectum. Physiological and Molecular Plant Pathology* **40,** 133–147.

Singh A, Singh M. 1993. Cell wall degrading enzymes in *Orobanche aegyptiaca* and its host *Brassica campestris. Physiologia Plantarum* **89,** 177–181.

Tagne A, Neergaard E, Hansen HJ, The C. 2002. Studies of host–pathogen interaction between maize and *Acremonium strictum* from Cameroon. *European Journal of Plant Pathology* **108,** 93–102.

Vallet C, Chabbert B, Czaninski Y, Monties B. 1996. Histochemistry of lignin deposition during sclerenchyma differentiation in alfalfa stems. *Annals of Botany* **78,** 625–632.

VanderMolen GE, Labavitch JM, Strand LL, DeVay JE. 1983. Pathogen-induced vascular gels: ethylene as a host intermediate. *Physiologia Plantarum* **59,** 573–580.

Young SA, Guo A, Guikema JA, White FF, Leach JE. 1995. Rice cationic peroxidase accumulates in xylem vessels during incompatible interactions with *Xanthomonas oryzae* pv. *oryzae. Plant Physiology* **107,** 1333–1341.

Zehhar N, Labrousse P, Arnaud MC, Boulet C, Bouya D, Fer A. 2003. Study of resistance to *Orobanche ramosa* in host (oilseed rape and carrot) and non-host (maize) plants. *European Journal of Plant Pathology* **109,** 75–82.

Annals of Applied Biology ISSN 0003-4746

RESEARCH ARTICLE

Resistance to broomrape (*Orobanche crenata*) in faba bean (*Vicia faba*): cell wall changes associated with prehaustorial defensive mechanisms

A. Pérez-de-Luque[1], M.D. Lozano[2], M.T. Moreno[1], P.S. Testillano[3] & D. Rubiales[2]

1 Área de Mejora y Biotecnología, Centro "Alameda del Obispo", IFAPA (Junta de Andalucía), Córdoba, Spain
2 Instituto de Agricultura Sostenible, CSIC, Córdoba, Spain
3 Department of Plant Development and Nuclear Organization, Centro de Investigaciones Biológicas, CSIC, Madrid, Spain

Keywords
Callose; defensive mechanisms; lignification; *Orobanche crenata*; parasitic plants; resistance; *Vicia faba*.

Correspondence
A. Pérez-de-Luque, Área de Mejora y Biotecnología, Centro "Alameda del Obispo", IFAPA (Junta de Andalucía), Apdo. 3092, E-14080 Córdoba, Spain.
Email: bb2pelua@uco.es

Received: 11 January 2007; revised version accepted: 15 May 2007.

doi:10.1111/j.1744-7348.2007.00164.x

Abstract

Broomrapes (*Orobanche* spp.) are parasitic angiosperms, which attach to the roots of the hosts to take water and nutrients from them. No complete control measures are available to date, but breeding for resistance remains as one of the most feasible and environmentally friendly methods. However, the mechanisms governing the interaction between these parasites and the host are not yet well understood. We studied the cellular changes associated with the resistance to *Orobanche crenata* in faba bean as mechanisms involved or responsible for resistance. Two cultivars of faba bean, resistant and susceptible to *O. crenata* infection, were used. The evolution of the infection and the changes in the cell and tissue organisation and wall components of the host cells were followed and evaluated in both genotypes. Samples of compatible and incompatible interactions were fixed and sectioned, and specific cytochemical methods for different cell components were applied, results being analysed under light and epifluorescence microscopy. A higher proportion of *O. crenata* seedlings unable to penetrate the root was found on the resistant genotype. Reinforcement of cell walls by callose deposition hampers parasite penetration through the cortex. Lignification of endodermal cells prevents further penetration of the parasite into the central cylinder.

Introduction

The existence of parasitic plants attacking crops is known from ancient times (Cubero & Moreno, 1996). This is particularly true for the broomrapes (*Orobanche* spp.), which are obligate root holoparasites. Devoid of chlorophyll, they totally depend on the hosts for the supply of carbon, nitrogen and inorganic solutes, which they obtain through a specialised structure (haustorium) connected to the vascular system of their host plants. This haustorium is formed after the parasite has germinated in the presence of stimulants from the host root, developed a seedling, attached to the host root and penetrated into the central cylinder (Parker & Riches, 1993; Press & Graves, 1995). Following vascular connection with the host, the parasite develops a tubercle that later on will originate an apex that will evolve into a flowering stem.

Orobanche crenata (crenate broomrape) is an important pest in legumes, affecting mainly faba bean (*Vicia faba*), pea (*Pisum sativum*), lentil (*Lens culinaris*), vetches (*Vicia* spp.), grass and chickling pea (*Lathyrus sativus* and *L. cicera*) and other grain and forage legumes in the Mediterranean basin and Middle East (Rubiales *et al.*, 2006). Despite several methods having been developed to control these parasites, including mechanical, biological and chemical practices (Parker & Riches, 1993;

Jurado-Expósito *et al.*, 1996, 1997; Joel, 2000; Rubiales *et al.*, 2003*a*; Eizenberg *et al.*, 2004; Pérez-de-Luque *et al.*, 2004*a*,*b*), breeding for resistance remains as the most economic, feasible and environmentally friendly method of control. However, resistance to *Orobanche* in legumes is a complex multicomponent event, difficult to access, scarce and of low heritability (Cubero & Hernández, 1991; Cubero, 1994; Cubero & Moreno, 1999), which makes breeding for resistance a difficult task. Hence, a detailed knowledge of the mechanisms underlying such resistance is necessary to improve breeding programmes and help breeders to identify new sources of resistance when turning to wild relatives.

Resistance to *Orobanche* spp. has been reported in different crops including sunflower (*Helianthus annuus*) (Labrousse *et al.*, 2001) and legumes (Rubiales *et al.*, 2003*a*,*b*, 2004; Pérez-de-Luque *et al.*, 2005*a*), but little is known about the basis of host resistance to these parasites (Joel *et al.*, 1996; Pérez-de-Luque *et al.*, 2005*b*). It is tempting to compare infection by parasitic plants with infection by fungi, but despite analogies being present, there are also many differences (Mayer, 2006). Studying resistance against parasitic plants presents some handicaps compared with that of other pathosystems, as parasite and host are relatively close organisms that share many morphological, physiological and biochemical traits. The question becomes more complicated because the interaction implies two plants that merge their tissues. At this point, cytological and cytochemical studies are powerful tools to unveil the mechanisms underlying the plant–parasitic plant interaction. These methodologies have been applied recently with success to study the *O. crenata*–pea (Pérez-de-Luque *et al.*, 2005*b*, 2006*a*), *O. crenata*–vetch (Pérez-de-Luque *et al.*, 2005*b*, 2006*b*) and *O. cumana*–sunflower interactions (Echevarría-Zomeño *et al.*, 2006).

The aim of the present work was to analyse, for the first time, the changes in cell and tissue organisation and components accompanying the resistant response as defence mechanisms implicated in the resistance of faba bean against *O. crenata*, specifically those which hamper parasite penetration into the host root and do not allow formation of the endophyte (haustorium) and connection with the vascular tissues.

Material and methods

Plant material and growth conditions

Orobanche crenata was grown on resistant and susceptible cultivars of faba bean (*Vicia faba*, Baraca and Prothabon, respectively). The glass rhizotron system described by Rubiales *et al.* (2006) was used. It involves growing host and parasite in sand and vermiculite (3:1) held in the gap between two glass sheets (Fig. 1). Two cork strips of 0.5 cm thickness are placed between both glasses in the left and right sides, and the lower side is sealed with a porous material (foam rubber) that allows nutrient solution to penetrate. A strip (11 × 12 cm) of glass fibre paper (Whatmann GF/A) with disinfected *O. crenata* seeds (40 mg) spread on it was inserted in the upper part

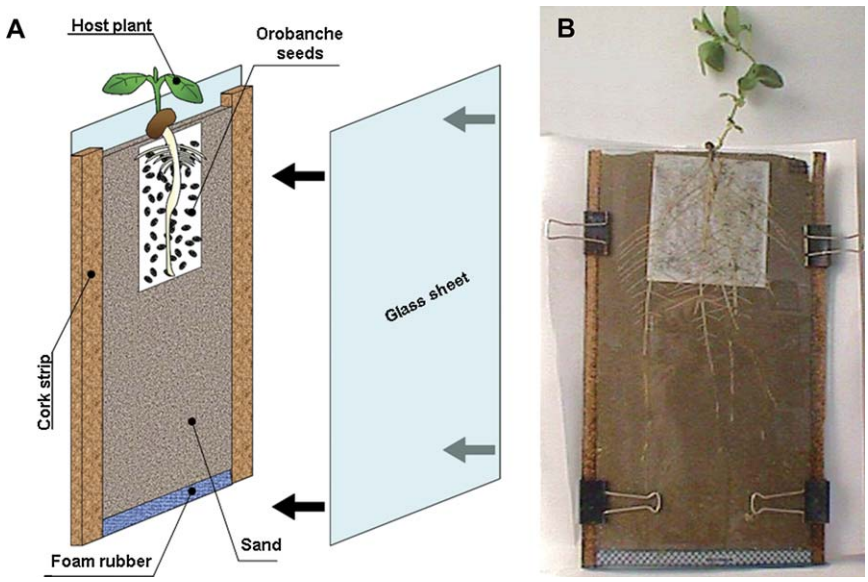

Figure 1 Glass rhizotron system for inoculation of faba bean with *Orobanche crenata*. (A) Schematic representation of the system. (B) General view of the system.

of the plate, on the sand. Faba bean seedlings, with a root length of about 5–6 cm, were placed on the paper in the upper side of the plates. Plates were placed vertically and irrigated with Hoagland nutrient solution (Hoagland & Arnon, 1950). The plants were grown in a controlled environment chamber with a day/night temperature of 20°C ± 0.5°C, a 14-h photoperiod and an irradiance of 200 μmol m^{-2} s^{-1}.

The *O. crenata* seed germination was evaluated 20 days after transplantation by using a binocular microscope (Nikon SMZ1000; Nikon Europe B.V., Badhoevedorp, The Netherlands). Five hundred seeds located close (<3 mm) to the faba bean root were observed, and the number of those germinated were counted and expressed as percentage of the total. Seeds were considered to be germinated when the germ tube was at least 0.1 mm long. At 25 days after transplanting, the number of *O. crenata* seedlings touching faba bean roots was counted. Those that became necrotic or caused darkening of the host at the point of contact were expressed as a percentage of the total number of successfully attached seedlings.

Faba bean root length and *O. crenata* tubercle formation were evaluated 40 days after transplanting. Root length was estimated according to Tennant (1975). Tubercles were counted and classified according to their developmental stage (Ter Borg *et al.*, 1994): S1, tubercles <2 mm; S2, tubercles >2 mm but without root formation; S3, tubercles with crown root; S4, sprout already visible remaining underground; S5, shoot emergence; S6, flowering; and S7, setting of seeds. Values were expressed as total number of tubercles per plant, number of tubercles per centimetre of host root length and number and percentage of tubercles at S1–S4 developmental stage. The percentage of germinated seeds that established a tubercle was also estimated.

Collection and processing of samples for cytochemistry

At 25 days after transplanting, seedlings of *O. crenata* were sampled at random with the corresponding attached parts of host roots. The sampled material was fixed either in FAA solution (ethanol 50% + formaldehyde 5% + glacial acetic acid 10%, in water) for 48 h or in Karnovsky's fixative (paraformaldehyde 4% + glutaraldehyde 5%, in 0.025 M cacodilate buffer) for 4 h.

The FAA-fixed samples were then dehydrated in an ethanol series (50%, 80%, 95%, 100%, 100%: 12 h each), transferred to an embedding solvent (xylene; Panreac Quimica S.A., Montcada i Reixac, Spain) through a xylene–ethanol series (30%, 50%, 80%, 100%, 100%: 12 h each) and finally saturated with paraffin (Paraplast Xtra; Sigma, St Louis, MO, USA). Sections (7 μm) were cut with a rotary microtome (Nahita 534; Auxilab S.A., Beriain, Spain) and attached to adhesive-treated microscope slides (polysine slides; Menzel GmbH & Co. KG, Braunschweig, Germany).

Karnovsky-fixed samples were dehydrated in an acetone series and embedded in an acrylic resin, Historesin 8100 (Leica Microsystems Wetzlar GmbH, Wetzlar, Germany). Resin polymerisation was performed at 4°C overnight. Semi-thin sections (2 μm) were cut with a glass knife in an ultratome Pyramitome (LKB, Stockholm, Sweden) and attached to microscope slides.

Cytochemical methods for light and epifluorescence microscopy

After removal of paraffin, FAA-fixed sections were stained with the following dyes: (a) alcian green–safranin (AGS) (Joel, 1983). The slides were dried and mounted with DePeX (BDH, Poole, UK) mounting medium. With this staining method, carbohydrates (including cell walls and mucilage) appeared green, yellow or blue, while lignified, cutinised and suberised walls as well as tannin and lipid material inside cells appeared red (Joel, 1983). (b) phloroglucinol (2% in ethanol)–HCl (35%) (Ruzin, 1999) stains the aldehyde groups of lignin and suberin but quenches lignin autofluorescence and retains suberin fluorescence (Baayen *et al.*, 1996; Rioux *et al.*, 1998). (c) aniline blue fluorochrome was used for callose detection under ultraviolet fluorescence. Samples were stained for 15–30 min in a solution of 0.1% aniline blue fluorochrome in water (Bordallo *et al.*, 2002).

Semi-thin (2 μm) historesin sections of Karnovsky-fixed samples were stained with 0.05% toluidine blue O (TBO) in phosphate buffer (pH 5.5) for 1 min (Ruzin, 1999). This method allows detection of phenolics as well as tannins, lignin and suberin (Baayen *et al.*, 1996; Bordallo *et al.*, 2002; Mellersh *et al.*, 2002; Crews *et al.*, 2003).

Sections were observed using a light microscope (Leica DM-LB, magnification ×100 to ×400; Leica Microsystems Wetzlar GmbH) and photographed using a digital camera (Nikon DXM1200F; Nikon Europe B.V.). Samples were also observed by epifluorescence under excitation at 450–490 nm (blue–violet) with the same microscope.

Statistical analysis

Assays were performed with 10 replicates per treatment with a completely randomised design. Statistical analysis (analysis of variance) was performed with SPSS 10.0 (SPSS Inc., Chicago, Illinois, USA) and Statistix 8.0 (Analytical Software, Tallahassee, Florida, USA) for Windows. Percentages were transformed according to the formula $Y = \arcsin(\sqrt{(X\%/100)})$.

Table 1 *Orobanche crenata* seed germination and tubercle formation in faba bean[a]

Faba Bean Cultivar	Germination at 0–3 mm from Host Root (%)[b]	Germinated Seeds that Establish a Tubercle (%)[b]	Number of Tubercles per Plant	Host Root Length (cm)	Tubercles per centimetre of Host Root Length
Baraca (resistant)	43.8 ± 2.4 (0.72 ± 0.03)	0.04 ± 0.01 (0.018 ± 0.004)	3.4 ± 0.9	336.7 ± 26.5	0.01 ± 0.00
Prothabon (susceptible)	46.4 ± 3.5 (0.75 ± 0.04)	1.34 ± 0.41 (0.107 ± 0.016)	127.0 ± 26.4	342.9 ± 24.3	0.38 ± 0.08

[a]Values are given as mean ± standard error; d.f. = 9.

[b]Log transformed data with standard error are shown in parentheses alongside back-transformed mean values.

Table 2 Attached *Orobanche crenata* seedlings unable to develop tubercles and developmental stage of already established tubercles[a]

Faba Bean Cultivar	Attached Seedlings Unable to Develop Tubercles (%)[b]	Developmental Stage							
		S1		S2		S3		S4	
		Number of Tubercles	Percentage[b]	Number of Tubercles	Percentage[b]	Number of Tubercles	Percentage[b]	Number of Tubercles	Percentage[b]
Baraca (resistant)	68.5 ± 1.8 (0.98 ± 0.02)	1.29 ± 0.7	37.5 ± 12.6 (0.38 ± 0.18)	1.9 ± 0.5	54.1 ± 15.3 (0.88 ± 0.22)	0.3 ± 0.2	8.4 ± 3.2 (0.12 ± 0.08)	0.0 ± 0.0	0.0 ± 0.0 (0.00 ± 0.00)
Prothabon (susceptible)	39.4 ± 2.3 (0.68 ± 0.02)	28.4 ± 7.7	22.4 ± 1.8 (0.48 ± 0.02)	70.1 ± 17.1	55.2 ± 2.5 (0.81 ± 0.03)	28.0 ± 3.4	22.1 ± 2.5 (0.52 ± 0.03)	0.4 ± 0.2	0.3 ± 0.2 (0.03 ± 0.02)

[a]Values are given as mean ± standard error; d.f. = 9.

[b]Log transformed data with standard error are shown in parentheses alongside back-transformed mean values.

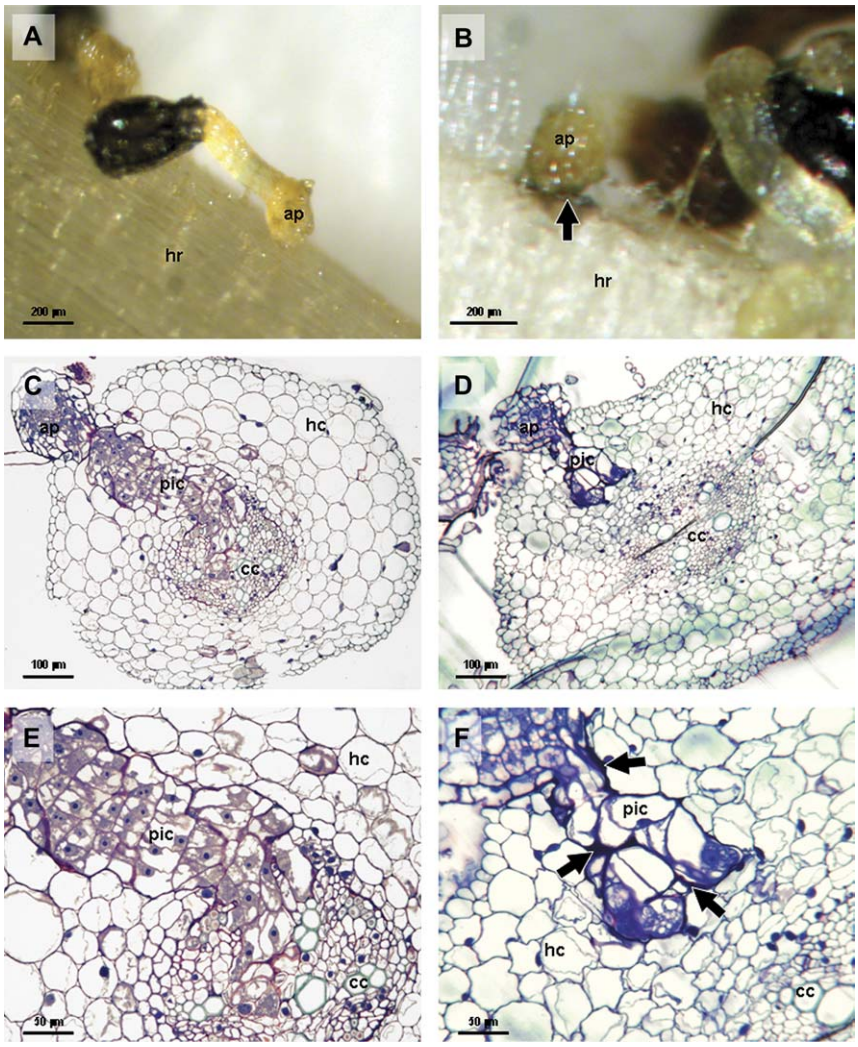

Figure 2 Compatible and incompatible reactions of *Orobanche crenata* in faba bean. (A) Successful attachment on and penetration into susceptible faba bean. (B) Incompatible reaction in resistant faba bean. Arrow indicates darkening of host tissues at the attachment point. (C) Cross-section of a compatible interaction stained with toluidine blue O (TBO) showing penetration of parasite cells through the host tissues. (D) Cross-section of an incompatible interaction stained with TBO showing parasite cells halted in the host cortex. (E) Detail of (C) showing how the parasite cells have reached the central cylinder of the host. (F) Detail of (D) showing accumulation of a dark stained deposit around the penetration pathway of the parasite (arrows). ap, parasite appressorium; cc, central cylinder; hc, host cortex; hr, host root; pic, parasite intrusive cells.

Results

Resistance against *Orobanche* has been divided into several steps, including induction of parasite germination, penetration/establishment and tubercle development. Resistant plants stop parasite infection and/or development in at least one of these steps. Both cultivars showed no significant differences in inducing germination of *O. crenata* seeds (about 45% of germination) (Table 1). The percentage of germinated *O. crenata* seeds developing a tubercle was higher in the susceptible cultivar Prothabon (1.34%) than in the resistant cultivar Baraca (0.04%) (more than 30 times). This resulted in 127.0 established tubercles per Prothabon plant whereas it resulted only in 3.4 per Baraca plant. No differences were found in the root length of both genotypes, but to avoid escape because of low root biomass, the number of established tubercles were referred to the root length. The relation remained between both cultivars, with Prothabon presenting the highest number of established tubercles per centimetre of root (0.38) compared with Baraca (0.01).

Most of the established tubercles in both cultivars remained in stages 1 and 2 of development at the end of the experiment (Table 2). Only in Prothabon did

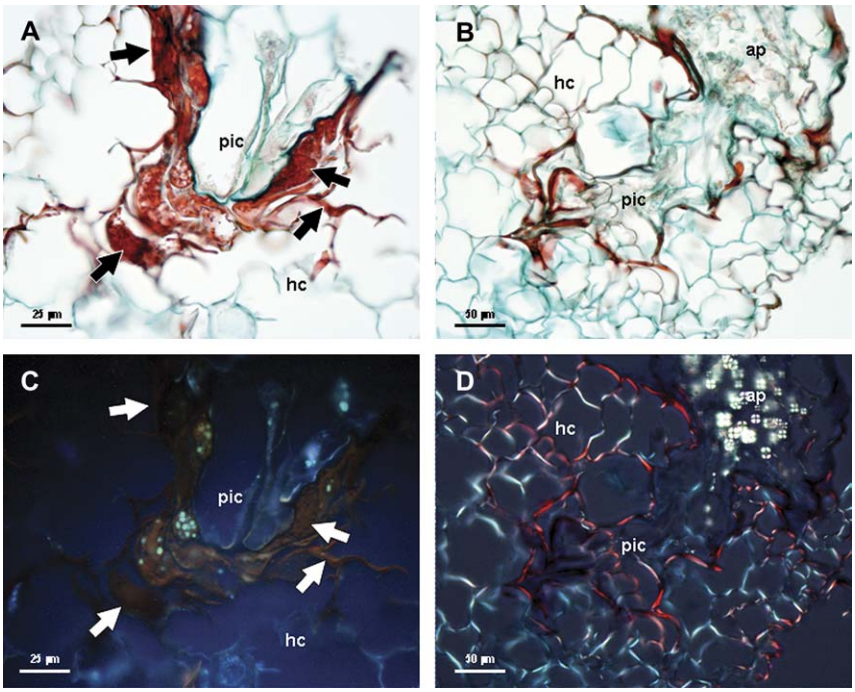

Figure 3 Incompatible interactions stained with alcian green–safranin. (A) Detail of parasite cells halted in the host cortex showing an intense red coloration of the material accumulated in the apoplastic interface. (B) Parasite intrusive cells showing a 'bottleneck' aspect because of difficulties found during the penetration attempt. (C) The same as (A) under epifluorescence showing absence of emission from the accumulated substances. (D) The same as (B) under polarised light showing the absence of suberised or lignified cell walls. ap, parasite appresorium; hc, host cortex; pic, parasite intrusive cells.

a significant number (22.1%) develop on the crown root (stage 3) and some (0.3%) also developed at the apex (stage 4).

Darkening of tissues around the attachment and penetration point was observed in some cases (Fig. 2b). The seedlings could not develop further, became dark and did not result in a tubercle. The percentage of these attached *O. crenata* seedlings unable to develop a tubercle was also determined for both genotypes (Table 2), resulting in a higher percentage of aborted penetration attempts in Baraca (68.5%) compared with that in Prothabon (39.4%).

To analyse the changes in cell structure and components associated with the mechanisms of resistance behind this reaction, cytochemical analyses were performed. Staining of historesin-embedded samples with TBO revealed a different level of penetration of the parasite intrusive cells in susceptible (Fig. 2c and Fig. 2e) and resistant (Fig. 2d and Fig. 2f) cultivars. In root cross-sections of Prothabon (susceptible) samples, the parasite cells were observed penetrating throughout the whole root and reaching the central cylinder (Fig. 2c and Fig. 2e). However, in resistant plants of Baraca cultivar, the parasite cells appeared to be stopped at the cortex (Fig. 2d and Fig. 2f). It seems that the parasite is unable to penetrate into the host central cylinder and appeared to be stopped in both the cortex and/or the endodermis (Fig. 2d and Fig. 2f). Moreover, an accumulation of dark-blue stained substances around the penetration pathway during incompatible interactions was observed (Fig. 2f).

Staining with AGS of paraffin-embedded samples also revealed that the penetration of the parasite is stopped at the root cortex in resistant plants (Fig. 3a and Fig. 3b). AGS staining makes carbohydrates (including cell walls and mucilage) to appear green, yellow or blue, while lignified, cutinised and suberised walls appear red. In the resistant plant roots, AGS-stained sections showed that the substances around the penetration pathway are of heterogeneous nature. The observation of these sections under epifluorescence microscopy with blue excitation showed no fluorescence emission from the substances or neighbouring host cells and walls (Fig. 3c). Also the observation under polarised light did not show any special feature (Fig. 3d).

Accumulation of callose around the penetration pathway of the parasite has been detected using aniline blue fluorochrome (Fig. 4a–d) as a key feature associated with the major mechanism responsible for stopping parasite

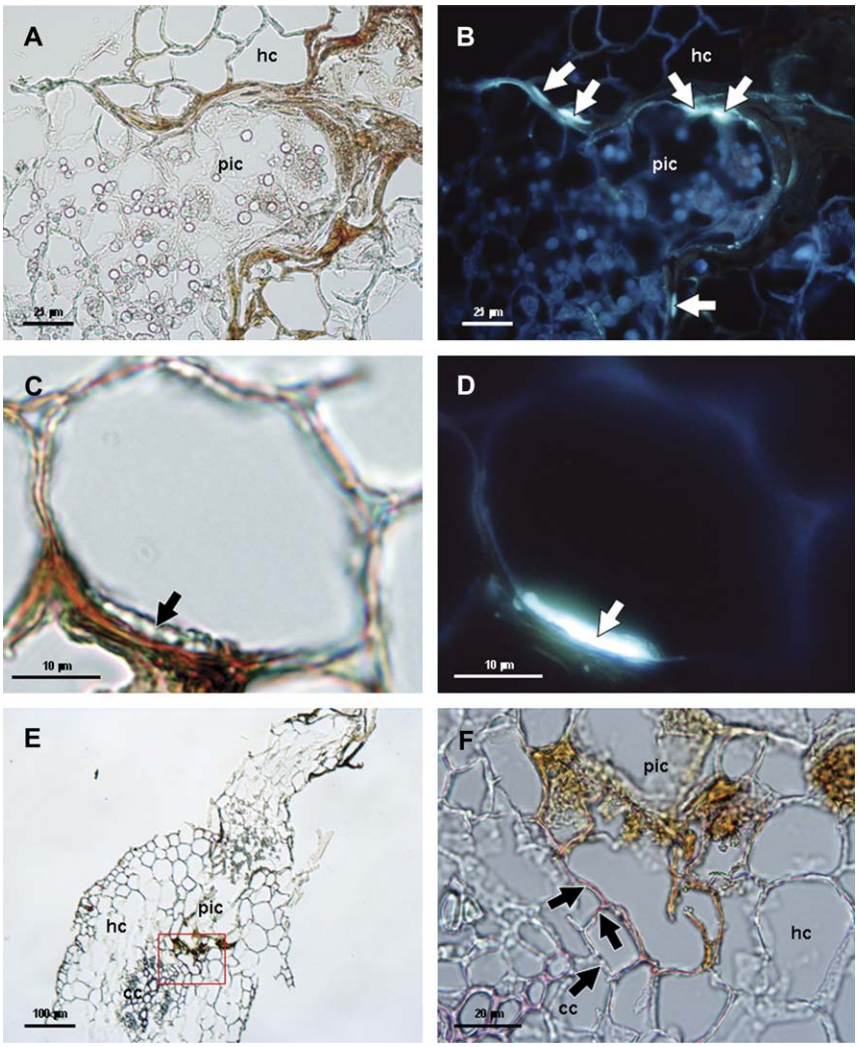

Figure 4 (A) Incompatible interaction stained with aniline blue fluorochrome and observed under light microscope. (B) The same as (A) observed under epifluorescence and showing accumulation of callose around the penetration pathway of the parasite (arrows). (C) Detail of a faba bean cell stained with aniline blue fluorochrome showing accumulation of material on the cell wall in contact with the parasite tissues (arrow). (D) The same as (C) but observed under epifluorescence and showing callose deposition on the cell wall (arrow). (E) Incompatible interaction stained with phloroglucinol–HCl and showing the parasite intrusive cells reaching the endodermis. (F) Detail of (E) showing lignification of endodermal cell walls in contact with parasite tissues (arrows). cc, central cylinder; hc, host cortex; pic, parasite intrusive cells.

penetration into the host cortex. As revealed by the aniline-blue-specific staining, the accumulation of callose occurred in the walls of the host cells surrounding the parasite, and this accumulation was localised mostly in certain wall regions, specifically in those directly in contact with the parasite cells (Fig. 4b–d). The reinforcement of host cell walls by callose accumulation originates a characteristic bottleneck aspect of the parasite intrusive tissues (Figs 2f, 3b and 4a). No callose depositions were detected in compatible interactions collected on susceptible plants (data not shown).

In some cases, in the resistant plants, the parasite is not being stopped in the cortex and reaches the endodermis (Fig. 4e and Fig. 4f). The phloroglucinol–HCl procedure for lignin provided specific staining of the endodermal cell walls at the point of the cessation of the parasite (Fig. 4e and Fig. 4f). This result indicates that a lignification of endodermal cell walls in contact with parasitic tissues takes place (Fig. 4e and Fig. 4f). Again, no presence of lignification was detected in samples collected on susceptible plants (data not shown).

Discussion

As clearly demonstrated in other studies (Labrousse *et al.*, 2001; Pérez-de-Luque *et al.*, 2005*a*), resistance to

Orobanche can be divided into different steps. In our work, contrary to previous results obtained with other legumes (Rubiales *et al.*, 2003*a*,*b*; Pérez-de-Luque *et al.*, 2005*a*; Sillero *et al.*, 2005, 2006), low induction of germination of parasite seeds does not seem to be a determinant factor in the resistant faba bean cultivar studied. However, stoppage of parasite penetration through host tissues and hampering of tubercle development appear as the main available defence responses found in the resistant faba bean. The darkening around the attachment and penetration point of the parasite has been widely described as an incompatible interaction in resistant plants against root parasitic angiosperms (Lane & Bailey, 1992; Dörr *et al.*, 1994; Goldwasser *et al.*, 1997; Pérez-de-Luque *et al.*, 2005*b*). Our study shows that it is a quantitative trait because it is present also in the susceptible cultivar Prothabon but to a lesser extent compared with that in the resistant Baraca. It is important to notice that the resistance found in Baraca is also incomplete; a few individuals are able to overcome the barriers and develop a tubercle. This confirms previous works assuring that resistance to *Orobanche* is complex (Cubero & Hernández, 1991; Cubero, 1994; Cubero & Moreno, 1999). This darkening around the attachment point has been usually assumed as a hypersensitive response (HR) because of the dark coloration of host tissues, but there is no conclusive evidence supporting that a HR really occurs in a manner similar to that described for fungal infection (Heath, 1999; Richael & Gilchrist, 1999). In fact, other studies about the incompatible interaction between *Orobanche* spp. and resistant hosts have shown that no HR is present (Rubiales *et al.*, 2003*b*; Pérez-de-Luque *et al.*, 2005*b*, 2006*a*; Echevarría-Zomeño *et al.*, 2006). For that reason, cytochemical studies were developed to unveil the nature of such defence response.

No HR was detected when samples of the incompatible interaction were dissected. The accumulation of substances around the penetration pathway of the parasite intrusive cells seems to be responsible for the dark coloration observed at the attachment point as previously reported (Pérez-de-Luque *et al.*, 2005*b*). This accumulation can only be observed in the case of incompatible interactions, and a possible explanation for it was given previously (Joel *et al.*, 1996; Pérez-de-Luque *et al.*, 2005*b*, 2006*b*): when the parasite is hampered during the penetration attempts, it releases higher amount of secretions (i.e. enzymes and adhesives) to overcome the host resistance. An analogous phenomenon was described for the interaction between parasites of the Santalaceae and incompatible hosts (Kuijt, 1969). The nature of these substances remains undetermined to date, but studies with *O. crenata* and other legumes suggests that such accumulation of substances would correspond with an excess of enzymes and adhesive substances excreted by the parasite and degraded products from the host cell walls (Pérez-de-Luque *et al.*, 2005*b*, 2006*a*). In other cases (*O. cumana–Helianthus annuus*), these secretions contain phenolic compounds excreted by the host leading to the creation of a toxic environment for the parasite (Echevarría-Zomeño *et al.*, 2006), but we have not found evidence for this in our study (i.e. fluorescence).

Reinforcement of host cell walls by callose deposition, a β-1,3-glucan polymer, appears as the main factor responsible for resistance in this case. This is a type of cell wall fortification rapidly developed under pathogen invasion (Hammond-Kosack & Jones, 1996; Brown *et al.*, 1998). Despite being previously reported in pea resistant to *O. crenata* (Pérez-de-Luque *et al.*, 2006*a*), this is the first time it is observed in sufficient amounts and locations to stop the parasite penetration. Because the reinforcement of cell walls by callose requires cross-linking of hydroxyproline-rich glycoproteins (Brown *et al.*, 1998), it is possible that protein cross-linking will also be taking place in this case, but we did not observe it (data not shown). Although the main role of callose here seems to be cell wall reinforcement, we cannot discard another role as a reservoir of β-glucans elicitors as suggested by Esquerré-Tugayé *et al.* (2000). In this case, β-glucans degraded from the cell walls would release oligosaccharides, which could play an important role as elicitors of defence responses (Aldington & Fry, 1993).

Complementary to callose depositions, if the parasite is able to pierce the cortex and reach the endodermis, lignification of the cells takes place. This lignification of host pericycle and endodermis was reported as the main resistance factor in *Vicia sativa* against *O. crenata* penetration (Pérez-de-Luque *et al.*, 2005*b*) and prevents the parasite reaching the central cylinder and establishing a haustorium with vascular connections. Other reports described lignification of host cortex and xylem elements (Dörr *et al.*, 1994; Antonova & Ter Borg, 1996) and unspecific tissues (De Ruck *et al.*, 1995; Goldwasser *et al.*, 1999). In this work, however, we have observed that lignification of cell walls is set in play after stoppage of parasite intrusive cells in the host cortex has been overcome.

In addition to these, a retarded development of the few established individuals was observed in resistant faba bean. This can be explained by delayed penetration and establishment as result of the barriers activated by the resistant host; it would take more time for the parasite to establish a functional haustorium because it must overcome the mechanisms of resistance. But at this point, we cannot discard other possible mechanism of resistance, such as partial occlusion of host xylem vessels by mucilage (Pérez-de-Luque *et al.*, 2005*b*, 2006*b*) but not being as

drastic as leading to parasite death. We also cannot discard an incompatibility between host and parasite tissues at the hormonal level, preventing a normal development of the haustorium and vascular connections. More studies are needed to investigate this hypothesis.

In conclusion, stoppage of *O. crenata* seedling penetration in the host root is a quantitative response in faba bean and is associated with reinforcement of host cell walls in contact with the parasite intrusive cells. In the first stage, reinforcement takes place in the cortex by callose deposition. However, if the parasite later overcomes this barrier, lignification of endodermal cells prevents further penetration into the central cylinder and formation of a haustorium.

Acknowledgements

We thank A. Moral for her help in the realisation of this work. A. P-d-L. was a visiting researcher at the Plant Development group at the CIB-CSIC (Madrid) funded by the Consejería de Innovación, Ciencia y Empresa de la Junta de Andalucía. A. P-d-L acknowledges a postdoctoral contract at the IFAPA funded by the programme 'Juan de la Cierva' of the Spanish Ministry of Education and Science. This research was supported by the project EUFABA (QLK5-CT-2002-02307-07).

References

Aldington S., Fry S.C. (1993) Oligosaccharins. *Advances in Botanical Research*, **19**, 1–101.

Antonova T.S., Ter Borg S.J. (1996) The role of peroxidase in the resistance of sunflower against *Orobanche cumana* in Russia. *Weed Research*, **36**, 113–121.

Baayen R.P., Ouellette G.B., Rioux D. (1996) Compartmentalization of decay in carnations resistant to *Fusarium oxysporum* f. sp. dianthi. *Phytopathology*, **86**, 1018–1031.

Bordallo J.J., Lopez-Llorca L.V., Jansson H.B., Salinas J., Persmark L., Asensio L. (2002) Colonization of plant roots by egg-parasitic and nematode-trapping fungi. *New Phytologist*, **154**, 491–499.

Brown I., Trethowan J., Kerry M., Mansfield J., Bolwell G.P. (1998) Localization of components of the oxidative cross-linking of glycoproteins and of callose synthesis in papillae formed during the interaction between non-pathogenic strains of *Xanthomonas campestris* and French bean mesophyll cells. *Plant Journal*, **15**, 333–343.

Crews L.J., McCully M.E., Canny M.J. (2003) Mucilage production by wounded xylem tissue of maize roots – time course and stimulus. *Functional Plant Biology*, **30**, 755–766.

Cubero J.I. (1994) Breeding work in Spain for *Orobanche* resistance in faba bean and sunflower. In *Biology and Management of Orobanche. Proceedings of the Third International Workshop on Orobanche and related Striga research*, pp. 465–473. Eds A.H. Pieterse, J.A.C. Verkleij and S.J. ter Borg. Amsterdam, the Netherlands: Royal Tropical Institute.

Cubero J.I., Hernández L. (1991) Breeding faba bean (*Vicia faba* L.) for resistance to *Orobanche crenata* Forsk. *Options Méditerranéennes*, **10**, 51–57.

Cubero J.I., Moreno M.T. (1996) Parasitic plant science: a quarter century. In *Advances in Parasitic Plant Research*, pp. 15–23. Eds M.T. Moreno, J.I. Cubero, D. Berner, D. Joel, L.J. Musselman and C. Parker. Sevilla, Spain: Junta de Andalucía, Consejería de Agricultura y Pesca.

Cubero J.I., Moreno M.T. (1999) Studies on resistance to *Orobanche crenata* in *Vicia faba*. In *Resistance to Broomrape, the State of the Art*, pp. 9–15. Eds J.I. Cubero, M.T. Moreno, D. Rubiales and J.C. Sillero. Sevilla, Spain: Junta de Andalucía, Consejería de Agricultura y Pesca.

De Ruck E., Tena M., Jorrín J. (1995) La lignificación como respuesta defensiva de girasol (*Helianthus* spp.) frente a la infección por plantas parásitas (*Orobanche cernua*). In *XIX Congreso de la Sociedad Española de Bioquímica*, pp. 225. Eds J. Cárdenas and E. Fernández Reyes. Córdoba, Spain: SEBBM.

Dörr I., Staack A., Kollmann R. (1994) Resistance of *Helianthus* to *Orobanche* – histological and cytological studies. In *Proceedings of the Third International Workshop on Orobanche and Related Striga Research*, pp. 276–289. Eds A.H. Pieterse, J.A.C. Verkleij, S.J. ter Borg. Amsterdam, the Netherlands: Royal Tropical Institute.

Echevarría-Zomeño S., Pérez-de-Luque A., Jorrín J., Maldonado A.M. (2006) Pre-haustorial resistance to broomrape (*Orobanche cumana*) in sunflower (*Helianthus annuus*): cytochemical studies. *Journal of Experimental Botany*, **57**, 4189–4200.

Eizenberg H., Goldwasser Y., Golan S., Plakhine D., Hershenhorn J. (2004) Egyptian broomrape (*Orobanche aegyptiaca*) control in tomato with sulfonylurea herbicides – greenhouse studies. *Weed Technology*, **18**, 490–496.

Esquerré-Tugayé M.T., Boudart G., Dumas B. (2000) Cell wall degrading enzymes, inhibitory proteins, and oligosaccharides participate in the molecular dialogue between plants and pathogens. *Plant Physiology and Biochemistry*, **38**, 157–163.

Goldwasser Y., Kleifeld Y., Plakhine D., Rubin B. (1997) Variation in vetch (*Vicia* spp.) response to *Orobanche aegyptiaca*. *Weed Science*, **45**, 756–762.

Goldwasser Y., Hershenhorn J., Plakhine D., Kleifeld Y., Rubin B. (1999) Biochemical factors involved in vetch resistance to *Orobanche aegyptiaca*. *Physiological and Molecular Plant Pathology*, **54**, 87–96.

Hammond-Kosack K.E., Jones J.D.G. (1996) Resistance gene-dependent plant defense responses. *Plant Cell*, **8**, 1773–1791.

Heath M.C. (1999) The enigmatic hypersensitive response: induction, execution, and role. *Physiological and Molecular Plant Pathology*, **55**, 1–3.

Hoagland D.R., Arnon D.I. (1950) *The Water-Culture Method for Growing Plants Without Soil. California Agricultural Experiment Station Circular 347*. Berkeley, CA, USA: University of California.

Joel D.M. (1983) AGS (Alcian Green Safranin) – a simple differential staining of plant material for the light microscope. *Proceedings of the Royal Microscopical Society*, **18**, 149–151.

Joel D.M. (2000) The long-term approach to parasitic weeds control: manipulation of specific developmental mechanisms of the parasite. *Crop Protection*, **19**, 753–758.

Joel D.M., Losner-Goshen D., Hershenhorn J., Goldwasser Y., Assayag M. (1996) The haustorium and its development in compatible and resistant host. In *Advances in Parasitic Plant Research*, pp. 531–541. Eds M.T. Moreno, J.I. Cubero, D. Berner, D. Joel, L.J. Musselman and C. Parker. Sevilla, Spain: Junta de Andalucía, Consejería de Agricultura y Pesca.

Jurado-Expósito M., Castejón-Muñoz M., García-Torres L. (1996) Broomrape (*Orobanche crenata*) control with Imazethapyr applied to pea (*Pisum sativum*) seed. *Weed Technology*, **10**, 774–780.

Jurado-Expósito M., Castejón-Muñoz M., García-Torres L. (1997) Broad bean and lentil seed treatments with imidazolines for the control of broomrape (*Orobanche crenata*). *Journal of Agricultural Science*, **129**, 307–314.

Kuijt J. (1969) *The Biology of Parasitic Flowering Plants*. Berkeley, CA, USA: University of California Press.

Labrousse P., Arnaud M.C., Serieys H., Bervillé A., Thalouarn P. (2001) Several mechanisms are involved in resistance of *Helianthus* to *Orobanche cumana* Wallr. *Annals of Botany*, **88**, 859–868.

Lane J.A., Bailey J.A. (1992) Resistance of cowpea and cereals to the parasitic angiosperm *Striga*. *Euphytica*, **63**, 85–93.

Mayer A.M. (2006) Pathogenesis by fungi and parasitic plants: similarities and differences. *Phytoparasitica*, **34**, 3–16.

Mellersh D.G., Foulds I.V., Higgins V.J., Heath M.C. (2002) H_2O_2 plays different roles in determining penetration failure in three diverse plant–fungal interactions. *Plant Journal*, **29**, 257–268.

Parker C., Riches C.R. (1993) *Parasitic Weeds of the World: Biology and Control*. Wallingford, UK: CAB International.

Pérez-de-Luque A., Jorrín J., Rubiales D. (2004*a*) Crenate broomrape control in pea by foliar application of benzothiadiazole (BTH). *Phytoparasitica*, **32**, 21–29.

Pérez-de-Luque A., Sillero J.C., Moral A., Cubero J.I., Rubiales D. (2004*b*) Effect of sowing date and host resistance on the establishment and development of *Orobanche crenata* in faba bean and common vetch. *Weed Research*, **44**, 282–288.

Pérez-de-Luque A., Jorrín J., Cubero J.I., Rubiales D. (2005*a*) Resistance and avoidance against *Orobanche crenata* in pea (*Pisum* spp.) operate at different developmental stages of the parasite. *Weed Research*, **45**, 379–387.

Pérez-de-Luque A., Rubiales D., Cubero J.I., Press M.C., Scholes J., Yoneyama K., Takeuchi Y., Plakhine D., Joel D.M. (2005*b*) Interaction between *Orobanche crenata* and its host legumes: unsuccessful haustorial penetration and necrosis of the developing parasite. *Annals of Botany*, **95**, 935–942.

Pérez-de-Luque A., González-Verdejo C.I., Lozano M.D., Dita M.A., Cubero J.I., González-Melendi P., Risueño M.C., Rubiales D. (2006*a*) Protein cross-linking, peroxidase and β-1,3-endoglucanase involved in resistance of pea against *Orobanche crenata*. *Journal of Experimental Botany*, **57**, 1461–1469.

Pérez-de-Luque A., Lozano M.D., Cubero J.I., González-Melendi P., Risueño M.C., Rubiales D. (2006*b*) Mucilage production during the incompatible interaction between *Orobanche crenata* and *Vicia sativa*. *Journal of Experimental Botany*, **57**, 931–942.

Press M.C., Graves J.D. (1995) *Parasitic Plants*. London, UK: Chapman & Hall.

Richael C., Gilchrist D. (1999) The hypersensitive response: a case of hold or fold? *Physiological and Molecular Plant Pathology*, **55**, 5–12.

Rioux D., Nicole M., Simard M., Ouellette G.B. (1998) Immunocytochemical evidence that secretion of pectin occurs during gel (gum) and tylosis formation in trees. *Phytopathology*, **88**, 494–505.

Rubiales D., Pérez-de-Luque A., Cubero J.I., Sillero J.C. (2003*a*) Crenate broomrape (*Orobanche crenata*) infection in field pea cultivars. *Crop Protection*, **22**, 865–872.

Rubiales D., Pérez-de-Luque A., Joel D.M., Alcántara C., Sillero J.C. (2003*b*) Characterization of resistance in chickpea to crenate broomrape (*Orobanche crenata*). *Weed Science*, **51**, 702–707.

Rubiales D., Alcántara C., Sillero J.C. (2004) Variation in resistance to crenate broomrape (*Orobanche crenata*) in species of *Cicer*. *Weed Research*, **44**, 27–32.

Rubiales D., Pérez-de-Luque A., Fernández-Aparicio M., Sillero J.C., Román B., Kharrat M., Khalil S., Joel D.M., Riches C. (2006) Screening techniques and sources of resistance against parasitic weeds in grain legumes. *Euphytica*, **147**, 187–199.

Ruzin S.E. (1999) *Plant Microtechnique and Microscopy*. New York, NY, USA: Oxford University Press.

Sillero J.C., Moreno M.T., Rubiales D. (2005) Sources of resistance to crenate broomrape in *Vicia* species. *Plant Disease*, **89**, 22–27.

Sillero J.C., Cubero J.I., Fernández-Aparicio M., Rubiales D. (2006) Search for resistance to crenate broomrape (*Orobanche crenata*) in *Lathyrus*. *Lathyrus Lathyrism Newsletters*, **4**, 7–9.

Tennant D. (1975) A test of a modified line intersect method of estimating root length. *Journal of Ecology*, **63**, 995–1001.

Ter Borg S.J., Willemsen A., Khalil S.A., Saber H.A., Verkleij J.A.C., Pieterse A.H. (1994) Field study of the interaction between *Orobanche crenata* Forsk. and some lines of *Vicia faba*. *Crop Protection*, **13**, 611–616.

Medicago truncatula as a Model for Nonhost Resistance in Legume-Parasitic Plant Interactions[1][C]

M. Dolores Lozano-Baena, Elena Prats, M. Teresa Moreno, Diego Rubiales, and Alejandro Pérez-de-Luque*

Consejo Superior de Investigaciones Científicas, Institute for Sustainable Agriculture, 14080 Cordoba, Spain (M.D.L.-B., E.P., D.R.); and Instituto de Investigación y Formación Agraria y Pesquera de Andalucía (Junta de Andalucía), Centro Alameda del Obispo, Área de Mejora y Biotecnología, 14080 Cordoba, Spain (M.T.M., A.P.-d.-L.)

Crenate broomrape (*Orobanche crenata*) is a root parasitic weed that represents a major constraint for grain legume production in Mediterranean and West Asian countries. *Medicago truncatula* has emerged as an important model plant species for structural and functional genomics. The close phylogenic relationship of *M. truncatula* with crop legumes increases its value as a resource for understanding resistance against *Orobanche* spp. Different cytological methods were used to study the mechanisms of resistance against crenate broomrape of two accessions of *M. truncatula*, showing early and late acting resistance. In the early resistance accession (SA27774) we found that the parasite died before a tubercle had formed. In the late resistance accession (SA4327) the parasite became attached without apparent problems to the host roots but most of the established tubercles turned dark and died before emergence. The results suggest that there are defensive mechanisms acting in both accessions but with a time gap that is crucial for a higher success avoiding parasite infection.

Crenate broomrape (*Orobanche crenata*) is one of the most important parasitic plants attacking legume crops in Mediterranean area, devastating crops and making unusable infested land (Rubiales, 2001, 2003; Rubiales et al., 2002). Being a broomrape (*Orobanche* sp.), crenate broomrape is an obligate root holoparasite lacking in chlorophyll and depending entirely on the host for its supply of nutrients (Joel et al., 2007). The knowledge of the mechanisms of resistance against the parasite is crucial to develop strategies of control, like breeding for resistance. With this purpose, we have chosen *Medicago truncatula* as a crenate broomrape host model plant due to its characteristics.

M. truncatula is an annual forage legume in the Mediterranean area. Contrary to other legume crops, *M. truncatula* is an autogamous self-fertile plant with a small and diploid genome, a short life cycle, and a prolific seed production (Blondon et al., 1994). Its simple genetics, the development of new tools and methods for molecular and genetic analysis, and the complete genome sequence (http://www.medicago.org) provide researchers with a valuable data set and making it interesting as a legume model species for laboratory studies (Cook et al., 1997; Cook, 1999) and also in pathogenic interactions (Ellwood et al., 2007; Pérez-de-Luque et al., 2007a).

Nowadays, the most numerous and important works about parasitic plants were focused on the development in susceptible host, as *Orobanche* spp. (Joel and Losner-Goshen, 1994; Neumann et al., 1999), *Striga* spp. (Dörr, 1997; Reiss and Bailey, 1998), *Cuscuta* spp. (Vaughn, 2002, 2003), *Viscum* spp. (Heide-Jørgensen, 1987), and others (Heide-Jørgensen and Kuijt, 1993, 1995). But little is known about the basis of host resistance to these parasites, just finding the work of Joel et al. (1996) introducing this subject. In the last years only some histological studies of the resistant interactions have been undertaken (Dörr et al., 1994; Antonova and Ter Borg, 1996; Gowda et al., 1999; Goldwasser et al., 2000; Labrousse et al., 2001; Rubiales et al., 2003; Zehhar et al., 2003; Pérez-de-Luque et al., 2005b, 2006a, 2006b).

This lack of knowledge is due to the complexity of this interaction. The study of this host-parasite interaction presents important limitations because they both are plants, which implies sharing similar morphological, physiological, and biochemical traits. To solve it, we have chosen cytological and cytochemical techniques as powerful tools to reveal the mechanisms underlying the host-parasitic plant interaction. These studies, complemented with omic studies using *M. truncatula* as a host model, will be a valuable addition to our knowledge about the plant-parasitic plant interactions.

In this work we have used two *M. truncatula* accessions previously evaluated against crenate broomrape infection (Rodríguez-Conde et al., 2004). We have identified one of them as early resistant to broomrape

[1] This work was supported by the project FP6–2002–FOOD–1–5062232004–2008. A.P.-d.-L. is a researcher at the Instituto de Investigación y Formación Agraria y Pesquera de Andalucía funded by the program Juan de la Cierva of the Spanish Ministry of Education and Science.

* Corresponding author; e-mail bb2pelua@uco.es.

The author responsible for distribution of materials integral to the findings presented in this article in accordance with the policy described in the Instructions for Authors (www.plantphysiol.org) is: Alejandro Pérez-de-Luque (bb2pelua@uco.es).

[C] Some figures in this article are displayed in color online but in black and white in the print edition.

www.plantphysiol.org/cgi/doi/10.1104/pp.107.097089

Table I. *Phenotypic components of the resistance to crenate broomrape observed in M. truncatula per plant*

Data shown as mean ± SE. Data with the same letter within the same column are not significantly different (HSD, $P < 0.05$). * From a total of 200 seedlings per plant.

Accession	15 d after GR24		22 d after GR24		30 d after GR24	
	Total No. of *Oc* Seedlings Attached to *Mt* Roots*	% *Oc* Seedlings Attached to *Mt* Roots*	Total No. of *Oc* Seedlings Attached to *Mt* Roots*	% *Oc* Seedlings Developed into Tubercle	Total No. of *Oc* Tubercles Established on *Mt* Roots	% of Unviable *Oc* Tubercles (Darkened)
SA4327	23.0a ± 1.58	11.5a ± 0.79	27.4a ± 2.87	80.5a ± 4.85	23.6a ± 2.36	67.9a ± 2.55
SA27774	23.4a ± 1.82	11.7a ± 0.91	31.6a ± 1.51	7.7b ± 1.45	4.3b ± 0.63	49.7a ± 9.30

infection (SA27774) because no establishment or development of parasites can be observed. The other one was characterized as late resistant (SA4327) because despite parasites established and developed, most of them were unable to evolve into mature plants. Cytochemical studies revealed that the defensive mechanisms are activated at different time points in each accession, which implies a different observation of the phenotype of the resistance and a higher success avoiding parasite infection for the early resistant accession.

RESULTS

Minirhizotron Studies

This system allowed the study of the infection process in both accessions of *M. truncatula* and the collection of samples at the right time for cytochemical analysis. It also permitted a quantitative study of the expression of the resistance, allowing characterization of both accessions as early and late resistant plants. Addition of GR24 to the minirhizotrons assured a high and homogeneous germination of crenate broomrape seeds (40%). A similar number of attachments was formed on both accessions during the first 3 weeks (Table I). However, both accessions differed already by this time on percentage of crenate broomrape germinated seeds in contact with *M. truncatula* roots that successfully formed a tubercle, being the success on tubercle formation much lower in SA27774 (7.7%). This reaction was characterized by stoppage of parasite seedlings penetration into the host root, usually accompanied by darkening of host and/or parasite tissues around the point of attachment. On the contrary, at the same observation date, most of the attachments in SA4327 had evolved to small tubercles. As a consequence, 30 d after GR24 application there were almost no tubercles (4.3) in accession SA27774 contrasting with the number of them established on SA4327 (23.6). But a new incompatible reaction was found at this point: More than half of the tubercles (67.9%) on SA4327 had become dark and stopped their development.

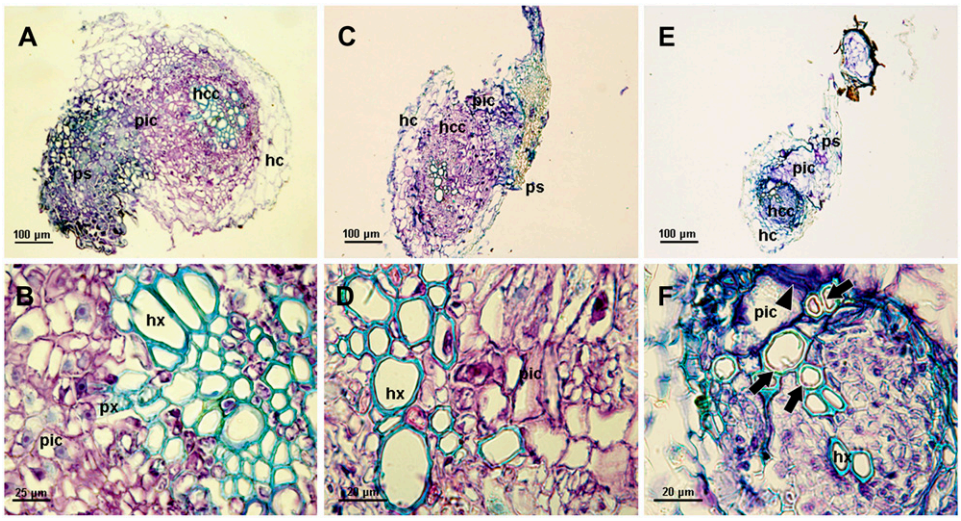

Figure 1. Sections stained with TBO. A, Cross section of a successful crenate broomrape seedling penetration on SA4087 accession of *M. truncatula*. B, Detail of A showing the central cylinder and host xylem vessels in contact with parasite cells. Some parasite vessels begin to develop connecting with the host xylem vessels. C, Cross section of a successful crenate broomrape seedling penetration on SA4327 accession of *M. truncatula*. D, Detail of C showing the central cylinder and host xylem vessels in contact with parasite cells. E, Cross section of an unsuccessful crenate broomrape seedling penetration on SA27774 accession of *M. truncatula*. F, Detail of E showing the thickening of host xylem walls (arrows) in contact with parasite cells and accumulation of a dark stained substance (arrowhead). ps, Parasite seedling; pic, parasite intrusive cells; hc, host cortex; hcc, host central cylinder; hx, host xylem vessels; px, parasite xylem vessels. [See online article for color version of this figure.]

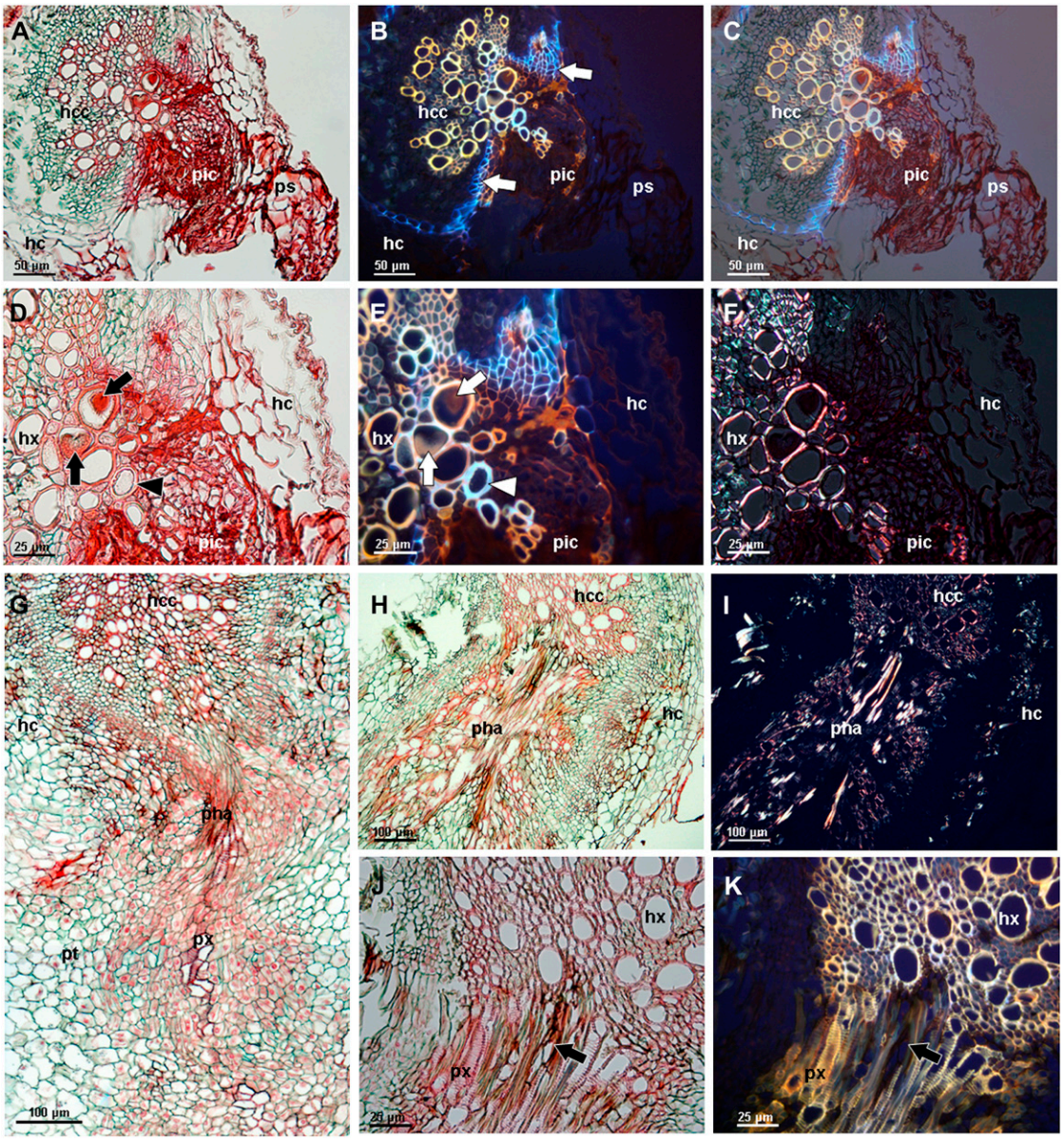

Figure 2. Sections stained with AGS. A, Cross section of an unsuccessful crenate broomrape seedling penetration on SA27774 accession of *M. truncatula*. B, The same section observed under UV excitation (340–380 nm) showing an intense fluorescence in host cells in contact with parasite tissues (arrows). C, Overlay of A and B showing the localization of the fluorescent cells. D, Detail of A showing accumulation of substances (noncarbohydrates) inside host xylem vessels (arrows) and thickening of xylem vessels in contact with parasite cells (arrowhead). E, The same section as D observed under UV excitation (340–380 nm) and showing blue fluorescence from the thickened xylem cell walls (arrowhead). F, The same section as D observed under polarized light showing no changes in the cell walls birefringence of thickened xylem vessels. G, Cross section of a successful established crenate broomrape tubercle on SA4087 accession. H, Cross section of a darkened established crenate broomrape tubercle on SA4327 accession. I, The same section as H observed under polarized light. J, Detail of a cross section of a darkened established crenate broomrape tubercle on SA4327 accession showing accumulation of a dark brown substance inside parasite xylem vessels and the apoplast of the haustorium (arrow). K, The same section as J observed under UV excitation (340–380 nm) and showing quenched autofluorescence from the vessels covered by the dark brown substance (arrow). ps, Parasite seedling; pic, parasite intrusive cells; hc, host cortex; hcc, host central cylinder; hx, host xylem vessels; pha, parasite haustorium; pt, parasite tubercle; px, parasite xylem vessels.

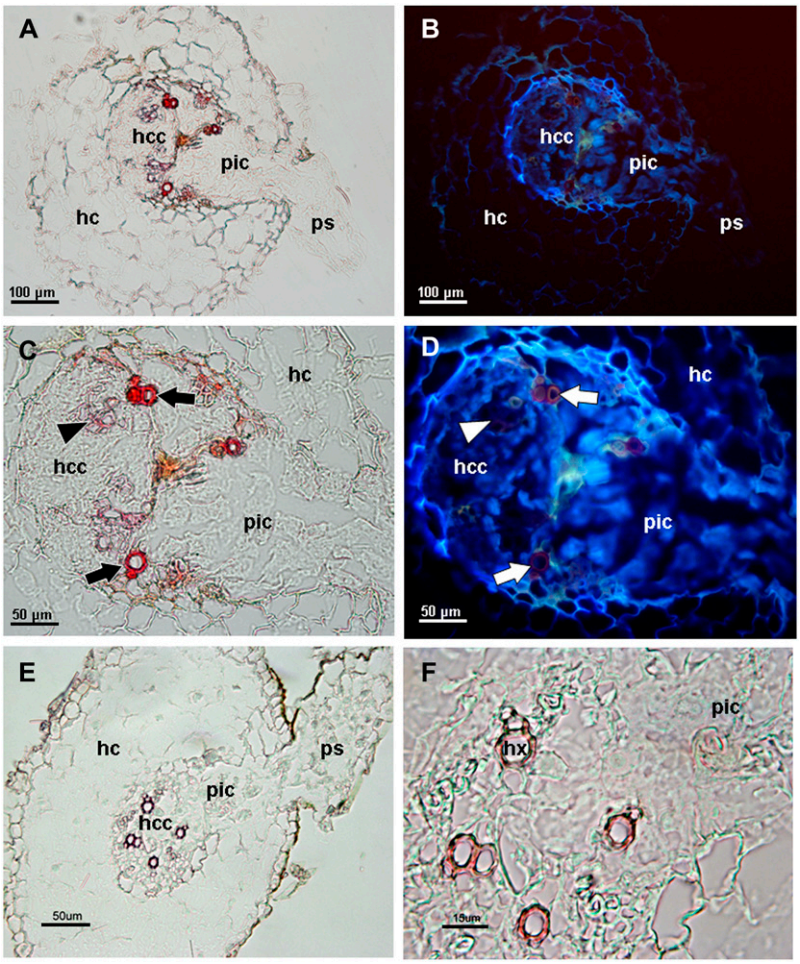

Figure 3. Sections stained with phloroglucinol-HCl. A, Cross section of an unsuccessful crenate broomrape seedling penetration on SA27774 accession of *M. truncatula*. B, The same section observed under UV excitation (340–380 nm). C, Detail of A showing accumulation of substances (polyphenols) inside host xylem vessels and thickening of their cell walls (arrows) compared with normal xylem vessels stained with the dye (arrowhead). D, The same section as C observed under UV excitation (340–380 nm) and showing blue fluorescence corresponding to suberin from endodermal cells, and the quenched fluorescence from normal lignified xylem walls (arrowhead) and thickened xylem walls (arrows). E, Cross section of a successful crenate broomrape seedling penetration on SA4087 accession of *M. truncatula*. F, Detail of E showing the normal staining of host xylem walls. ps, Parasite seedling; pic, parasite intrusive cells; hc, host cortex; hcc, host central cylinder; hx, host xylem vessels. [See online article for color version of this figure.]

Samples of both kinds of incompatible interactions and compatible interactions were collected and used for cytochemical studies.

Light and Fluorescence Microscopy

To characterize the mechanisms of resistance setting in play by the host, different histochemical procedures were employed. For comparison, tissues of the *M. truncatula* accession SA4087 were included as controls. This accession is the most susceptible one to crenate broomrape attack described to date (Rodríguez-Conde et al., 2004).

Sections of both successful and unsuccessful penetration attempts are presented in Figure 1, corresponding to accessions SA4087 (Fig. 1, A and B), SA4327 (Fig. 1, C and D), and SA27774 (Fig. 1, E and F), respectively. The toluidine blue O (TBO) staining was used as a general dye to get preliminary information about the incompatible interaction. In accessions SA4087 and SA4327 the parasite was able to pierce through the cortex and penetrated into the host central cylinder, beginning the development of the haustorium. Parasite intrusive cells in SA27774 also reached the host central cylinder but some abnormalities were observed. A dark stained deposit accumulated at the interface between host and parasite and a wall thickening inside host xylem vessels next to parasite tissues was developed (Fig. 1F).

Staining of sections from the early resistance accession with alcian green safranin (AGS) confirmed that parasite intrusive cells reached the host central cylinder, but an intense red coloration of the parasite tissues (corresponding to noncarbohydrate substances) was observed (Fig. 2, A and D), contrary to the common green staining (carbohydrates) expected for normal and healthy tissues in SA4087 (Fig. 2G). The parasite tissues also presented a disrupted and disorganized aspect. Accumulation of a red-stained material in the apoplast within and around the penetration pathway of the parasite was observed (Fig. 2, A and D) corresponding with the dark-stained material (unspecific substances) found using the TBO procedure. Host cells in contact and near the parasite tissues were impregnated with this red substance and it was also present inside some host xylem vessels (Fig. 2D). Observation of samples under UV excitation (340–380 nm) revealed a strong blue-white fluorescence from the walls and middle lamellae of cells surrounding the parasite intrusive tissues, including some xylem vessels (Fig. 2,

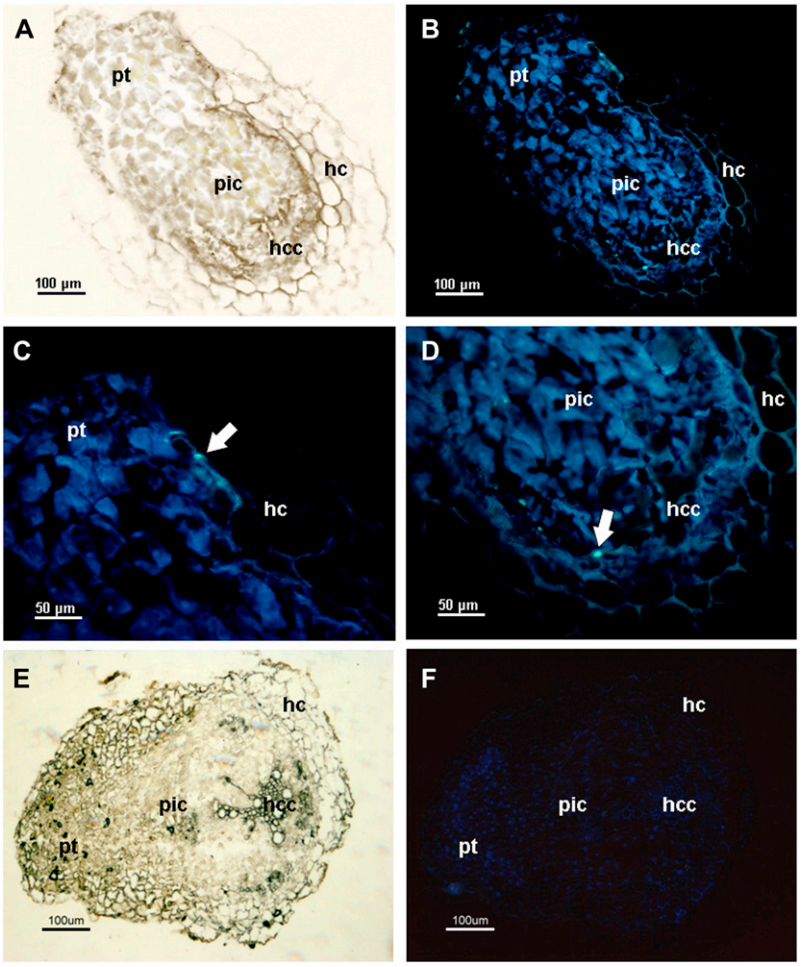

Figure 4. Sections stained with aniline blue fluorochrome. A, General view of a cross section of an incompatible interaction on SA27774 accession of *M. truncatula* observed under bright field. B, The same section as A observed under UV excitation (340–380 nm). C, Detail of B showing callose depositions (arrow) in cell walls from the host cortex in contact with parasite cells. D, The same section as C showing callose depositions (arrow) in cell walls from the host central cylinder. E, Cross section of a compatible interaction on SA4087 accession of *M. truncatula* observed under bright field. F, The same section as E observed under UV excitation (340–380 nm). No presence of callose is detected. pt, Parasite tubercle; pic, parasite intrusive cells; hc, host cortex; hcc, host central cylinder.

B, C, and E). This fluorescence was shown only in host vessels near or in contact with the parasite cells (Fig. 2, C and E), but not in those located away from the infection point. The thickening of the cell walls found inside the xylem vessels also presented this fluorescence (Fig. 2E). Observation of samples under polarized light proved that the secondary thickening of xylem walls was not due to birefringence (O'Brien and McCully, 1981), as it is common in the case of lignified and suberized walls (Fig. 2F). Sections of tubercles becoming dark on the late resistant accession and stained with the same technique (AGS) showed a normal aspect at the first sight (Fig. 2H) compared with those corresponding to healthy tubercles (Fig. 2G). However, a few details were observed: First, the presence of a dark brown deposit in the apoplast and some vessels from the haustorium (Fig. 2J), which did not stain; and second, the presence of a slight blue-white fluorescence in host xylem walls in contact with the haustorium (Fig. 2K). The dark deposit did not present fluorescence and quenched that of the impregnated vessels (Fig. 2K). It also eliminated the birefringence of the affected vessels (Fig. 2I) under polarized light. The blue-white fluorescence was very similar to that found in the case of the early resistant accession (Fig. 2, B, C, and E).

To check the possible role of lignins and suberins in this resistance, phloroglucinol-HCl staining was used (Fig. 3). In compatible interactions on SA4087, xylem walls appeared with a light pink stain (Fig. 3, E and F), indicating their normal lignification. However, an intense red coloration was observed in walls of xylem vessels near the parasite intrusive cells in sections of incompatible interactions on SA27774 (Fig. 3, A and C). These vessels presented also the thickened walls observed with TBO and AGS staining. Some xylem vessels were also filled with a material that was strongly stained with this method. When observed under UV excitation (340–380 nm; Fig. 3, B and D), lignin autofluorescence was quenched by the staining and only suberin fluorescence remained. As can be seen in Figure 3, B and D, only the suberized walls corresponding to the endodermal cells showed fluorescence; lignified cell walls did not fluoresce.

To identify other mechanisms implicated in reinforcement of host cell walls against *Orobanche* penetration, aniline blue fluorochrome was used for identification of callose under UV excitation (340–380 nm; Fig. 4). Our results showed that host cell walls from the cortex (Fig. 4C) in contact with parasite intrusive tissues and some cells in the central cylinder

(Fig. 4D) presented a slight accumulation of callose. No presence of callose was detected in compatible interactions (Fig. 4F).

Observations of fresh hand cut sections were taken under UV excitation (340–380 nm; Fig. 5) to detect the presence of phenolic compounds. No fluorescence in tissues was detected neither in uninfected roots (Fig. 5, A and B) or compatible interactions (Fig. 5, C and D). On the contrary, a strong fluorescence was found in host tissues adjacent to parasite intrusive cells (Fig. 5, E and F) and haustoria (Fig. 5, G and H) in sections of incompatible interactions.

Confocal Laser Scanning Microscopy

Confocal microscopy studies were developed to get a more secure localization of phenolic compounds in tissues (Fig. 6). The emission spectra were collected using two channels (green and red) for the same excitation, to check differences in the fluorescence of the accumulated compounds. The fluorescence was detected within the host central cylinder (Fig. 6, A–D) and cortical cells (Fig. 6, E–H) in incompatible interactions on the early resistant accession (SA27774). Also, accumulation of phenolics was observed in the

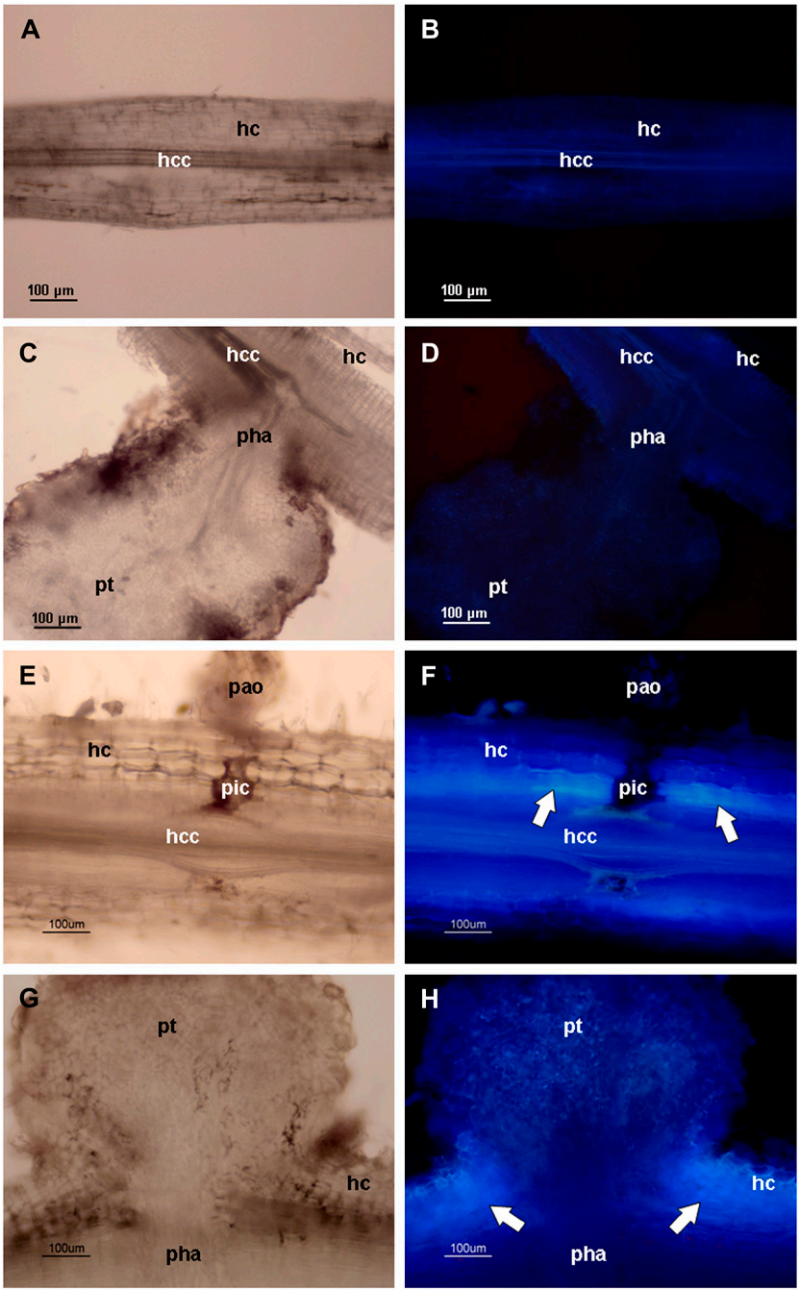

Figure 5. Hand cut fresh sections for fluorescence observation. A, Longitudinal section of an uninfected *M. truncatula* root observed under bright field. B, The same section as A observed under UV excitation (340–380 nm). C, Longitudinal section of a successful established crenate broomrape tubercle on SA4327 accession of *M. truncatula* observed under bright field. D, The same section as C observed under UV excitation (340–380 nm). E, Longitudinal section of an unsuccessful crenate broomrape seedling penetration on SA27774 accession of *M. truncatula* observed under bright field. F, The same section as E observed under UV excitation (340–380 nm) and showing a strong fluorescence from host cells in contact with parasite tissues (arrows). G, Cross section of a darkened crenate broomrape tubercle on SA4327 accession observed under bright field. H, The same section as G observed under UV excitation (340–380 nm) and showing a strong fluorescence from host cells in contact with parasite tissues (arrows). hc, Host cortex; hcc, host central cylinder; pha, parasite haustorium; pt, parasite tubercle; pao, parasite attachment organ; pic, parasite intrusive cells.

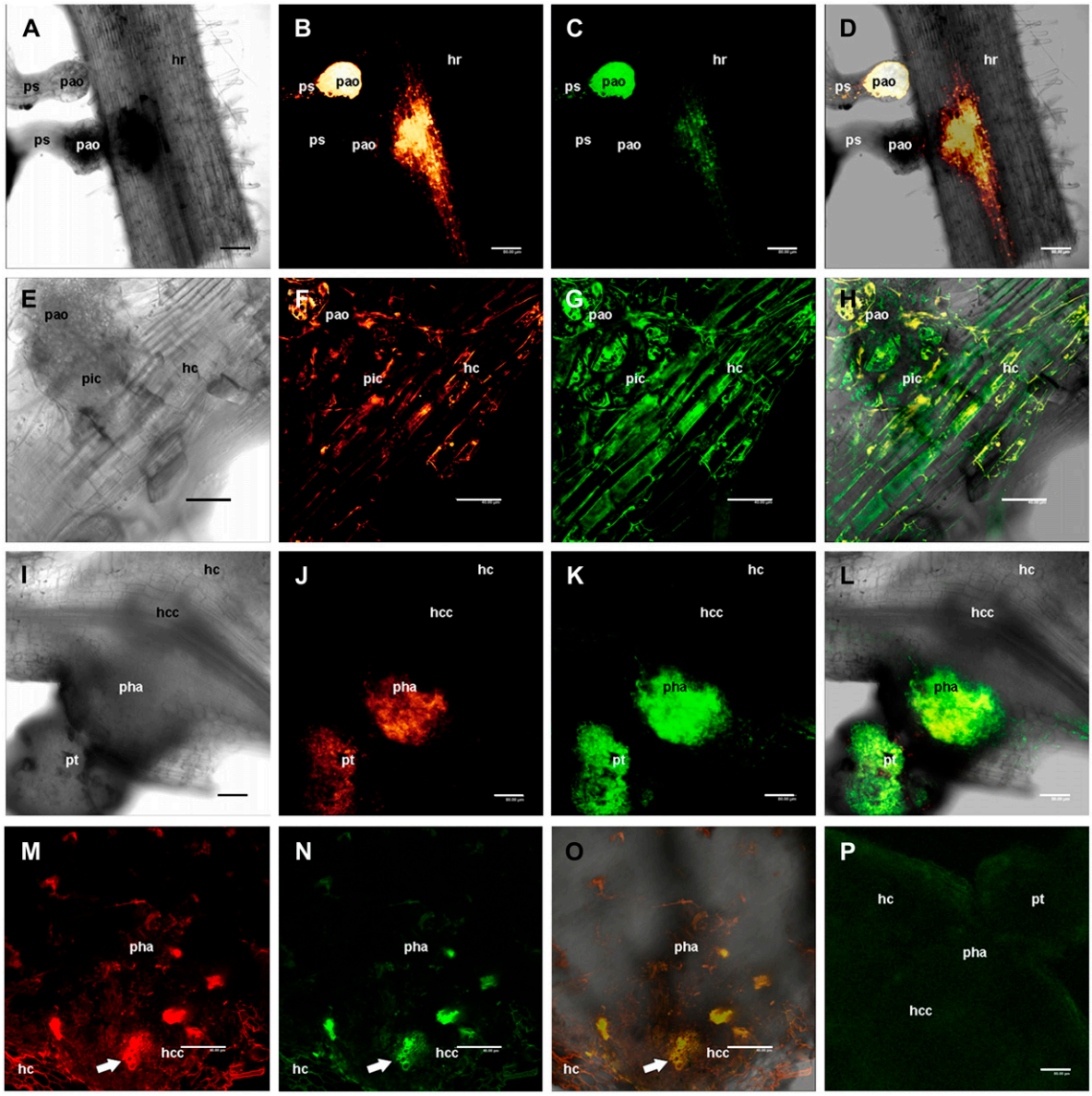

Figure 6. Localization of phenolic compounds using confocal laser microscopy. The images are single optical sections in B, C, F, G, J, K, M, N, and P. Figures B, F, J, and M correspond to emission spectra collected within the red channel (590–670 nm). Figures C, G, K, N, and P correspond to emission spectra collected within the green channel (515–590 nm). A, Incompatible interaction of crenate broomrape on SA27774 accession of *M. truncatula* (transmission). A darkening of the attachment organ and root tissues can be observed. B, Optical section of A showing intense fluorescence (red channel) in the host central cylinder and in the youngest attachment organ. C, The same section as B through the green channel. D, Overlay of A, B, and C showing the localization of the fluorescence in tissues. E, Detail of an unsuccessful crenate broomrape seedling penetration on SA27774 accession (transmission). F, Optical section of E showing intense fluorescence (red channel) in the host cells and in the parasite intrusive cells. G, The same section as F through the green channel. H, Overlay of E, F, and G showing the localization of the fluorescence in tissues. I, Darkened crenate broomrape tubercle on SA4327 accession of *M. truncatula* (transmission). J, Optical section of I showing intense fluorescence (red channel) in the haustorium and distal parts of the tubercle. K, The same section as J through the green channel. L, Overlay of I, J, and K showing the localization of the fluorescence in tissues. M, Optical section of a darkened crenate broomrape tubercle on SA4327 accession showing intense fluorescence (red channel) in the host xylem vessels (arrow). N, The same section as M through the green channel. O, Overlay of M and N with a transmission image showing the localization of the fluorescence in tissues. P, Optical section of a normal crenate broomrape tubercle on SA4327 accession. No fluorescence (green channel) can be detected. ps, Parasite seedling; pao, parasite attachment organ; hr, host root; pic, parasite intrusive cells; hc, host cortex; hcc, host central cylinder; pha, parasite haustorium; pt, parasite tubercle. Scale bar: 80 μm in A to D, I to L, and P; 40 μm in E to H and M to O.

attachment organ of some parasites in contact with the host root (Fig. 6, A–D). Regarding incompatible interactions on the late resistant accession (SA4327), accumulation of phenolics was observed in the haustoria and tubercles of the parasite (Fig. 6, I–L) and within host xylem vessels connected with the parasite haustorium (Fig. 6, M–O). No presence of phenolics compounds was detected in compatible interactions on both accessions SA4327 (Fig. 6P) and SA4087 (data not shown).

Cell Viability Assay

Trypan blue staining was used in fresh hand cut sections to check the viability of the cells in compatible and incompatible interactions (Fig. 7). In compatible interactions (Fig. 7, A and B) and uninfected roots (Fig. 7E) all the cells exclude the dye, confirming they were alive. However, the parasite intrusive cells and those corresponding to the attachment organ (Fig. 7, C and D) in incompatible interactions were clearly stained by the dye, indicating no viable cells. Moreover, parasite cells located in the distal part of the tubercle in incompatible interactions on the late resistant accession were also stained (Fig. 7F) and consequently were not viable.

Identification of Phytoalexins

Thin-layer chromatography (TLC) plates showed the presence of known phytoalexins in the methanolic extracts of inoculated plants from both soluble and cell wall-bound phenolics fractions (Fig. 8). Medicarpin and maackiain were found in the soluble phenolic fraction of inoculated plants of both *M. truncatula* accessions. Scopoletin was identified in the cell wall-bound phenolic fraction of inoculated plants of *M. truncatula* accession SA4327. Pisatin was not detected in any of the extracts. Several other compounds appeared on the TLC plate corresponding to soluble phenolics from inoculated plants but they did not correlated with any of the phytoalexins used as standards. The retention factor of the known phytoalexins was 0.158 for scopoletin, 0.526 for pisatin, 0.595 for maackiain, and 0.632 for medicarpin.

DISCUSSION

Mechanisms of resistance against crenate broomrape were characterized in two genotypes of *M. truncatula*. One of them, SA27774, shows an early expression of the resistance to this parasitic plant and does not allow

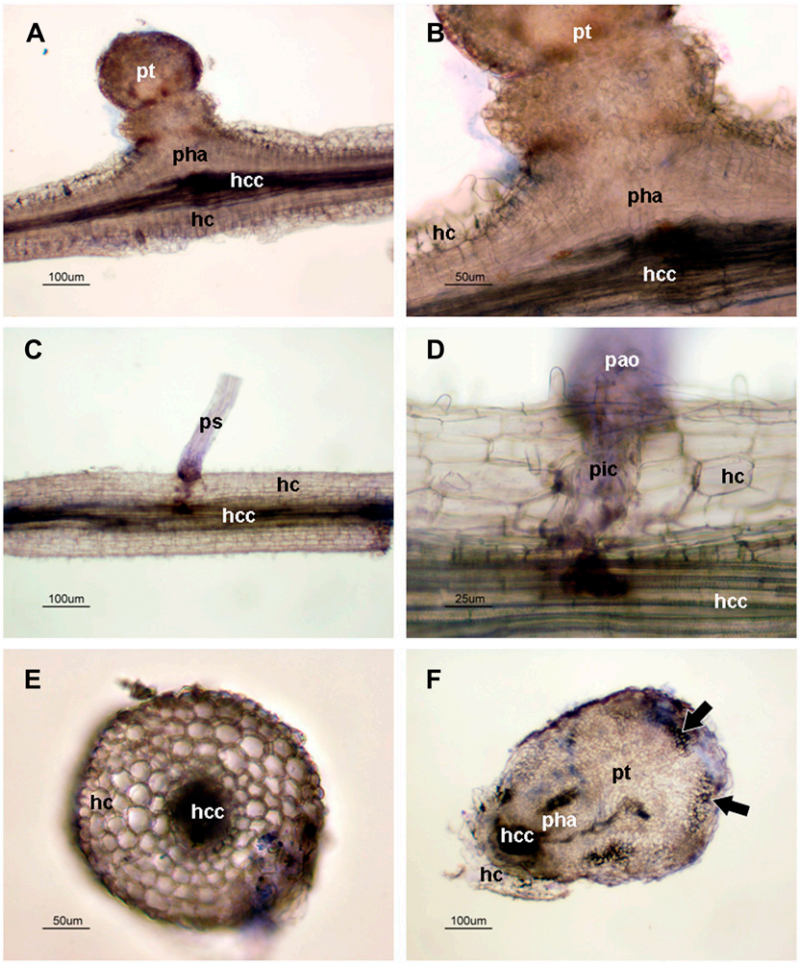

Figure 7. Hand cut fresh sections stained for cell viability. A, Longitudinal section of a normal crenate broomrape tubercle on SA4327 accession of *M. truncatula*. B, Detail of A showing the absence of stained cells in host and parasite tissues. C, Longitudinal section of an unsuccessful crenate broomrape seedling penetration on SA27774 accession of *M. truncatula*. D, Detail of C showing stained cells corresponding to the parasite intrusive cells and the attachment organ, indicating their loss of viability. E, Cross section of an uninfected *M. truncatula* root showing the absence of stained cells. F, Cross section of a darkened crenate broomrape tubercle on SA4327 accession showing stained cells (arrows) in the distal part of the tubercle. pt, Parasite tubercle; pha, haustorium; hc, host cortex; hcc, host central cylinder; ps, parasite seedling; pao, parasite attachment organ; pic, parasite intrusive cells.

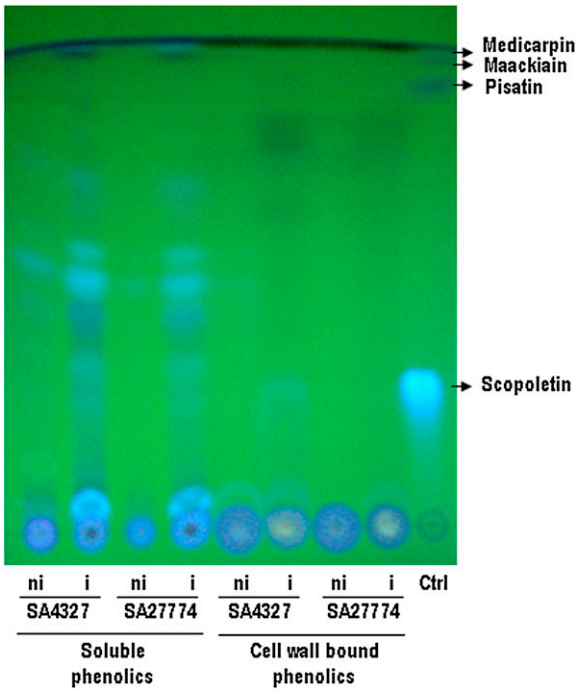

Figure 8. TLC plate of the methanolic extract from root samples of crenate broomrape inoculated (i) and noninoculated (ni) *M. truncatula* plants. Ctrl, Control with standard phytoalexins (scopoletin, medicarpin, pisatin, and maackiain).

the establishment of the parasite. On the contrary, SA4327 is infected with crenate broomrape and allows the establishment and development of parasite tubercles. However, it is not completely susceptible to the pathogen attack and a late resistance is expressed after tubercles establishment. This does not prevent completely the development of the parasitic plant, but limits the amount of individuals of the pathogen growing on it. Both kind of incompatible interactions, appearing before or after the development of the parasite haustorium, have been previously reported in resistant host to parasitic plants (Labrousse et al., 2001; Serghini et al., 2001; Rubiales et al., 2003; Zehhar et al., 2003; Pérez-de-Luque et al., 2005a, 2005b, 2006a, 2006b; Echevarría-Zomeño et al., 2006). They are indicative of resistance, but the exact nature of the mechanisms underlying such resistance is not well understood. For example, stoppage of seedling penetration has been usually associated to a hypersensitive response (HR; Dörr et al., 1994; Goldwasser et al., 1997), but there is no conclusive evidence that a HR really occurs in these interactions (Rubiales et al., 2003; Pérez-de-Luque et al., 2005b) in a manner similar to that described for fungal attack (Heath, 1999; Richael and Gilchrist, 1999). For that reason, histological and histochemical studies are of great value to know what is really happening inside host tissues.

The cytological data show that the penetration of crenate broomrape in the early resistant *M. truncatula* accession (SA27774) is stopped once the parasite intrusive cells have reached the host central cylinder. To our knowledge, this is the first time that a prehaustorial mechanism of resistance against parasitic root plants is located inside the central cylinder of the host. Usually, the prehaustorial defensive mechanisms against parasitic plants have been located in the host cortex (Echevarría-Zomeño et al., 2006; Pérez-de-Luque et al., 2006a, 2007b) or the endodermis (Pérez-de-Luque et al., 2005b, 2006a, 2007b). This kind of resistance is also different to that found in rice (*Oryza sativa*) and maize (*Zea mays*) against the parasite *Striga* spp. (Gurney et al., 2003, 2006) where the parasite is stopped before penetrating the central cylinder, probably due to physical barriers as described in the case of *Orobanche* spp. But once the parasite reached the central cylinder, a haustorium was developed connecting with the hosts vascular tissues and resistance relied on posthaustorial mechanisms such as sealing of vessels by mucilage (Pérez-de-Luque et al., 2005a, 2006b). Moreover, to our knowledge, for the first time is also described a posthaustorial defensive mechanism different from the sealing of vessels (Pérez-de-Luque et al., 2005a, 2006b) in the late resistant *M. truncatula* accession (SA4327).

The only physical barrier detected against the parasite intrusion is the thickening of host xylem walls. This was reported some time ago (Dörr et al., 1994), and our results indicate that the secondary thickening of the xylem walls is composed of some kind of lignin, or at least (because no birefringence was detected) by some kind of polyphenol. Although some callose depositions were located, their presence was not enough or well located enough to stop broomrape penetration as has been recently found in faba bean (*Vicia faba*; Pérez-de-Luque et al., 2007b). In this last case, big callose depositions were located in host cell walls in contact with parasite tissues (i.e. at the point of the resistance) stopping the parasite penetration. However, we cannot discard a possible role of callose as a reservoir of β-glucans elicitors (Esquerré-Tugayé et al., 2000) as suggested in the case of pea (*Pisum sativum*)-crenate broomrape (Pérez-de-Luque et al., 2006a).

So the lack of strong physical barriers preventing the parasite penetration into the host must be complemented and reinforced by another type of defensive mechanism: The fluorescence points toward the presence of phenolic compounds (phytoalexins) as the mechanism responsible to stop parasite intrusion, as has been recently reported in the sunflower (*Helianthus annuus*)-crenate broomrape interaction (Echevarría-Zomeño et al., 2006). However, contrary to what has been shown in that work, in which suberization plays a crucial role stopping crenate broomrape penetration in the cortex, no physical barriers appear in *M. truncatula* roots and the parasite intrusive cells are able to pierce easily through the cortex and the endodermis, reaching the vascular cylinder. At this moment, an intense release of phenolic compounds at the infection point

takes place through the host cells in contact with the parasite tissues and the xylem vessels. Medicarpin and maackiain have been found as part of the soluble phenolics fraction in inoculated plants and both phytoalexins have been previously reported as implicated in defense against pathogens (Cachinero et al., 2002). This maybe creates an unpleasant environment for the parasite intrusive cells, contributing to their further death and avoiding the development of an haustorium. Moreover, these phenolic compounds seem to be secreted to the external part of the root, affecting broomrape seedlings attached near a previous unsuccessful penetration attempt. This is not strange, because accumulation and secretion of phytoalexins against parasitic plants has been previously reported (Goldwasser et al., 1999; Serghini et al., 2001; Echevarría-Zomeño et al., 2006). The absence of dead host cells in this case, confirmed by the viability test, supports that this defensive mechanism is not a HR. However, other mechanisms of resistance acting at the same time cannot be discarded. For example, hormonal compatibility between host and parasite is needed to develop a functional haustorium (D.M. Joel and A. Pérez-de-Luque, unpublished data) and a lack of this compatibility could affect the normal parasite growth.

In the case of the late resistance found in SA4327, the accumulation and secretion of phenolic compounds seems to be operating but at a later stage. Once the parasite has formed a haustorium and established vascular connections with the host, the last one produces phenolic compounds that are translocated through the vascular system and reach the parasite. The first evidence for this is the presence of a dark deposit in parasite vessels of the haustorium. This deposit probably corresponds with the oxidation of phenolic compounds, which usually originates dark brown components (Takahama, 2004). The fluorescence found in host vessels, haustoria, and tubercles implies that the host is poisoning the parasite established tubercles releasing phytoalexins through the vascular connections. These phytoalexins accumulate in the tubercles by the sink effect that crenate broomrape has once it has been connected with the host root. The presence of parasite dead cells in the same areas where phenolic compounds accumulate within the tubercles could indicate that the accumulation of toxic metabolites (phenolics) from the host plant is killing the parasite. The presence of soluble phenolics like medicarpin and maackiain also supports the idea of excretion of phytoalexins. As in the previous case, other(s) defensive mechanism(s) cannot be discarded, including the lack of hormonal compatibility. The presence of scopoletin in the cell wall-bound phenolics fraction could be indicative of further development of physical barriers not detected at this point by cytochemical methods.

All these results are in accordance with those obtained by Dita et al. (2007), who found an activation of genes related with the synthesis of phenolic compounds also in early and late resistant accessions to crenate broomrape. The main difference was, like in this case, a matter of time: Similar genes were activated but with a time gap between them.

CONCLUSION

Recent studies have revealed that multiple factors are involved in resistance to parasitic plants. Behind the observation of incompatible interactions (unsuccessful attachment penetration and darkening of established tubercles) underlies a complex system of multiple mechanisms of resistance. To date, most of those described were based mainly in physical barriers preventing parasite penetration into the host central cylinder (prehaustorial mechanisms) and blocking of host vessels disrupting the nutrient fluxes between host and parasite (posthaustorial mechanisms). In this work we presented one mechanism of resistance, accumulation of phytoalexins (phenolic compounds), that does not rely on physically stopping parasite penetration into the host: The parasite penetrates reaching the central cylinder, but it seems to be poisoned and killed before developing a haustorium. Despite other mechanisms of resistance that could be involved, a crucial difference between both accessions is the moment at which the host detects and reacts against the parasite. It determines a more effective resistance against the pathogen: The earliest the parasite is detected, the most effective are the defensive mechanisms activated, and the infection is lower.

MATERIALS AND METHODS

Plant Material and Growth Conditions

Crenate broomrape (*Orobanche crenata*) was grown on accessions of *Medicago truncatula* showing early or late resistance to this pathogen (accessions SA27774 and SA4327, respectively).

The petri dish system described by Pérez-de-Luque et al. (2005a) and Rubiales et al. (2006) was used for in vitro cultivation of the *M. truncatula* plants and inoculation with crenate broomrape seeds.

M. truncatula seeds were supplied from the South Australian Research and Development Institute Genetic Resource Centre in Australia (origin: Yugoslavia for SA4327 and Morocco for SA27774). Seeds were scarified with a metal sheet and sterilized in commercial bleach (20% in sterile water) for 10 min. For synchronize germination, seeds were place at 4°C for 36 h in sterile water. During this period, we replaced sterile water two or three times to help germination. After that, seeds were rinsed with sterile water at room temperature for 3 or 4 h, changing it six or eight times. Finally, seeds were placed in petri dishes on wet glass fiber filter papers (Whatmann GF/A) and kept in darkness at 20°C for 1 to 2 d. When the radicle reached 2 cm length, seedlings were transferred to new dishes (15 cm diameter) with perlite and new glass fiber papers (Pérez-de-Luque et al., 2005a).

Crenate broomrape seeds were collected from infected faba bean (*Vicia faba*) plants at Córdoba during 2000. They were disinfected with formaldehyde according to González-Verdejo et al. (2005) and spread on the glass fiber paper (approximately 8 mg) where the *M. truncatula* roots were growing. To prevent exposure of the parasite seeds and host roots to direct light, the dishes containing test plants inoculated with parasite seeds were sealed with parafilm and covered with aluminum foil. Then, the upward growing host plants were placed vertically in trays with Hoagland nutrient solution (Hoagland and Arnon, 1950) and grown in a controlled environment chamber at 20°C ± 0.5°C with a day/night 14 h photoperiod and an irradiance of 200 μmol m^{-2} s^{-1}.

At the same time plants were growing, crenate broomrape seeds were conditioned. For conditioning, parasite seeds need to be in darkness at 20°C for 10 d (Pérez-de-Luque et al., 2005a).

After conditioning period, we applied 5 mL of the synthetic stimulant GR24 (1 mg/mL; Magnus et al., 1992) on the paper with the seeds (for crenate broomrape homogenous germination induction; Rubiales et al., 2003).

Minirhizotron Studies

The infection process was followed using a binocular microscope (Nikon SMZ1000; Nikon Europe B.V.). Fifteen days after GR24 application, the percentage of crenate broomrape attach seedlings on *M. truncatula* roots was calculated. The total of 200 crenate broomrape seedlings close (<3 mm) to the *M. truncatula* roots were visualized in each petri dish and the number of attached seedlings was referred to the total number of seedlings. At 22 d after GR24 application, the percentage of compatible and incompatible attachments against total attachments was scored. An attachment was considered compatible when it resulted in tubercle formation. Finally, 30 d after GR24 application established broomrapes were quantified and expressed as absolute value per plant. In addition, the number of darkened tubercles was recorded and expressed as a percentage respect to the total number of established tubercles per plant.

Collection and Fixation of Samples

Observations were taken using a binocular microscope. At 15 d after GR24 application, seedlings of crenate broomrape were sampled at random with the corresponding attached parts of host roots.

For staining methods and confocal laser scanning microscopy, the samples were fixed in 4% formaldehyde in phosphate-buffered saline (PBS), pH 7.3 at 4°C overnight. After washing in PBS (3 × 15 min), they were stored in 0.1% formaldehyde in PBS at 4°C.

Fixed samples were then dehydrated in ethanol series (50%, 80%, 95%, 100%, and 100%: 12 h each) and transferred to an embedding solvent (Xylene; Panreac Quimica S.A.) through a xylene-ethanol series (30%, 50%, 80%, 100%, 100%: 12 h each) and finally saturated with paraffin (Paraplast Xtra; Sigma). Seven micrometer-thick sections were cut with a rotary microtome (Nahita 534; Auxilab S.A.) and attached to adhesive-treated microscope slides (polysine slides; Menzel GmbH & Co. KG).

Staining Methods

After removal of paraffin, sections were stained with different dyes: (1) Staining with 0.05% TBO in PO_4 buffer (pH 5.5) during 5 to 10 min was used. In this case the dye was applied before removal of paraffin (Ruzin, 1999). This method allows the detection of phenolics as well as tannins, lignin, and suberin (Baayen et al., 1996; Bordallo et al., 2002; Mellersh et al., 2002; Crews et al., 2003). (2) AGS (Joel, 1983): The slides were dried and mounted with DePeX (BDH Chemicals). With this staining method, carbohydrates (including cell walls and mucilage) appeared green, yellow, or blue, while lignified, cutinized, and suberized walls, as well as tannin and lipid material inside cells appeared red (Joel, 1983). Nonstained sections were kept as control and for examination under the fluorescence microscope. (3) Phloroglucinol (2% in ethanol)-HCl (35%; Ruzin, 1999) were applied covering tissue sections for 30 min and observed by using light and fluorescence microscopy. This compound stains the aldehyde groups of lignin and suberin but quenches lignin autofluorescence and retains suberin fluorescence (Baayen et al., 1996; Rioux et al., 1998). (4) Aniline blue fluorochrome was used for callose detection under UV fluorescence (340–380 nm). The samples were stained during 15 to 30 min in a solution of 0.1% aniline blue fluorochrome in water (Bordallo et al., 2002).

Transverse sections were observed using a light microscope (Leica DM-LB, magnification ×100–×400; Leica Microsystems Wetzlar GmbH) and photographed using a digital camera (Nikon DXM1200F; Nikon Europe B.V.). The samples were also observed by epifluorescence under excitation at 340 to 380 nm (UV).

Fluorescence Microscopy

Hand cut sections (with a razor blade) were obtained from fresh root samples to observe accumulation of phenolic compounds by epifluorescence under excitation at 340 to 380 nm (UV).

Confocal Laser Scanning Microscopy

Ten fresh samples of crenate broomrape seedlings with the corresponding attached parts of host roots were immersed in a solution of 0.1% (w/v) diphenyl boric acid 2-aminoethylester (Naturstoffreagenz A: NA) in buffer (100 mM KPi pH 6.8, 1% NaCl [w/v]) according to Hutzler et al. (1998). This treatment induces secondary fluorescence of flavonoids. Confocal optical section stacks were collected using a Leica TCS-SP2-AOBS-UV confocal laser scanning microscope (Leica Microsystems Wetzlar GmbH) with an excitation wavelength of 488 nm and emission spectra monitored from 515 to 670 nm. The emission spectra corresponding to 515 to 590 nm was monitored through one channel (green channel), and the emision spectra corresponding to 590 to 670 nm was monitored through another channel (red channel). Analysis of confocal images was performed with the LEICA software LCS, version 2.5 Build 1227.

Cell Viability Assay

Trypan blue dye exclusion was used to assess cell viability. Samples were immersed in a commercial Trypan Blue solution of 50% (Sigma) and observed using a light microscope. Viable (alive) and nonviable (dead) cells were identified microscopically under bright field optics, as those that had excluded and taken up the trypan blue stain, respectively.

Extraction of Total Phenolics and Identification of Phytoalexins

The petri dish system was used for plant material collection from *M. truncatula* accessions showing early or late resistance (SA27774 and SA4327, respectively) to crenate broomrape as described before. *M. truncatula* roots from noninfected and infected plants were sampled 30 d after GR24 application, the date corresponding to establishment of the parasite. For noninfected plants, small root pieces (approximately 1 cm) were sampled at random. For infected plants, parts of the root with a crenate broomrape attachment were sampled, removing the parasite tissues. Then, samples were washed with tap and then distilled water, blotted dry with filter paper, frozen in liquid nitrogen, and stored at −80°C until biochemical analysis (Pérez-de-Luque et al., 2005a).

Frozen root tissue (0.04 g fresh weight) was homogenized in 1 mL methanol by using a pestle and mortar. After filtering off the solvent extract, the residue was further sequentially extracted twice with a similar volume of methanol and centrifuged twice at 15,000*g* for 15 min. The combined solvent extracts were dried and phenolic compounds were resuspended in 0.24 mL of methanol. The pellet residue was resuspended in 0.08 mL of 2 M NaOH and incubated at 70°C for 16 h. The suspension was cooled down, neutralized with 0.08 mL of 2 M HCl, and centrifuged (15,000*g* for 15 min). Then, the suspension was dried and resuspended in the same volume of methanol.

TLC analysis of the methanolic extract was performed according to Prats et al. (2003) by using Silicagel 60 F254 plates (Merk) and diethyleter:hexane (70:30 v/v) as the mobile phase. Plate was visualized under UV light (254 nm) lamp. Scopoletin (Sigma), medicarpin, pisatin, and maackiain (from Plantech) were used as standards.

Statistical Analysis

Minirhizotron assays were performed with two plants per petri dish and 10 petri dishes per *M. truncatula* accession (SA27774 and SA4327). Data were recorded from three randomized areas in each plant. To study possible interactions due to cultivation of plants in different dishes, each petri dish was treated as a block and an ANOVA was performed (Statistix v1.1 for Windows). No significant differences were found between blocks so each petri dish was considered as a replicate. For cytochemical and confocal studies, at least 10 samples were selected at random from several petri dishes for each study. Percentages were transformed according to the formula $Y = \arcsin(\sqrt{[X\%/100]})$ prior to statistical treatment.

ACKNOWLEDGMENT

We thank the microscopy service of the University of Córdoba-Servicio Centralizado de Apoyo a la Investigación where confocal laser microscopy observations were made.

Received February 1, 2007; accepted August 6, 2007; published August 10, 2007.

LITERATURE CITED

Antonova TS, Ter Borg SJ (1996) The role of peroxidase in the resistance of sunflower against *Orobanche cumana* in Russia. Weed Res **36:** 113–121

Baayen RP, Ouellette GB, Rioux D (1996) Compartmentalization of decay in carnations resistant to *Fusarium oxysporum* f. sp. dianthi. Phytopathology **86:** 1018–1031

Blondon F, Marie D, Brown S, Kondorosi A (1994) Genome size and base composition in *Medicago sativa* and *M. truncatula* species. Genome **37:** 264–275

Bordallo JJ, Lopez-Llorca LV, Jansson HB, Salinas J, Persmark L, Asensio L (2002) Colonization of plant roots by egg-parasitic and nematode-trapping fungi. New Phytol **154:** 491–499

Cachinero JM, Hervás A, Jiménez-Díaz RM, Tena M (2002) Plant defence reactions against fusarium wilt in chickpea induced by incompatible race 0 of *Fusarium oxysporum* f.sp. ciceris and nonhost isolates of *F. oxysporum*. Plant Pathol **51:** 765–776

Cook DR (1999) *Medicago truncatula*: a model in the making. Curr Opin Plant Biol **2:** 301–304

Cook DR, VandenBosh K, De Bruijn FJ, Huguet T (1997) Model legumes get the nod. Plant Cell **9:** 275–281

Crews LJ, McCully ME, Canny MJ (2003) Mucilage production by wounded xylem tissue of maize roots—time course and stimulus. Funct Plant Biol **30:** 755–766

Dita MA, Die JV, Román B, Krajinski F, Küster H, Moreno MT, Cubero JI, Rubiales D (2007) Gene expression profiling of *Medicago truncatula* roots in response to the parasitic plant *Orobanche crenata*. Planta (in press)

Dörr I (1997) How *Striga* parasitizes its host: a TEM and SEM study. Ann Bot (Lond) **79:** 463–472

Dörr I, Staack A, Kollmann R (1994) Resistance of Helianthus to *Orobanche*—histological and cytological studies. *In* AH Pieterse, JAC Verkleij, SJ ter Borg, eds, Biology and Management of *Orobanche.* Proceedings of the Third International Workshop on *Orobanche* and Related *Striga* Research. Royal Tropical Institute, Amsterdam, pp 276–289

Echevarría-Zomeño S, Pérez-de-Luque A, Jorrín J, Maldonado AM (2006) Pre-haustorial resistance to broomrape (*Orobanche cumana*) in sunflower (*Helianthus annuus*): cytochemical studies. J Exp Bot **57:** 4189–4200

Ellwood S, Lichtenzveig J, Pfaff T, Kamphuis L, Oliver R (2007) Fungi. *In* U Mathesius, EP Journet, LW Sumner, eds, The Medicago truncatula Handbook. The Samuel Roberts Noble Foundation, Ardmore, OK, pp 1–6

Esquerré-Tugayé MT, Boudard G, Dumas B (2000) Cell wall degrading enzymes, inhibitory proteins, and oligosaccharides participate in the molecular dialogue between plants and pathogens. Plant Physiol Biochem **38:** 157–163

Goldwasser Y, Hershenhorn J, Plakhine D, Kleifeld Y, Rubin B (1999) Biochemical factors involved in vetch resistance to *Orobanche aegyptiaca*. Physiol Mol Plant Pathol **54:** 87–96

Goldwasser Y, Kleifeld Y, Plakhine D, Rubin B (1997) Variation in vetch (*Vicia* spp.) response to *Orobanche aegyptiaca*. Weed Sci **45:** 756–762

Goldwasser Y, Plakhine D, Kleifeld Y, Zamski E, Rubin B (2000) The differential susceptibility of vetch (*Vicia* spp.) to *Orobanche aegyptiaca*: anatomical studies. Ann Bot (Lond) **85:** 257–262

González-Verdejo CI, Barandiaran X, Moreno MT, Cubero JI, Di-Pietro A (2005) An improved axenic system for studying pre-infection development of the parasitic plant *Orobanche ramosa*. Ann Bot (Lond) **96:** 1121–1127

Gowda BS, Riopel JL, Timko MP (1999) NRSA-1: a resistance gene homolog expressed in roots of non-host plants following parasitism by *Striga asiatica* (witchweed). Plant J **20:** 217–230

Gurney AL, Grimanelli D, Kanampiu F, Hoisington D, Scholes JD, Press MC (2003) Novel sources of resistance to *Striga hermonthica* in *Trypsacum dactyloides* a wild relativesof maize. New Phytol **160:** 557–568

Gurney AL, Press MC, Scholes JD (2006) A novel form of resistance in rice to the angiosperm parasite *Striga hermonthica*. New Phytol **169:** 199–208

Heath MC (1999) The enigmatic hypersensitive response: induction, execution, and role. Physiol Mol Plant Pathol **55:** 1–3

Heide-Jørgensen HS (1987) Development and ultrastructure of the haustorium of *Viscum minimum*. I. The adhesive disk. Can J Bot **67:** 1161–1173

Heide-Jørgensen HS, Kuijt J (1993) Epidermal derivatives as xylem elements and transfer cells: a study of the host-parasite interface in two species of *Triphysaria* (Scrophulariaceae). Protoplasma **174:** 173–183

Heide-Jørgensen HS, Kuijt J (1995) The haustorium of the root parasite *Triphysaria* (Scrophulariaceae), with special reference to xylem bridge ultrastructure. Am J Bot **82:** 782–797

Hoagland DR, Arnon DI (1950) The Water-Culture Method for Growing Plants Without Soil. California Agricultural Experiment Station Circular 347. University of California, Berkeley

Hutzler P, Fischbach R, Heller W, Jungblut TP, Reuber S, Schmitz R, Veit M, Weissenbock G, Schnitzler J (1998) Tissue localization of phenolic compounds in plants by confocal laser scanning microscopy. J Exp Bot **49:** 953–965

Joel DM (1983) AGS (alcian green safranin)—a simple differential staining of plant material for the light microscope. Proc RMS **18:** 149–151

Joel DM, Hershenhorn Y, Eizenberg H, Aly R, Ejeta G, Rich PJ, Ransom JK, Sauerborn J, Rubiales D (2007) Biology and management of weedy root parasites. *In* J Janick, ed, Horticultural Reviews, Vol 33. John Wiley & Sons, Hoboken, NJ, pp 267–349

Joel DM, Losner-Goshen D (1994) The attachment organ of the parasitic angiosperms *Orobanche cumana* and *O. aegyptiaca* and its development. Can J Bot **72:** 564–574

Joel DM, Losner-Goshen D, Hershenhorn J, Goldwasser Y, Assayag M (1996) The haustorium and its development in compatible and resistant host. *In* MT Moreno, JI Cubero, D Berner, D Joel, LJ Musselman, C Parker, eds, Advances in Parasitic Plant Research. Junta de Andalucía, Consejería de Agricultura y Pesca, Sevilla, Spain, pp 531–541

Labrousse P, Arnaud MC, Serieys H, Bervillé A, Thalouarn P (2001) Several mechanisms are involved in resistance of *Helianthus* to *Orobanche cumana* Wallr. Ann Bot (Lond) **88:** 859–868

Magnus EM, Stommen PLA, Zwanenburg B (1992) A standardized bioassay for evaluation of potential germination stimulants for seeds of parasitic weeds. J Plant Growth Regul **11:** 91–98

Mellersh DG, Foulds IV, Higgins VJ, Heath MC (2002) H_2O_2 plays different roles in determining penetration failure in three diverse plant-fungal interactions. Plant J **29:** 257–268

Neumann U, Vian B, Weber HC, Sallé G (1999) Interface between haustoria of parasitic members of the Scrophulariaceae and their host: a histochemical and inmunocytochemical approach. Protoplasma **207:** 84–97

O'Brien TP, McCully ME (1981). The Study of Plant Structure. Principles and Selected Methods. Termarcarphi Pty. Ltd., Melbourne, Australia

Pérez-de-Luque A, González-Verdejo CI, Lozano MD, Dita MA, Cubero JI, González-Melendi P, Risueño MC, Rubiales D (2006a) Protein cross-linking, peroxidase and β-1,3-endoglucanase involved in resistance of pea against *Orobanche crenata*. J Exp Bot **57:** 1461–1469

Pérez-de-Luque A, Jorrín J, Cubero JI, Rubiales D (2005a) Resistance and avoidance against *Orobanche crenata* in pea (*Pisum* spp.) operate at different developmental stages of the parasite. Weed Res **45:** 379–387

Pérez-de-Luque A, Lozano MD, Cubero JI, González-Melendi P, Risueño MC, Rubiales D (2006b) Mucilage production during the incompatible interaction between Orobanche crenata and Vicia sativa. J Exp Bot **57:** 931–942

Pérez-de-Luque A, Lozano MD, Maldonado AM, Jorrín JV, Dita MA, Die J, Román B, Rubiales D (2007a) *Medicago truncatula* as a model for studying interactions between root parasitic plants and legumes. *In* U Mathesius, EP Journet, LW Sumner, eds, The Medicago truncatula Handbook. The Samuel Roberts Noble Foundation, Ardmore, OK, pp 1–31

Pérez-de-Luque A, Lozano MD, Testillano PS, Moreno MT, Rubiales D (2007b) Resistance to broomrape (*Orobanche crenata*) in faba bean (*Vicia faba*): cell wall changes associated with pre-haustorial defensive mechanisms. Ann Appl Biol **151:** 89–98

Pérez-de-Luque A, Rubiales D, Cubero JI, Press MC, Scholes J, Yoneyama K, Takeuchi Y, Plakhine D, Joel DM (2005b) Interaction between *Orobanche crenata* and its host legumes: unsuccessful haustorial penetration and necrosis of the developing parasite. Ann Bot (Lond) **95:** 935–942

Prats E, Bazzalo ME, Leon A, Jorrin J (2003) Accumulation of soluble phenolic compounds in sunflower capitula correlates with resistance to *Sclerotinia sclerotiorum*. Euphytica **132:** 321–329

Reiss GC, Bailey JA (1998) *Striga* gesnerioides parasitising cowpea: development of infection structures and mechanisms of penetration. Ann Bot (Lond) **81:** 431–440

Richael C, Gilchrist D (1999) The hypersensitive response: a case of hold or fold? Physiol Mol Plant Pathol **55:** 5–12

Rioux D, Nicole M, Simard M, Ouellette GB (1998) Immunocytochemical evidence that secretion of pectin occurs during gel (gum) and tylosis formation in trees. Phytopathology **88:** 494–505

Rodríguez-Conde MF, Moreno MT, Cubero JI, Rubiales D (2004) Characterization of the *Orobanche-Medicago truncatula* association for studying early stages of the parasite-host interaction. Weed Res **44:** 218–223

Rubiales D (2001) Parasitic plants: an increasing threat. Grain Legumes **33:** 10–11

Rubiales D (2003) Parasitic plants, wild relatives and the nature of resistance. New Phytol **160:** 459–461

Rubiales D, Pérez-de-Luque A, Fernández-Aparicio M, Sillero JC, Román B, Kharrat M, Khalil S, Joel DM, Riches C (2006) Screening techniques and sources of resistance against parasitic weeds in grain legumes. Euphytica **147:** 187–199

Rubiales D, Pérez-de-Luque A, Joel DM, Alcántara C, Sillero JC (2003) Characterization of resistance in chickpea to crenate broomrape (*Orobanche crenata*). Weed Sci **51:** 702–707

Rubiales D, Sillero JC, Román MB, Moreno MT, Fondevilla S, Pérez-de-Luque A, Cubero JI, Zermane N, Kharrat M, Khalil S (2002) Management of broomrape in Mediterranean agriculture. *In* AEP, ed, Legumed: Grain Legumes in the Mediterranean Agriculture. European Association for Grain Legume Research, Rabat, Morocco, pp 67–73

Ruzin SE (1999) Plant Microtechnique and Microscopy. Oxford University Press, Oxford

Serghini K, Pérez-De-Luque A, Castejón-Muñoz M, García-Torres L, Jorrín JV (2001) Sunflower (*Helianthus annuus L.*) response to broomrape (*Orobanche cernua* Loefl.) parasitism: induced synthesis and excretion of 7-hydroxylated simple coumarins. J Exp Bot **52:** 2227–2234

Takahama U (2004) Oxidation of vacuolar and apoplastic phenolic substrates by peroxidase: physiological significance of the oxidation reactions. Phytochem Rev **3:** 207–219

Vaughn KC (2002) Attachment of the parasitic weed dodder to the host. Protoplasma **219:** 227–237

Vaughn KC (2003) Dodder hyphae invade the host: a structural and immunocytochemical characterization. Protoplasma **220:** 189–200

Zehhar N, Labrousse P, Arnaud MC, Boulet C, Bouya D, Fer A (2003) Study of resistance to *Orobanche ramosa* in host (oilseed rape and carrot) and non-host (maize) plants. Eur J Plant Pathol **109:** 75–82

Annals of Botany

ORIGINAL ARTICLE

Title: Resistance to *Orobanche crenata* in the model legume *Medicago truncatula*: the flavonoid response

Authors: María D. Lozano-Baena[1*], Elena Prats[1], Diego Rubiales[1] and Alejandro Pérez-de-Luque[2]

[1] *CSIC (Institute for Sustainable Agriculture), Apdo. 4084, 14080 Córdoba, Spain* and

[2] *IFAPA, Avda. Menendez Pidal s/n, PO Box 3092, 14004 Córdoba, Spain*

[*] For correspondence. E-mail: b72lobam@gmail.com

Running title: Flavonoids against crenate broomrapes attack

- ***Background and Aims*** *Orobanche crenata* Forsk. (crenate broomrape) is a weedy root parasite that represent the major constraint for legume crops in Mediterranean Basin and West Asia. This obligate root holoparasite depends completely on its host for all nutritional requirements. Little is known on resistance mechanisms in legume crops such as faba bean, vetches and pea what is hampered by their complex genome and physiology and the little genomic resources available. To facilitate identification of genes and metabolic pathways activated in resistance reactions we have studied the response against *O. crenata* attack using the model legume *Medicago truncatula* Gaertn. (barrel medic). *M.*

truncatula seems to defend from *O. crenata* infection mainly using chemical compounds i.e. flavonoids (phytoalexins). These phenolic compounds are well known in plant kingdom due to their antifungal and antimicrobial activity. In this work we identified and quantified by the first time some of the flavonoids acting against *O. crenata* invasion using two *M. truncatula* accessions with different resistances.

- ***Methods*** To identify and quantify some of the flavonoids produced by *M. truncatula* as response to the *O. crenata* attack, we have used high performance liquid chromatography with UV and mass spectrometric detection (LC-MS/MS) systems as well recognized methods to profile flavonoids in plant tissue extracts.
- ***Key Results*** Three of the standards (naringenin, daidzein and formononetin) were identified and quantified in the analysed root tissues for soluble phenolic samples but only formononetin appeared in both inoculated and non inoculated roots (naringenin and daidzein were only detected in inoculated roots of the SA4327 accession). No standard was detected in cell wall-bound phenolic extracts. Medicarpin, genistein, chlorogenic acid and scopoletin were not detected in any case and maackiain could not be analysed due to its instability.
- ***Conclusions*** This is the first report of flavonoids presents in the plant-plant parasite interaction *M. truncatula-O. crenata* such as defence response against this parasite. Our results probed that the model legume *M. truncatula* produces certain flavonoids (phytoalexins), defending itself and avoiding *O. crenata* attack.

Key words: *Orobanche crenata*, *Medicago truncatula*, legumes, phenolics, phenylpropanoid pathway, formononetin, resistance, parasitic plants.

Introduction

Crenate broomrapes (*Orobanche crenata* Forsk.) are root holoparasitic plants specialized in attacking cool season legume crops. This parasitic weed represents the major constraint for grain and forage legume production in Mediterranean and West Asian countries, resulting in complete yield loss with severe infestations and removing otherwise productive land from effective use for very long periods of time (Rubiales et al., 2006; Joel et al., 2007). Legumes are an important crop family to humans as a source of food, feed for livestock and raw materials for industry (Graham and Vance, 2003).

Phytoalexins are polycyclic compounds (phenolics) commonly-know by plant pathologists due to their antifungal, antiinsect and antimicrobial activity (Dakota and Phillips, 1996). These compounds are synthesized "de novo" in response to pathogen elicitors or damages via phenylpropanoid pathway (Dixon et al., 2002; Yu and McGonigle, 2005). Legumes are known to produce and accumulate specific phytoalexins named isoflavonoids as defence against different attacks including UVB light, anaerobic mediums, heavy metals, herbivorous and pathogens (Aoki et al., 2000; Dixon and Sumner, 2003). Phenolics have recently been shown to as plant defence compounds against broomrapes (Pérez-de-Luque et al., 2005a; Echevarría-Zomeño et al., 2006; Lozano-Baena et al., 2007) as in other plant-plant parasite interactions (Ueda and Sugimoto, 2010). For this reason, qualitative and quantitative determination of isoflavonoids expressed in legume crops against pathogens is important to understand plant defences and to design control strategies.

Unfortunately, little genomic resources are available for most cool season grain and forage legumes such as faba beans (*Vicia faba* L.), lentils (*Lens culinaris* Medik), peas (*Pisum sativum* L.) or vetches (*Vicia sativa* L.). Nevertheless, *Medicago truncatula* Gaertn. (barrel medic) has been selected as a model legume (Benedito et al., 2008; Rispail et al., 2010) because

of its small diploid genome, self-fertility, short life cycle, high seed production, ease of cultivation and possibility of genetic transformation. Development of techniques and methods for molecular and genetic analysis and the genome sequence (http://www.medicago.org) provide new tools which make *M. truncatula* a suitable model for legume genomic research.

Different mechanisms of resistance against *O. crenata* have been reported in *M. truncatula* germplasm (Rodríguez-Conde et al., 2004; Fernández-Aparicio et al., 2008). Accessions SA4327 and SA27774 have been the subject of recent cytological and molecular studies revealing that both accessions present similar defence mechanisms but acting at different timing, being the resistance of SA27774 early acting and that of SA4327 late acting (Lozano-Baena et al., 2007; Pérez-de-Luque et al., 2007; Castillejo et al., 2009). Thus, resistance act in SA27774 during host tissues invasion, whereas in SA4327 acts after establishment of vascular connections.

Cytological studies showed that resistance is due to accumulation of compounds (i.e. phenolics) (Lozano-Baena et al., 2007) in host tissues around infection points that accumulate into parasite. The same reaction has been described in the interaction of *O. cumana* with its host sunflower (*Helianthus annus* L.) where fluorescence and confocal laser microscopy (CLM) observations revealed accumulation of phenolic compounds during the incompatible reaction (Echevarría-Zomeño et al., 2006). Sealing of vessels or callose found before in sunflower (Echevarría-Zomeño et al., 2006) was not evident if *M. truncatula*.

In the present study, we identified and quantified some of the flavonoids produced by *M. truncatula* as response to the *O. crenata* attack using high performance liquid chromatography with UV and mass spectrometric detection (LC-MS/MS) systems as well recognized methods to profile flavonoids in plant tissue extracts (Prasain et al., 2004; Deavours and Dixon, 2005). As standards, we have selected some of the main *M. truncatula* flavonoids of the phenylpropanoid

pathway probed as defence compounds in pathogen invasions (Naoumkina et al., 2007; Farag et al., 2008; Lozano-Baena et al., 2007), in its close relative alfalfa (*M. sativa* L.) (He and Dixon, 2000), as well as in other species (Shimada et al., 2000) (Fig. 1). Specifically, chlorogenic acid is a product of cinnamic acid metabolism (Steck, 1968), an important intermediate of lignin biosynthesis with anti-pathogenic properties (Jöet et al., 2010) and has been reported to be produced by alfalfa under stress conditions (Jorrín and Dixon, 1990). Scopoletin is a coumarin, a class of secondary metabolites with antimicrobial properties and derived from phenylpropanoid pathway in plants, that is involved too in lignin biosynthesis (Kai et al., 2008). Naringenin were selected due to be the start point to other phenolic synthesis (i.e. flavones, flavonols, anthocyanins and condensed tannins) with defensive roles against parasites, and the precursor of the mainly isoflavonoids analysed (Deavours and Dixon, 2005; Farag et al., 2008; Limem et al., 2008) (Fig. 2) i.e. daidzein and genistein (next steps in this metabolic pathway). Moreover, these simple isoflavonoids are not only phytoalexin precursors but they inhibit the growth of microorganisms themselves (Dakota and Phillips, 1996). Daidzein plays another important role in this pathway due to be the precursor of phytoalexins in legume plants (Dixon et al., 1996; He and Dixon, 2000; Shimada et al., 2000; Dixon et al., 2002; Deavours and Dixon, 2005; Yu and McGonigle, 2005), specifically, two pterocarpans directly related with *M. truncatula* defence response: medicarpin (the major phytoalexin produced in alfalfa) and its precursor formononetin (Dixon et al., 1996; Naoumkina et al., 2007; Farag et al., 2008). And finally, maackiain is an important phytoalexin pterocarpan with antifungal activity and precursor of pisatin (another phytoalexin), present in pea (Aoki et al., 2000).

Therefore, to identify the presence and concentration of these standards in samples could help in understanding *M. truncatula* / *O. crenata* interaction.

Materials and methods

Plant material and growth conditions

Crenate broomrape was grown on two *Medicago truncatula* accessions showing early and late resistance to this pathogen (accessions SA27774 and SA4327, respectively). The petri dish system described by Pérez-de-Luque et al. (2005a) was used for in vitro cultivation of the *M. truncatula* plants and inoculation with *O. crenata* seeds. *M. truncatula* seeds were supplied from the South Australian Research and Development Institute Genetic Resource Centre in Australia (origin: Morocco for SA27774 and Yugoslavia for SA4327). Seeds were scarified slightly scratching the cuticle with a razor blade and sterilized in commercial bleach (20% in sterile water) for 10 min. For synchronized germination, seeds were placed at 4ºC for 36 h in sterile water. During this period, sterile water was replaced two or three times to help germination. After that, seeds were rinsed with sterile water at room temperature for 3 h, changing it six times. Finally, seeds were placed in petri dishes on wet glass fibre filter papers (Whatmann GF/A) and kept in darkness at 20ºC for 1 to 2 days. When the radicle reached 2 cm length, seedlings were transferred to new dishes (15 cm diameter) with perlite and new glass fibre papers (Pérez-de-Luque et al., 2005a). *O. crenata* seeds were collected from infected faba bean (*Vicia faba*) plants at Córdoba (Spain) during 2000. They were disinfected with formaldehyde according to González-Verdejo et al. (2005) and spread on the glass fibre paper (approximately 8 mg) where *M. truncatula* roots were growing. At the same time, some seedlings were kept without inoculation as controls. To prevent exposure of the parasite seeds and host roots to direct light, the dishes containing test plants were covered with aluminium foil. Then, the upward growing host plants were placed vertically in trays with Hoagland nutrient solution (Hoagland and Arnon, 1950) and grown in a controlled environment chamber at 20ºC ± 0.5ºC with a day/night 14 h photoperiod and an irradiance of 200 µmol m^{-2} s^{-1}. At the same time plants were growing, crenate

broomrape seeds were conditioned. For conditioning, parasite seeds need to be in a humid environment in darkness at 20ºC for 10 days (Pérez-de-Luque et al., 2005a).

After conditioning period, we applied 5 ml of the synthetic stimulant GR24 (0.01 mg/ml; Magnus et al., 1992) on the paper with the seeds for *O. crenata* homogenous germination induction.

Collection of samples

Root samples were harvested 15 days after GR24 application, time at which many of the haustorium are formed (Fig. 3) and plant defence mechanisms are expected to be acting. Another indication of the best moment to collect samples was the aspect that *O. crenata* radicles showed during collection. When samples were harvested, we could observe morphological differences between *M. truncatula* accessions and *O. crenata* parasites corresponding with the aspect described before (Fig. 3). Tissue samples collected from SA4327 showed a healthy appearance and growing as expected but *O. crenata* radicles infecting SA27774 had stopped their development and both, host and parasite close tissues seemed dark.

For non inoculated plants, small root pieces (approximately 1 cm) were sampled at random. For inoculated plants, parts of the root with a crenate broomrape attachment were sampled, removing the parasite tissues. Then, samples were washed with tap and distilled water, blotted dry with filter paper, frozen in liquid nitrogen, and stored at -80ºC until biochemical analysis (Pérez-de-Luque et al., 2005a).

Observations were taken using a binocular microscope (Nikon SMZ1000; Nikon Europe B.V.). Triplicate biological replicates were collected for both control and inoculated samples.

Extraction of phenolics

Frozen root tissues (0.04 g fresh weight) were homogenized in 1 ml methanol (MeOH) by using a pestle and mortar. After filtering off the solvent extract, the residue was further sequentially extracted twice with a similar volume of MeOH and centrifuged twice at 15,000g for 15 min. The combined solvent extracts were dried and phenolic compounds were resuspended in 0.24 ml of MeOH for further analysis of soluble phenolics. The pellet residue was resuspended in 0.08 ml of 2 M NaOH and incubated at 70ºC for 16 h. The suspension was cooled down, neutralized with 0.08 ml of 2 M HCl, and centrifuged (15,000g for 15 min). Then, the suspension was collected and analysed as extract of cell wall-bound phenolics.

Chemicals

The flavonoids (used as standards) formononetin, daidzein, genistein, naringenin, maackiain and medicarpin were purchased from Plantech (www.plantechuk.co.uk, Reading, UK); scopoletin and chlorogenic acid were purchased from Sigma-Aldrich (www.sigmaaldrich.com) (Fig. 1). Standards were chosen based on their previous reported role in the plant defence process and represent the principal steps of the phenylpropanoid pathway.

Quantification of total phenolics

The determination of total phenolic content was performed by the Folin-Ciocalteu method (Prats, 2002). Absorbance of both, soluble and cell wall-bound phenolic extracts was measured colorimetrically in a Synergy HT multi-detection microplate reader (Biotek Instruments, Winooski, VT, USA). Data analysis was carried out using BioTek's Gen5 Data Analysis Software.

LC-ESI-MS/MS Analyses: Identification and quantification of phytoalexins

A Varian 1200 L Triple-Quadrupole tandem mass spectrometer (S.C.A.I., UCO) was used equipped with an electrospray ionization (ESI) source under negative ionization (NI). Chromatographic separation was performed on a C18 column 150 x 2 mm inner diameter (id). The mobile phase consisted of (A) double distilled water containing 0.1% formic acid and (B) a solution of acetonitrile 75% and methanol 25% (v/v). The mobile phase was pumped at a flow rate of 0.2 ml/ min and the injection volume was 10 μl. The gradient started with 10% B and increased linearly to 100% B over 10 min. Compounds were subjected to collision-induced dissociation in the multiple reaction monitoring (MRM) mode.

Statistical Analysis

Total phenolic determination assays were performed with 4 replicates per treatment and LC-ESI-MS/MS analyses with three replicates per treatment, with a completely randomized design. Statistical analysis (ANOVA) was performed with Statistix 9.0 for Windows.

Results

O. crenata seeds germinated 7 days after GR24 application and broomrape attachments on *M. truncatula* roots were developed 15 days after GR24 application as usual. At this point, we could observe differences in the aspect of the attached seedlings between accessions: SA4327 attached seedlings presented a healthy appearance (Fig. 3A and B). On the contrary, SA27774 attached seedlings and the host tissues surrounding parasite attachment showed a dark appearance and no further healthy tubercles developed (Fig. 3C and D).

Quantification of total phenolics

Total soluble and cell wall-bound phenolic content was determinated in *M. truncatula* root tissue extracts of non inoculated and inoculated plants with *O. crenata* parasite corresponding to plants sampled 15 days after GR24 application (a synthetic germination stimulant). Data are presented in Fig. 4.

Root extracts from inoculated plants presented a twofold higher phenolic level, both soluble and cell wall-bound respect to non inoculated plants. However, significant differences between accessions were not detected (Fig. 4A, B).

For soluble phenolics (Fig. 4A), values ranged between 1935 μg of phenolics per g of fresh in inoculated tissues of accession SA27774 and 505.5 $\mu g \cdot g^{-1}$ of fresh tissues corresponding to non inoculated tissues of SA4327. Roots from SA4327 inoculated tissues and SA27774 non inoculated tissues had 1710.6 and 750 μg of phenolics per gr of fresh tissues respectively. Cell wall-bound phenolics data showed similar results with the highest phenolic concentration in SA27774 inoculated tissues (4920 $\mu g \cdot g^{-1}$ of fresh tissues) and the lowest value of SA4327 non inoculated tissues (1281 $\mu g \cdot g^{-1}$ of fresh tissues) (Fig. 4B).

LC-ESI-MS/MS Analyses

LC-MS technique was used to identify and quantify phytoalexins produced by *M. truncatula* cell roots in response to *O. crenata* attack (Fig. 5). Our samples were analysed using both: positive-ion ESI mass spectra, which provided a greater number of fragment ions for each component that aided in structural identification, and negative-ion ESI, which yielded better sensitivity and higher signal to noise ratios (Huhman and Sumner, 2002). However no differences were observed between these methods in analysed samples.

Three of the standards (naringenin, daidzein and formononetin) were identified and quantified in the analysed root tissues for soluble phenolic samples but only formononetin appeared in both inoculated and non inoculated roots (naringenin and daidzein were only detected in inoculated roots of the SA4327 accession). No standard was detected in cell wall-bound phenolic extracts. Medicarpin, genistein, chlorogenic acid and scopoletin were not detected in any case and maackiain could not be analysed due to its instability.

Significant differences between samples were detected in formononetin accumulation. Firstly, although formononetin was identified in control samples its presence is more than twice in inoculated tissue extracts. Secondly, we found differences between accessions so that the highest and lowest formononetin concentration (i.e. 4108.4 and 1096.2 ngr gr^{-1} fresh tissues respectively) appears in SA27774 accession. However, formononetin concentration in SA4327 non inoculated samples is higher than SA27774 non inoculated. In this sense, SA4327 inoculated samples have lower formononetin levels than the inoculated SA27774 roots.

Regarding standards found in SA4327 accession, formononetin concentration in inoculated samples (3308.9 ngr gr^{-1} fresh tissues) is so much higher in comparison with

naringenin and daidzein (74.187 and 85.57 ngr gr^{-1} fresh tissues respectively). No significant differences between naringenin and daidzein concentration were detected.

When chromatograms of inoculated and non inoculated samples were compared, we could observe that LC-MS detected other peaks, apart from our standards, present in inoculated samples that did not appear in non inoculated. Now, we are working in order to identify these compounds present only in infected samples.

Discussion

O. crenata invasion process can be divided into different phases and plant hosts have developed different resistance mechanisms which act in all of them (Pérez-de-Luque et al., 2008). In the first phase of *O. crenata* life cycle, parasite seeds germinate and grow towards host stimulated by the presence in the soil of some specific chemicals exuded by its roots. Because *M. truncatula* is a poor host of *O. crenata* the percentage of *O. crenata* seeds germinated in presence of *M. truncatula* root exudates is very low (Rodriguez-Conde et al., 2004). To solve this problem, researchers normally use exogenous application of the synthetic germination stimulant GR24. With its addition, the percentage of *O. crenata* germinated seeds reach the 40-50% increasing the number of contacting radicles and attached seedlings (Fernández-Aparicio et al., 2008). For this reason, we have chosen the GR24 application such as start point of *O. crenata* infection process. Afterwards, we can observe the first emerged radicles 5 days after its application and the 40-50% of germinated seeds in a week. After that, infection process continues as normally, appearing attached tubercles to *M. truncatula* roots growing 15 days after GR24 application.

We centred our work in the next phase of *O. crenata* life cycle when radicles start to penetrate *M. truncatula* root tissues. At this level, host plants activate the pre-haustorial resistance mechanisms aiming to hamper the parasite attempt to reach the central cylinder and establish vascular connection with host vessels. However, whether parasite reaches to establish host vascular connections, it starts to develop the haustorium (a specialized structure to suck water and nutrient from host). In order to avoid this, host plant activates the post-haustorial mechanisms of resistance and finally, try to stop parasite tubercle growth (Pérez-de-Luque et al., 2008). Whatever the resistance mechanism which is acting in this interaction, it should be taking place at this phase. For this reason, samples were collected at this time gap in order to determine this defence reaction.

Quantification of total phenolics

In general, phytoalexins are not detectable in healthy tissues or they can be found in very low concentrations (i.e. constitutive metabolism) or as sugar conjugates stored in vacuoles (then named phytoanticipins) (Dixon et al., 1996; Dakota and Phillips, 1996). They are secreted as defence compounds by cells immediately adjacent to infected sites and accumulate in dead and dying cells within these localized regions. These compounds are synthesized rapidly after infection due to the de novo activation of secondary metabolic pathways (i.e. phenylpropanoid pathway), which divert primary metabolic precursors into the production of phytoalexins (Yu and McGonigle, 2005).

In legumes, isoflavonoid phytoalexins are the products of the phenylpropanoid pathway involved in defence against pathogens (Dixon et al., 1996). In our previous study (Lozano-Baena et al., 2007), we showed that *M. truncatula* produced some toxic compounds against *O. crenata* infection, stopping parasite growth. These observations suggested the possibility of phenolic compound accumulation as a defence strategy by infected legume plants. They inhibited development of *O. crenata* attached seedlings and caused a browning reaction in radicles and tubercles.

Our results show high concentration of phenolics in extracted samples (Fig. 4). Phenolics were detected in all samples with no significant differences between host accessions but with pathogen presence. The presence of phenolics in non inoculated samples could be due to constitutive metabolism (Dakota and Phillips, 1996; Farag et al., 2007). But, our results probe that inoculation (i.e. infection) process induced a very high increase of these compounds in samples, duplicating their concentration (Fig. 4).

The increase of phenolic compounds was observed in both soluble and cell wall-bound fractions but it was higher in cell wall-bound extracts where inoculated SA4327 accession has more than three times the concentration regarding to non inoculated samples. A similar fact occurs in SA27774 accession (Fig. 4). This suggest that cell wall-bound phenolics have a more important role in *M. truncatula* defence response but the less concentration of phenolics in soluble fractions can be explained in a different way. In this sense, soluble phenolics are synthesised and excreted close to parasite tissues and confocal studies have shown that parasite accumulate these phenolics within itself (Lozano-Baena et al., 2007). Indeed, they established a flux between host and parasite in which *O. crenata* radicles and tubercles showed an accumulation of phenolics removing them from host root tissues. Moreover, once phenolics reach parasite intrusive tissues and due to their strong antioxidant properties (Limem et al., 2008), they are rapidly oxidated into other chemical forms and getting their toxic function. These two facts, could contribute to detect a lower concentration of soluble phenolics in root samples. On the contrary, cell wall-bound phenolics are fixed into cell walls and extraction method recovers them in all their original form and concentration.

On the other hand, the high level of cell wall-bound phenolics in samples suggests that cells are accumulating these compounds in walls with defensive function acting such as physical barriers reinforcing cell walls and trying to hamper parasite penetration (Pérez-de-Luque et al., 2005b). Using specific stainings Lozano-Baena et al. (2007) showed the thickening of host vascular cell walls by phenolics accumulation but showed that these thickened walls presented no lignins which could strengthen them. Thus, it is not clear that these phenolics are from metabolic branch of lignins synthesis (normal pathway to imparts mechanical strength to stems and trunks, and hydrophobicity to water-conducting vascular elements) (Dixon et al., 1996) and moreover, these phenolics do not stopped parasite intrusion because it reached the endodermis and vascular

vessels of the host. This suggests that the accumulation of these phenolics does not act as strong physical barrier and probably could have other function.

LC-ESI-MS/MS Analyse

Total phenolic determination just provides evidences about the presence and concentration of phenolic compounds in harvested samples but no identification and quantification of them are possible. For this reason, LC-MS technique was selected in this work because of its reliability, high sensitivity and selectivity identifying and quantifying specific compounds in a complex mixture (Caboni et al., 2008). Other authors have presented plant phenolic compounds as defence against Orobanche ssp. (Serghini et al., 2001; Echevarría-Zomeño et al., 2006; Lozano-Baena et al., 2007) but this is the first time that a work analyze and quantify their role in the interaction between *O. crenata* and the model legume *M. truncatula*.

Using LC-MS technique, neither chlorogenic acid nor scopoletin were detected in any of analysed samples. These phenolics are directly involved in phenylpropanoid pathway, for example as precursors of lignin biosynthesis (Fig. 2). In agreement with this, lignins were not observed before in inoculated roots of *M. truncatula* (Lozano-Baena et al., 2007).

On the other hand, phenylpropanoid pathway is responsible for flavonoid synthesis (Fig. 2) such as naringenin and LC-MS analysis confirms the presence of this flavanone such as soluble phenolic but only in SA4327 inoculated samples (Fig. 5B). This fact point naringenin, as principal step of this pathway, as one of the first flavonoids appeared in host tissues after parasite intrusive cells detection. Once naringenin is metabolized, the first isoflavonoids of the phenylpropanoid pathway are daidzein and genistein. Genistein were not detected by LC-MS analysis and daidzein had a similar concentration as naringenin and appeared in the same samples (i.e. SA4327 inoculated samples) (Fig. 5A).

All this data support the idea that phenylpropanoid pathway is activated in *M. truncatula* defence response. Indeed, no control (i.e. non inoculated) samples have showed traces of any of the standard flavonoids used except formononetin (Fig. 5). This suggests that no defence response is acting in this samples and formononetin detection is due to basal metabolism (Dakota and Phillips, 1996). Furthermore, LC-MS analysis confirmed that intrusive cells of *O. crenata* parasite induce the accumulation of formononetin like soluble phenolic in all *M. truncatula* extracted root tissues nearby infected point (Fig. 5C). Formononetin (derived from daidzein metabolization) is the precursor of medicarpin, a constitutive polyphenol of *M. truncatula* (Farag et al., 2007) and its close relative alfalfa, and main isoflavonoid responsible of its defence response to pathogens (He and Dixon, 2000; Deavours and Dixon, 2005; Naoumkina et al., 2007; Farag et al., 2008).

In this sense, LC-MS analysis of inoculated samples revealed a considerable accumulation of formononetin of non inoculated roots. In addition, we found significant difference between accessions, so inoculated SA27774 samples have more concentration of formononetin than inoculated SA4327 (Fig. 5C). This may be due to the difference between defence reactions occurring in *M. truncatula* accessions and the time-gap selected to collect samples.

The final step of phenylpropanoid pathway in *M. truncatula* is the conversion of formononetin into the phytoalexin medicarpin (Dixon et al., 1996). Other authors have demonstrated that cell suspensions of *M. truncatula* accumulated the isoflavonoid phytoalexin medicarpin in response to yeast elicitor or methyl jasmonate (Naoumkina et al., 2007) and to fungi (Harrison and Dixon, 1993). Results indicate that mechanisms underlying accumulation of medicarpin differ depending on the nature of the stimulus.

Unfortunately, we could not detect medicarpin in root tissue as expected. The absence of medicarpin could be explaining by several reasons: firstly, we chose as time sampling 15 days

after GR24 application, period of time necessary to allow pathogen germinate, take contact with host roots and initiate host tissue invasion. Hence, when we collected samples probably we selected them in another pathway step so medicarpin levels could not be detected. Secondly, the extraction method separate detected compounds depending on their state in plant tissues (i.e. soluble or cell wall-bound). TLC analysis identified medicarpin as part of the soluble phase in extracted samples (Lozano-Baena et al., 2007) and if medicarpin is secreted by *M. truncatula* root cells and transported to *O. crenata* parasite to stop its intrusion, this fact could difficult its detection in root extracted samples. This circumstance was showed by Lozano-Baena et al (2007) where phenolic flux from host tissues to parasite and further accumulation was detected in *O. crenata* established seedlings and tubercles by fluorescence.

Because no standards were detected in cell wall-bound analysed samples, we conclude that these compounds are not involved in this defence reaction. Therefore, phytoalexins responsibles of host cell walls reinforcement could not be identified. In this sense, phenylpropanoid pathway produce many different polyphenols that could be the cause of this reaction i.e. flavones, flavonols, etc (Fig. 2). These polyphenols act bounded to cell wall perhaps limiting the absorption of water and nutrients by the parasite from host vessels, and reducing tubercles growth.

Altogether, in this work we have demonstrated that the model legume *M. truncatula* produces certain compounds i.e. flavonoids as phytoalexins in order to defend itself from the *O. crenata* parasite attack. These compounds (derived from phenylpropanoid pathway) have been identified and their concentration in host tissues quantified to determine their role in this plant-parasitic plant interaction.

Acknowledgements

This work was supported by project AGL2008-01239.

References

Aoki T, Akashi T, Ayabe S. 2000. Flavonoids of Leguminous plants: Structure, biological activity and biosinthesis. *Journal Plant Research* 113: 475-488.

Benedito VA, Torres-Jerez I, Murray JD, Andriankaja A, Allen S, Kakar K, Wandrey M, Verdier J, Zuber H, Ott T, Moreau S, Niebel A, Frickey T, Weiller G, He1 J, Dai1 X, Zhao PX, Tang Y, Udvardi MK. 2008. A gene expression atlas of the model legume *Medicago truncatula*. *The Plant Journal* 55: 504-513.

Caboni P, Sarais G, Angioni A, Vargiu S, Pagnozzi D, Cabras P, Casida JE. 2008. Liquid chromatography-Tandem mass spectrometric ion-switching determination of chlorantraniliprole and flubendiamide in fruits and vegetables. *Journal of Agricultural and Food Chemistry* 56: 7696-7699.

Castillejo MA, Maldonado AM, Dumas-Gaudot E, Fernández-Aparicio M, Susin R, Rubiales D, Jorrín J. 2009. Differential expression proteomics to investigate responses and resistance to *Orobanche crenata* in *Medicago truncatula*. *BMC Genomic*s 10: 294. doi:10.1186/1471-2164-10-294.

Dakota FD, Phillips DA. 1996. Diverse functions of isoflavonoids in legumes transcend anti-microbial definitions of phytoalexins. *Physiological and Molecular Plant Pathology* 49: 1-20.

Deavours B.E. and Dixon R.A. (2005) Metabolic Engineering of Isoflavonoid Biosynthesis in alfalfa. *Plant Physiology* 138: 2245-2259.

Dixon RA, Sumner LW. 2003. Legume natural products: understanding and manipulating complex pathways for human and animal health. *Plant Physiology* 131: 878-885.

Dixon RA, Lamb CJ, Masoud S, Sewalt VJH, Paiva NL. 1996. Metabolic engineering: prospects for crop improvement through the genetic manipulation of phenylpropanoid biosynthesis and defence responses - a review. *Gene* 179: 61-71.

Dixon RA, Achnine L, Kota P, Liu C, Reddy MSS, Wang L. 2002. The phenylpropanoid pathway and plant defence-a genomics perspective. *Molecular Plant Pathology* 3: 371-390.

Echevarría-Zomeño S, Pérez-de-Luque A, Jorrín J, Maldonado AM. 2006. Pre-haustorial resistance to broomrape (*Orobanche cumana*) in sunflower (*Helianthus annuus*): cytochemical studies. *Journal of Experimental Botany* 57: 4189-4200.

Farag MA, Huhman DV, Lloyd Z, Sumner LW. 2007. Metabolic profiling and systematic identification of flavonoids and isoflavonoids in roots and cell suspension cultures of *Medicago truncatula* using HPLC-UV-ESI-MS and GC-MS. *Phytochemistry* 68: 342-354.

Farag MA, Huhman DV, Dixon RA, Sumner LW. 2008. Metabolomics reveals novel pathways and differential mechanistic and elicitor-specific responses in phenylpropanoid and isoflavonoid biosynthesis in *Medicago truncatula* cell cultures. *Plant Physiology* 146: 387-402.

Fernández-Aparicio M, Pérez-de-Luque A, Prats E, Rubiales D. 2008. Variability of interaction between barrel medic (*Medicago truncatula*) genotypes and *Orobanche* species. *Annals of Applied Biology* 153: 117-126.

González-Verdejo CI, Barandiaran X, Moreno MT, Cubero JI, Di-Pietro A. 2005. An improved axenic system for studying pre-infection development of the parasitic plant *Orobanche ramosa*. *Annals of Botany* 96: 1121-1127.

Graham PH, Vance CP. 2003. Legumes: importance and constraints to greater use. *Plant Physiology* 131: 872-877.

Harrison MJ, Dixon RA. 1993. Isoflavonoid accumulation and expression of defence gene transcripts during the establishment of vesicular-arbuscular mycorrhizal associations in roots of *Medicago truncatula*. *Molecular Plant-Microbe Interactions* 6: 643-654.

He XZ, Dixon RA. 2000. Genetic manipulation of isoflavone 7-O-methyltransferase enhances biosynthesis of 4'-O-methylated isoflavonoid phytoalexins and disease resistance in alfalfa. *The Plant Cell* 12: 1689-1702.

Hoagland DR, Arnon DI. 1950. The water-culture method for growing plants without soil. California Agricultural Experiment Station Circular 347. University of California, Berkeley.

Huhman D, Sumner L. 2002. Metabolic profiling of saponins in *Medicago sativa* and *Medicago truncatula* using HPLC coupled to an electrospray ion-trap mass spectrometer. *Phytochemistry* 59: 347-360.

Joel DM, Hershenhorn Y, Eizenberg H, Aly R, Ejeta G, Rich PJ, Ransom JK, Sauerborn J, Rubiales D. 2007. Biology and Management of Weedy Root Parasites. In: J. Janick ed. Horticultural Reviews. Hoboken, 33: 267-350.

Jöet T, Salmona J, Laffargue A, Descroix F, Dussert S. 2010. Use of the growing environment as a source of variation to identify the quantitative trait transcripts and modules of co-expressed genes that determine chlorogenic acid accumulation. *Plant, Cell and Environment* 33: 1220-1233.

Jorrín J, Dixon A. 1990. Stress Responses in Alfalfa (*Medicago sativa* L.) II. Purification, Characterization, and Induction of Phenylalanine Ammonia-Lyase Isoforms from Elicitor-Treated Cell Suspension Cultures. *Plant Phisiology* 92: 447-455.

Kai K, Mizutani M, Kawamura N, Yamamoto R, Tamai M, Yamaguchi H, Sakata K, Shimizu B. 2008. Scopoletin is biosynthesized via ortho-hydroxylation of feruloyl CoA by a 2-oxoglutarate-dependent dioxygenase in *Arabidopsis thaliana*. *The Plant Journal* 55: 989-999.

Limem I, Guedon E, Hehn A, Bourgaud F, Ghedira LC, Engasser JM, Ghoul M. 2008. Production of phenylpropanoid compounds by recombinant microorganisms expressing plant-specific biosynthesis genes. *Process Biochemistry* 43: 463-479.

Lozano-Baena MD, Moreno MT, Rubiales D, Pérez-de-Luque A. 2007. *Medicago truncatula* as a model for non-host resistance in legume-parasitic plant interactions. *Plant Physiology* 145: 437-449.

Magnus EM, Stommen PLA, Zwanenburg B. 1992. A standardized bioassay for evaluation of potential germination stimulants for seeds of parasitic weeds. *Journal of Plant Growth Reguation* 11: 91-98.

Naoumkina M, Farag MA, Sumner LW, Tang Y, Liu CJ, Dixon RA. 2007. Different mechanisms for phytoalexin induction by pathogen and wound signals in *Medicago truncatula*. *PNAS* 104: 17909-17915.

Pérez-de-Luque A, Jorrín J, Cubero JI, Rubiales D. 2005a. *Orobanche crenata* resistance and avoidance in pea (*Pisum* spp.) operate at different developmental stages of the parasite. *Weed Research* 45: 379-387.

Pérez-de-Luque A, Rubiales D, Cubero JI, Press MC, Scholes J, Yoneyama K, Takeuchi Y, Plakhine D, Joel DM. 2005b. Interaction between *Orobanche crenata* and its host legumes: unsuccessful haustorial penetration and necrosis of the developing parasite. *Annals of Botany* 95: 935-942.

Pérez-de-Luque A, Lozano-Baena MD, Maldonado AM, Jorrín JV, Dita MA, Die J, Román B, Rubiales D. 2007. *Medicago truncatula* as a model for studying interactions between root parasitic plants and legumes. In: U Mathesius, EP Journet, LW Sumner, eds. The *Medicago truncatula* Handbook. The Samuel Roberts Noble Foundation, Ardmore: OK 1-31.

Pérez-de-Luque A, Moreno T, Rubiales D. 2008. Host plant resistance against broomrapes (*Orobanche* spp.): defence reactions and mechanisms of resistance. *Annals of Applied Biology* 152: 131-141.

Pérez-de-Luque A, Fondevilla S, Pérez-Vich B, Aly R, Thoirons S, Simiers P, Castillejo MA, Fernández-Martínez JM, Jorrín J, Rubiales D, Delavaults P. 2009. Understanding *Orobanche* and *Phelipanche*-host plant interactions and developing resistance. *Weed Research* 49: 8-22.

Prasain JK, Wang CC, Barnes S. 2004. Mass spectrometric methods for the determination of flavonoids in biological samples. *Free Radical Biology and Medicine* 37: 1324-1350.

Prats E, Rubiales D, Jorrín J. 2002. Acibenzolar-s-methylinduced resistance to sunflower rust (*Puccinia helianthi*) is associated with an enhancement of coumarins on foliar surface. *Physiological and Molecular Plant Pathology* 60: 155-162.

Rispail N, Kaló P, Kiss GB, Ellis THN, Gallardo K, Thompson RD, Prats E, Larrainzar E, Ladrera R, González EM, Arrese-Igor C, Ferguson BJ, Gresshoff PM, Rubiales D. 2010. Model legumes contribute to faba bean breeding. *Field Crops Research* 115: 253-269.

Rodríguez-Conde MF, Moreno MT, Cubero JI, Rubiales D. 2004. Characterization of the *Orobanche-Medicago truncatula* association for studying early stages of the parasite-host interaction. *Weed Research* 44: 218-223.

Rubiales D, Pérez-de-Luque A, Fernández-Aparicio M, Sillero JC, Román B, Kharrat M, Khalil S, Joel DM, Riches C. 2006. Screening techniques and sources of resistance against parasitic weeds in grain legumes. *Euphytica* 147: 187-199.

Serghini K, Pérez-De-Luque A, Castejón-Muñoz M, García-Torres L, Jorrín JV. 2001. Sunflower (*Helianthus annuus* L.) response to broomrape (*Orobanche cernua* Loefl.) parasitism: induced synthesis and excretion of 7-hydroxylated simple coumarins. *Journal of Experimental Botany* 52: 2227-2234.

Shimada N, Akashi T, Aoki T, Ayabe S. 2000. Induction of isoflavonoid pathway in the model legume *Lotus japonicus*: molecular characterization of enzymes involved in phytoalexin biosynthesis. *Plant Science* 160: 37-47.

Steck W. 1968. Metabolism of cinnamic acid in plants: Chlorogenic acid formation. *Phytochemistry* 7: 1711-1717.

Ueda H, Sugimoto Y. 2010. Vestitol as a chemical barrier against intrusion of parasitic plant *Striga hermonthica* into *Lotus japonicas* roots. *Bioscience biotechnology and biochemistry* 74: 1662-1667.

Yu Oliver, McGonigle B. 2005. Metabolic engineering of isoflavone biosynthesis. *Advances in Agronomy* 86: 147-190.

Figures

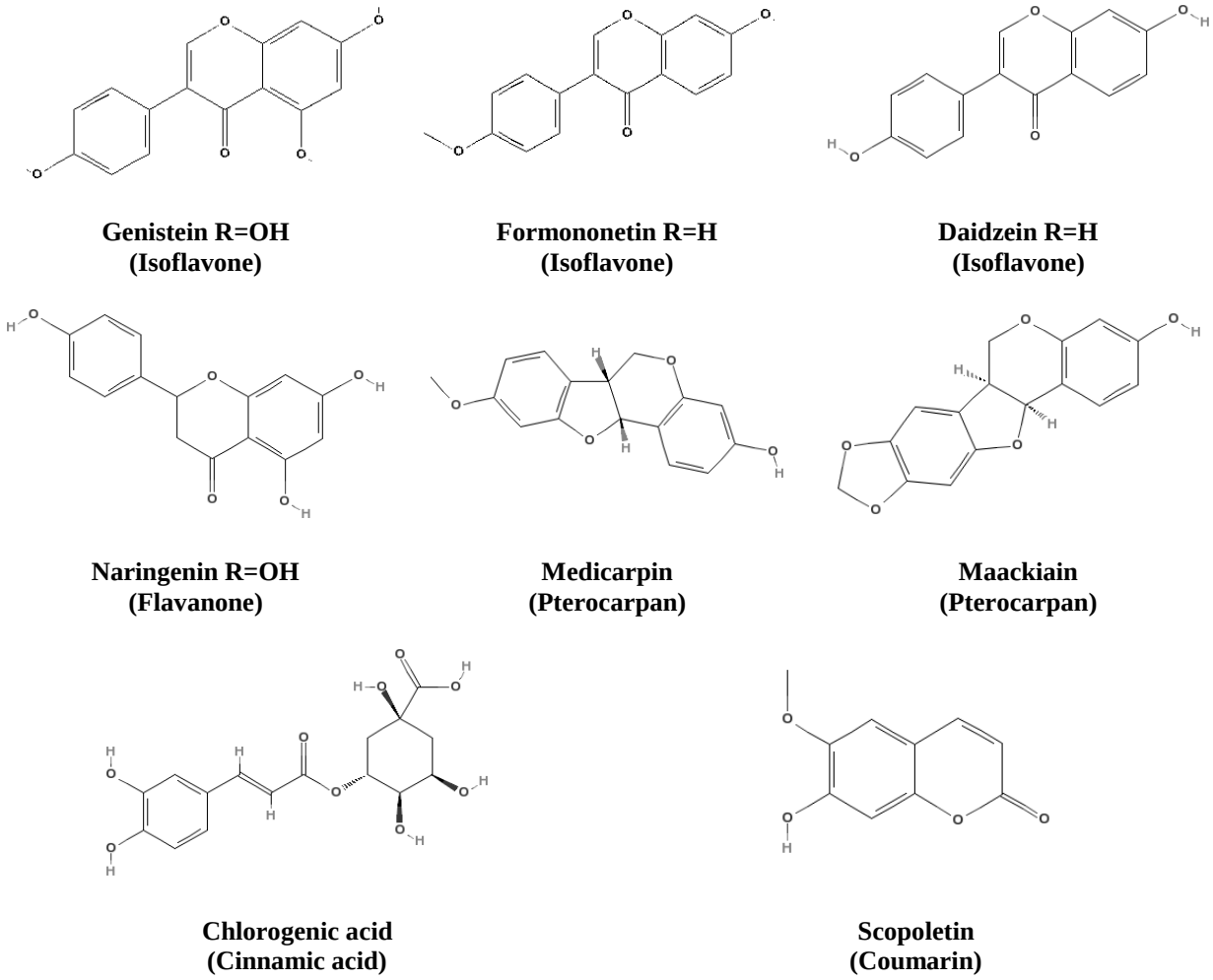

Fig. 1. Structure of analysed phytoalexins.

Fig. 2. Phenylpropanoid pathway

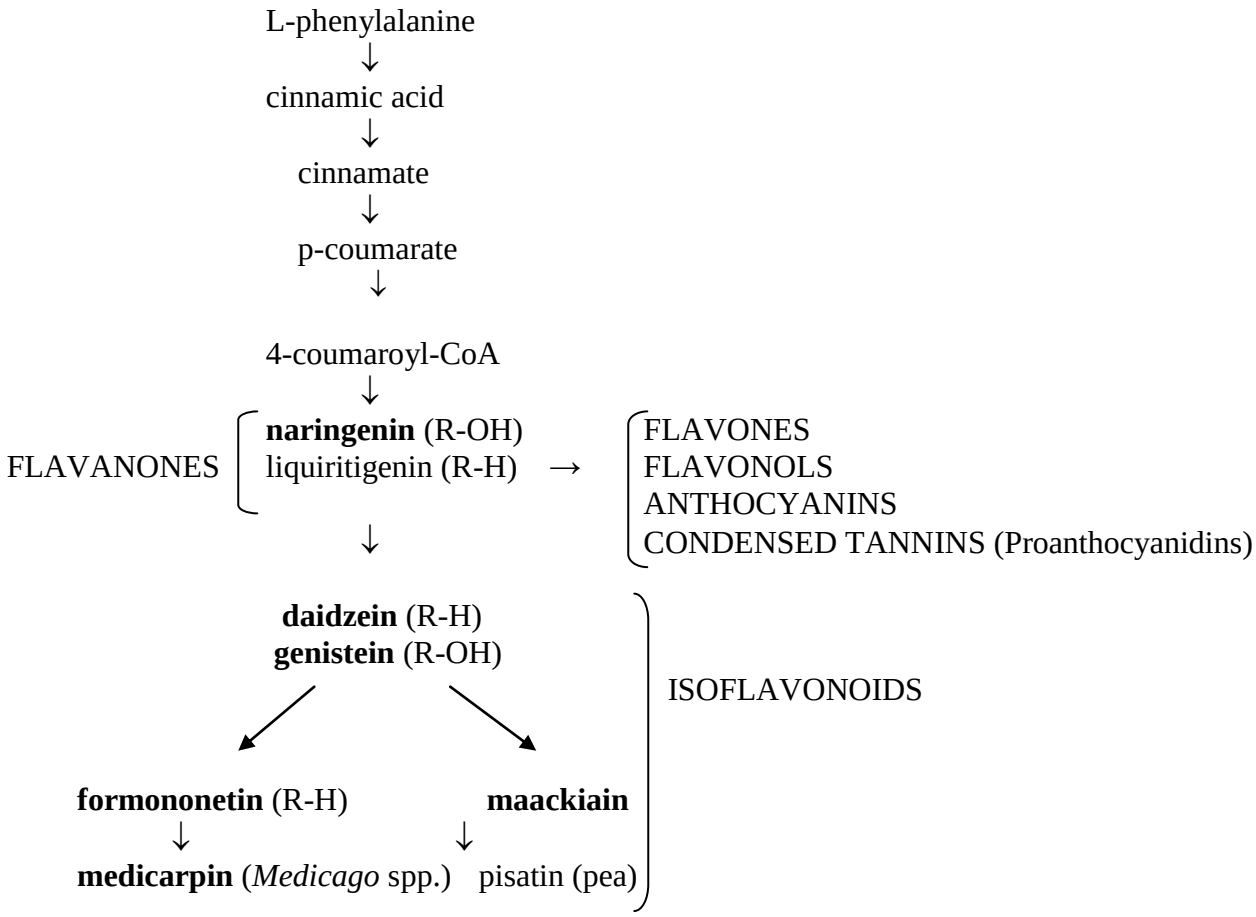

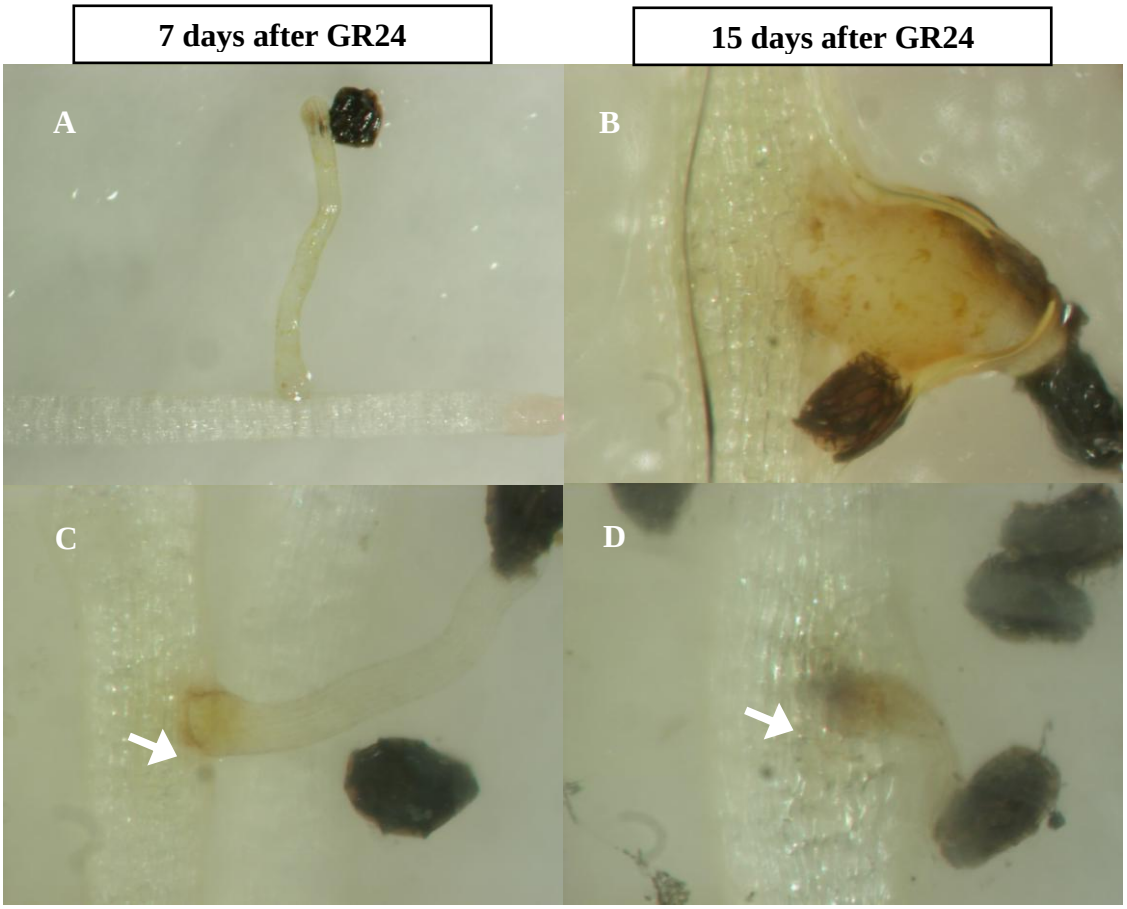

Fig. 3. Images illustrate *O. crenata* parasite attacking *M. truncatula* roots in "initial" infection stage (7 days after GR24 application) and "well develop" stage (15 days after GR24) observed under bright field. Images A and B show roots from *M. truncatula* SA4327 accession with *O. crenata* attached seedlings and tubercle (respectively). Images C and D show roots from SA27774 accession with attached seedlings. No SA27774 tubercles were observed in this time gap. Arrows shows the darkening around the infection point observed in SA27774 and parasite tissues.

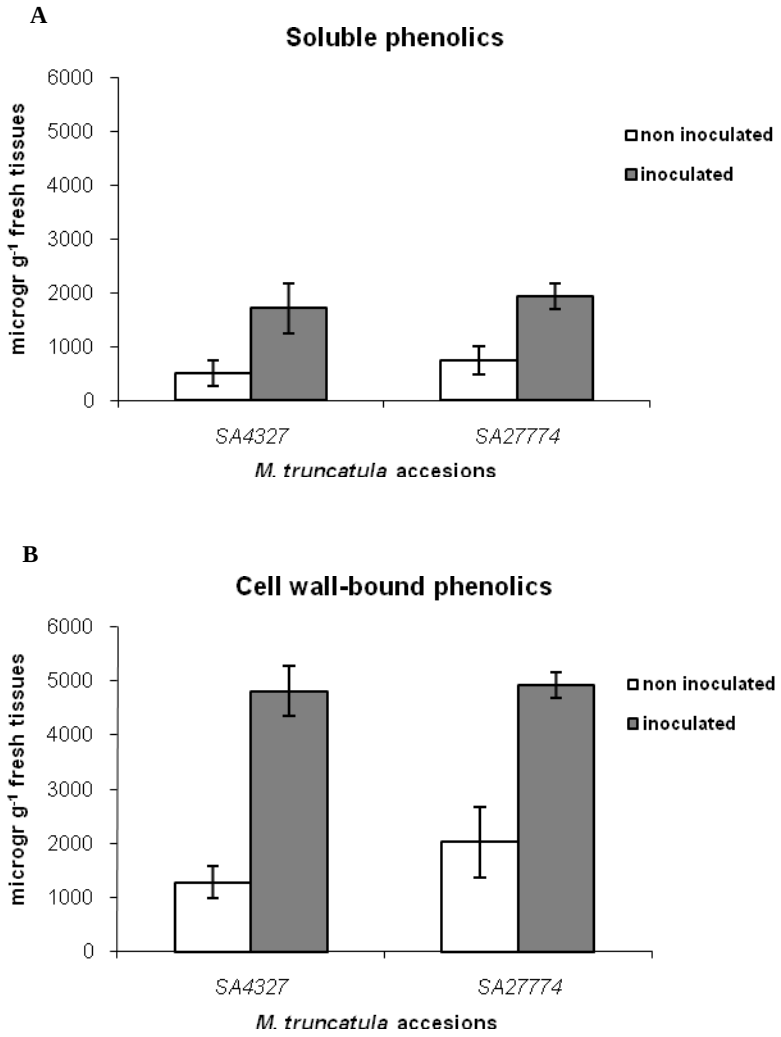

Fig. 4. Total soluble (A) and cell wall-bound (B) phenolics in non inoculated and *O. crenata* inoculated *M. truncatula* roots. Plant root samples were collected 15 days after GR24 application. Concentration of phenolics is indicated as micrograms of chlorogenic acid per gram of fresh tissues.

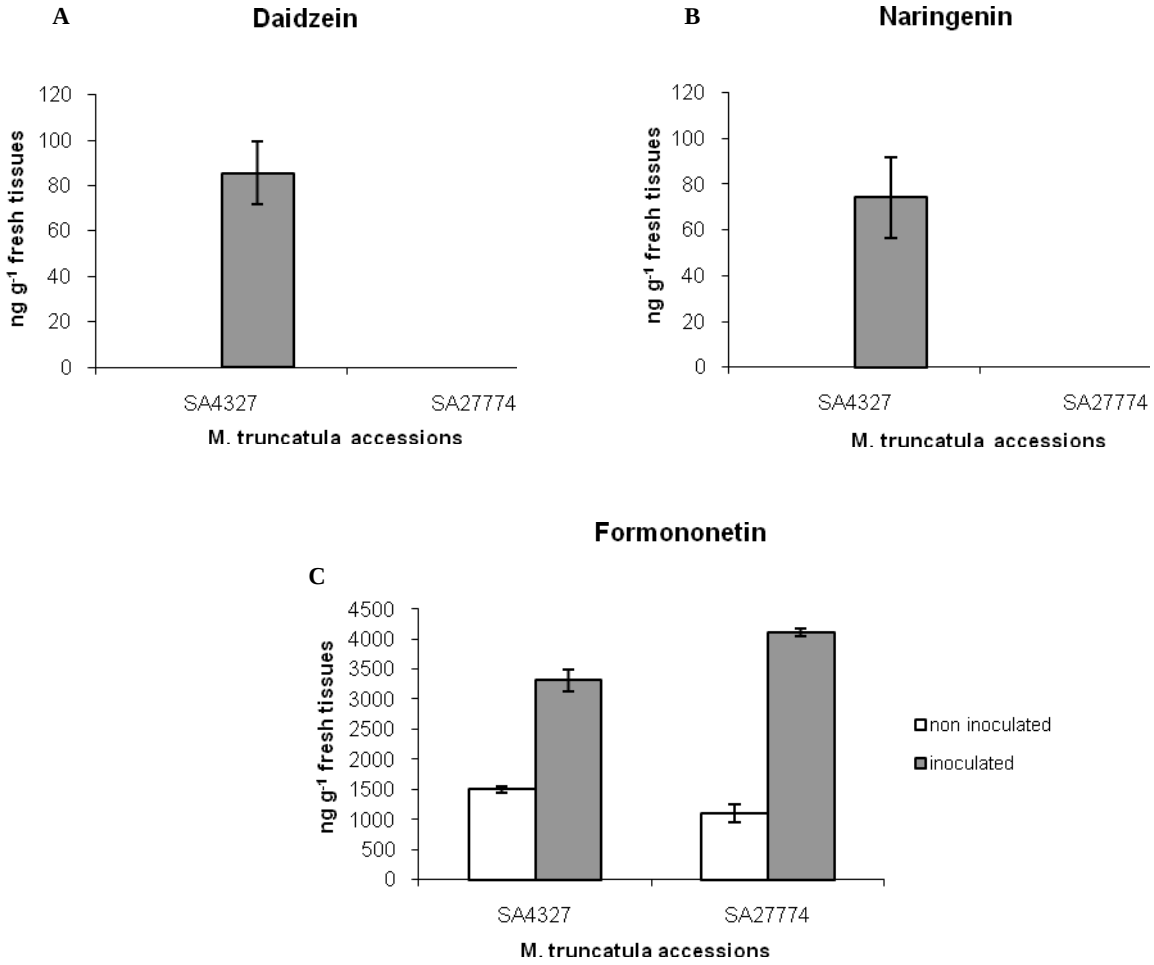

Fig. 5. LC-MS Analysis: naringenin (A), daidzein (B) and formononetin (C) concentration in non inoculated and *O. crenata* inoculated *M. truncatula* roots corresponding to soluble phenolic samples. Plant root samples were collected 15 days after GR24 application.